



**Functional characterization of splicing-associated  
kinases in the blood stages of the  
malaria parasite *Plasmodium falciparum***

Funktionelle Charakterisierung von Splicing-assoziierten Kinasen in  
den Blutstadien des Malariaerregers *Plasmodium falciparum*

Doctoral thesis for the completion of a doctoral degree  
at the Graduate School of Life Sciences,  
Julius-Maximilians-Universität Würzburg  
Section Infection and Immunity

submitted by

**Selina Melanie Kern**

from

Mutlangen

**Würzburg 2014**

Submitted on .....

Office stamp

Members of the *Promotionskomitee*:

Chairperson: Prof. Dr. Thomas Hünig

Primary Supervisor: Prof. Dr. Gabriele Pradel

Second Supervisor: Prof. Dr. Sven Krappmann

Third Supervisor: Prof. Dr. Jude Przyborski

Date of Public Defense:.....

Date of Receipt of Certificates:.....

## Affidavit

I hereby confirm that my doctoral thesis entitled "Functional characterization of splicing-associated kinases in the blood stages of the malaria parasite *Plasmodium falciparum*" is the result of my own work. I did not receive any help or support from commercial consultants. All sources and/or materials applied are listed and specified in the thesis.

Furthermore, I confirm that this thesis has not yet been submitted as a part of another examination process neither in identical nor in similar form.

I did not acquire, or try to acquire, yet another academic degree besides the within the approval documented degrees.

---

Place, Date

---

Signature

## Eidesstattliche Erklärung

Hiermit erkläre ich an Eides statt, die vorliegende Dissertation „Funktionelle Charakterisierung von Splicing-assoziierten Kinasen in den Blutstadien des Malariaerregers *Plasmodium falciparum*“ eigenständig, d.h. insbesondere selbständig und ohne Hilfe eines kommerziellen Promotionsberaters, angefertigt und keine anderen als die von mir angegebenen Quellen und Hilfsmittel verwendet zu haben. Wörtlich oder sinngemäß übernommenes Gedankengut habe ich als solches kenntlich gemacht.

Des Weiteren erkläre ich, dass diese Dissertation weder in gleicher noch in ähnlicher Form bereits in einem anderen Prüfungsverfahren vorgelegen hat.

Ich habe bisher außer den mit dem Zulassungsgesuch urkundlich vorgelegten Graden keine weiteren akademischen Grade erworben oder versucht zu erwerben.

---

Ort, Datum

---

Unterschrift

## Acknowledgements

The present study has been accomplished in the research group of Prof. Dr. Gabriele Pradel at the Research Center for Infectious Diseases (ZINF), University of Würzburg from May 2009 to November 2011 and at the Institute for Molecular Biotechnology, RWTH Aachen University from December 2011 to July 2013. Here I would like to acknowledge the following persons and institutions that contributed to the completion of my PhD thesis:

First and foremost I address my deepest gratitude to **Prof. Dr. Gabriele Pradel**, who gave me the opportunity to accomplish my PhD thesis in her working group and who initiated my fascination for such a complex yet intriguing organism as *Plasmodium falciparum* and the enthusiasm for scientific research. She gave me constant and excellent supervision, guidance and always the encouragement to define my targets and to do my utmost to achieve this doctoral thesis.

I am also very grateful to **Prof. Dr. Sven Krappmann** and **Prof. Dr. Jude Przyborski** who agreed to be the co-supervisors of my doctoral thesis for excellent supervision and taking time for helpful advices throughout the entire course of my thesis.

Further, I thank **Prof. Dr. Jörg Vogel** as well as **Prof. Dr. Rainer Fischer** for providing me the possibility to work in two very well equipped institutes.

I am indebted to **Prof. Dr. Franz Bracher** and his co-workers for fruitful discussions as well as providing me the library of CLK inhibitors. Without this help, the inhibitor part of this thesis would not have been feasible to conduct in the way it was. I also like to thank all collaborators that were involved in the studies encompassing this thesis for excellent collaboration, especially **Prof. Dr. Christian Doerig** for helpful advices and sharing so much valuable information on *Plasmodium* kinases, and **Prof. Dr. Andrew Tobin** for providing the antibodies against PfCLK-3 and all the information on it.

I would like to acknowledge the past and present **members of AG Pradel** for an amazing working environment throughout all these years. I thank Dr. Shruti Agarwal for introducing me into the field of PfCLKs and into numerous techniques like the kinase activity assays, for providing the transfection plasmids, transfected cultures and for handing over parts of her project to me, therefore forming the sound basis for my PhD thesis. I am indebted to Dr. Nina Simon for introduction into several techniques like Western blotting, IFA and protein purification methods and guidance and support regarding the animal work. Furthermore, I would like to thank Dr. Matthias Scheuermayer for constant help when it came to questions on kinase peculiarities, excellent support especially regarding confocal microscopy and for providing IFA preparations, pictures and valuable antibodies. I am grateful to Ludmilla Sologub for providing such a well-organized work in the lab and for perfectly introducing me into Malstat assays, gametocyte toxicity and exflagellation assays and to all required cell culture methods. I thank Veronika Klinger for all the help regarding the expression of SR proteins and inhibitor screening studies during her time as undergraduate student in the Pradel lab. I am very indebted to Christine Wirth for her studies on PfCLK-3 already during her

undergraduate student time in the lab and even more when she became a constant member of the Pradel lab. I thank her for all the significant work on the manuscript, for providing several excellent IFAs and Co-IPs for this thesis and for assisting perfectly with the confocal microscopy. She critically proofread the manuscript as well as this thesis and gave me valuable input and advices. Throughout the years, she became more than a lab colleague, but also a close friend who frequently motivated me to accomplish this doctoral thesis. Finally, I am thankful to all members of the AG Pradel I have not mentioned yet, especially Dr. Andrea Kühn, Dr. Nigel Aminake, Dr. Julius Ngwa, Tim Weißbach, Andreas v. Bohl, Vanesa Ngongang and Tom Brügl for an amazing amicable atmosphere inside and outside the laboratory and for having a lot of laughs and good times together throughout my lab times.

I would like to thank the **MALSIG 7<sup>th</sup> framework programme** of the EU for financially enabling these studies and for giving me the opportunity to participate in excellent scientific meetings in amazing surroundings like India or Rome, having distinguished discussions on the field of malaria research. Moreover, I am indebted to the **“Qualification program for Female Scientists”** of the University of Würzburg for the six-months financial grant. I thank the **Graduate School of Life Sciences** for administrative assistance and constant effort providing a variety of excellent courses mediating essential skills for a scientific career.

Finally, I thank my family for steady support (financial and moral), for putting their trust in me and bearing my nagging and my moods whenever something in the lab did not work out immediately as I anticipated. I like to thank all my close friends for their belief in me, especially Nadine who critically proofread the thesis and always found words of comfort and encouragement when I was in doubts.

To close with, I thank everybody who contributed directly or indirectly to the successful achievement of my doctoral thesis.

“Somewhere, something incredible is waiting to be known.”

CARL SAGAN

## Table of contents

<b>1</b>	<b>Introduction .....</b>	<b>1</b>
1.1	The tropical disease malaria .....	1
1.2	The malaria pathogen <i>Plasmodium falciparum</i> .....	3
1.3	Malaria control strategies .....	6
1.3.1	Vaccine development.....	6
1.3.2	Antimalarial chemotherapy .....	8
1.4	The kinome of <i>P. falciparum</i> .....	12
1.5	Evaluation of protein kinases as drug targets.....	15
1.6	The CLK kinases of <i>P. falciparum</i> .....	17
1.7	Splicing in <i>P. falciparum</i> .....	19
1.8	Objective of this study .....	22
<b>2</b>	<b>Materials and Methods .....</b>	<b>24</b>
2.1	Materials .....	24
2.1.1	Bioinformatical tools and computer programs.....	24
2.1.2	Laboratory Equipment .....	24
2.1.3	Chemicals and consumables .....	25
2.1.4	Inhibitors used in the study .....	26
2.1.5	Enzymes and commercial kits .....	32
2.1.6	Buffers, reagents and solutions .....	32
2.1.7	Media and solutions for <i>Plasmodium falciparum</i> cultivation.....	35
2.1.8	Media and agar plates for bacterial cultivation.....	36
2.1.9	Plasmodial and bacterial cell lines .....	36
2.1.10	Plasmids .....	37
2.1.11	Antibodies and antisera .....	39
2.1.12	Oligonucleotides .....	41
2.1.13	Gene IDs .....	43
2.1.14	DNA and protein ladders.....	43
2.2	Methods .....	44
2.2.1	Microbiological and cell biology methods .....	44
2.2.1.1	Cultivation and storage of bacterial cells.....	44
2.2.1.2	Transformation of competent bacterial cells.....	44
2.2.1.3	<i>In vitro</i> cultivation and maintenance of <i>Plasmodium falciparum</i> .....	45
2.2.1.4	Synchronization and purification of asexual blood stage parasites.....	47
2.2.1.5	Purification of gametocytes using Percoll® .....	48
2.2.1.6	Malstat assay .....	48
2.2.1.7	Limiting dilution.....	50
2.2.1.8	Exflagellation inhibition assay .....	50

2.2.1.9	Gametocyte toxicity assay.....	51
2.2.1.1	Stage-of-inhibition assay.....	51
2.2.1.2	Indirect immunofluorescence assay (IFA).....	52
2.2.2	Molecular biology methods.....	52
2.2.2.1	Genomic DNA isolation.....	52
2.2.2.2	Polymerase chain reaction.....	53
2.2.2.3	Agarose gel electrophoresis.....	54
2.2.2.4	Purification of DNA fragments.....	54
2.2.2.5	DNA digestion via restriction endonucleases.....	54
2.2.2.6	Ligation of DNA fragments.....	55
2.2.2.7	Amplification and extraction of plasmid DNA.....	55
2.2.2.8	Colony PCR and control digestion.....	56
2.2.2.9	Sequencing.....	57
2.2.2.10	Genotype characterization by diagnostic integration PCR.....	57
2.2.3	Protein biochemistry methods.....	57
2.2.3.1	Expression of recombinant proteins.....	57
2.2.3.2	Purification of recombinant proteins.....	58
2.2.3.3	Immunization of mice and generation of mouse polyclonal antibodies.....	60
2.2.3.4	Preparation of parasite lysates and nuclear extract.....	60
2.2.3.5	SDS polyacrylamide gel electrophoresis.....	61
2.2.3.6	Western blot analysis.....	62
2.2.3.7	Co-immunoprecipitation assay.....	63
2.2.3.8	Kinase activity assay.....	64
<b>3</b>	<b>Results.....</b>	<b>66</b>
3.1	Functional characterization of the PfCLKs.....	66
3.1.1	Protein expression analysis of PfCLK-3 and PfCLK-4 in <i>P. falciparum</i> stages.....	66
3.1.2	Reverse genetic studies on PfCLK-3 and PfCLK-4.....	72
3.1.3	Kinase activity assays on PfCLK-3 and PfCLK-4-specific precipitate.....	76
3.2	Identification of putative interaction partners of the PfCLKs.....	77
3.2.1	Expression of recombinant proteins in <i>E. coli</i> .....	78
3.2.2	Kinase activity assays with putative SR proteins.....	82
3.2.3	Localization studies on putative SR proteins.....	85
3.3	Evaluation of potential PfCLK inhibitors.....	90
3.3.1	Antiplasmodial activity of CLK inhibitors against blood stages of <i>P. falciparum</i> .....	90
3.3.2	Effect of CLK inhibitors on PfCLK-mediated phosphorylation.....	91
3.3.3	Effect of CLK inhibitors on specific blood stages.....	93
3.3.4	Effect of CLK inhibitors on gametocyte maturation.....	95
3.3.5	Effect of CLK inhibitors on microgametocyte exflagellation.....	95
<b>4</b>	<b>Discussion.....</b>	<b>98</b>
4.1	Functional characterization of PfCLK-3 and PfCLK-4.....	99
4.2	PfCLK-3 and PfCLK-4 are essential for the asexual replication cycle.....	102

4.3	Identification of putative CLK interaction partners .....	104
4.4	CLK inhibitors block parasite development and impair phosphorylation activity...	106
<b>5</b>	<b>Conclusions and future perspectives .....</b>	<b>109</b>
<b>6</b>	<b>Summary.....</b>	<b>111</b>
<b>7</b>	<b>Zusammenfassung.....</b>	<b>113</b>
<b>8</b>	<b>References .....</b>	<b>115</b>
<b>9</b>	<b>Appendix.....</b>	<b>130</b>
9.1	Antiplasmodial activity of the CLK inhibitor library. ....	130
9.2	Sequences of genes investigated in this study .....	132
9.3	List of abbreviations .....	140
9.4	List of tables .....	142
9.5	List of figures .....	143



# 1 Introduction

## 1.1 The tropical disease malaria

The unicellular eukaryotic parasites of the genus *Plasmodium* are responsible for malaria, affecting more than 200 million people and killing roughly 655 000 people annually (WHO, 2013), thus historically being one of mankind's most lethal diseases to date. The disease is most prevalent in Sub-Saharan Africa, Southeast Asia, India and South and Central America (Fig. 1.1).

Malaria parasites of the genus *Plasmodium* belong to the phylum Apicomplexa. This phylum is a wide-ranging category of protists exhibiting an apical complex that bestows the parasite to penetrate the host cell, as exemplified by the invasion of plasmodial parasites into host erythrocytes during blood stage infection. Malaria parasites are transmitted by the bite of infected female mosquitoes of more than 30 *Anopheles* species (WHO, 2013). Whereas *A. gambiae* is the major insect vector for malaria in Africa, mosquitoes belonging to the *A. stephensi*-complex show up to be highly adaptable and potent vectors in the Middle East and the Indo-Pakistan subcontinent (Kamali et al., 2011). Globally, a reckoned 3.3 billion people were at risk of malaria in 2011, with populations living in Sub-Saharan Africa having the highest risk of acquiring malaria: Approximately 80 % of cases and 90 % of deaths are estimated to occur in the African region, with pregnant women and children under five years of age most ruthlessly affected (WHO, 2013).

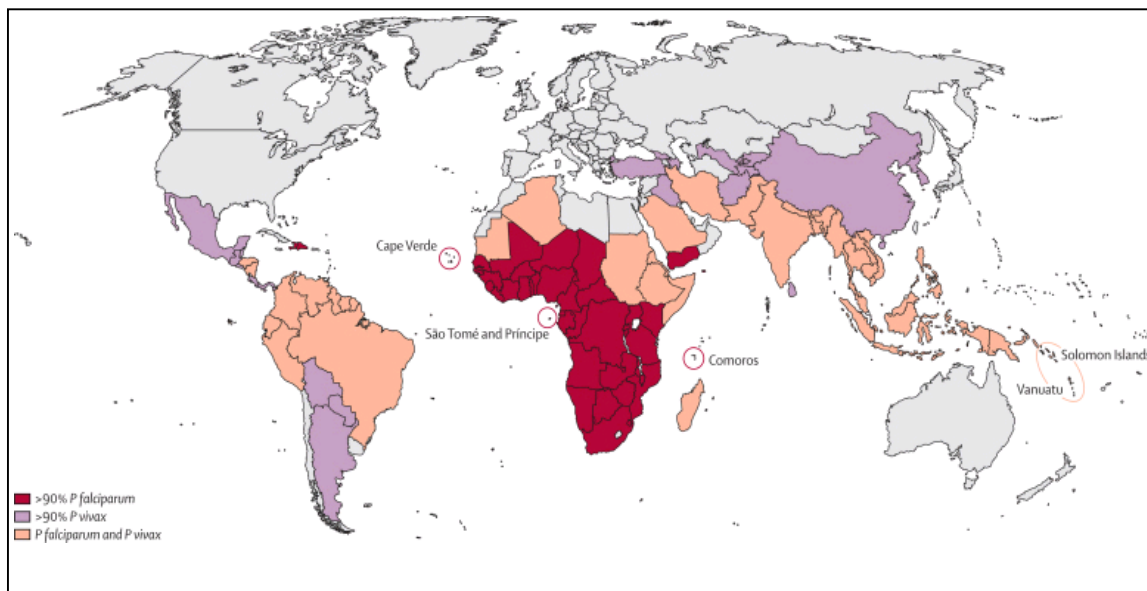


**Fig. 1.1: Worldwide distribution of vivax and falciparum malaria.** World map displaying the proportion of human malaria caused by *P. falciparum* and *P. vivax* by country (Feachem et al., 2010). *P. falciparum* malaria is predominant in Africa, whereas *P. vivax* is more prevalent in Southeast Asia as well as Central and South America. As *P. malariae*, *P. ovale* and *P. knowllesi* contribute to a much lower extent to malaria morbidity and mortality, these species are not taken into consideration in this figure.

Malaria is caused by five species of parasites of the genus *Plasmodium* that affect humans, which are:

*P. falciparum*,

*P. vivax*,

*P. ovale*,

*P. malariae*,

*P. knowlesi*.

Malaria tropica caused by *P. falciparum* is the most fatal form which predominates in Africa (WHO, 2013) and accounts for practically all deaths from this disease as well as high levels of morbidity, thus representing a serious barrier to social and economic progress of second and third world countries (reviewed in (Sachs and Malaney, 2002, Kokwaro, 2009)). On the contrary, *P. vivax* is less dangerous but more prevalent (Fig. 1.1), especially outside Africa; whereas *P. ovale* as well as *P. malariae* are found much less frequently and are rarely lethal (WHO, 2013). Interestingly, *P. knowlesi* as the fifth genus of human pathogenic plasmodial species habitually infects monkeys, occurring in certain forested areas of Southeast Asia (Cox-Singh et al., 2008; Lim et al., 2013). It was recently reported to infect humans (Singh et al, 2004; Jongwutiwes et al, 2011), rendering *P. knowlesi* as significant human pathogenic malaria parasite (Cox-Singh et al., 2008; Lim et al., 2013).

The public health system in malarious countries is affected by the burden of malaria as well as all aspects of educational systems and economic or social structures of many developing countries with endemic parasites, particularly in Africa (reviewed in (Sachs and Malaney, 2002; Breman et al., 2004; Sims and Hyde, 2006; Kokwaro, 2009)). To mention only a few educational problems that arise from the burden of malaria, there are school absenteeism of elder children and depletion in learning ability or cognitive development already in pre-school children (reviewed in Sachs and Malaney, 2002). Being most vulnerable due to loss of maternal immunity and having not yet developed specific immunity to malaria infection, children between six months and five years of age are mostly at risk of malaria. Herein, malaria manifests through various clinical symptoms: cerebral malaria, severe anemia, renal failure, hypoglycemia or pulmonary edema; occurring reclusively or in combinations (reviewed in Schumacher and Spinelli, 2012). Upon being exposed frequently to malarial infections, a person may develop a partially protective immunity, the so called "semi-immunity" (Bull et al., 1998). Principally, semi-immune persons still can be infected, but do not progress severe disease and often lack any typical malarial symptoms. Irrespective of this protective semi-immunity, pregnant women become highly susceptible to malaria due to diminished immunity (Roll Back Malaria Partnership, 2008), especially during first or second time pregnancies. Malaria infection of pregnant women impacts on fetal development and contributes to an increase in maternal deaths, miscarriages, several complications like maternal anemia or low birth weight, and the likelihood of stillborn children (reviewed in Rogerson et al., 2007).

## 1.2 The malaria pathogen *Plasmodium falciparum*

*Plasmodium falciparum* displays the most fatal plasmodial species (WHO, 2013), which deviates from the other *Plasmodium* species in several properties. One of the most devastating features of *P. falciparum* is its ability to confer cytoadhesive characteristics to its surrounding host erythrocyte, which contributes in large parts to the *P. falciparum* pathogenesis (reviewed in Doerig et al., 2010). The adhesion of infected red blood cells (RBCs) to uninfected RBCs (rosetting) and to endothelial cells (sequestration) are involved in both host pathogenesis and parasite survival. These phenomena are facilitated by different host and parasite derived proteins on the surface of infected RBCs (reviewed in Kirchgatter and Del Portillo, 2005). Major players in cytoadherence are the parasite-encoded surface antigen PfEMP1, a modified host erythrocyte membrane protein (band 3) as well as receptors on the endothelium (reviewed in (Sherman et al., 2003; Carvalho et al., 2013; Ho, 2014; Aird et al., 2014)). PfEMP-1 mediates cytoadherence of the infected RBCs to the endothelium of the vascular system with intercellular adhesion molecule 1 (ICAM-1) as one key receptor of the endothelium (reviewed in (Kirchgatter and Del Portillo, 2005; Miller et al., 2013)). ICAM-1 is an endothelial molecule that also acts as receptor for infected erythrocytes (Berendt et al. 1989), thus leading to the sequestration of mature trophozoites and schizonts from the peripheral circulation (reviewed in Kirchgatter and Del Portillo, 2005). ICAM-1 has been reported to play crucial roles in cerebral malaria (Berendt et al., 1989; Fernandez-Reyes et al. 1997). This phenomenon plays an important role in the pathogenicity of the disease, resulting in occlusion of small blood vessels and thus contributing to failure of many organs (reviewed in (Miller et al., 2002; Kirchgatter and Del Portillo, 2005)). Rosetting signifies the formation of rosettes due to adhesion of erythrocytes infected with mature parasite forms to uninfected RBCs. It is likely to increase microvascular obstruction of the blood circulation by clumping (reviewed in (Miller et al., 2002; Kirchgatter and Del Portillo, 2005)). Both sequestration and rosetting result in limited oxygen supply, thus causing organ damage in brain, heart, lung, liver, kidney or subcutaneous tissues leading to death or coma of infected patients (reviewed in Miller et al., 2002).

*P. falciparum* exhibits a complex life cycle, alternating between the human intermediate host, where asexual replication and multiplication takes place, and the anopheline insect host, where sexual propagation occurs (Fig. 1.3). Upon one human being bitten by an infected female mosquito, sporozoites are injected into the blood stream and migrate through the blood vessels to the liver. The parasites are subsequently invading hepatocytes followed by a first asexual replication cycle, giving rise to hepatic schizonts. Approximately seven days post infection, these liver schizonts rupture and release thousands of newly developed invasion stages, called merozoites, into the bloodstream. Each merozoite invades one RBC, residing inside the same and undergoing various morphologically distinct developmental changes (Fig. 1.2). During the subsequent ring stage, a parasitophorous vacuole (PV) is formed. Ring stages start to feed on host cell hemoglobin and other nutrients from the extracellular milieu (Kumar et al., 2014). The parasite thereby enters a highly metabolic maturation phase, termed trophozoite stage, which subsequently merges into the schizont stage (Bozdech et al., 2003). In this stage, the parasite prepares for reinvasion of fresh RBCs. Following mitotic division, the

developing erythrocytic schizont matures so that it encompasses about 16 to 32 new merozoites. Upon rupture of the schizont and subsequent release, these merozoites invade fresh erythrocytes resulting in higher parasitemia and the manifestation of the disease. Residence of *P. falciparum* in human erythrocytes is the major cause of malarial pathology and a key step for the parasites' development and propagation. This erythrocytic schizogony occurs in a cyclic manner every 48-72 h (reviewed in Hill, 2006).

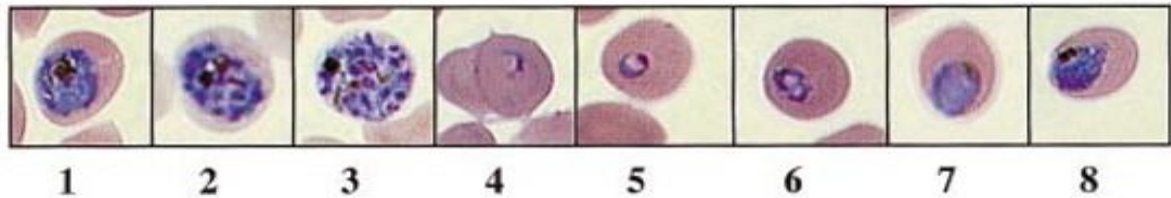


**Fig. 1.2: Representative asexual blood stage parasites in Giemsa-stained blood smears.** 1: Schizont, 24 h after synchronization. 2 & 3: Transition from schizont to segmenter. 4: Ring stage parasite. 5: Early trophozoite. 6 – 8: Trophozoite stages (modified from Bracchi-Ricard et al., 2000).

Given unknown factors, a subset of predetermined merozoites develops into sexual precursor stages, the male and female gametocytes (reviewed in Hill, 2006). Commitment to the sexual cycle already occurs in the trophozoites of the preceding asexual generation (reviewed in Talman et al., 2004), corroborated by the observation that all gametocytes arisen from one schizont are either male or female (Silvestrini et al., 2000). Density stress due to high parasitemia is one assumed factor triggering the induction of the formation of gametocytes (Bruce et al., 1990).

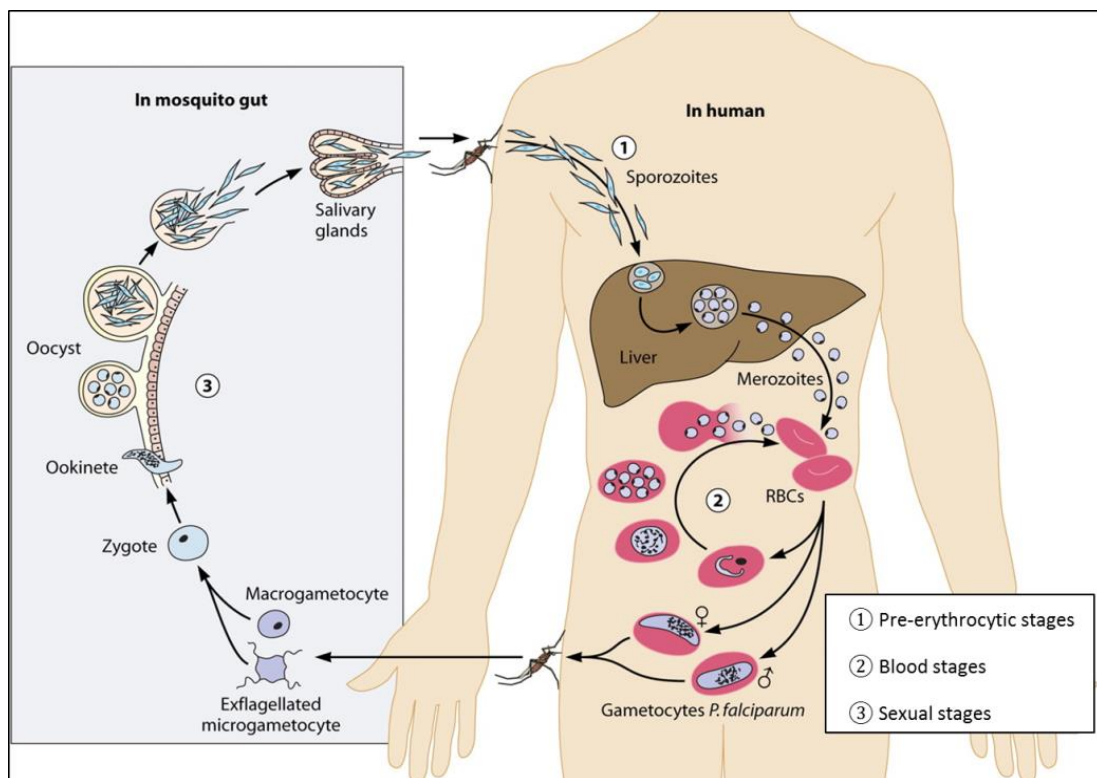


**Fig. 1.3: Schematic of the life cycle of *P. falciparum*** (modified from Bousema and Drakeley, 2011).

The process of arising gametocytes from asexual blood stage parasites in humans is called gametocytogenesis (reviewed in Talman et al., 2004) and takes approximately 10 days. Over this period of time, maturing gametocytes represent five morphologically recognizable stages, which can be distinguished by means of Giemsa-stained blood smears (Fig. 1.4).

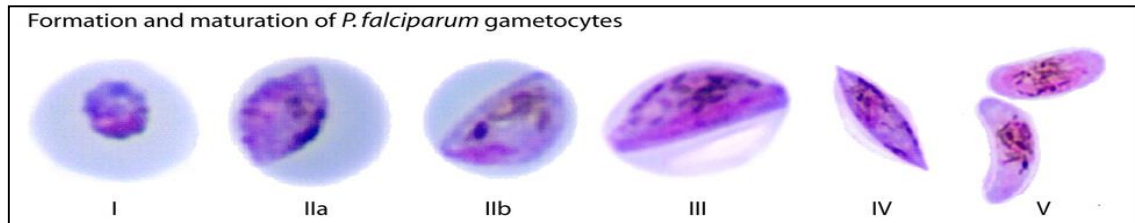


**Fig. 1.4: Gametocytes of *P. falciparum* in Giemsa-stained blood smears.** The five developmental stages of *P. falciparum* gametocytes (stage I–V). Whereas Giemsa-stained stage I gametocytes resemble young asexual trophozoites, stages II–V are easily distinguishable in a blood smear (modified from Bousema and Drakeley, 2011).

Whereas mature gametocytes (stage V, Fig. 1.4) are released into circulation and are accessible to mosquitoes taking a blood meal, immature stages from I to IV are sequestered away from the blood circulation, presumptively to avoid splenic immune clearance (reviewed in Bousema and Drakeley, 2011; Fig. 1.4). Upon ingestion of mature gametocytes by a female mosquito during a blood meal, the emergence of gametocytes from surrounding erythrocytes follows. Triggered by diverse factors within the mosquito midgut, including a decrease in temperature of 5°C below that of the vertebrate host, an increase of carbon dioxide and the presence of the mosquito-specific molecule xanthurenic acid (Billker et al., 1998; Arai et al., 2001), the gametocytes get activated and the egress of gametes from the red blood cells occurs. Noteworthy, this emergence is mediated by proteases in an inside-out manner (Sologub et al., 2011). The female macrogametocyte subsequently transforms into a spherical extracellular and non-motile macrogamete, whereas the male microgametocyte releases eight motile flagellated microgametes after replicating its genome three times (reviewed in Kuehn and Pradel, 2010), which is called gametogenesis. Upon activation, exflagellation occurs in the mosquito midgut, which is the process in which the cells form rosettes due to adherence of the newly emerged microgametes to adjacent erythrocytes. This rosetting cells are called exflagellation centers and counting of them is a routine measurement of gametocyte activation potential. During exflagellation, the female macrogametes are fertilized by the motile male microgametes, thus resulting in a zygote by rapid meiotic division, with the zygote being the only diploid stage in the parasite's life cycle (Lobo and Kumar, 1999). Within 24 hours, the zygote transforms into a motile tetraploid ookinete (reviewed in Pradel, 2007), being capable of traversing the mosquito midgut epithelium and forming an oocyst. Replication takes place subsequently and the oocyst gives rise to a large amount of newly emerged invasion stages, the sporozoites. For perpetuating the parasite life cycle, the sporozoites migrate to the mosquito's salivary glands, where they await discharge into a new host during the mosquito's blood meal, and subsequently invade blood capillaries of the human intermediate host (Lobo and Kumar, 1999).

### 1.3 Malaria control strategies

Given high incidences of resistances against the widely used antimalarial chloroquine as well as the sulfadoxine-pyrimethamine combination therapy, malaria still is pervasive, along with the fact that alternative medications are practically too expensive for the population of malarious countries (reviewed in Wiesner et al., 2003). Control strategies are further subverted by co-infections with HIV, severe poverty and the lack of health services and well-established infrastructures (reviewed in Breman et al., 2004; WHO, 2013). To aggravate the situation, the efficacy of transmission control by means of widely used insecticide-treated bed nets and indoor residual spraying is dropping because of resistances (reviewed in Ranson et al., 2011; Ndiath et al., 2014). Even if there have been major gains during the last 13 years in malaria control in many endemic countries including many in Africa (reviewed in O'Meara et al., 2010), subsisting malaria control strategies still are vastly vulnerable to emerging resistances. Therefore there is an urgent demand of research and development of new effective and affordable malaria control strategies (reviewed in Doerig and Meijer, 2007). Furthermore, there are particular African countries with a static or even deteriorated situation regarding malaria transmission control, especially in the highland areas of East Africa (reviewed in O'Meara et al., 2010), rendering the continuation and improvement of malaria control strategies.

#### 1.3.1 Vaccine development

In spite of, or exactly because of the complex life cycle of *P. falciparum* providing a plurality of antigenic targets for vaccine development, there is currently no effective vaccine available against malaria (reviewed in Good et al., 2001; Santos et al., 2013). Opposed to vaccines that are developed for various diseases relying on the basic principle of a whole cell antigen complex of the respective organism in killed or attenuated form, this is not feasible for malaria vaccines to this date. The reason is that malaria parasites require human erythrocytes for growth or culturing and a whole-cell vaccine is consequently considered to be potentially unsafe and impracticable for a disease for which 40 % of the world's population is theoretically at risk (reviewed in Good et al., 2001). Therefore, malaria vaccine development is attempted to generate a subunit vaccine. Out of the five known human pathogenic *Plasmodium* species, there are only two species represented in vaccine development, with over 40 vaccine projects for *P. falciparum* and only one for *P. vivax* to reach clinical trial stage (reviewed in Schwartz et al., 2012).

Vaccine development against malaria can be subdivided into their ability of targeting different life cycle stages, for example vaccines targeting pre-erythrocytic stages like sporozoites and liver stage parasites. They can be mentioned as the first category, in contrast to vaccines of the second category that target blood stage parasites which are responsible for clinical symptoms and thus the pathology of malaria. The vast majority of vaccination strategies aim to target this intraerythrocytic developmental cycle (Bozdech et al., 2003; reviewed in Hill, 2006). As a third class, there are vaccines that aim at blocking sexual stages and are therefore called transmission blocking vaccines (TBV).

Being classified as a pre-erythrocytic vaccine, RTS,S/AS01E is by far the most advanced candidate, hence being at least 5 to 10 years ahead of all other malaria vaccine projects (reviewed in Schwartz et al., 2012). RTS,S is a protein particle vaccine (comprised of polypeptides RTS and S) targeting the *P. falciparum* circumsporozoite protein (CSP), fused to a hepatitis B surface antigen including a new potent adjuvant (WHO, 2013). The vaccine manufacturer is focusing on African children resident in malaria-endemic countries. RTS,S was capable to induce clinical efficacy in the 25-60 % range, depending on the respective clinical settings. It is assumed that the WHO recommends RTS,S for use in 2015, depending on the outcome of the current trials (reviewed in Schwartz et al., 2012). Recent reports give account on the accomplished clinical trial phase II. The immunogenicity of RTS,S vaccines containing Adjuvant System AS01 or AS02 was evaluated as compared with non-adjuvanted RTS,S in healthy, malaria-naïve adults in a randomized, double-blind study. The result revealed acceptable safety profiles of the adjuvanted vaccines, with the anti-CSP antibody response being significantly higher as RTS,S/AS01 combination than RTS,S/AS02. Therefore, RTS,S/AS01 is being selected for clinical phase III in Africa (Leroux-Roels et al., 2014).

Blood stage vaccines principally aim at targeting antigens that are expressed on the surface of merozoites. There are at least two plasmodial antigens worth mentioning (reviewed in Hill, 2006). These two are, at least subunits of it, currently under clinical trials: merozoite surface protein 1 (MSP-1) and apical membrane antigen 1 (AMA-1). Firstly, there is much knowledge about the immune effector mechanisms of MSP-1. It is expressed from the onset of schizogony and involved in erythrocyte invasion by merozoites (reviewed in Schwartz et al., 2012). Antibodies against MSP-1 revealed to be implicated in a diminished risk of clinical malaria (reviewed in Fowkes et al., 2010). Secondly, AMA-1 antibodies were observed in patients with acquired natural immunity, with repeated natural exposure leading to high AMA-1 antibody titers (Udhayakumar et al., 2001; Courtin et al., 2009). MSP-1 as well as AMA-1 are highly polymorphic and display complex folding patterns (reviewed in Good, 2001).

Although receiving revived attention, sexual stage vaccines display the third and still most underrepresented vaccine category. They are intended to block the life cycle in mosquitoes by utilizing antisera that are raised against sexual stage-specific antigens (Vogel, 2010). Vaccines protecting from liver stage or blood stage parasites and thus from the symptoms of malaria are still not capable of clearing all the parasites from the patient. Consequently, a vaccinated person could be symptom-free, but still be infected and, moreover, still infect others (Vogel, 2010). This is the starting approach for transmission blocking vaccines (TBVs). Currently there are only a few sexual stage vaccines in pre-clinical development, at least one phase 1 trial is underway: A vaccine candidate that is based on Pfs25, supplemented with a meliorated adjuvant formula, as previous studies revealed low antibody titers and only marginal transmission blocking activity (Qian et al., 2007; Qian et al., 2008). An addition of aluminum hydroxide gel and an oligodeoxynucleotide that acts as Toll-like receptor 9 (TLR9) agonist elicited a significant increase in functional antibody levels in mice, compared to the same formulation without the supplementation (Qian et al., 2007; Qian et al., 2008). Both transmission blocking efficacy and antibody titers were auspicious in subsequent studies, however both vaccines revealed unanticipated reactogenicity for further development (Wu et

al., 2008). Due to the observed systemic adverse events including erythema nodosum associated with the vaccine formulation, current efforts are focused on the development of a well tolerated formulation capable of inducing strong immune responses (Wu et al., 2008).

### 1.3.2 Antimalarial chemotherapy

Likewise to the development of antimalarial vaccines, the complex parasite life cycle offers several points of attack for chemotherapeutical intervention. Similarly, antimalarials can be distinguished into 3 classes that represent the different life cycle compartments of *P. falciparum*: Drugs that zero in on the asymptomatic liver stages are primarily utilized for prophylactic chemotherapy by preventing blood stage infection, i.e. for travellers (reviewed in Doerig et al., 2010). As a second and best-represented category, drugs that target erythrocytic stages are deployed for the treatment of the disease. The vital importance of these drugs is inappropriately accompanied by their high susceptibility to the emergence of drug resistances (reviewed in Doerig et al., 2010). Out of the presently amenable armamentarium, a vast majority of current drug resistances occur among schizonticidal drugs (reviewed in Doerig et al., 2010). Lastly, a third implement of antimalarial control is to obstruct the parasite sexual stages. An interference of drugs with sexual stage parasites is feasible either at the level of gametocytogenesis or within the mosquito host during sporogony (reviewed in (Pradel, 2007; Doerig et al., 2010)), thus blocking the transmission of malaria parasites from the human host to the insect vector and therefore obviating or reducing parasite propagation.

The onset of antimalarial chemotherapy took place in the early 18<sup>th</sup> century when the bark of South American cinchona trees was used for malaria treatment (reviewed in Wongsrichanalai et al., 2002). The latter isolated bark compound quinine is a quinoline alkaloid and has been the mainstay for treating severe malaria in children, but even it reveals high efficacy, there are concerns that the value of quinine is retrograding in parts of Southeast Asia (Pukrittayakamee et al., 1994; reviewed in Praygod et al., 2008) and South America (Zalis et al., 1998). Additionally, isolated cases of quinine resistant *P. falciparum* malaria have been reported from East Africa, confirming an association of a special mutation in the *pfmdr-1* gene with reduced susceptibility (Jelinek et al., 1995). Quinine is presently set aside as a second- or third-line drug, only being used in case of severe malaria (reviewed in Wongsrichanalai et al., 2002).

Being firstly manufactured in Germany, the quinine-derived quinoline chloroquine (CQ) gained attention as overwhelmingly effective synthetic antimalarial not before the 1940s during World War II (reviewed in Wongsrichanalai et al., 2002). Becoming the cornerstone of antimalarial chemotherapy, it was widely used and turned out to be the affordable drug of choice until its efficacy began to decline when parasite strains acquired resistance to CQ firstly in the 1960s (reviewed in Schlitzer, 2007). Resistances are nowadays widespread with the WHO no longer considering CQ as adequate antimalarial chemotherapeutic. Regarding several related quinolines, for example mefloquine and piperazine, there are reported resistances (reviewed in Schlitzer, 2007). Presently used quinine-derived antimalarials are halofantrine or amodiaquine in combination with artesunate (reviewed in Hyde, 2005).



As gametocytes exhibit susceptibility towards primaquine (PQ) and other 8-aminoquinolines, they might be utilized as transmission blocking drugs, thus reducing the transmission and therefore the incidence of malaria. PQ is the only currently available drug that actively clears mature *P. falciparum* gametocytes and prevents malaria transmission to mosquitoes (White, 2013; Eziefula et al., 2013). However, PQ is also known to have potentially grave side effects in people with an enzyme deficiency common in several malaria endemic regions (glucose-6-phosphate dehydrogenase deficiency; G6PD; Eziefula et al., 2014). In these patients, high doses of PQ administered over several days occasionally destroys erythrocytes, causing anaemia and possibly life-threatening effects (Alving et al., 1956; reviewed in Beutler, 1959; Eziefula et al., 2013; Eziefula et al., 2014). Consequently, in 2013 the WHO revised the previously recommended single dose to 0.25 mg/kg from initially 0.75 mg/kg due to concerns about safety (reviewed in Graves et al., 2014).

Sulfadoxine (SDX) and pyrimethamine (PYR), a combination of antimalarial antifolates, have been used widely in many parts of Africa in order to replace CQ treatment since the emergence of CQ resistance (Eriksen et al., 2008). Contrary to its great advantage that the SDX/PYR treatment can be administered by one single dose, reported resistances raise serious doubts if this affordable and practical combination therapy will have a prolonged life span in the treatment of malaria (Warsame et al., 2002; Barnes et al., 2006). Mutations in the antifolate resistance genes coding for dihydrofolate reductase (*dhfr*) and dihydropteroate synthase (*dhps*) confer resistance to SDX and PYR by reducing the parasite's chemosensitivity towards these compounds (Inoue et al., 2014). Pharmacogenetic studies revealed that the current SDX/PYR dosing is inadequate especially in young infants and that the children's age has critical impact on the pharmacokinetic features of the compounds (Barnes et al., 2006). These findings emphasize the need for appropriately designed prospective pharmacokinetic studies especially for young children to ensure optimal dosing of all antimalarial drugs.

Another drug type which is of particular importance as recently licensed antimalarial drug is atovaquone. Being solely used in combination with the antifolate drug proguanil and listed as commercially available Malarone<sup>®</sup>, it was successfully used for a period of time, especially for travellers (reviewed in (Marra et al., 2003; Hyde, 2007)). It is still used effectively as prophylactic drug, nevertheless some cases of resistance to Malarone<sup>®</sup> treatment have been reported in West Africa as well as in Thailand (Kuhn et al., 2005; Krudsood et al, 2007).

Implying an urgent need of alternatives, artemisinin and its derivatives (artemether, arteether and artesunate) are taken into account as potent and rapidly acting schizontocide against all *Plasmodium* species, having an exceptional broad activity against asexual parasites and young gametocytes (Kumar and Zheng, 1990; Sutanto et al., 2013). It was originally used and is still deployed successfully in combination with mefloquine in areas of persistent multidrug-resistance, for example in Southeast Asia (reviewed in Hyde, 2007). Artemisinin derivatives are now being assessed as artemisinin combination therapies (ACT) in several other combinations with antimalarials like lumefantrine, amodiaquine or SDX/PYR (Roll Back Malaria Partnership, 2008). The slower-acting non-artemisinin partners of these formulations are aimed to exterminate small portions of parasites that were able to escape the rapidly metabolized artemisinin, which has a short plasma-half life of only four hours (reviewed in Hyde, 2007). However, the effectiveness of ACTs is doubtful, with an already compromised

partner drug to artemisinin (Duffy et al., 2006). It is of tremendous significance for millions of malaria-affected people to generate an effective antimalarial drug, with ACT proposing the utmost anticipation (Roll Back Malaria Partnership, 2008). Nevertheless, proceeded research as well as continued surveillance is necessary to monitor which drug combination is the most sustainable in different populations, as emerging resistances to ACT would be a massive failure and regression regarding antimalarial combat strategies by the use of drugs (Duffy et al., 2006; Ferreira et al., 2013). There is strong disagreement over the implication of putative newly emerged artemisinin susceptibility observations (Dondorp and Ringwald, 2013; reviewed in Krishna and Kremsner, 2013). Particularly, the term of “artemisinin resistance” is currently under discussion, since recent research observed artemisinin resistance prevalent across mainland Southeast Asia which is associated with distinct mutations in *kelch13* gene locus (Dondorp et al., 2009; Ashley et al., 2014). The authors of this specific study attribute a high significance to these observations (Dondorp and Ringwald, 2013). Moreover, recent observations report a case of malaria in a patient returning to Vietnam after several years in Angola that did not respond to intravenous artesunate and clindamycin or an oral artemisinin-based combination (Van Hong et al., 2014). On the contrary, other findings report merely a slow clearance rate of parasites by ACT as a result of a drop in susceptibility among young ring stages, whereas the susceptibility is sustained in mature stages (Ferreira et al., 2013; Witkowski et al., 2013). Nevertheless, according to these authors the clinical relevance of these findings still remains elusive since these infections could still be successfully treated with ACTs (reviewed in Krishna and Kremsner, 2013; Lun et al., 2014).

With constantly emerging resistances against a variety of applied antimalarials, antibiotic substances as a special class of antimalarial drugs are currently taken more and more into account. The first antibiotics that have been reported to counteract malaria parasites were chloramphenicol, chlortetracycline and oxytetracycline (reviewed in Pradel and Schlitzer, 2010). Antibiotics exhibit a slowly acting antimalarial activity; therefore it is often used in combination therapy with faster acting drugs. Nowadays, clindamycin and doxycycline are used in combination with artemisinin derivatives or quinine, and this combination is moreover recommended as malarial second line treatment and chemoprophylaxis in most Western countries (Briolant et al., 2010; WHO 2013). Antimalarial activity of antibiotics is traced back to the fact that the mitochondrion as well as the apicoplast of *Plasmodium sp.* are of prokaryotic origin, being semiautonomous structures within the parasite and possessing sovereign genomes (reviewed in (Wiesner et al., 2003; Pradel and Schlitzer, 2010)). Due to the fact that bacterial co-infections are often fundamental complications of malaria, antibiotics are supplementarily administered. As antibiotics mostly impede bacterial translation processes, they are slowly acting; furthermore for some antibiotics, a delayed death effect was observed and postulated in *P. falciparum* (Barthel et al., 2008; reviewed in Pradel and Schlitzer, 2010).

Being solely administered as ectopic antiseptic, chlorhexidine (CHX) exhibited an antimalarial effect among other antibiotic compounds. CHX is commonly applied externally as antibiotic in dentistry and is used in general skin cleansing, skin decolonization, preoperative showering and bathing, vascular catheter site preparation, impregnated catheters and oral

decontamination (reviewed in Milestone et al., 2008). CHX exhibits the highest antibiotic activity against gram-positive cocci, whereas acid-fast bacteria, enveloped viruses and spores are CHX resistant. The mode of action of this strongly basic compound on *E. coli* and *S. aureus* is given by its capability to adsorb to the bacterial surface and integrate into the bacterial membrane, thereby damaging the permeability barriers. After entering the bacterial cell, CHX reacts with free solutions of the cytoplasm, hence leading to precipitation of the cytoplasm (Davies, 1975). The first experimental evidence of antimalarial activity of CHX was provided by *in vivo* examinations (Curd and Rose, 1946). Based on these observations, the antiplasmodial activity of CHX was further assessed by culture testings utilizing the Trager-Jensen system (Geary and Jensen, 1983). There, it revealed an  $IC_{50}$  of approximately 0.316  $\mu$ M, determined by concentration-effect curves. Moreover, CHX demonstrated to effect on human cyclin-dependent kinase-like kinases (CLKs), therefore affecting alternative splicing (Younis et al., 2010; Wong et al., 2011).

To counteract uprising resistances against antimalarial drugs, there are general prerequisites that have to be fulfilled. As first and most important premise, a combination therapy of two different compounds is required with the components targeting different metabolic reactions, hereby decreasing the risk of developing rapid mutations that confer resistance to the malaria parasites (reviewed in Farooq and Mahajan, 2004; Smith et al., 2010). To prevent the further propagation of surviving parasites in the patient, the ideal medication should also have transmission-blocking capabilities (reviewed in (White 2004; Doerig 2005)). As schizonticidal drugs can select randomly occurring mutations that could confer resistance to the parasite population, these resistant parasites then develop into gametocytes, transmitting drug-resistant phenotypes to the insect vector (reviewed in Doerig et al., 2007). Consequently, drug-resistant parasites are spread into the human population. Transmission blocking drugs (TBD) would be the method of choice in this scenario, being co-administered with schizonticidal compounds. An example is artemisinin, which also kills young gametocytes, in addition to its schizonticidal properties (Kumar and Zheng, 1990; reviewed in Doerig et al., 2010; Sutanto et al., 2013). As gametocytes do not divide, resistant genotypes would not be selectively amplified by the application of TBDs (reviewed in (Doerig et al., 2007, Doerig et al., 2010)). Moreover, one of the combination partners of the drug of choice must possess a fast clearance rate in such a way that the surviving parasites are not exposed to sub-therapeutic drug levels, thereby supporting the emergence of resistance-conferring mutations. In contrast, the other member of the combination drug should exhibit a long termination half life (White, 1998; Dormoi et al., 2014).

Taken all of the above mentioned premises into account, this approach could represent a strategy to prevent emerging resistances against antimalarial compounds, thus taking one step towards worldwide eradication of malaria (Feachem et al., 2008; reviewed in Greenwood et al., 2008).

## 1.4 The kinome of *P. falciparum*

Reversible protein phosphorylation catalyzed by protein kinases is ubiquitous in all aspects of cellular processes, such as proliferation, differentiation, metabolism and gene expression (Hanks, 2003). The addition of phosphate groups leads to remarkable changes in terms of enzymatic activity, stability, binding properties or subcellular localization of the protein substrates (reviewed in Kappes et al., 1999), rendering protein kinases (PK) as key regulators of cellular life. Since their early discovery by the 1992 Medicine Nobel Prize laureates Edwin G. Krebs and Edmond H. Fischer, human protein kinases have been the subject-matter of elaborate research (reviewed in Doerig et al., 2007). Moreover, the substantial importance of eukaryotic protein kinases (ePK) is displayed by the number of these specific enzymes present in eukaryotes: In the human genome for example, approximately 1.7 % of all genes encode protein kinases (reviewed in Manning et al., 2002), whereas in budding yeast, protein kinase genes consist of even 2 % of the total genome (Johnson et al., 1998). Dysfunction of protein phosphorylation has been identified as major cause or consequence of human diseases such as cancer, inflammation, neurodegenerative disorders, diabetes or viral infections (reviewed in Cohen et al., 2002).

ePKs are modularly organized with regard to specific substrate recognition, localization to substrate sites and a determined mode of regulation. The identification of ePKs is conducted by database mining, which is based on the presence of a distinct conserved kinase domain. This specific kinase domain is further sectioned into twelve conserved subdomains that fold into a common catalytic core structure (reviewed in Hanks and Hunter, 1995; Fig. 1.5). All of them carry a conserved amino acid motif that is required for the kinase activity (Hanks, 2003; depicted in Fig. 1.5). Of certain importance for the kinase's catalytic function is on the one hand the invariant lysine (K73) in subdomain II and on the other hand the conserved aspartate (D) present in subdomain VII. These motifs conduct binding and positioning of ATP in the catalytic cleft of the enzyme (Hanks and Quinn, 1995; Hanks, 2003). The glycine triad of subdomain I forms a hairpin which encloses a part of the ATP molecule (reviewed in Ward et al., 2004). Conversely, the invariant aspartate present in subdomain VIB is assumed to mediate the phosphotransfer reaction, whereas peptide-substrate recognition is implemented by subdomain VIB as well as VIII and the highly conserved APE motif (Johnson et al., 1998). The APE motif is furthermore responsible for structural stability of the large lobe (Hanks and Quinn, 1995; reviewed in (Hanks and Hunter, 1995; Ward et al., 2004)).

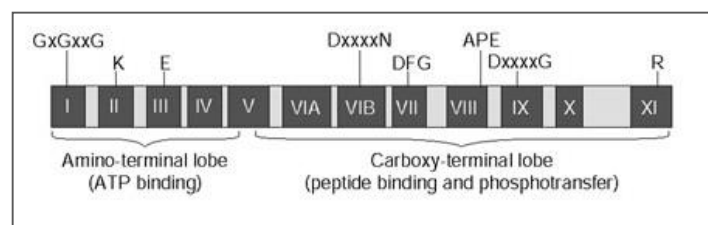


**Fig. 1.5: Schematic of the typical ePK catalytic subdomain structure.** Roman numerals indicate the 12 conserved subdomains. The positions of amino acid (aa) residues and motifs highly conserved throughout the ePK superfamily are indicated above the domains (single letter aa code with x as any aa). Hanks, 2003.

Generally, subdomains I to V comprise the amino- (N-)terminal lobe required for ATP binding, whereas the stretch of domain V to XI is referred to as carboxy- (C-)terminal lobe and mediates peptide binding and phosphotransfer (reviewed in Hanks and Hunter, 1995; Hanks, 2003).

Eukaryotic protein kinases can be classified into two superfamilies, based on their sequence similarity and their enzymatic specificity (reviewed in Kappes et al., 1999). The first superfamily, the Ser, Thr and Tyr kinases, catalyze the transfer of phosphate residues from ATP to serine, threonine or tyrosine, respectively, whereas the second superfamily of His kinases autophosphorylates conserved histidine residues (reviewed in (Hanks and Hunter, 1995; Kappes et al., 1999)). The superfamily of Ser, Thr and Tyr kinases can be further partitioned into five major groups by means of phylogenetic tree construction (reviewed in Kappes et al., 1999). Noteworthy, the plasmodial kinome displays a comparatively small kinome, encompassing less than 100 kinases (reviewed in Lucet et al., 2012). Given the outstanding importance of ePKs, several protein kinases of *P. falciparum* have been identified in recent years and were classified according to the above mentioned scheme, based on the general characteristics of the respective eukaryotic kinase group (reviewed in Kappes et al., 1999), leading to the classification of the plasmodial kinome as follows:

#### 1) CMGC group

This vast group comprises 18 plasmodial members from four different families: i) the family of cyclin-dependent protein kinases (CDKs), ii) mitogen-activated protein kinases (MAPK), iii) the glycogen-synthase kinase 3 (GSK-3) family, iv) the CDK-like kinase (CLK) family and other close relatives (reviewed in Manning et al., 2002). CDKs have been identified in all eukaryotes investigated so far and are principally implied in cell cycle regulation (reviewed in (Kappes et al., 1999; Doerig et al., 2002)). In *P. falciparum*, five related CDKs have been described so far (reviewed in Doerig et al., 2002) and two previously characterized MAPKs, Pfmap-1 and Pfmap-2, cluster together with a member of the MAPK family (Doerig et al., 1996; Dorin et al., 1999). Interestingly, PfPK6 and Pfcrc-4 display features of both CDKs and MAPKs (Bracchi-Ricard et al., 2000; reviewed in Ward et al., 2004). Two subfamilies are grouped to the GSK-3 family: the GSK-3 family itself and the casein kinase 2 (CK2)-type enzyme family (reviewed in Kappes et al., 1999). *P. falciparum* encodes three GSKs, sharing a sequence similarity of greater than 45 % with other eukaryotic GSKs (Anamika et al., 2005). Conversely, only one CK2 homologue is encoded in the parasite genome: PfCK2, which possesses two beta subunit species and is most likely involved in the chromatin assembly pathway (Holland et al., 2009; Dastidar et al., 2012). Four CLK kinases are identified in *P. falciparum*, which are involved in RNA metabolism, processing and transport (Li et al., 2001; Dixit et al., 2010; Agarwal et al., 2011) and are investigated in detail in this study (section 1.7).

#### 2) AGC group

This group (cyclic-nucleotide & calcium/phospholipid-dependent kinase group) is represented in *P. falciparum* by five kinases out of which cGMP-dependent PfPKG, cAMP-dependent PfPKA and calcium/calmodulin-dependent PfPKB have been described so far (Li et al., 2000; Deng et al., 2002; Diaz et al., 2006; Vaid et al., 2006) There appears to be no homologue of the protein

kinase C (PKC) subfamily in *P. falciparum*, but it is assumed that the calcium-dependent protein kinase (CDPK) homologue PfCDPK7 may perform functions analogous to mammalian PKCs that are activated by calcium and phospholipids (reviewed in Kappes et al., 1999). PfCDPK7 is an atypical parasite CDPK, possessing two calcium-binding EF-hands and being of particular importance for the survival of erythrocytic asexual stages (Kumar et al., 2014).

### 3) CK1 group

Merely one plasmodial kinase has been identified and characterized hitherto from the casein kinase 1 group, PfCK1 (Barik et al., 1997) whereas this group is vastly expanded in other kinomes. *C. elegans*, for example, retains 85 genes which are assigned to the CK1 group (reviewed in Ward et al., 2004). Characterization of PfCK1 led to the hypothesis that it interacts with Rab GTPases of the parasite, suggesting to play a role in early and late endosome function in malaria parasites (Rached et al., 2012).

### 4) CamK group

The calmodulin-dependent kinase (CamK) group comprises 13 PfkPKs, underlining the importance of calcium signalling in the parasite (reviewed in (Garcia, 1999; Ward et al., 2004)). A tight cluster is formed by PfCDPK1-7 that share the canonical CDPK structure which is exclusively found in plants and alveolates, but not in metazoans and therefore mammals (reviewed in Ward et al., 2004). In these organisms, they are predominantly involved in stress and hormone responses, germination and most likely membrane biogenesis (Hegeman et al., 2006). In the malaria parasite, CDPKs might substitute for the function of the CamKs or PKC isoenzymes, as this is also suggestive to be the case in plants (reviewed in Kappes et al., 1999).

### 5) TKL group

The fifth malarial kinome group, the tyrosine kinase-like (TKL) family, encompasses five plasmodial enzymes (reviewed in Ward et al., 2004). PfTKL3 was characterized previously as essential kinase for asexual proliferation and co-localizes with cytoskeleton microtubules in gametocytes (Abdi et al., 2010). Moreover, it was anticipated as amenable drug target. Recently identified PfTKL2 is described to be exported to the host erythrocyte and successively secreted into the medium of asexual parasite cultures. It is suggested that PfTKL2 might have immunomodulatory functions, promoting the parasites' survival in the human host (Abdi et al., 2013).

Up to date, no plasmodial protein kinase was identified that clusters within the tyrosin kinase (TyrK) group, albeit it was recently investigated by global phosphorylation analyses that PfGSK3 as well as PfCLK-3 are autophosphorylated at tyrosine residues within their activation loop and that the tyrosine phosphorylation is responsible for full kinase activity (Solyakov et al., 2011). TyrK family members are as well absent in yeast and in most, but not all unicellular eukaryotes (Shiu et al., 2004). STE kinases are kinases identified in sterile yeast mutants. Members of this group are absent in malaria parasites similar to TyrK group members. This

finding is consistent with the failure of *in vitro* and *in silico* attempts to identify MAPKK malarial homologues (Dorin et al., 2001; Dorin et al., 2005). This indicates a divergent organization of the MAPK pathways in malaria parasites (reviewed in Ward et al., 2004; further specified in section 1.5).

Moreover, there are plasmodial kinases that have no orthologues in the human host as they do not cluster within any of the above mentioned groups. Hence they are denoted as “orphan kinases” or “other protein kinases” (reviewed in (Kappes et al., 1999; Doerig et al., 2008)). For example, the *P. falciparum* kinome encompasses a family of four protein kinases that cluster within the NIMA (never-in-mitosis) family: Pfnek-1 to Pfnek-4. Previously characterized Pfnek-1 is non-redundant in asexual parasites and displays a potential target for antimalarial intervention (Dorin et al., 2001; Dorin-Semblat et al., 2011). Pfnek-2, -3 and -4 are predominantly expressed in gametocytes, and a role for Pfnek-2 and Pfnek-4 in meiosis has been described (Reininger et al., 2009; Dorin-Semblat et al., 2011). NIMA-related kinases in other organisms display a conserved family of kinases with critical roles in the regulation of mitosis as well as meiosis and an association with centrosomes, spindle poles and other components of the cell division apparatus are reported (Dorin-Semblat et al., 2011).

Furthermore, the *P. falciparum* proteome comprises a family of putative kinases called FIKKs, some of which are exported to the host RBC and might play a role in erythrocyte remodeling and alteration of the host cell surface, thus ensuring the parasite survival in the host circulation (Nunes et al., 2007; Nunes et al., 2010; reviewed in Lim et al., 2012). This ePK group is exclusively found in Apicomplexa and termed after the conserved Phe-Ile-Lys-Lys motif in subdomain II of the catalytic domain present in all members of the family (reviewed in Ward et al., 2004; Schneider and Mercereau-Puijalon, 2005). Notably, the FIKK group encompasses the largest kinase family in *P. falciparum* with 21 members (Solyakov et al., 2011). Remarkably, most FIKK genes are arranged in the subtelomeric region of chromosomes encoding for genes that are involved in antigenic variation such as the *var* genes (Schneider and Mercereau-Puijalon, 2005).

In addition, several PfePKs exist that exhibit features from more than one conventional ePK family, being referred to as “composite” or “dual” kinases”. Pfcrk-4 as well as PfPK6 display characteristics of both CDKs and MAPKs (Bracchi-Ricard et al., 2000). It remains elusive if these “composite” enzymes reflect mutual ancestors to subsequently diverging kinase families or if they originated from domain shuffling between existing kinase genes (reviewed in Ward et al., 2004).

## 1.5 Evaluation of protein kinases as drug targets

One of the first inhibitory drugs that apply their potency on targeting a protein kinase used clinically was rapamycin (Cohen, 2001). This immunosuppressant acts as inhibitor of the serine-threonine kinase mTOR, thus blocking the signal transduction cascade which is activating and propagating the cell cycle of T-cells from the G1 to the S-phase. Consequently, rapamycin is the immunosuppressive agent of choice to prevent rejection after kidney

transplantations (Cohen, 2001). In general, kinase inhibitor research is most progressive in the field of combating cancer, neurodegenerative and inflammatory diseases (reviewed in Doerig and Meijer, 2007).

In case of targeting plasmodial kinases for antimalarial control strategies, only minor progress has been reported so far. Given the lack of an effective vaccine up to date and several drawbacks in antimalarial drug development as well as arising insecticide resistances, there is an urgent need for the development of new antimalarials. Since recent years, the characterization of the *P. falciparum* kinome has disclosed grave divergences between the malaria parasite and the human host, rendering plasmodial kinases as potent targets for antimalarials (reviewed in (Doerig and Meijer, 2007; Lucet et al., 2012)). It requires the verification that a distinct kinase is indispensable for the parasite's growth or differentiation to validate the same as an effective drug target. Therefore, one promising tool might constitute gene knock-out attempts by reverse genetic approaches, resulting in the demonstration of the indispensability of the respective parasite kinase (reviewed in Kappes et al., 1999). Several investigations have been undertaken up to date to determine whether a parasite kinase is essential for the parasite's survival in order to identify potential novel drug targets. For this purpose, reverse genetic approaches by disrupting the kinase gene locus were utilized to generate gene-disruptant parasite lines to investigate the phenotype (Dorin-Semblat et al., 2007). To this day, numerous plasmodial kinases were scrutinized that are crucial for *P. falciparum* (reviewed in Lucet et al., 2012), for example Pbcrk-1, Pfmap-2 or PfCK2 (Rangarajan et al., 2006; Dorin-Semblat et al., 2007; Holland et al., 2009; Solyakov et al., 2011). Regarding curative drugs, the kinase of interest should ideally be essential for the asexual multiplication of the parasite, whereas an indispensability for the sexual development renders a kinase as potential target for transmission blocking drugs (reviewed in Doerig and Meijer, 2007).

Secondly, to consider a kinase as a promising drug target the protein must be distinguishable from its human counterpart in such a way that interfering molecules can exploit a given substrate specificity of the kinase of choice. With *P. falciparum* belonging to the phylum Apicomplexa, this taxonomic group displays a phylogenetically significant distance from the Opisthokonta branch that includes animals and fungi (Baldauf, 2003; Solyakov et al., 2011). Recently, two independent studies of the *P. falciparum* kinome utilizing genome wide analyses of the collectivity of protein kinase encoding genes were undertaken (reviewed in Ward et al., 2004; Anamika et al., 2005). It was figured out that there exist vast divergences between *P. falciparum* and mammalian protein kinases on several levels. Numerous orphan kinases have been identified that do not cluster within any established family from yeast or mammalian kinomes. One of the largest groups comprising orphan plasmodial kinases display the FIKKs (reviewed in Ward et al., 2004; Nunes et al., 2007; Nunes et al., 2010; Solyakov et al., 2011). Secondly, the malaria parasite possesses a family of four protein kinases that cluster within the NIMA family that does not occur in the human host (Dorin et al., 2001; Dorin-Semblat et al., 2011). The family of calcium-dependent protein kinases (CDPKs) encompasses members in the malarial kinome, whereas representatives of this family are found in plants and ciliates, but not in mammalian cells (reviewed in (Ward et al., 2004; Doerig and Meijer, 2007)).



On the other hand, even if most established ePK groups have orthologue members in the plasmodial kinome, there is strong evidence that the malarial parasite lacks tyrosine kinases as well as members of the STE kinases, indicating a divergence regarding the MAPK pathways in *P. falciparum* (Dorin et al., 2001; reviewed in Ward et al., 2004; Dorin et al., 2005; Solyakov et al., 2011). Noteworthy, atypical MAPKs are present in *P. falciparum*, but no typical MAPKs are identified so far in the malaria parasite (reviewed in Doerig and Meijer, 2007).

Even in case an individual kinase orthologue can be identified in *P. falciparum*, this candidate still can exhibit deviations from the human host enzyme. It is of high importance that these divergences can be exploited in the search for parasite-specific kinase inhibitors. Many orthologues still possess atypical characteristics compared to their human counterpart, such as large insertions, extensions or variant regulatory sites (reviewed in (Doerig, 2004; Doerig and Meijer, 2007)). For instance, the plasmodial MAPK lacks the usual TxY motif (Doerig et al., 1996; reviewed in Doerig and Meijer 2007).

## 1.6 The CLK kinases of *P. falciparum*

In *P. falciparum* there are four kinases that resemble CDK-like kinases (CLK) which are involved in mRNA splicing and transport. These plasmodial kinases are referred to as PfCLK-1, PfCLK-2, PfCLK-3 and PfCLK-4 and, in its entirety, PfCLKs. PfCLK-1 is also denoted as LAMMER kinase, as it shows homology to the LAMMER kinase family (Li et al., 2001) which is conserved among eukaryotes and share the common motif EHLAMMERILG (Yun et al., 1994; Talevich et al., 2011). The PfCLKs are annotated in PlasmoDB as putative Ser/Thr kinases, most likely with a further function of tyrosine phosphorylation. PfCLK-1, PfCLK-2 as well as PfCLK-4 possess intron-less gene sequences whilst PfCLK-3 contains eight introns, with exons encoding large polypeptides.

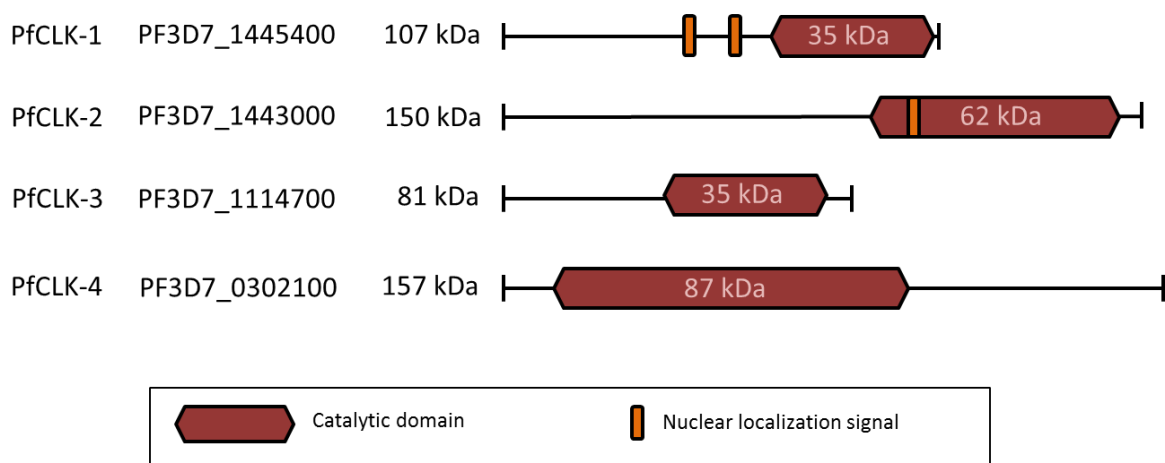


**Fig. 1.6: Domain structures of the PfCLKs.** Schematic of the plasmodial PfCLKs depicting the catalytic domains (red) with molecular mass and nuclear localization signals (orange).

Regarding the catalytic domains of the PfCLKs, these are located at the C-terminus for PfCLK-1 to PfCLK-3 and N-terminal for PfCLK-4 (Fig. 1.6). Two nuclear localization signals upstream of the C-terminal catalytic domain were evidenced for PfCLK-1 by the use of *in silico* analysis, whereas for PfCLK-2, one signal was predicted (Agarwal, 2010; Agarwal et al., 2011; Fig. 1.6). The evidence of these signals emphasizes a possible localization of PfCLK-1 and PfCLK-2 within nuclear speckles, subcellular organelles which display dynamic storage sites for splicing components like serine/arginine-rich (SR) proteins within the cell nucleus (Gui et al., 1994). For PfCLK-3 and PfCLK-4, no nuclear localization signals could be observed. Nevertheless, the subcellular localization is suggestive of promyelocytic leukemia bodies (PML bodies) and nucleoplasm for the two PfCLK kinases, respectively (Agarwal, 2010).

Noteworthy, PfCLK-4 exhibits 45% sequence homology with the kinase domain of human SRPK1 (Dixit et al., 2010). For this reason, PfCLK-4 is often referred to as PfSRPK1, and PfCLK-2 is denoted as SRPK2 (Dixit et al., 2010). Moreover, PfCLK-4/SRPK1 possesses all the conserved kinase subdomains as well as an insertion between domain VIb and VII, which is a signature of SRPKs (Dixit et al., 2010). In contrast, PfCLK-2/SRPK2 revealed distinct differences compared to PfCLK-4 and human SRPK1, as PfCLK-2 lacks the typical glycines in the ATP binding pocket (Dixit et al., 2010; Talevich et al., 2011). These results agree with previous report on the kinome of *P. falciparum*, which predicted PfCLK-2 and PfCLK-4 as members of SRPK family (reviewed in Ward et al., 2004).

In preceding investigations, *in silico* analysis of the four PfCLKs was conducted (Agarwal, 2010; Agarwal et al., 2011) by aligning the catalytic domain sequences of the PfCLKs with the homologous kinase Sky1p from the yeast *Saccharomyces cerevisiae* (Nolen et al., 2001). Sky1p is a non-essential serine-arginine (SR) protein kinase which is well researched and known to be involved in splicing and transport of mRNA in budding yeast (Siebel et al., 1999). The analysis' outcome revealed a remarkable homology in terms of catalytic domain sequences between Sky1p and all four PfCLKs. In addition, further sequence alignment with Sky1p discovered matches between substrate binding residues of the PfCLKs with the substrate binding site of Sky1p. The yeast kinase has a specific substrate, Npl3p, which shuttles between the nucleus and the cytoplasm of *S. cerevisiae* and therefore displays an mRNA transport protein which is regulated by reversible phosphorylation conducted by Sky1p (reviewed in Fu et al., 1995; Siebel et al., 1999; Lukasiewicz et al., 2007). On the basis of Npl3p representing the kinase substrate for homologous yeast kinase, various plasmodial proteins were identified that display homology to Npl3p and to mammalian CLK substrate SF2/ASF (Agarwal, 2010). Among them, plasmodial proteins were found that are putative splicing factors or RNA binding proteins. Noteworthy, the hypothetical splicing factor PfSR-1 (PF3D7\_0517300) also exhibited homology to Npl3p (29%) and mammalian SF2/ASF (52%), which was shown in previous studies to interact with PfCLK-4 (Dixit et al., 2010). For further investigation of interaction partners of the PfCLKs, four hypothetical plasmodial proteins were selected for this study which revealed substantial homology to the yeast protein and the mammalian splicing factor (Tab. 3.1): PfASF-1 (PF3D7\_1119800), PfSRSF12 (PF3D7\_0503300), PfSFRS4 (PF3D7\_1022400) and PfSF-1 (PF3D7\_1321700).

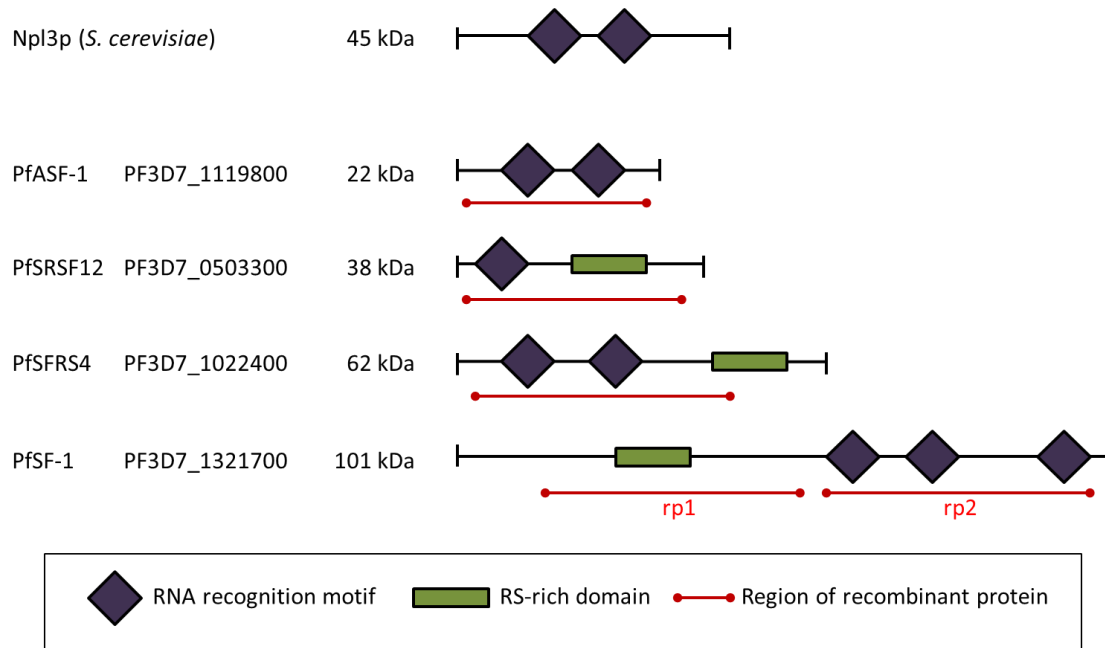


**Fig. 1.7: Domain structures of yeast splicing factor Npl3p and the four homologous plasmodial factors.** The regions of recombinantly expressed proteins are indicated by red lines. All investigated plasmodial factors possess RNA recognition motifs (RRM), whilst RS-rich domains are only found in PfsRSF12, PfsFRS4 and PfsF-1.

## 1.7 Splicing in *P. falciparum*

There exists a multitude of ways to control gene expression at different levels, for example transcriptional and post-transcriptional regulation, translational regulation and mRNA degradation (reviewed in Deitsch et al., 2007). One of the most important post-transcriptional mechanisms is pre-mRNA splicing. This is the molecular process that mediates the removal of intervening, noncoding intronic sequences and the joining of coding exons to form mature mRNA for subsequent translation (Aubol et al., 2013; reviewed in Naro and Sette, 2013). Whereas constitutive splicing results in solely one mature mRNA and thus one protein isoform from a specific primary transcript, alternative splicing (AS) displays the phenomenon of a single pre-mRNA giving rise to multiple mature mRNAs and thus protein isoforms, depending on the combination of exons of one gene being included within or excluded from the processed mRNA (reviewed in (Stojdl and Bell, 1999; Black, 2003)).

AS enables eukaryotic organisms to enlarge their protein repertoire out of a comparatively small number of genes (reviewed in Hagiwara, 2005; Pajares et al., 2007; Eshar et al., 2012). These different protein isoforms out of one gene can have diverse biological properties, such as changes in protein/protein interaction, subcellular localization or catalytic abilities (reviewed in (Black, 2003; Stamm, 2008)). In mammals, 90% of multiexon genes undergo alternative splicing (Fedorov et al., 2011; reviewed in (Keren and Lev-Maor, 2010; Naro and Sette, 2013)). Splicing typically occurs inside the nucleus, governed by a multicomponent complex, the spliceosome. This dynamic structure is assembled by five small nuclear ribonucleoprotein particles (snRNP; U1, U2, U4, U5 and U6 snRNPs) and more than 200 supportive proteins (reviewed in (Long and Cáceres, 2009; Naro and Sette, 2013)). The

assembly of the spliceosome is initiated by the recognition of short conserved sequences, the 5' and 3' splice sites, by the U1 snRNP subunit and auxiliary factors. After recruiting the U2 subunit to the branch point in an ATP dependent manner, further recruitment and association of the tri snRNP complex U4/U6-U5 with the pre-mRNA leads to structural rearrangements, resulting in the catalytically active spliceosomal C complex (reviewed in Long and Cáceres, 2009), leading to the cleavage of the 5' and 3' ends of the intron from the adjacent exons.

Splicing involves reversible phosphorylation of serine/arginine-rich (SR) proteins, which directly mediate splice site selection in eukaryotic mRNA (reviewed in (Huang and Steitz, 2005; Godin and Varani, 2007)). They are phosphorylated by two protein kinase families which display major keyplayers in these events: SRPKs and CLKs (Talevich et al., 2011; Aubol et al., 2013). SRPKs and CLKs possess pronounced differences regarding substrate specificity and enzymatic kinetics in phosphorylation of SR proteins (Colwill et al., 1996a; Colwill et al., 1996b). SRPK phosphorylation of splicing factors displays a comparatively limited activity due to a specific docking interaction (Bullock et al., 2009). By contrast, CLK activity is less constrained due to specific kinase domain insertions (Bullock et al., 2009; Aubol et al., 2013). Moreover, a distinct regiospecificity of both kinase families in regard to SR protein phosphorylation has been confirmed by mass spectrometric mapping previously (Velazquez-Dones et al., 2005). Kinases of the Clk/Sty family are able to transfer phosphates to the majority of serine residues in the RS domain of SR proteins, whereas SRPKs are highly restricted to a block of RS repeats in the N-terminal half of the RS domain.

Even though AS is such a crucial mechanism in eukaryotes, the regulation of splicing events as well as the AS machinery itself are poorly understood in *P. falciparum*. Moreover, *Plasmodium* possesses a high degree of developmental control of gene expression (Le Roch et al., 2004) in contrast to a rather small genome with approximately 5 700 genes (Gardner et al., 2002). The blood stage antigen P41-3 precursor (Knapp et al., 1991) as well as the adenylyl cyclase (Muhia et al., 2003) were firstly reported to undergo AS in *P. falciparum*, giving rise to different isoforms of the respective protein. Another example for a conserved AS event across *Plasmodium* evolution is the splicing of the *maebi* gene in different *Plasmodium* species, whose gene product is involved in red blood cell invasion (Singh et al., 2004). More recent genome wide studies using RNA sequencing of different life cycle stages during the intraerythrocytic development cycle were carried out, implying that over 300 AS events occur in approximately 4 % of genes of the malaria genome (Otto et al., 2010; Sorber et al., 2011). In *Plasmodium*, about 54 % of the genes contain introns (Gardner et al., 2002), with 30 % of them possessing at least two introns (Eshar et al., 2012). Noteworthy, genes of malaria parasites and other unicellular organisms have larger exons with fewer and smaller introns than metazoans (Singh et al., 2004). Previously, a putative homologue of the SF2/ASF splicing factor was identified in *P. falciparum*, affecting alternative splice site selection by antagonizing other SR proteins and binding to ribosomes (Iriko et al., 2009). Moreover, the splicing branch points that give rise to the excised lariat intron are also unusual in *P. falciparum*: The 5' splice site is poorly conserved and tolerates various nucleotide substitutions (Zhang et al., 2011; reviewed in Hull and Dlamini, 2014). Noteworthy, some

introns also have numerous branch points indicating a further mechanism for alternative splicing and possessing flexibility in branch point nucleophilic attack (Zhang et al., 2011).

It is proposed that AS may play an important role in the ability of endoparasites to evade the immune system of the human host, as AS gives rise to different isoforms of antigenic proteins. This may imply a further mechanism for immune evasion by the parasite to avoid immune detection (reviewed in Hull and Dlamini, 2014). In order to survive the hostile environment of the host organism, endoparasites like *P. falciparum* change their antigenic surface molecules during an infection. There are various antigenic proteins in *P. falciparum* that are known to have isoforms originating from AS, for example the blood antigen P41-3 (Knapp et al., 1991) or the surface antigen UB05, which is the target of IgG antibodies from semi-immune adults infected with *P. falciparum* (Sorber et al., 2011). In addition, the mRNA of the surface antigen PF70 (PF3D7\_1002100) reacting with anti *P. falciparum* serum contains a 5' alternative splice site, resulting in a different protein isoform than the full-length transcript (Sorber et al., 2011). Recently, an alternate stop codon has been described for MSP-5, a member of the merozoite surface proteins (MSP), which are of great interest regarding a putative malaria vaccine (Otto et al., 2010). This finding could decrease its usefulness as vaccine target, as increased variation is implied by the alternatively spliced isoform. Apart from the alternatively spliced *maebi* gene which is involved in erythrocyte binding and invasion (Singh et al., 2004), another RBC-binding protein is expressed in different isoforms by AS. Cytoadherence linked asexual gene 9 (clag 9), which is required to bind to endothelial cell receptors and is immunogenic, was found to be alternatively spliced (Otto et al., 2010; reviewed in Hull and Dlamini, 2014). However, the specific roles played by these antigen isoforms still remain elusive.

## 1.8 Objective of this study

The sequencing and subsequent annotation of the *P. falciparum* genome in 2002 offered the possibility to identify parasite proteins which might display targets for innovative antimalarial intervention strategies. In *P. falciparum*, the phylogenetic tree classifies the four identified members of the cyclin-dependent kinase-like kinases (PfCLKs) to the conventional branch of the CMGC group. This comparatively large group of typical ePKs are key regulators of mRNA splicing processes in other eukaryotes. There are numerous CLKs in other organisms that have been assigned to phosphorylation of SR proteins that act as splicing factors, governing pre-mRNA processing with the collaboration of other components of the splicing machinery. Up to date, little information is available about the individual compartments of this complex. Therefore, gaining deeper insight into the function and putative interaction partners of the parasite CLKs will unwind the intricate regulation of the malarial spliceosomal complex. Preceding studies showed that two members of the PfCLKs, PfCLK-1 and PfCLK-2, are predominantly expressed in the parasite nucleus, which is consistent with the findings that both kinases possess nuclear localization signals. Both kinases are furthermore associated with phosphorylation activity *in vitro* and are indispensable for the asexual replication cycle. To successfully accomplish the study on the four CLKs of *P. falciparum*, this present study is conducted to gain deeper insight into the two remaining members of the parasite CLK family, PfCLK-3 and PfCLK-4. This will be achieved by scrutinizing the protein expression profile and subcellular localization of both kinases by means of Western blot analyses and indirect immunofluorescence assays. Therefore, antibodies directed against the catalytic domains of both PfCLKs are to be generated to study the expression pattern. Further, reverse genetic studies are intended to evaluate if the respective kinase loci can be genetically disrupted in order to determine the resulting phenotype in the parasite life cycle. Subsequent phosphorylation studies are planned to verify the *in vitro* phosphorylation capability. The functional characterization of PfCLK-3 and PfCLK-4 is complementing preceding studies in such a way that these four enzymes are validated in regard to their specific function in the parasite, and moreover, as potential targets for prospective antimalarial intervention strategies.

Leading over to the principal part of the present thesis, all four kinases have previously been acknowledged to display a notable homology to the yeast protein Sky1p. This protein phosphorylates a specific SR protein, Npl3p, in the mRNA splicing and transport process in this organism. Therefore, the investigations in the course of this thesis are undertaken to find putative interaction partners of the four parasite CLKs that represent SR proteins and most likely act as splicing factors. For this purpose, recombinant proteins are expressed in *E. coli* and utilized in kinase activity assays to investigate the *in vitro* interaction with the PfCLKs. These proteins are the yeast kinase substrate Npl3p and the four homologous plasmodial proteins PfASF-1, PfSRSF12, PfSFRS4 and PfSF-1. These parasite SR proteins show remarkable homology to Npl3p as well as to the mammalian splicing factor SF1/ASF. In addition, the four plasmodial SR proteins would be characterized with respect to their subcellular localization. By scrutinizing potential interaction partners of the four PfCLKs, these findings will set the

platform for future approaches to unravel the malarial spliceosome, thus finding potential drug targets as splicing displays such an indispensable mechanism of cellular life in eukaryotes, and in particular in *P. falciparum*.

Taking another step towards the identification of targets for antimalarial strategies on the chemotherapeutic level, the third and concluding part of the present study includes the screening of a small compound library which is already available for intervention against human and microbial CLKs. Out of this CLK inhibitor library, it is intended to identify putative PfCLK inhibitors. In an additional approach, the study aims at characterizing the inhibitory effect of chlorhexidine, an antiseptic which was previously reported to affect human CLKs besides its reported antimalarial activity. For the purpose of defining specific PfCLK inhibitors, Malstat viability assays are to be carried out in an initial approach. Subsequent stage-of-inhibition assays, gametocyte toxicity assays and exflagellation assays are aimed at deciphering the specific effect of the inhibitors on the asexual stages, gametocyte development and gamete formation, respectively. In order to define the specific inhibition of the compounds on the PfCLKs, kinase activity assays are to be carried out. Moreover, bearing in mind that a lot of *P. falciparum* kinases can not be knocked out by conventional strategies, finding specifically acting and effective small compounds would display a powerful tool to chemically knock-out the CLKs. This in turn could contribute to phenotypically characterize the PfCLKs.

Taken together, all these studies were aimed at functionally characterizing components of the malarial splicing machinery and unravel regulatory mechanism of the same. With the background of the urgent need of innovative antimalarial chemotherapeutics, this study should target at identifying novel compounds for chemically intervention of the plasmodial CLKs.

## 2 Materials and Methods

### 2.1 Materials

#### 2.1.1 Bioinformatical tools and computer programs

- Adobe Acrobat Pro/Photoshop CS
- BioEdit
- GIMP 2.8.4
- GraphPad PRISM 5
- GraphPad QuickCalcs ([www.graphpad.com/quickcalcs/](http://www.graphpad.com/quickcalcs/)) for calculation of IC<sub>80</sub> values
- ImageJ
- Leica LAS AF Lite
- LSM Image Browser
- Microsoft Office® Excel/Word/PowerPoint 2010
- NCBI/BLAST/blastp suite
- PlasmoDB v.9.2 [www.plasmodb.org](http://www.plasmodb.org)
- Primer3 v.0.4.0 <http://frodo.wi.mit.edu/>
- SMART/EMBL Heidelberg [smart.embl-heidelberg.de](http://smart.embl-heidelberg.de)
- [www.bioinformatics.org/sms/prot\\_mw.html](http://www.bioinformatics.org/sms/prot_mw.html) for prediction of protein molecular weight
- [www.yeastgenome.org](http://www.yeastgenome.org)

#### 2.1.2 Laboratory Equipment

<b>Instrument</b>	<b>Company</b>
Accu Jet® Pro	Brand, Wertheim
Assistent RM5 Tube Agitator	Karl Hecht KG, Sondheim
Bunsen burner Gasi	Schütt, Göttingen
Centrifuge Megafuge 1.OR	Heraeus, Hanau
Confocal microscope LSM 510	Zeiss, Oberkochen
Confocal microscope TC S SP5 II	Leica, Solms
Consort electrophoresis power supply E835	Sigma-Aldrich, Taufkirchen
Developing machine CURIX 60	Agfa, Cologne
Electrophoresis chamber Mini-Protean 3	Bio-Rad, Munich
French® Press SLM Aminco FA078	Heinemann, Schwäbisch Gmünd
Gel documenter Gel Doc 2000	Bio-Rad, Munich
Gel drying apparatus 14x14 cm	Carl Roth, Karlsruhe
Geldryer Model 583	Biorad, Munich
Heating block Bio TBD-100 & TBD-120	Lab4you, Berlin
Heating table OTS 40	Medite GmbH, Burgdorf
Incubator HERAcCell	Heraeus, Hanau
Incubator Model 100-800	Memmert, Schwalbach



LB 124 SCINT contamination monitor	Berthold Technologies, Bad Wildbad
Light microscope Leica DMLS	Leica, Solms
Light microscope Leitz Laborlux 11	Leitz, Wetzlar
Microcentrifuge Biofuge <i>pico</i>	Heraeus, Hanau
Microscope camera AxioCam	Zeiss, Oberkochen
Microwave	Durabrand, Wal-Mart, Arkansas, USA
Mini-Rocker Shaker MR1	Lab4you, Berlin
Mini-Shaker for immunology PSU-2T	Lab4you, Berlin
pH-Meter inoLab® 7110	WTW, Weilheim
Pipettes	Eppendorf AG, Hamburg
Programmable thermal controller PTC-100™	MJ Research Inc., St. Bruno, Canada
Refrigerated microcentrifuge Biofuge <i>fresco</i>	Heraeus, Hanau
Scales 440-47N & 440-33	Kern & Sohn GmbH, BL-Frommern
Sonicator Sonopuls HD70	Bandelin, Berlin
Spectrophotometer Multiskan Ascent	Thermo Scientific, Waltham, USA
Spectrophotometer NanoDrop ND-2000	Peqlab, Erlangen
Sterile bench HERAsafe	Heraeus, Hanau
Test tube Vortexer Power Mix L46	Labinco, Breda, The Netherlands
Thermocycler Primus 25 advanced	Peqlab, Erlangen
Thermomixer compact	Eppendorf AG, Hamburg
Universal shaker SM 30 control	E. Bühler GmbH, Tübingen
Vacuum pump Laboport	KNF, Freiburg
Water bath Hecht 3185 WTE	K. Hecht KG, Sondheim
Western blot apparatus Mini-Trans-Blot	Bio-Rad, Munich

### 2.1.3 Chemicals and consumables

#### Chemicals

Chemicals were purchased from the following companies:

- AppliChem, Darmstadt
- ATCC, Manassas, USA
- Carl Roth, Karlsruhe
- Dianova, Hamburg
- GE Healthcare/Amersham, Munich
- Invitrogen/Gibco, Molecular Probes, Karlsruhe
- Merck/Novagen, Darmstadt
- Pharmacia/Pfizer, Vienna
- Roche Diagnostics, Penzberg
- Santa Cruz Biotechnology, Heidelberg
- Sigma Aldrich/Fluka, Taufkirchen
- WAK Chemie, Darmstadt

### Consumables

Consumables were purchased from the following companies or suppliers:

- BD Falcon, Heidelberg
- Bio-Rad, Munich
- Carl Roth, Karlsruhe
- Eppendorf, Hamburg
- Greiner, Flacht
- Laborbedarf Hartenstein, Würzburg
- Millipore, Schwalbach
- Noras, Höchberg
- Sarstedt, Nürnberg
- VWR International, Darmstadt

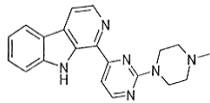
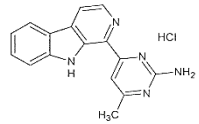
### Miscellaneous

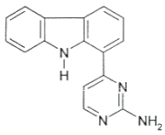
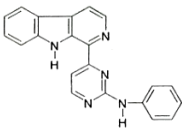
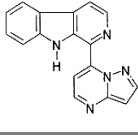
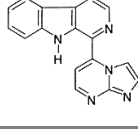
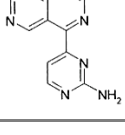
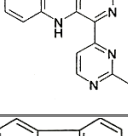
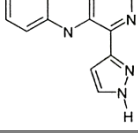
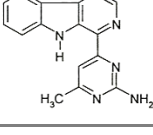
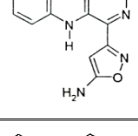
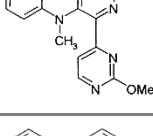
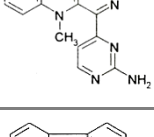
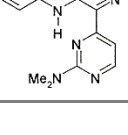
- Human A<sup>+</sup> serum and erythrocytes used for cell culture were obtained from Bayerisches Rotes Kreuz (BRK), Würzburg and the University Hospital of Aachen.
- Six weeks old female NMRI-mice for immunization were purchased from Charles River Laboratories, Sulzfeld.
- Gas cylinders containing a mixture of 5 % O<sub>2</sub>, 5 % CO<sub>2</sub> in 90 % N<sub>2</sub> used as gas supplement to *Plasmodium* cultures was purchased from Tyczka Industriegase, Würzburg or Westfalen AG, Münster, respectively.
- Cell culture medium RPMI 1640 + 25 mM HEPES/L-Glutamine/Sodium bicarbonate was obtained from Invitrogen/Gibco, Karlsruhe.
- $\gamma^{32}\text{P}$ -labeled ATP was purchased from Hartmann Analytic GmbH, Braunschweig.

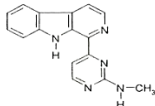
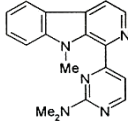
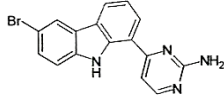
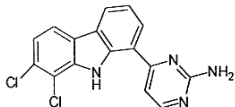
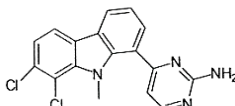
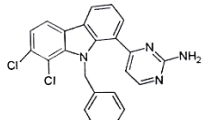
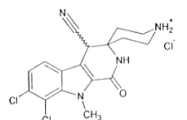
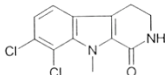
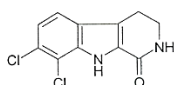
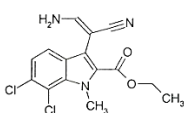
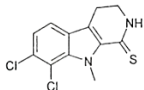
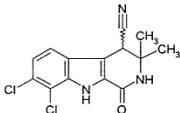
### 2.1.4 Inhibitors used in the study

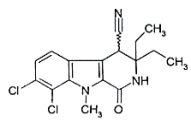
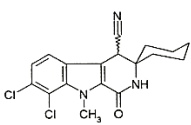
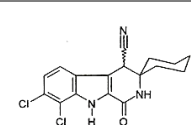
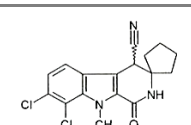
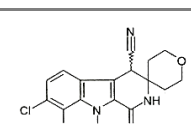
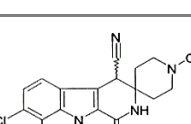
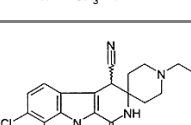
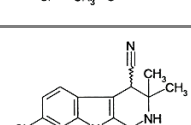
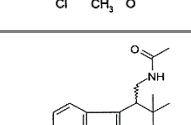
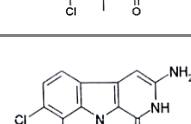
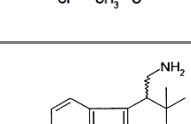
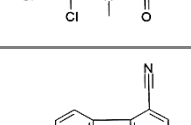
All CLK-inhibitors used in this study except of chlorhexidine were kindly provided by Dr. Franz Bracher (Department of Pharmacy, Center for Drug Research, Ludwigs-Maximilians-University, Munich; tab. 2.1). Chlorhexidine was purchased from Sigma-Aldrich, Taufkirchen. All compounds were prepared as stock solutions of 100 mM and were dissolved in DMSO and stored at -20°C until further use.

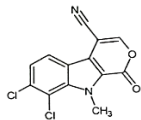
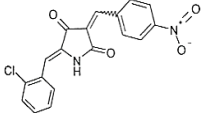
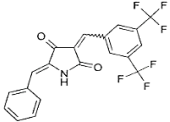
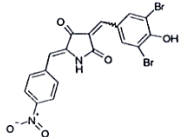
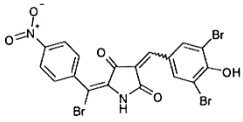
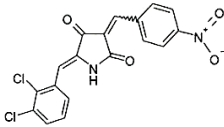
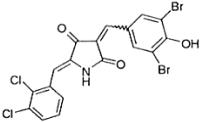
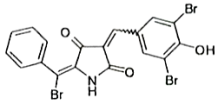
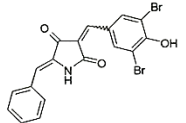
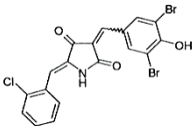
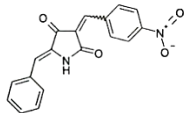
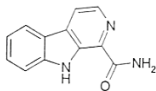
**Tab. 2.1: List of CLK-inhibitors used in the present study, sorted by chemical substance classes.**

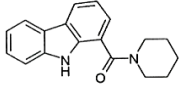
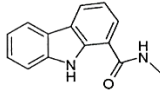
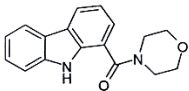
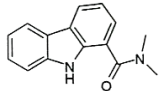
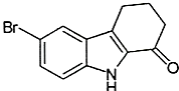
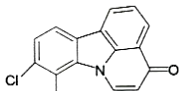
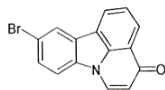
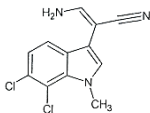
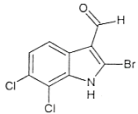
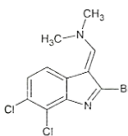
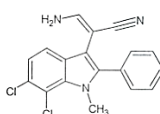
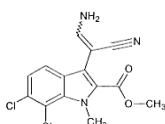
Substance	Molecular weight [g/mol]	Structure
<b>Aminopyrimidines</b>		
<b>C-117</b>	344.41	
<b>Kast180-HCl</b>	311.8	

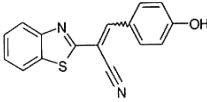
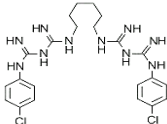
<b>C81</b>	260.3	
<b>C-129</b>	337.4	
<b>C-666-42-72</b>	285.3	
<b>C-667</b>	285.3	
<b>EK-28</b>	279.1	
<b>Kast-24</b>	260.3	
<b>Kast-25</b>	234.3	
<b>Kast-27</b>	275.3	
<b>Kast-50</b>	250.3	
<b>Kast-73</b>	211.2	
<b>Puzik-V8</b>	275.3	
<b>Puzik-V12</b>	289.3	

<b>Puzik-V16</b>	275.3	
<b>Puzik-V23.1</b>	303.4	
<b>gea-27</b>	339.2	
<b>gea-50</b>	329.2	
<b>gea-70</b>	343.2	
<b>gea-75</b>	419.3	
<b>Oxo-β-carbolines</b>		
<b>KH-CARB13xHCl</b>	399.7	
<b>Pohl-2</b>	269.1	
<b>Pohl-17</b>	255.1	
<b>KH-CB19T</b>	338.2	
<b>AR7</b>	285.2	
<b>KH-CARB1</b>	308.2	

<b>KH-CARB8</b>	350.2	
<b>KH-CARB3A</b>	362.3	
<b>KH-CARB3B</b>	348.2	
<b>KH-CARB7</b>	348.2	
<b>KH-CARB9</b>	364.2	
<b>KH-CARB10</b>	377.3	
<b>KH-CARB11</b>	391.3	
<b>KH-CARB2</b>	322.2	
<b>KH-DTCMA</b>	368.3	
<b>KH-CARB6</b>	282.1	
<b>KH-AMTC</b>	326.2	
<b>KH-CB5</b>	292.1	

NIH85	293.1	
<b>Tetramic acids</b>		
KH-HP05	354.8	
KH-HP11	411.3	
KH-HP01	494.1	
KH-HP02	494.1	
KH-HP03	389.2	
KH-HP04	518.0	
KH-HP06	528.0	
KH-HP07	449.1	
KH-HP08	483.6	
KH-HP09	320.3	
<b>Carbolines/Carbazoles</b>		
CS-14	211.2	

<b>CS02</b>	278.4	
<b>CS04</b>	224.3	
<b>CS06</b>	280.3	
<b>CS07</b>	238.3	
<b>gea_11</b>	264.1	
<b>gea_49</b>	288.1	
<b>gea_55</b>	298.1	
<b>Indoles/Benzothiazoles</b>		
<b>NIH08</b>	266.1	
<b>NIH11</b>	292.9	
<b>NIH16</b>	320.0	
<b>NIH39</b>	342.2	
<b>NIH54</b>	324.2	

<b>KH-CM16</b>	278.3	
<b>Antibiotics</b>		
<b>Chlorhexidine</b>	505.4	

## 2.1.5 Enzymes and commercial kits

Tab. 2.2: List of commercial kits and enzymes used in this study and their suppliers.

Enzymes and Kits	Suppliers
Alkaline Phosphatase, Calf Intestinal (CIP)	New England Biolabs, Ipswich, USA
GoTaq® DNA Polymerase & buffer	Promega GmbH, Mannheim
NucleoSpin® Blood	Macherey-Nagel, Düren
NucleoSpin® Extract II	Macherey-Nagel, Düren
NucleoSpin® Plasmid	Macherey-Nagel, Düren
Phusion® High-Fidelity DNA Polymerase & buffer	New England Biolabs, Ipswich, USA
Restriction endonucleases & buffers	New England Biolabs, Ipswich, USA
T4 DNA Ligase & buffer	New England Biolabs, Ipswich, USA

## 2.1.6 Buffers, reagents and solutions

Unless specified otherwise, buffers were stored at RT.

Tab. 2.3: List of solutions, reagents and buffers used and their compositions.

Buffers, reagents and solutions	Ingredients and concentrations
<b>1 x TE (Tris-ETDA) buffer</b>	10 mM Tris pH 8.0 1 mM EDTA pH 8.0 in H <sub>2</sub> O <sub>bidest</sub>
<b>10 % Ammonium peroxosulphate (APS)</b>	10 g APS, <i>ad</i> 100 ml H <sub>2</sub> O <sub>bidest</sub> , store at 4°C
<b>10 % Triton X-100</b>	5 ml of 100 % Triton X-100 in 50 ml H <sub>2</sub> O <sub>bidest</sub>
<b>10 x DNA loading buffer</b>	0.1 % Bromophenol blue (w/v) 0.1 % Xylene cyanol (w/v) 50 % Glycerol (w/v) in 1 x TAE
<b>10 x SDS-PAGE running buffer</b>	29 g Tris 144 g Glycine 10 g SDS <i>ad</i> 1000 ml H <sub>2</sub> O <sub>bidest</sub>
<b>10 x Tris-buffered saline (TBS)</b>	12.1 g Tris 87.3 g NaCl <i>ad</i> 1000 ml H <sub>2</sub> O <sub>bidest</sub> , adjust pH to 7.5
<b>10 x Phosphate-buffered saline (PBS)</b>	80 g NaCl 2 g KCl 11.5 g Na <sub>2</sub> HPO <sub>4</sub> 2 g KH <sub>2</sub> PO <sub>4</sub>



	<i>ad</i> 1000 ml H <sub>2</sub> O <sub>bidest</sub> , adjust pH to 7.4
<b>100 mM phenylmethanesulfonyl fluoride (PMSF)</b>	17.42 mg/ml Methanol
<b>2 x SDS sample buffer</b>	2.5 ml 500mM Tris-HCl pH 6.8 2.0 ml Glycerol (100 %) 4.0 ml 10 % SDS 0.5 ml 0.1 % Bromophenol blue <i>ad</i> 10 ml H <sub>2</sub> O <sub>bidest</sub> , store at 4°C
<b>5 x Kinase buffer for kinase activity assay</b>	20 mM Tris-HCl pH 7.5 20 mM MgCl <sub>2</sub> 2 mM MnCl <sub>2</sub> 10 mM 1 M NaF (Sigma) 10 mM 1 M β-glycerophosphate (Sigma) 10 μM ATP 0.37 MBq γ- <sup>32</sup> P-ATP Dissolve in the required volume of H <sub>2</sub> O <sub>bidest</sub> prior to kinase activity assay, pre-chill at 4°C
<b>50 x TAE electrophoresis buffer</b>	242 g Tris 57.1 g Acetic acid 100 ml 0.5 M EDTA pH 8.0 <i>ad</i> 1000 ml H <sub>2</sub> O <sub>bidest</sub> , adjust pH to 8.0
<b>Blocking solution Western blot</b>	50 ml 1 x TBS 0.5 g BSA (Fraction V albumin) 2.5 g Milk powder
<b>Buffer A for nuclear extraction</b>	10 mM HEPES pH 7.9 10 mM KCl 0.1 mM EDTA 1 mM DTT 10 % IGEPAL 1 x Incomp. PIC
<b>Buffer B for nuclear extraction</b>	20 mM HEPES pH 7.9 0.4 M NaCl 1 mM EDTA 10 % Glycerol 1 mM DTT 1 x incomp. PIC
<b>Column buffer MaBP purification</b>	50 mM Tris pH 8.0 1 mM EDTA 100 mM NaCl in H <sub>2</sub> O <sub>bidest</sub>
<b>Detergent buffer inclusion bodies</b>	20 mM Tris/HCl pH 7.5 2 mM EDTA pH 8.0 200 mM NaCl 1 % Deoxycholic acid 1 % Nonidet P-40 in H <sub>2</sub> O <sub>bidest</sub> , store at 4°C
<b>Elution buffer GST purification</b>	50 mM Tris pH 8.0 10 mM reduced Glutathione in H <sub>2</sub> O <sub>bidest</sub> Store at 4°C, should not be frozen and thawed more than five times

<b>Elution buffer MaBP purification</b>	50 mM Tris pH 8.0 1 mM EDTA 100 mM NaCl 10 mM Maltose in H <sub>2</sub> O <sub>bidest</sub>
<b>Equilibration buffer Western blot</b>	12.1 g Tris 5.8 g NaCl 10.2 g MgCl <sub>2</sub> <i>ad</i> 1000 ml H <sub>2</sub> O <sub>bidest</sub> , adjust pH to 9.5
<b>Ketamine/Xylazine solution</b>	1000 µl 10 % Ketamine (in H <sub>2</sub> O) 150 µl 2 % Xylazine (in methanol)
<b>Lysis buffer GST purification</b>	20 ml 50 mM Tris-HCl/10 % Glycerol pH 8.0 1.4 ml 5 M NaCl 20 µl β-mercaptoethanol 216 µl 20 % (v/v) IGEPAL 216 µl Imidazole
<b>Lysis buffer inclusion bodies</b>	50 mM Tris/HCl pH 8.0 0.25 % Sucrose 1 mM EDTA, pH 8.0 in H <sub>2</sub> O <sub>bidest</sub> , adjust pH to 8.0
<b>Lysis buffer MaBP purification</b>	50 mM Tris pH 8.0 1 mM EDTA 100 mM NaCl in H <sub>2</sub> O <sub>bidest</sub>
<b>Lysozyme solution</b>	10 mg Lysozyme in 1 ml H <sub>2</sub> O <sub>bidest</sub> , prior to lysis
<b>Permeabilization/blocking solution for IFA</b>	0.5 % BSA 0.01 % Saponin (Sigma-Aldrich) in 1 x PBS pH 7.4
<b>PMSF lysis buffer for preparation of cell lysate</b>	20 µl 1 M Tris-HCl pH 8.0 20 µl 0.5 M EDTA pH 8.0 80 µl 5 M NaCl 10 µl 1 M PMSF 10 µl 1 M β-glycerophosphate 10 µl 1 M NaF 5 µl 1 x PIC (Roche Diagnostics) 3 µl 10 % Triton X-100 <i>ad</i> 1000 µl 1 x PBS, prepare fresh prior to lysis
<b>Solution 1 for Dirty mini of plasmid DNA</b>	25 mM Tris/HCl pH 8.0 50 mM Glucose 10 mM EDTA pH 8.0 5 mg/ml Lysozyme
<b>Solution 2 for Dirty mini of plasmid DNA</b>	200 mM NaOH 1 % SDS
<b>Solution 3 for Dirty mini of plasmid DNA</b>	3 M KAc pH 4.8
<b>Stop buffer Western blot</b>	1.2 g Tris 0.4 g EDTA <i>ad</i> 1000 ml H <sub>2</sub> O <sub>bidest</sub> , adjust pH to 8.0
<b>TBS milk (TBSM)</b>	3 % Milk powder in 1 x TBS
<b>TBS-T buffer solution Western blot</b>	990 ml 1 x TBS

	10 ml 10 % Tween 20
<b>Transfer buffer Western blot</b>	3.03 g Tris 14.4 g Glycine 200 ml Methanol <i>ad</i> 1000 ml H <sub>2</sub> O <sub>bidest</sub>
<b>Washing buffer inclusion bodies</b>	0.5 % Triton X-100 1 mM EDTA pH 8.0 in H <sub>2</sub> O <sub>bidest</sub>

### 2.1.7 Media and solutions for *Plasmodium falciparum* cultivation

All solutions were sterile filtered either using syringe filter (0.22 µm) or bottle-top filter (Millipore) prior to use. Unless specified otherwise, solutions and media were stored at 4°C.

Tab. 2.4: List of media and solutions for *P. falciparum* cultivation.

Medium or solution	Ingredients and concentration
<b>0.2 % Dextrose/0.9 % NaCl for thawing of cultures</b>	0.1 g Dextrose 0.45 g NaCl in 50 ml H <sub>2</sub> O <sub>bidest</sub>
<b>1 mM Xanthurenic acid</b>	0.05 g Xanthurenic acid (Sigma-Aldrich) 1 ml 0.5 M NH <sub>4</sub> OH 243 ml H <sub>2</sub> O <sub>bidest</sub>
<b>1.6 % NaCl for thawing of cultures</b>	0.8 g NaCl in 50 ml H <sub>2</sub> O <sub>bidest</sub>
<b>10 % AlbuMax II™ stock</b>	10 g AlbuMax II™ (Gibco), dissolve in 100 ml H <sub>2</sub> O <sub>bidest</sub>
<b>10 % Saponin</b>	5 g Saponin (Sigma-Aldrich), <i>ad</i> 50 ml 1 x PBS
<b>10 x Giemsa buffer</b>	0.7 g KH <sub>2</sub> PO <sub>4</sub> 1.0 g Na <sub>2</sub> HPO <sub>4</sub> <i>ad</i> 1000 ml H <sub>2</sub> O <sub>bidest</sub> and adjust pH to 7.2
<b>10 x RPMI incomplete medium (ICM)</b>	10.43 g RPMI 1640 powder (Gibco) 5.94 g HEPES 0.05 g Hypoxanthine <i>ad</i> 1000 ml H <sub>2</sub> O <sub>bidest</sub>
<b>1000 x Hypoxanthine stock</b>	0.05 g/ml in NaOH
<b>12 % NaCl for thawing of cultures</b>	6 g NaCl in 50 ml H <sub>2</sub> O <sub>bidest</sub>
<b>5 % Sorbitol</b>	2.5 g Sorbitol (AppliChem), dissolve in 50 ml 1 x ICM
<b>A<sup>+</sup> medium (RPMI complete medium)</b>	To 500 ml RPMI 1640 (Gibco), add: 50 ml heat inactivated human A <sup>+</sup> serum 550 µl Gentamycine (10 mg/ml, Gibco) 550 µl 1000 x Hypoxanthine stock solution
<b>AlbuMax II™ medium</b>	To 500 ml RPMI 1640 (Gibco), add: 25 ml 10 % AlbuMax II™ 525 µl Gentamycine (10 mg/ml, Gibco) 525 µl 1000 x Hypoxanthine stock solution
<b>Blasticidine (BSD) stock solution</b>	5 mg Blasticidine (Invitrogen) per ml H <sub>2</sub> O <sub>bidest</sub>
<b>BSD medium (2.5 µg/ml)</b>	To 500 ml RPMI 1640 (Gibco), add: 50 ml Heat inactivated human A <sup>+</sup> serum 550 µl Gentamycine (10 mg/ml, Gibco) 550 µl 1000 x Hypoxanthine stock solution 275 µl BSD stock solution

<b>Giemsa staining solution</b>	3.5 ml Giemsa stock solution (Roth) in 70 ml 1 x Giemsa buffer
<b>Glycerolyte 57 solution</b>	26.66 g Sodium lactate 584 mg NaH <sub>2</sub> PO <sub>4</sub> x 2 H <sub>2</sub> O (Monohydrate, monobasic) 300 mg KCl 570 g Glycerol 2344 mg Na <sub>2</sub> HPO <sub>4</sub> x 7 H <sub>2</sub> O (Anhydrate, dibasic) <i>ad</i> 1000 ml H <sub>2</sub> O <sub>bidest</sub>
<b>Malstat reagent</b>	1 ml 10 % Triton X-100 1 g L(+) Lactate 0.33 g Tris 0.033 g 3-Acetylpyrimidin-adenine dinucleotide (3-APAD) dissolve in 100 ml H <sub>2</sub> O <sub>bidest</sub> , adjust pH to 9.0, store at 4°C for approx. 2 weeks

### 2.1.8 Media and agar plates for bacterial cultivation

Media and agar used in this study was autoclaved (121°C for 20 min) prior to use.

**Tab. 2.5:** List of media and agar used in this study for bacterial cultivation.

<b>Medium or agar</b>	<b>Ingredients and concentrations</b>
<b>1000 x Ampicillin</b>	100 mg/ml in H <sub>2</sub> O <sub>bidest</sub>
<b>LB agar</b>	10 g Tryptone 5 g Yeast extract 5 g NaCl 15 g Agar <i>ad</i> 1000 ml H <sub>2</sub> O <sub>bidest</sub>
<b>Lysogeny broth (LB) medium</b>	10 g Tryptone 5 g Yeast extract 5 g NaCl <i>ad</i> 1000 ml H <sub>2</sub> O <sub>bidest</sub> , pH 7.0
<b>Super optimal broth with catabolite repression (SOC) medium</b>	20 g Tryptone 5 g Yeast extract 0.5 g NaCl 10 ml 0.25 M KCl 5 ml 2 M MgCl <sub>2</sub> 20 ml 1 M Glucose <i>ad</i> 1000 ml H <sub>2</sub> O <sub>bidest</sub>

### 2.1.9 Plasmodial and bacterial cell lines

Cell lines of *Plasmodium falciparum*

***P. falciparum* wild type strain NF54** (MRA-1000) is a gametocyte producing strain which is chloroquine-sensitive. Isolated 1982 from a Dutch patient, the parasite was presumed of West African origin (Ponnudurai et al., 1981; [www.mr4.org](http://www.mr4.org)).

***P. falciparum* clone 3D7** (MRA 102) is derived from wild type strain NF54 via limiting dilution (Rosario et al., 1981; [www.mr4.org](http://www.mr4.org)).

***P. falciparum* strain F12** is a gametocyte-less strain obtained by limiting dilution after long-term cultivation of 3D7 isolate for 20 months (Walliker et al., 1987). By courtesy of Dr. Pietro Alano, Rome, Italy.

***P. falciparum* strain Dd2** (MRA 150) is derived from W2-Mef, which was selected from clone W2 for resistance to mefloquine. Furthermore CQ-resistant (intermediate) and pyrimethamine-resistant. (Wellems et al., 1990; [www.mr4.org](http://www.mr4.org)).

#### Cell lines of *Escherichia coli*

***E. coli* BL21-CodonPlus®-(DE3)-RIL** (Stratagene, Heidelberg): Chemically competent *E. coli* cells appropriate for protein expression. Genotype *E. coli* B F<sup>-</sup> *ompT hsdS* (*r<sub>B</sub><sup>-</sup> m<sub>B</sub><sup>-</sup>*) *dcm*<sup>+</sup> Tet<sup>r</sup> *E. coli gal* λ (DE3) *endA Hte* [*argU ileY leuW Cam*<sup>r</sup>]

***E. coli* Nova Blue** (Stratagene, Heidelberg): Chemically competent *E. coli* transformation cell line. Genotype *endA1 hsdR17* (*r<sub>K12</sub><sup>-</sup> m<sub>K12</sub><sup>+</sup>*) *supE44 thi-1 recA1 gyrA96 relA1 lac F*'[*proA<sup>+</sup>B<sup>+</sup> lacI<sup>q</sup>ΔM15::Tn10*] (Tet<sup>R</sup>)

***E. coli* OneShot®Top10-Competent Cells** (Invitrogen, Karlsruhe): Chemically competent *E. coli* transformation cell line. Genotype F<sup>-</sup> *mcrA Δ(mrr-hsdRMS-mcrBC) φ80lacΔM15 ΔlacX74 recA1 araD139 Δ(ara-leu)7697 galU galK rpsL(Str<sup>R</sup>) endA1 nupG λ<sup>-</sup>*

## 2.1.10 Plasmids

### pGEX-4T-1

It is a high-copy protein expression vector conferring ampicillin resistance and a Glutathione-S-transferase (GST) tag to the gene of interest for recombinant protein purification (GE Healthcare, Munich).

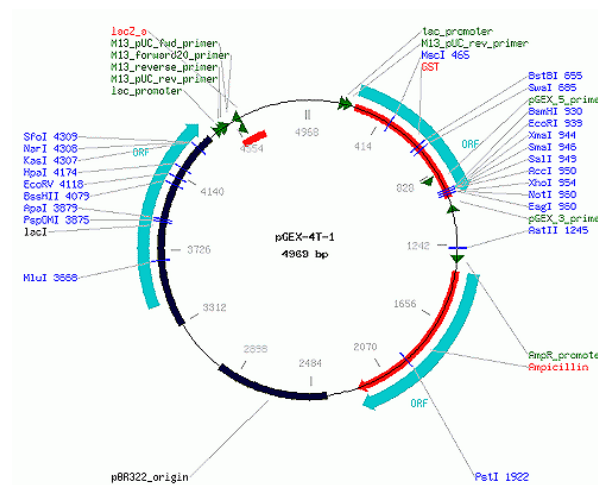


**Fig. 2.1:** Vector map of the expression vector pGEX-4T-1. Used in this study for the generation of GST fusion proteins.

pih902/pMAL-c

The pIH902 expression vector is a precursor of the subsequently designed pMAL-c and its derivatives (Maina et al., 1988; New England Biolabs, Frankfurt). It was kindly provided by Kim Williamson, Chicago. The plasmid encodes a maltose binding protein (MaBP)-tag as well as 6-His-tag and a *lacZ* $\alpha$ -gene for blue/white screening. For selection of positive clones it confers an ampicillin resistance to the transformant bacteria.

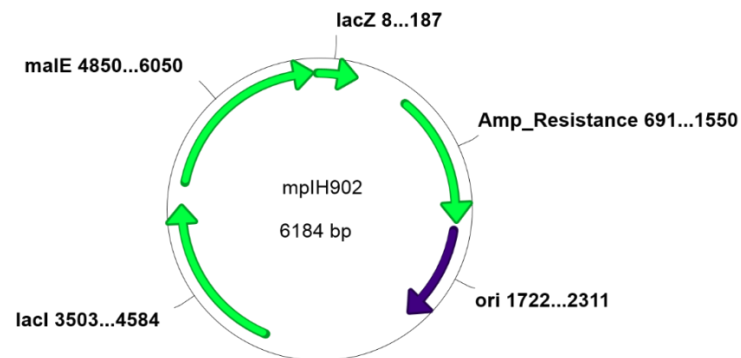


**Fig. 2.2:** Vector map of the expression vector pIH902. Used in this study for the generation of MaBP fusion proteins.

pCAM-BSD vector

For the purpose of achieving gene-disruption or gene-tagging, respectively, pCAM-BSD vector was used to create a single cross-over homologous recombination (Sidhu et al., 2005), carrying a blasticidine as well as an ampicillin resistance cassette. It was kindly provided by Prof. Christian Doerig, Clayton, Australia.

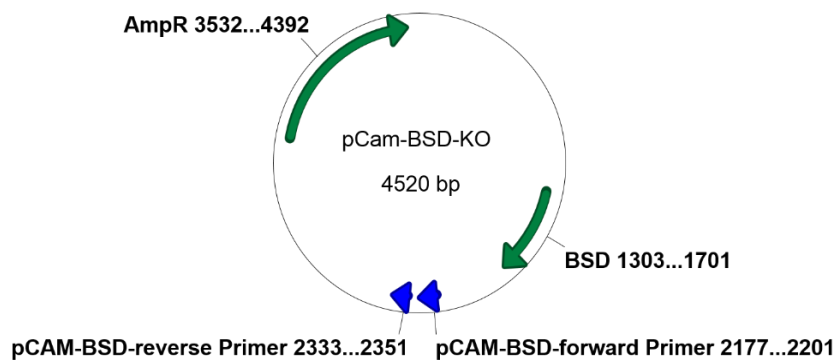


**Fig. 2.3:** Vector map of pCAM-BSD for disrupting a specific gene locus.

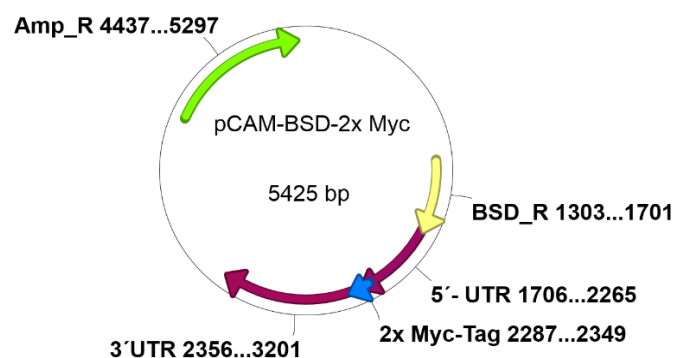


**Fig. 2.4:** Vector map of pCAM-BSD-Myc for gene-tagging.

### 2.1.11 Antibodies and antisera

**Tab. 2.6: List of antibodies used in this study, their properties and suppliers.** If not mentioned otherwise, all antibodies are of polyclonal origin.

Antibody	Origin	Working dilution		Suppliers and source
		Western blot	IFA	
<b>Primary antibodies</b>				
<b>anti-PfCLK-1</b>	rabbit	1:50	1:50	Biogenes, Berlin; Agarwal, 2010 PhD thesis; Agarwal et al., 2011.
<b>anti-PfCLK-2</b>	mouse	1:50	-	Biogenes, Berlin; Agarwal, 2010 PhD thesis; Agarwal et al., 2011.
<b>anti-PfCLK-3</b>	mouse	1:15	-	Pradel lab, this study
<b>anti-PfCLK-3</b>	rat	-	1:20	A. Tobin, Leicester, UK; Solyakov et al., 2011.
<b>anti-PfCLK-4</b>	mouse	1:75	1:75	Pradel lab, this study
<b>anti-PfASF-1</b>	mouse	-	1:15	Pradel lab, this study
<b>anti-PfSRSF12</b>	mouse	-	1:50	Pradel lab, this study
<b>anti-PfSFRS4</b>	mouse	-	1:30	Pradel lab, this study
<b>anti-PfSF-1</b>	mouse	-	1:50	Pradel lab, this study
<b>anti-PfMSP-1</b>	mouse	-	1:150	Pradel lab
<b>anti-PfMSP-1</b>	rabbit	-	1:1000	ATCC/MR4, Manassas, USA (MRA-33)
<b>anti-Pf230-C</b>	rabbit	-	1:200	Biogenes, Berlin
<b>anti-Pf39</b>	mouse	1:500	-	Pradel lab; Scholz et al., 2008.
<b>anti-PKRP</b>	mouse	1:50	1:20	Pradel lab

<b>anti-GST-tag</b>	goat	1:4000	-	GE Healthcare, Munich
<b>anti-MaBP-tag</b>	mouse	1:100	1:50	Pradel lab
<b>anti-Myc-tag</b>	rabbit	1:200	1:200	Cell Signaling
<b>Neutral mouse serum</b>	mouse	same as tested antibody		Pradel lab
<b>Neutral rabbit serum</b>	rabbit	same as tested antibody		Biogenes, Berlin
<b>Neutral goat serum</b>	goat	same as tested antibody		Sigma-Aldrich, Taufkirchen
<b>Neutral rat serum</b>	rat	same as tested antibody		Sigma-Aldrich, Taufkirchen
<b>Secondary antibodies</b>				
<b>anti-mouse Alexa Fluor®488</b>	goat	-	1:1000	Invitrogen, Karlsruhe
<b>anti-mouse Alexa Fluor®594</b>	goat	.	1:1000	Invitrogen, Karlsruhe
<b>anti-rat Alexa Fluor®488</b>	goat	-	1:1000	Invitrogen, Karlsruhe
<b>anti-rabbit Alexa Fluor®594</b>	goat	-	1:1000	Invitrogen, Karlsruhe
<b>anti-rabbit Alexa Fluor®488</b>	goat	-	1:1000	Invitrogen, Karlsruhe
<b>anti-mouse alkaline phosphatase</b>	goat	1:5000	-	Sigma-Aldrich, Taufkirchen
<b>anti-goat alkaline phosphatase</b>	rabbit	1:5000	-	Sigma-Aldrich, Taufkirchen
<b>anti-rabbit alkaline phosphatase</b>	goat	1:5000	-	Sigma-Aldrich, Taufkirchen



### 2.1.12 Oligonucleotides

All oligonucleotides were, if not already accessible in our working group, synthesized by and purchased from either biomers.net, Ulm or Eurofins MWG Operon, Ebersberg.

**Tab. 2.7:** List of primers used in this study for recombinant protein expression and gene modification. Restriction sites are underlined and stop codons are labeled in bold type.

Gene locus/ name	Name, restriction site	5'-3' sequence	Product length
<b>Primers for recombinant protein expression</b>			
PfCLK-3 rp1	CLK3rp1.for, EcoRI	TA <u>GAA TTC</u> AAG GGA AAT GCA GAT ACA	1 155 bp
PfCLK-3 rp1	CLK3rp1.rev, NotI	TA <u>GCGGCCGC</u> <b>TTA</b> TGG TTG AAG GGA AAT AGC CCT AAA	
PfCLK-3 rp2	CLK3rp2.for, EcoRI	TA <u>GAA TTC</u> GAT GAT TTT GAT ATG TTT TCC TGT	828 bp
PfCLK-3 rp2	CLK3rp2.rev, NotI	TA <u>GCGGCCGC</u> <b>TTA</b> GCC CTT ATA TTC CAT CAT CAG	
PfCLK-4 rp4	0105RP4.for, BamHI	TA <u>GGATCC</u> TCC AAT AAC AGC AAC AGT	1 403 bp
PfCLK-4 rp4	0105RP4.1.rev, SmaI	TA <u>CCCGGG</u> <b>TTA</b> TTT GGT AAT CCC TTC CGC TTT	
PfASF-1	ASF1-rp1-S1, EcoRI	AA <u>GAATTC</u> ATG AAA AAG TTA ATT AAT TGT GGC	600 bp
PfASF-1	ASF1-rp1-AS1- NOT, NotI	TT <u>GCGGCCGC</u> <b>TTA</b> ATT TAG TTC CTT TGG AGA	
PfSRSF12	SR1-RP2.for, EcoRI	AA <u>GAATTC</u> ATG AAA AAG TTA ATT AAT TGT GGC	901 bp
PfSRSF12	SR1- RP2.Not.rev,	TT <u>GCGGCCGC</u> <b>TTA</b> TTC ATT TTC CTT TCT CTT	
PfSFRS4	RP1.S1, BamHI	TA <u>GGATCC</u> GAT GAT GGT GTT GGT CCA	681 bp
PfSFRS4	RP1.Sal.rev, Sall	TA <u>GTCGAC</u> <b>TTA</b> CAT TTT CAT GTC CTG CAT TAG	
PFSF-1 rp1	Mal13RP1.for, BamHI	GCGTA <u>GGATCC</u> ATG GAA GAG AAC TCA TAT TTT GAG GCA	1 455 bp
PFSF-1 rp1	Mal13RP1.rev, Sall	TACGC <u>GTCGAC</u> <b>TTA</b> TTT TAA TCT TCT TTC TTC	
PFSF-1 rp2	Mal13RP2.for, EcoRI	TA <u>GAATTC</u> GAA GAA ATG GAA GAA GCA AAA AGG GAT	1 167 bp
PFSF-1 rp2	recMal13.rev, NotI	TA <u>GCGGCCGC</u> <b>TTA</b> CTT TGG AAG ACA AGT CAT ATC CCA TAC ATC	
<b>Primers for gene disruption using pCAM-BSD vector</b>			
PfCLK-3-KO	pCAM-CLK3KOS	CCT GTA GCT GTA AAA GTT	435 bp
PfCLK-3-KO	pCAM- CLK3KOAS	TTA TGC TCT ATA AAA TCT ACT	
PfCLK-4-KO	pCAM-CLK4KOS	TGT ACG AGC AGT AAA GAA	525 bp

PfCLK-4-KO	pCAM-CLK4KOAS	TTA GTC GTT CTT TTC GGA ATC	
<b>Primers for gene tagging using pCAM-BSD vector</b>			
PfCLK-3-Myc	pCAM-CLK3-tag-S	GGA AGT GCA AGT GAT ATA TCA	561 bp
PfCLK-3-Myc	pCAM-CLK3-tag-AS	TTC ATT TTG AGA TTT TGA	
PfCLK-4-Myc	pCAM-CLK4-tag-S	GAA GGA CAA GAA CAT GAT GCT	651 bp
PfCLK-4-Myc	pCAM-CLK4-tag-AS	AGT ATA TGC ACA AGA GTT	

**Tab. 2.8: List of primers used in this study for genotype characterization.** Primer pair combinations were used for diagnostic PCR investigating the genotype of transfected parasites and the expected PCR product lengths. WT: detection of wild type gene locus (primer combination A); Epi: detection of transfection episome (B); 5'-int: 5'-region of gene locus modified by vector integration (C); 3'-int: 3'-region of modified locus (D).

Region of interest	Oligonucleotide	5'-3' sequence	Product length
<b>PfCLK-3-KO</b>			
WT	pCAM-KOS	CTT GTA GCT GTA AAA GTT	594 bp
	0156-IP3-new	GTA TCA ATC CCC TGT GGT	
Epi	pCAM-BSD-F	TAT TCC TAA TCA TGT AAA TCT TAA A	794 bp
	pCAM-BSD-R	CAA TTA ACC CTC ACT AAA G	
5'-int	pCAM-KOS	CTT GTA GCT GTA AAA GTT	1 200 bp
	pCAM-BSD-R	CAA TTA ACC CTC ACT AAA G	
3'-int	pCAM-BSD-F	TAT TCC TAA TCA TGT AAA TCT TAA A	1 000 bp
	0156-IP3-new	GTA TCA ATC CCC TGT GGT	
<b>PfCLK-3-Myc</b>			
WT	WT2S	TA ATG TCC AAA GAT AAG AGA	1 920 bp
	WT2AS	AT ATC TTT ATT TAT CTG ATC	
Epi	pCAM-BSD-F	TAT TCC TAA TCA TGT AAA TCT TAA A	1 940 bp
	pCAM-BSD-R	CAA TTA ACC CTC ACT AAA G	
5'-int	WT2S	TA ATG TCC AAA GAT AAG AGA	1 740 bp
	pCAM-BSD-R	CAA TTA ACC CTC ACT AAA G	
3'-int	pCAM-BSD-F	TAT TCC TAA TCA TGT AAA TCT TAA A	1 390 bp
	WT2AS	AT ATC TTT ATT TAT CTG ATC	
<b>PfCLK-4-KO</b>			
WT	RPP1S	AGT AGT AGT GAA GAT GCT	1 480 bp
	RPP1AS	TCG GAT CCT TCT TTG CTC	
Epi	pCAM-BSD-F	TAT TCC TAA TCA TGT AAA TCT TAA A	672 bp
	pCAM-BSD-R	CAA TTA ACC CTC ACT AAA G	
5'-int	RPP1S	AGT AGT AGT GAA GAT GCT	1 380 bp
	pCAM-BSD-R	CAA TTA ACC CTC ACT AAA G	
3'-int	pCAM-BSD-F	TAT TCC TAA TCA TGT AAA TCT TAA A	770 bp
	RPP1AS	TCG GAT CCT TCT TTG CTC	
<b>PfCLK-4-Myc</b>			
WT	0105-RTPC2H	ATG ATG GAT CAT GAC ACA	1 400 bp
	0105-IP3	AAA TGT ACC CGT TAG GTT	

Epi	pCAM-BSD-F	TAT TCC TAA TCA TGT AAA TCT TAA A	1 700 bp
	pCAM-BSD-R	CAA TTA ACC CTC ACT AAA G	
5'-int	0105-RTPC2H	ATG ATG GAT CAT GAC ACA	2000 bp
	pCAM-BSD-R	CAA TTA ACC CTC ACT AAA G	
3'-int	pCAM-BSD-F	TAT TCC TAA TCA TGT AAA TCT TAA A	900 bp
	0105-IP3	AAA TGT ACC CGT TAG GTT	

### 2.1.13 Gene IDs

**Tab. 2.9: Gene IDs of investigated genes proteins.** The following gene identifiers are assigned to the proteins investigated in this study. Gene IDs and names were retrieved from PlasmoDB website ([www.plasmodb.org](http://www.plasmodb.org)) and yeast genome database ([www.yeastgenome.org](http://www.yeastgenome.org)).

Gene ID	previous Gene ID	Gene name
PF3D7_1445400	PF14_0431	PfCLK-1; PflAMMER
PF3D7_1443000	PF14_0408	PfCLK-2
PF3D7_1114700	PF11_0156	PfCLK-3
PF3D7_0302100	PFC0105w	PfCLK-4; SRPK1
PF3D7_1119800	PF11_0205	PfASF-1; alternative splicing factor
PF3D7_0503300	PFE0160c	PfSRSF12; putative Ser/Arg-rich splicing factor
PF3D7_1022400	PF10_0217	PfSFRS4; putative pre-mRNA splicing factor
PF3D7_1321700	MAL13P1.120	PfSF-1; putative splicing factor
YDR432W	-	Npl3p, RNA-binding protein of <i>Saccharomyces cerevisiae</i>

### 2.1.14 DNA and protein ladders

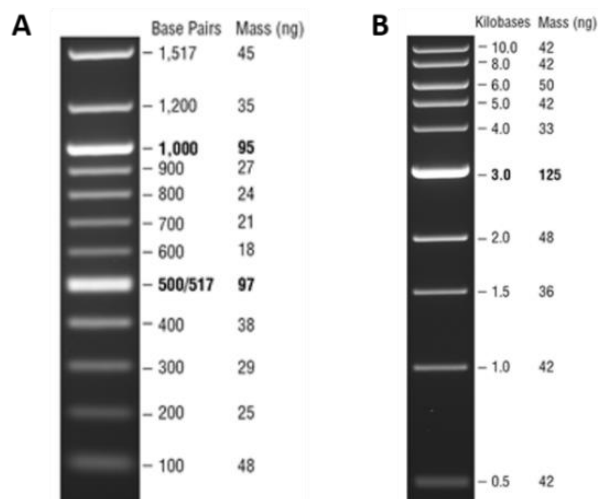


**Fig. 2.5:** The DNA molecular weight standards for agarose gel electrophoresis. As DNA marker the 100 bp DNA Ladder (A) and the 1 kb DNA Ladder (B) from NEB, Frankfurt were utilized. Depending on the size of the gel pockets, 2 to 10  $\mu$ l of the respective standard were applied.

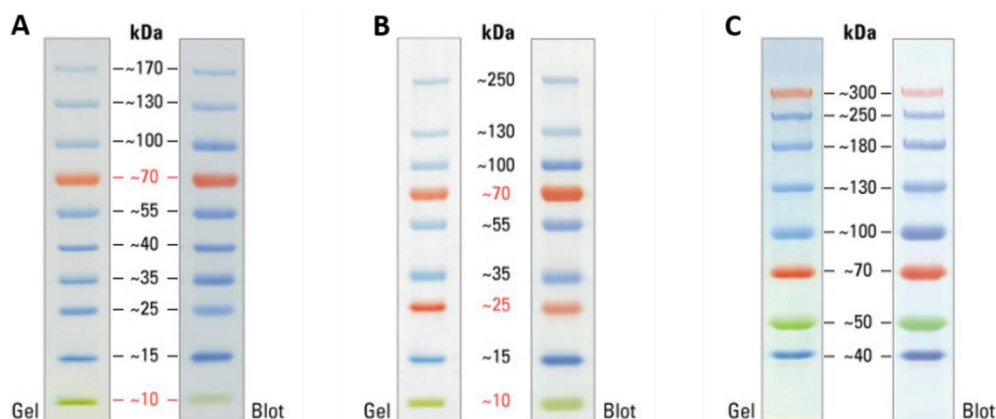


**Fig. 2.6:** The protein molecular weight standards used for SDS-PAGE. PageRuler™ Prestained Protein Ladder (A) and PageRuler™ Plus Prestained Protein Ladder (B) were utilized for normal molecular weight proteins and 4  $\mu$ l of the respective weight standard was applied per gel lane. For high molecular weight proteins, 10  $\mu$ l per lane of the Spectra™ Multicolor High Range Protein Ladder (C) served as molecular weight standard. All three protein ladders were purchased from Fisher Scientific, Schwerte.

## 2.2 Methods

### 2.2.1 Microbiological and cell biology methods

#### 2.2.1.1 Cultivation and storage of bacterial cells

Bacterial cells were cultivated in LB medium under antibiotic pressure, referring to the appropriate selection conditions, in a shaking incubator at 180-220 rpm. Agar plates were put in storage headfirst in an incubator. Optimal growing temperature for plasmid preparations was 37°C, and for bacterial cultivation and protein expression 18°C or room temperature (RT), respectively.

Short-term storage of bacteria on agar plates for days or weeks was carried out at 4°C. Bacteria destined for protein expression were not deposited for more than two days due loss of expression efficacy and thus transformed freshly prior to subsequent cultivation and expression.

Long-term storage of bacteria was facilitated by suspending 800  $\mu$ l of overnight cultures in 200  $\mu$ l sterile 80 % Glycerol solution in cryovials and subsequently freezing them at -80°C.

#### 2.2.1.2 Transformation of competent bacterial cells

Chemically competent *E. coli* bacteria were used in this study for plasmid transfer. Commercially available cell line BL21-CodonPlus-(DE3)-RIL was employed for recombinant protein expression, OneShot-Top10-cells or NovaBlue cell lines were used for replication of plasmid DNA (see 2.1.8). For transformation of the plasmid of interest, one aliquot of 20-50  $\mu$ l of competent cells was thawed on ice and mixed gently with 100 ng of plasmid DNA or 20  $\mu$ l of a ligation reaction and kept on ice for 30 min. Subsequent heat shock for 45 sec at 42°C led to the uptake of free plasmid DNA by increased bacterial membrane permeability. After heat-

shocking, cells were incubated on ice for further 2 min and 600  $\mu$ l of SOC medium were added to the specimen and incubated for 1 h at 37°C on a bacterial shaker at 220 rpm. Lastly, bacteria were streaked on LB<sub>Amp</sub> agar plates and incubated at 37°C overnight. Single colonies were picked the following day either for colony PCR, plasmid mini-preparation or mini-expression of recombinant protein.

### **2.2.1.3 *In vitro* cultivation and maintenance of *Plasmodium falciparum***

For performing the functional characterization of PfCLK kinases included in the study, *Plasmodium falciparum* was used as the model organism. Parasites were cultivated and harvested at their respective optimal conditions for subsequent experiments.

#### **2.2.1.3.1 Cultivation of *P. falciparum***

Since the development of Trager and Jensen in 1976, *in vitro* cultivation and propagation of *P. falciparum* blood cultures is commonly feasible in the laboratory. To maintain continuous asexual cultures, parasites were cultivated in small 25 cm<sup>2</sup>-cell culture flasks in a volume of 5 ml cell culture medium and A<sup>+</sup> red blood cells to reach a final hematocrit of 5 %. The medium was replenished every second day followed by gassing to obtain an optimal gas environment of 5 % O<sub>2</sub>, 5 % CO<sub>2</sub>, and 90 % N<sub>2</sub>. Once a parasitemia of 2 % was reached, the culture was passaged, whereby a parasitemia of approximately 0.5 to 1 % was not exceeded to avoid density stress and subsequent formation of sexual stages. Parasitemia was measured by preparing thin blood smears and estimating the percentage of infected erythrocytes (section 2.2.1.3.4). To purify various blood stages, the remaining culture from passaging was cultivated in 75-cm<sup>2</sup>-cell culture flasks with appropriate medium and erythrocytes.

Gametocyte maturation was performed by passaging asexual cultures with approximately 1 % parasitemia to 75 cm<sup>2</sup>-cell culture flasks and adding 15 ml cell culture medium as well as red blood cells to reach a final hematocrit of 5 %. Throughout cultivation for 10 to 20 days, sexual stage cultures were not passaged as high cell density induces formation and maturation of gametocytes. No more erythrocytes were added to the cell culture flasks for the same reason. Medium was aspirated daily and replenished, and stage progression was monitored microscopically preparing Giemsa-stained slides (section 2.2.1.3.4).

#### **2.2.1.3.2 Thawing of *P. falciparum* cultures**

The fundamental principle of thawing and recultivation of frozen plasmodial cultures displays the gentle adjustment to the level of salinity. Given the high salt level of the freezing solution, adaptation to the low salt level of the physiological conditions of the cell culture medium is indispensable. Therefore, the frozen culture was thawed on ice and transferred to a 15 ml centrifuge tube and 200  $\mu$ l of 12 % NaCl solution was added dropwise under constant agitation. After letting rest for two minutes at RT, 10 ml of a 1.6 % NaCl solution was added dropwise while shaking gently. The mixture was subsequently centrifuged for 5 min at 1 300  $\times$  g and the supernatant was discarded. For final adjustment of salt content, the cell pellet was lastly resuspended thoroughly in 10 ml of 0.2 % Dextrose/0.9 % NaCl solution, once more added dropwise. After repeated centrifugation, the cell pellet was finally resuspended

in 5 ml of the appropriate RPMI medium on 5 % hematocrit and transferred to a 25 cm<sup>2</sup>-cell culture flask for consecutive cultivation.

#### 2.2.1.3.3 Freezing and storage of *P. falciparum* cultures

For successful cryopreservation, asexual cultures with high parasitemia (3-4 %) and preferably mostly ring stage parasites were frozen by transferring the culture into a 15 ml centrifuge tube and pelleting at 1 300 × g for 5 min. After aspirating the resulting supernatant, the cell pellet was resuspended in the fivefold of the pellet's volume of Glycerolyte 57 freezing solution and relocated to 2 ml-cryotubes. After letting rest for 5 min, the tubes were frozen at -80°C for long-term storage until further required.

#### 2.2.1.3.4 Blood smear preparation and estimation of parasitemia

For preparation of Giemsa-stained blood smears, a 100 µl-aliquot of the respective culture was collected in a 1.5 ml tube and centrifuged at 3 500 × g for 1 min. The supernatant except of a twofold volume of the pellet was discarded. The cell pellet was subsequently resuspended in the remaining fluid and transferred to a glass slide. To attain a thin film of cells on the slide, a second glass slide was used (method depicted in Fig. 2.7).

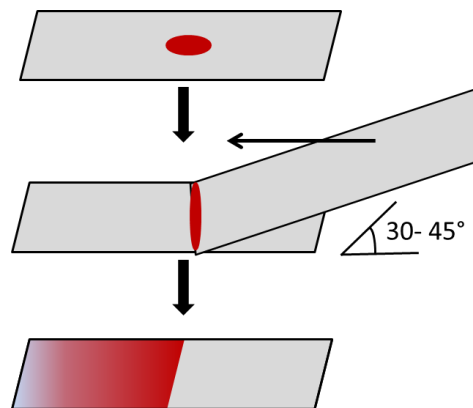


**Fig. 2.7: Preparation of a thin blood smear for determination of parasitemia.** The edge of a second slide (spreader slide) is brought in contact with the drop of blood on the first slide. The drop is allowed to bank evenly behind the spreader, which is positioned in an angle of 30-45° relative to the lying slide. Subsequently the spreader slide is pushed along the first slide in a smooth, quick motion to prepare a smear covering approximately half the glass slide.

After letting air-dry, the slides were immersed in methanol for fixation and allowed to dry followed by 5-15 min of staining with Giemsa stain solution (1:25 dilution of commercially available Giemsa stain solution with Giemsa buffer). After rinsing the stained slides with H<sub>2</sub>O<sub>bidest</sub> to remove excessive stain and subsequent air-drying, the blood smear was evaluated with a light microscope at 1 000 x magnification in oil immersion. By means of Giemsa dyeing of cells, nuclei of protozoans appear magenta, whereas the cytoplasm is colored bluish. On the contrary, erythrocytes appear light reddish. For estimation of infected RBCs, the number of parasites per 100 erythrocytes was counted for five to eight optical fields. Average parasitemia in percent was then calculated using the following formula:

$$\frac{\text{Number of infected RBCs} \times 100}{\text{Total number of RBCs (infected + non-infected)}}$$

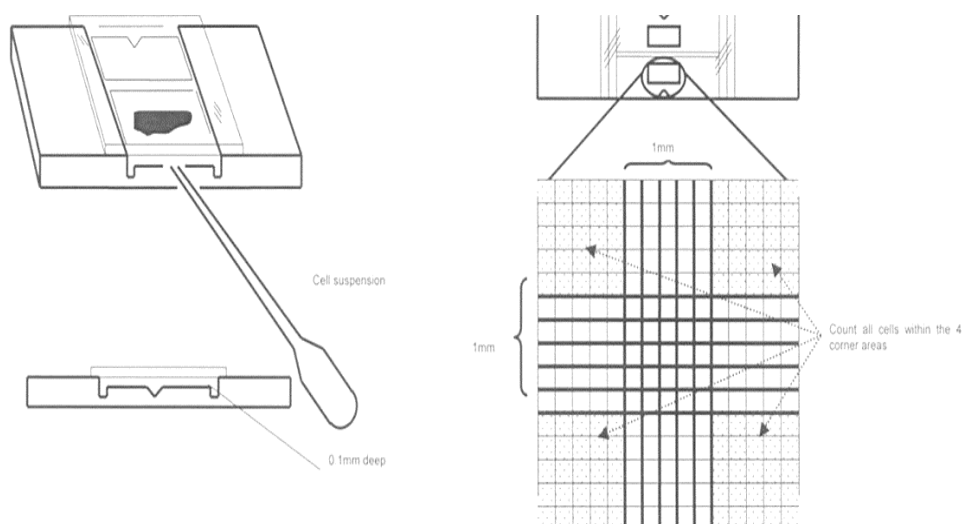


**Fig. 2.8: Neubauer hemocytometer and schematic representation of counting grid.** For determining the total number of cells per ml, the mean value of cells in the four corner areas (depicted by arrows) are multiplied with Neubauer chamber factor  $10^4$  and combined with total volume of cells, i.e. 10 ml. ([http://www.who.int/vaccines/en/poliolab/webhelp/manu779\\_04-a\\_files/image005.jpg](http://www.who.int/vaccines/en/poliolab/webhelp/manu779_04-a_files/image005.jpg)).

When seeding parasites for limiting dilution (section 2.2.1.7) or determining gametocytemia, a Neubauer hemocytometer was used for counting the number of cells in a suspension. This was conducted by placing a volume of 10  $\mu$ l of diluted sample into the chamber and counting the number of cells or parasites, respectively, in 64 small squares. Then the number of cells in 10 ml was reckoned using the below formula:

$$\text{Total number of gametocytes} = \text{mean value of gametocytes} \times 10^4 \times 10 \text{ ml}$$

#### 2.2.1.4 Synchronization and purification of asexual blood stage parasites

As the asexual development of *P. falciparum* is characterized by asynchronous stage appearance, it is indispensable to synchronize the asexual cultures when needed for stage-specific expression analyses or Malstat assay. Upon having approximately 2 % early ring stages, the parasite cultures were synchronized with 5 % sorbitol, which acts by conferring an osmotic shock to schizonts and thereby killing them. Initially, the culture was transferred into a centrifuge tube and centrifuged at  $1\,300 \times g$  for 2 min to gently pellet the cells. After aspirating the medium, the cells were resuspended thoroughly in five times pellet volume of 5 % prewarmed sorbitol solution and incubated at 37°C for 10 min, followed by centrifuging as previously to remove sorbitol. The pellet was washed once by resuspending the cells in the same volume of complete medium as sorbitol earlier and centrifuging yet again. Finally the pellet was resuspended once more in the appropriate volume of complete medium, transferred to a new culture flask and taken into culture at 37°C under appropriate gas conditions. Above procedure was repeated once at an interval of 4 h to remove newly emerged schizonts. The medium of the synchronized culture was replenished the following day after the procedure to remove dead schizonts and metabolic remnants.

To extract genomic DNA or attain purified asexual parasites for protein lysates for several applications, enveloping RBCs were lysed to release parasites. Firstly the asexual parasite culture with approximately 6-8 % parasitemia was transferred to centrifuge tubes and centrifuged at  $1\,300 \times g$  for 5 min. The resulting pellet was washed once in ice-cold 1 x PBS and subsequently resuspended thoroughly in 0.15 % saponin solution in 1 x PBS to lyse RBCs. Lysis was accomplished after 10 min of incubation on ice, then the mixture was centrifuged at  $3\,220 \times g$  for 10 min in a pre-chilled centrifuge resulting in a dark solid parasite pellet, which was washed once with 1 x PBS and consecutively stored at  $-20^{\circ}\text{C}$  or immediately resuspended in 5 x pellet's volume of lysis buffer and further processed.

#### 2.2.1.5 Purification of gametocytes using Percoll®

Gametocytes were cultured until the desired stage was obtained and purified as described previously (Kariuki et al., 1998) to attain DNA or parasites for protein lysates. All centrifugation steps and utilized solutions were carried out and prewarmed at  $37^{\circ}\text{C}$  to obviate gametocyte activation. Gametocyte cultures were pelleted at  $1\,300 \times g$  for 5 min, washed once with 10 ml RPMI incomplete medium (ICM) and taken up in 2 ml 1 x ICM. Percoll® was diluted to 90 % by addition of 10 x ICM. This solution was then diluted further with 1 x ICM to generate 80 %, 65 %, 50 % and 35 % Percoll® solutions, two ml of which were utilized as layers for a gradient, starting from the bottom with the heaviest (80 %, Fig. 2.8). The ICM-cell suspension was layered thoroughly onto the above gradient and centrifuged for 10 min at  $1\,000 \times g$ . The interphase between the 35 % and 50 % percoll layer was collected as it contains gametocytes and washed once in 1 x ICM. The gametocyte pellet was kept and stored at  $-20^{\circ}\text{C}$  for proceeding experiments.

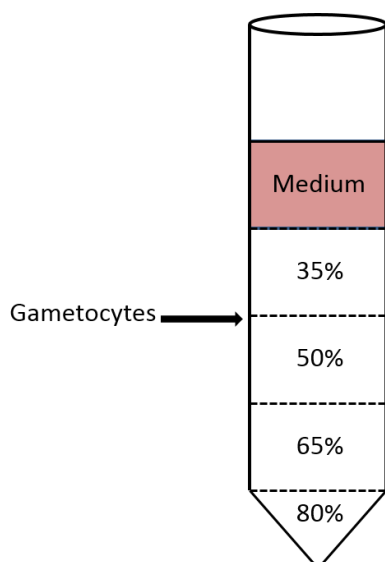


**Fig. 2.9:** Schematic depicting the different layers for percoll step gradient centrifugation method for gametocyte purification. The gametocytes are located at the interphase between the 35 % and 50 % percoll layer (indicated by arrow).

#### 2.2.1.6 Malstat assay

The CLK inhibitors were assessed in this study for evaluation of growth inhibition activity against asexual parasites of *P. falciparum* by means of a microdilution assay. Different concentrations of the compounds to be tested were utilized in Malstat viability assay as described previously (Makler and Hinrichs, 1993; Makler et al., 1993; Aminake et al., 2011). Malstat viability assay relies on the detection of the *Plasmodium*-specific enzyme lactate



dehydrogenase (pLDH), which is capable of using 3-acetylpyridine adenine dinucleotide (APAD) as NAD analogue for the back reaction of lactate to pyruvate. In contrast, human lactate dehydrogenase (hLDH) is not able to use the synthetic dinucleotide as coenzyme for redox reactions. In Malstat assay, pLDH is offered APAD along with lactate, which is metabolized to pyruvate subsequently by this enzyme. The reaction of lactate fermentation is subsequently measured in a colorimetric reaction (Makler et al., 1993). Being an essential enzyme in anaerobic glycolysis, pLDH catalyzes the reduction of pyruvate by utilizing  $\text{NADH} + \text{H}^+$  to lactate and therefore plays an important role in ATP supply during the asexual erythrocytic stage of the parasite. Employing the generated  $\text{NAD}^+$  for further process of glycolysis, *P. falciparum* utilizes the glucose metabolism pathway of the erythrocytes and expresses the hLDH homologue pLDH, which has a 200 fold faster kinetic for catalysis of APAD than the human counterpart (Gomez et al., 1997).

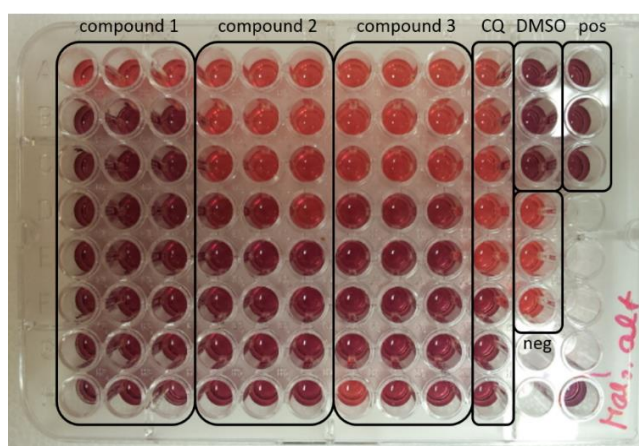


**Fig. 2.10: Malstat plate depicting a typical Malstat assay.** Compound 1, 2 and 3 are tested in triplicates (vertical rows with descending concentrations from top to bottom well), whereas chloroquine (CQ) as the positive control was tested in one column per plate. DMSO alone in a concentration of 0.5 % on parasites (DMSO) as well as parasite culture alone (pos) served as positive controls with purple colours in the wells indicating viable parasites. As negative control (neg), uninfected RBCs in a final hematocrit of 5 % were plated, with the light red coloured wells indicating the absence of viable parasites.

The CLK inhibitors were screened for growth inhibition against *P. falciparum* strain 3D7 at concentrations between 6.4 nM and 500  $\mu\text{M}$  using the Malstat assay. Sorbitol-synchronized ring stages were plated in triplicates in 96-well plates (200  $\mu\text{l}$ /well) at a parasitemia of 1 % in the presence of the compounds dissolved in DMSO. Chloroquine (diphosphate salt, Sigma-Aldrich; dissolved in double-distilled water) served as positive control in the experiments. Incubation of parasites with DMSO alone at a concentration of 0.5% vol. was used as negative control. Parasites were cultivated *in vitro* for 72 h, resuspended, and aliquots of 20  $\mu\text{l}$  were transferred and added to 100  $\mu\text{l}$  of the Malstat reagent to initiate the formation of pyruvate from parasite lactate dehydrogenase (LDH) and the release in the reaction of reduced APAD (APADH) in a 96-well microtiter plate. The assessment of pLDH activity was obtained by adding 20  $\mu\text{l}$  of a mixture of NBT (nitroblue tetrazolium)/diaphorase (1:1; 1mg/ml stock each) to the Malstat reaction and optical densities were measured at 630 nm. Each compound was tested two to four times, and the  $\text{IC}_{50}$  values were calculated from variable slope sigmoidal dose-response curves using the GraphPad Prism program version 5.

### 2.2.1.7 Limiting dilution

Upon obtaining integrant populations that were confirmed by diagnostic PCR (section 2.2.2.10), it is inevitable to separate single wild type-free parasites of the integrant population from the mixed parasite culture. For this purpose, a thin blood smear was primarily prepared to monitor parasitemia using the above mentioned formula (section 2.2.1.4.3) by counting parasites and RBCs for at least 8-15 fields. Hereinafter the number of cells per ml was then determined applying a Neubauer chamber (section 2.2.1.3.4) as follows:

$$\frac{\text{Number of erythrocytes} \times 10\,000 \times \text{dilution factor}}{\text{Number of corner squares counted}}$$

Total number of parasites per ml (p/ml) was thereafter ascertained by using succeeding formula:

$$\frac{\text{Average parasitemia}}{100} \times \frac{(\text{p/ml})}{\text{Total number of cells}}$$

In a series of dilution (three times 1:50), 24 parasites were finally plated into two 96-well microwell plates upon 5 % hematocrit and placed into the incubator within an air-tight chamber following gassing. Excess culture was cultured under normal conditions in a 25 cm<sup>2</sup>-cell culture flask and served as control for parasite growth. For each well, 160 µl of medium supplemented with BSD was replenished every second day and the plates were cultured for two to four weeks. Fresh blood was added once a week to attain a final hematocrit of 5 %. The control flask was treated accordingly. As soon as parasites could be monitored in the control flask, 20 µl of each well was transferred to new 96-well microtiter plates and parasites were detected by Malstat detection assay (section 2.2.1.6). Wells with parasites were taken into culture, checked for integration by integration PCR and integrant clones devoid of wild type bands were used for proceeding experiments.

### 2.2.1.8 Exflagellation inhibition assay

In the life cycle of malaria parasites, the maturation of microgametocytes, i.e. exflagellation, takes place in the mosquito midgut succeeding an infectious blood meal. Exflagellation inhibition assays were performed to scrutinize the activity of the evaluated CLK-inhibitors on gamete formation. Preceding the assay, an aliquot of 100 µl of the mature wild type culture was collected from the flask and activated by incubation with xanthurenic acid (XA) at a final concentration of 100 µM for 15 min. The suspension was pelleted by centrifugation at 3 500 × g for 1 min and 95 µl of the supernatant was discarded. After resuspension in the remaining 15 µl, the activated parasites were placed onto a glass slide and coated with a cover slip. The number of exflagellation centers per optical field was counted using a light microscope at 400-fold magnification. If a minimum quantity of 5 exflagellation centers per optical field were monitored, the culture was applicable for the inhibition assay. To perform the assay, the culture was preincubated for 15 min with the respective compound ranging between 0.1 and 1 000 mM or DMSO as solvent control to a final concentration of 0.5 % at 37°C. Subsequently the specimens were activated using XA for another 15 min and thereby

transferred to RT. After incubation, the suspension was yet again centrifuged and the resulting pellet processed as described above. Exflagellation centers were counted in 30 fields for each compound and DMSO-control in triplicates in two independent experiments. Exflagellation inhibition was calculated as a percentage of the number of exflagellation centers in compound-treated cultures in relation to the number of exflagellation centers in untreated DMSO controls. The  $IC_{50}$  values were calculated from variable-slope sigmoidal dose-response curves using GraphPad Prism version 5.

#### **2.2.1.9 Gametocyte toxicity assay**

In this study, gametocyte toxicity assay was utilized to evaluate the capacity of CLK inhibitors to inhibit gametocytes at their early stages, therefore preventing the formation of mature gametocytes, which is necessary for parasite transmission. *P. falciparum* wild type parasites were cultured at high parasitemia to promote gametocyte commitment. Upon obtaining stage II gametocytes, 1 ml of culture was aliquoted in triplicates in a 24-well-plate in the presence of respective inhibitor  $IC_{50}$  concentrations. As positive control, the proteasome inhibitor epoxomicin was used in a final concentration of 30 nM (Aminake et al., 2011). In contrast, chloroquine (CQ) in a final concentration of 40 nM served as negative control, as CQ has the ability to kill asexual parasites, but not sexual stage parasites. This compound rather stimulates gametocyte commitment due to stress reasons (Buckling et al., 1999). Besides negative and positive control, DMSO was used as solvent control, as all tested inhibitors were solved in DMSO. The aliquots were cultivated within the influence of the inhibitors for 48 h. After the 48 h-treatment, the cultures in the wells were further maintained for additional five days to allow healthy gametocytes to mature to stage IV and V in compound-free medium. Medium was replenished daily by replacing 800  $\mu$ l compound-free medium. At day 7, Giemsa-stained blood smears were prepared and gametocytemia was monitored by counting the numbers of gametocyte stages IV and V in a total amount of 1 000 erythrocytes per inhibitor/well. The gametocytes in each setting were counted in triplicates. Two independent experiments were performed and the mean gametocytemia was calculated for each compound. Data from the experimental cultures was normalized to the DMSO control, which was set to 100 % and the Student's t-test was performed for statistical analysis of the obtained data.

#### **2.2.1.1 Stage-of-inhibition assay**

To determine the stage of inhibition, synchronized ring stage parasites (T0) were supplemented with CHX, KH-CARB10, KH-CARB11, KH-CARB13xHCl and gea-27 in concentrations of their determined  $IC_{50}$  values (0.8, 7.5, 6.1, and 4.0  $\mu$ M, respectively; determined by Malstat viability assay, section 2.2.1.6) and  $IC_{80}$  values (4.0, 37.0, 30.0 and 20.0, respectively; calculated by usage of GraphPad QuickCalcs), plated in triplicates in 96-well plates. Blood smear samples were taken at 12 h, 24 h, 36 h, 48 h, 60 h and 72 h of inhibitor incubation. The numbers of ring stages, trophozoites, schizonts as well as amounts of dead parasites were counted for a total number of 100 infected erythrocytes for each setting. Ring stage parasites initially treated with 0.5 % DMSO served as negative control parasites.

### 2.2.1.2 Indirect immunofluorescence assay (IFA)

To study the stage-specific expression and cellular localization of the PfCLK kinases and SR proteins in *P. falciparum* in this study, indirect immunofluorescence assays were conducted. Aliquots of synchronized parasite cultures at ring, trophozoite and schizont stages as well as non-activated gametocytes were obtained (according to the experimental design), centrifuged for 1 min at 3 550 × g and the supernatant was discarded to a great extent. Cells were resuspended and placed in thin layers onto the wells of Teflon IFA slides (Carl Roth). Following air-drying, fixation was carried out by incubating the slides for 10 min in -80°C cold methanol. To label the SR proteins, parasites were fixed with 4 % paraformaldehyde (pH 7.4). Dried IFA slides were incubated in permeabilization/blocking solution for 30 min at RT and subsequently further blocked for 30 min in permeabilization/blocking solution supplemented with 1 % neutral goat serum (Sigma-Aldrich) to block unspecific binding sites. In case of paraformaldehyde-fixed samples, permeabilization was deployed with 0.1 % vol. Triton X-100 and 125 mM glycine (Carl Roth) in PBS for 30, followed by blocking with 3 % BSA in PBS for 1 h. Specimens were then incubated for 1.5 -2 h at 37°C with primary antibodies against the respective kinase, diluted in blocking solution. For double-labeling experiments, slides were consecutively incubated with the respective primary stage-specific antibody originating from different animal species than the kinase antibody. Thereafter, specimens were washed twice with IFA blocking solution to remove unbound antiserum. Binding of primary antibodies was subsequently prepared for visualization by incubating the slides with fluorophore-conjugated goat-derived secondary antibody (Alexa Fluor® 488 or Alexa Fluor® 594, respectively, Molecular Probes) against the origin species of primary antibodies used in the experiment. Incubation of secondary antibody was carried out for 1 h at 37°C. To avoid bleaching of the conjugated fluorescence dye, all succeeding washing and staining steps were protected from light. Final washing steps in 1 x PBS removed exceeding secondary antibodies. After rinsing of slides twice times for 5 min in 1 x PBS, samples were finally counterstained with Hoechst nuclear stain (diluted 1:5 000 in 1 x PBS; Molecular Probes) for dyeing of nuclei. After repeated rinsing in 1 x PBS for two times, specimens were dried and subsequently mounted in Antifading CitiFluor® Mounting Medium (LTD, London), subsequently covered with a cover slip and sealed with nail polish to avoid drying out of the specimens. Immunolabeled IFA slides were subsequently examined by confocal fluorescence microscope (Leica or Zeiss). Digital images were processed using the manufacturers' image editing software of the respective microscope or Adobe Photoshop CS software.

## 2.2.2 Molecular biology methods

### 2.2.2.1 Genomic DNA isolation

Genomic DNA was isolated from purified asexual blood stages of *P. falciparum* using the NucleoSpin® Blood Kit according to the manufacturers' protocol. Prior to the isolation, parasites were purified with 0.15 % saponin as mentioned above (section 2.2.1.4). For DNA elution, 50 µl of sterile H<sub>2</sub>O<sub>bidest</sub> were used instead of the buffer provided by the manufacturer. The DNA concentration was subsequently determined photometrically using NanoDrop spectrophotometer (Peqlab) measuring absorption at 260 nm.

### 2.2.2.2 Polymerase chain reaction

Polymerase chain reaction (PCR) was used to amplify kinase and splicing factor (subunit) sequences for recombinant protein expression as well as diagnostic PCR to identify episomal integration of the pCAM-BSD plasmid for reverse genetic studies. Two diverse polymerases were utilized in this study: Regarding the cloning procedure preparative to recombinant protein synthesis, Phusion® High-Fidelity DNA Polymerase was used as this enzyme possesses a 3'→5'-exonuclease activity that reduces the error rate and furthermore generates blunt-ended products. Gene-specific nucleotide sequences of desired proteins were obtained from the PlasmODB database and the program Primer3 was employed to design primers for each of the constructs. In case of introns prevailing in the gene of interest, cDNA was used as PCR template, which was kindly provided by Dr. Shruti Agarwal.

For colony PCR as well as integration PCR, GoTaq® DNA Polymerase was employed as proof reading activity is abdicable for these purposes. Its provided 5 x Buffer is supplemented with blue and yellow dyes which renders further adding of loading buffer dispensable.

The master mix for a PCR reaction was prepared as follows:

**Table 2.10: Pipetting scheme for PCR reactions using GoTaq® or Phusion® Polymerase, respectively.**

GoTaq® DNA Polymerase		Phusion® High-Fidelity DNA Polymerase	
Reagent	Final conc.	Reagent	Final conc.
gDNA*	100ng/μl	gDNA/cDNA	100ng/μl
5 x GoTag® Flexi buffer	1 x	5 x Phusion® HF buffer	1 x
MgCl <sub>2</sub> (25 mM)	2 mM	-	-
dNTPs (10 mM stock)	0.2 mM	dNTPs (10 mM stock)	0.2 mM
Sense primer (100 μM)	1 μM	Sense primer (100 μM)	1 μM
Antisense primer (100 μM)	1 μM	Antisense primer (100 μM)	1 μM
GoTaq® DNA Polymerase (5 U/μl)	1.25 U	Phusion® High-Fidelity DNA Polymerase (2 U/μl)	1.0 U

\*in case of colony PCR, one single colony was diluted in 10 μl of distilled water.

The PCR reaction was supplemented with sterile H<sub>2</sub>O<sub>bidest</sub> to reach a final volume of 50 μl. Following program was employed for amplification of gene products of interest:

**Table 2.11: Thermocycler programs for GoTaq® and Phusion® polymerase. T<sub>M</sub> = Primer melting temperature.**

Step type	GoTaq® DNA Polymerase		Phusion® High-Fidelity DNA Polymerase	
	Temperature	Time	Temperature	Time
Initial Denaturation	95°C	2 min	98°C	30 s
Denaturation	95°C	40 s	98°C	7 s
Primer annealing	lowest T <sub>M</sub> -5°C	50 s	lowest T <sub>M</sub> -5°C	30 s
Elongation	72°C	1 min/kb	72°C	30 s/kb
Final elongation	72°C	5 min	72°C	5 min
Cycle number	35		33	

### **2.2.2.3 Agarose gel electrophoresis**

As the phosphate residues confer a negative charge to nucleic acids, the same can be separated in an electric field due to their size. For this purpose, an inert matrix of agarose was utilized in this study. Resolved DNA fragments were visualized by using ethidium bromide (EtBr) solution. Ethidium bromide intercalates into the major groove of DNA and fluoresces when exposed to ultraviolet (UV) light, thus visualizing the migrated DNA fragments. In this study, 1.0 % agarose gels were employed to evaluate PCR products as well as to resolve digested DNA fragments out of a certain plasmid for subsequent gel purification (section 2.2.2.4).

For preparing 1 % agarose gels, the appropriate amount of agarose was solved in 1 x TAE buffer and subsequently brought to the boil. After cooling down to roughly 50°C, either EtBr was supplemented to a final concentration of 0.5 µg/ml or the latter gel with separated fragments was incubated for 15 min in a bath which was diluted with EtBr 1:10 000 in H<sub>2</sub>O<sub>bidest.</sub> After polymerization, samples were resuspended in 6 x DNA sample buffer for increase of density and denaturation of secondary structures. Subsequently specimens were loaded on gel, as well as a DNA size standard for estimation of fragment sizes (section 2.1.14). The gel was run with electric field strength of 6 V/cm. If the gel was not yet supplemented with EtBr previous to loading and running, the same was incubated in an EtBr solution bath after separating the fragments entirely. The separated DNA fragments were visualized and documented with a transilluminator and images were processed with Adobe Photoshop CS software.

### **2.2.2.4 Purification of DNA fragments**

DNA fragments were either purified directly after PCR/digestion or, in case of purification of vector-containing insert, firstly separated on an agarose gel and excised by using the NucleoSpin® Extract II Kit (Macherey-Nagel) according to the manufacturer's protocol. The underlying principle of the purification kit is based on the DNA's ability to bind to silica membranes in the presence of high saline buffers. In contrast, contaminations like oligonucleotides, genomic DNA or enzymes pass the silica column as they are not capable of binding to silica membranes. After washing of DNA, it can be easily eluted from the silica column by resuspension with water or TE buffer.

### **2.2.2.5 DNA digestion via restriction endonucleases**

Restriction endonucleases are enzymes of prokaryotic origin which are able to recognize palindromic sequences and cut DNA specifically at this sequences. In this study, restriction endonucleases were purchased from New England Biolabs (NEB) for preparing spin-purified inserts as well as target vectors for final ligation destined to cloning.

Digestion of inserts/vectors was carried out as follows:

**Tab. 2.12: Pipetting scheme for digestion reactions.**

Reagent	Digestion of insert	Digestion of vector
DNA	3 µg	5 µg
10 x buffer (NEB)	5 µl	5 µl
10 x BSA	5 µl	5 µl
Restriction enzyme 1	1 µl	1 µl
Restriction enzyme 2	1 µl	1 µl
H <sub>2</sub> O <sub>bidest</sub> , sterile	add up to 50 µl	add up to 50 µl

The reaction mixture was incubated for at least 2 h at 37°C. Concerning vector digestion, 1 h prior to the experiment's end, 1 µl of calf intestine phosphatase (CIP) was added to the digestion reaction. CIP removes phosphate residues from DNA ends and thus averts vector religation. The digested vectors were loaded on agarose gels where the respective bands were cut out and spin-purified or, in case of insert fragments, merely spin-purified to remove residual enzymes and contaminations prior to ligation.

#### 2.2.2.6 Ligation of DNA fragments

For ligation of DNA fragments, T4 DNA Ligase was used which catalyzes the joining of double stranded DNA by generation of phosphoric diester bonds between 3'-hydroxy residues and 5'-phosphate residues. For cloning in this study, the molar ratio of vector to insert was set 1:3. The amount of insert required for ligation was calculated using the following formula:

$$\text{Amount of insert [ng]} = \frac{\text{amount of vector [ng]} \times \text{fragment length [bp]} \times 5}{\text{length of vector [bp]}}$$

The reaction volume was prepared as depicted in Tab. 2.13 and incubated for at least 3 h at 16°C or overnight at 4°C. For further transformation, 2 µl of the ligation reaction was added to competent *E. coli* cells (section 2.2.1.2).

**Tab. 2.13: Pipetting scheme for ligation reactions.**

Reagent	Volume
Digested insert DNA	x µl
Digested vector DNA [50ng/µl]	y µl
10 x Ligation buffer	2 µl
T4 DNA ligase (NEB)	1 µl
H <sub>2</sub> O <sub>bidest</sub>	add up to 20 µl

#### 2.2.2.7 Amplification and extraction of plasmid DNA

Transformed *E. coli* strains (section 2.2.1.2) were cultivated in 3-5 ml LB medium under appropriate selection conditions overnight at 37°C on a bacterial shaker. Cells were harvested and underwent alkaline lysis for extraction of plasmid DNA. Depending on the projected purpose, two distinct kinds of preparation were used: on the one hand, a curtailed type of preparation was employed for analysis of bacterial clones after transformation of ligation reactions (Dirty mini). On the other hand, if DNA of higher purity was required for

transformation or sequencing, plasmid mini preparation was utilized by means of commercially available NucleoSpin® Plasmid Kit (Macherey-Nagel) according to the manufacturer's protocol. Principally both preparations are premised on the same alkaline lysis step associated with precipitation with isopropyl alcohol; however the commercially available kit employs silicate membranes for further increase of purity of DNA.

For the variant of Dirty mini plasmid preparation, 3 ml of bacterial culture were inoculated and kept shaking overnight at 37°C. After harvesting cells via centrifugation at 13 000 × g for 5 min, they were resuspended in 100 µl of Solution 1, which was supplemented with RNase. Subsequently cells were lysed by addition of 200 µl of Solution 2 and gently mixed by inverting the tubes, as vortexing would lead to an unwanted shearing of DNA, and incubated on ice for 5 min. For neutralization, 150 µl of Solution 3 were supplemented and specimens were again inverted and incubated on ice for further 5 min. Thereafter, RNA was removed by adding 450 µl of 5 M LiCl and centrifuged for 15 min at 16 060 × g after 5 min incubation on ice. The resulting supernatant was transferred to a new tube and DNA was precipitated using 0.6 proportion of volume isopropyl alcohol, for these tubes were inverted, incubated at RT for 10 min and finally centrifuged for 10 min at 16 060 × g. The resulting DNA pellet was subsequently washed once with 200 µl of 70 % ethanol and dried at RT until no ethanol residues could be traced. The pellet was resuspended lastly in 30 µl H<sub>2</sub>O<sub>bidest</sub> and stored at -20°C for future purposes.

#### 2.2.2.8 Colony PCR and control digestion

For analysis of single transformant bacterial colonies, colony PCR as well as control digestion analysis was conducted. Regarding colony PCR, five single colonies were picked separately the following day after transformation (section 2.2.1.2) with a disposable pipette tip and transferred into PCR reaction tubes containing 10 µl H<sub>2</sub>O<sub>bidest</sub>. The single colonies were resuspended and PCR reaction was prepared using GoTaq® DNA polymerase as described previously (Tab. 2.7). For amplification of inserts prevailing in transformed bacterial colonies, insert primers respective to the cloned insert were employed. Thermocycler program for GoTaq® DNA polymerase was used as mentioned above (Tab. 2.8). In case of positive clones attained by colony PCR, gDNA of overnight cultures was prepared as itemized in section 2.2.2.4. Isolated plasmid DNA was control digested using the following pipetting scheme:

**Tab. 2.14: Pipetting scheme for control digestion of purified plasmid DNA from transformant bacterial colonies.**

Reagent	Volume
10 x Reaction buffer	1 µl
10 x BSA	1 µl
Miniprep-DNA	5 µl
Restriction enzyme 1	0.5 µl
Restriction enzyme 2	0.5 µl
H <sub>2</sub> O <sub>bidest</sub>	2 µl



Restriction endonucleases were purchased from New England Biolabs (NEB) in conjunction with provided buffers.

### 2.2.2.9 Sequencing

Upon having verified correct size of vector and insert fragment by control digestion, the purified plasmid DNA from plasmid mini preparation (section 2.2.2.4) was quantified using spectrophotometer NanoDrop ND-2000 (Peglab). 700 ng of purified plasmid DNA and 20 pmol of the appropriate sequencing primer were subsequently added to sterile H<sub>2</sub>O<sub>bidest</sub> to a final volume of 7 µl and sent for “Extended HotShot sequencing” to SeqLab sequence laboratories (Göttingen). Sequences were analyzed utilizing BioEdit or Clone Manager, respectively, and NCBI nucleotide BLAST®.

### 2.2.2.10 Genotype characterization by diagnostic integration PCR

Vectors used for transfecting asexual parasite stages were cloned and transfected (kindly provided and carried out by Dr. Shruti Agarwal). Once the transfectant parasite population was growing, gDNA was isolated from enriched asexual parasites as mentioned (section 2.2.1.5 and 2.2.2.1) and utilized in diagnostic PCR for genotype characterization. For that purpose, primers were designed that bind to the 5′- and 3′-end of the amplified kinase gene locus.

Primers were used in the following combinations (see section 2.1.12):

Combination A	Amplification of wild type gene locus
Combination B	Amplification of episome (epi)
Combination C	Amplification of 5′-integrated gene locus (5′int)
Combination D	Amplification of 3′-integrated gene locus (3′int)

Diagnostic PCR reactions were carried out using GoTaq® DNA polymerase and were composed of reagents as mentioned above (Tab. 2.7). Reaction parameters are listed in Tab. 2.8.

## 2.2.3 Protein biochemistry methods

### 2.2.3.1 Expression of recombinant proteins

*P. falciparum* proteins were expressed recombinantly in *E. coli* for generation of antigens to raise mouse polyclonal antibodies as well as to directly apply the recombinant proteins in interaction studies like kinase activity assays. Depending on the size and the demanded part of the respective protein, either a small fraction of a protein domain or the full size recombinant protein was designed and generated. Recombinant proteins were expressed as fusion proteins with a GST-tag using the pGEX 4T1 vector or with a MaBP-tag using the pIH vector (section 2.1.10) in *E. coli* BL21-CodonPlus®-(DE3)-RI cells. Cloning was conducted by addition of restriction sites to the ends of PCR-amplified gene fragments complying with the respective protein domains (Fig. 1.6).

### Mini protein expression

To confirm protein expression of the respective tagged recombinant protein, single colonies of transformed *E. coli* BL21-CodonPlus®-(DE3)-RIL cells were picked and transferred into 3 ml LB<sub>Amp/Cam</sub> overnight preculture. The following day, each preculture was diluted in duplicates 1:5 with LB<sub>Amp/Cam</sub> as one reaction serves as negative control. The diluted cultures were subsequently grown in a shaking incubator at 37°C until the optical density reached 0.5 at a wavelength of 600 nm (OD<sub>600</sub>). At this time point, the bacteria are in the log phase of growth. As both expression plasmids possess the *lac* operon, protein expression can be initiated by adding the artificial substrate IPTG (isopropyl-β-D-thiogalactoside, Life Technologies). One of the two cultures yielded by one single clone was induced by supplementing IPTG at a final concentration of 0.75 mM whilst the other culture served as negative uninduced control. Cultures were shaken and incubated for further 3 h at 30°C for expression of recombinant protein. Thereafter, 30 µl of samples were acquired, diluted with 2 x SDS sample buffer containing 25 mM DTT and boiled at 95°C for 10 min to denature protein structures. Samples were finally loaded onto a SDS-gel and separated for analysis (section 2.2.3.5).

### Maxi protein expression

Upon having verified the proper expression of recombinant proteins by mini protein expression mentioned above, protein expression was conducted in a large scale to attain an appropriate concentration of the recombinant protein. Consequently, 20 to 50 ml of freshly transformed overnight culture was diluted 1:10 in an appropriate volume (2-6 l per recombinant protein construct) and further grown at 37°C on a shaking platform. Once the OD<sub>600</sub> of 0.5 and hence the exponential growth phase was reached, cultures were initially cooled down for 30 min to RT or 18°C and subsequently induced with IPTG in a final concentration of 0.75 mM as mentioned above. To ensure a slower and thus more precise expression and folding of the synthesized recombinant protein in bacteria, temperature was decreased for that purpose to RT or preferably 18°C. Incubation of induced cultures on a shaking platform was carried out for at least 4 h to overnight and thereafter harvested by centrifugation of the bacterial cultures for 5 min at 4°C and 5 000 × g. Cell pellets were subjected to lysis immediately or stored until further use at -20°C.

#### **2.2.3.2 Purification of recombinant proteins**

All steps were conducted on ice as well as all samples, buffers, centrifuges and tubes were prechilled at 4°C.

### Purification of soluble recombinant GST-tagged proteins

Bacterial pellets attained above were resuspended initially in lysis buffer and incubated for at least 1 h on a tumbler at 4°C. Cell disruption was thereafter performed using a French® Press by applying 1 200 psi pressure in three subsequent cycles, whereas DNA degradation was conducted furthermore by pulse sonication of the sample for 2 min at 50 % intensity and 50 cycles. The resultant sample was centrifuged at 15 000 × g for 1.5 h at 4°C to separate the proteinaceous supernatant from the remaining cell debris. Clear supernatant was

subsequently collected and filtered through a 0.22  $\mu\text{m}$  syringe filter. At the same time, Glutathione sepharose 4FastFlow beads (GE Healthcare) were prepared by washing three times with ice-cold 1 x PBS. 500  $\mu\text{l}$  of washed beads were added to the above filtered protein containing supernatant and incubated overnight on a tumbler under gentle rotation at 4°C to favour selective binding of GST-tagged proteins to sepharose beads. The following day, the mixture was loaded onto a PolyPrep® column (Bio-Rad) and allowed to pass through the matrix where GST-tagged proteins selectively bound to sepharose were retained, whereas unbound proteins passed through the matrix. Three times washing with 1 x PBS followed whereby all flow-through washing steps were retained for analysis. Lastly the proteins were eluted with GST elution buffer in three fractions of 1-3 ml each. Fractions were stored at -20°C, destined to SDS-PAGE and protein yield and concentration were corroborated by comparing band intensities of purified proteins with protein bands of known BSA concentrations.

#### Purification of soluble recombinant MaBP-tagged proteins

The harvested cell pellet acquired from maxi expression was washed once with 1 x PBS and thereafter resuspended in 3 ml of MaBP lysis buffer containing 1 mM PMSF and 80  $\mu\text{l}$  of lysozyme (stock 10 mg/ml) per g pellet. DNA degradation was conducted by sonicating the sample for 2 min at 50 % intensity and 50 cycles. Cell lysis was then induced by adding 6  $\mu\text{l}$  of 1 M  $\text{MgCl}_2$  and 0.08 g NaCl per ml to the lysate followed by incubation on a rotating mixer for 1 h at 4°C. Subsequent separation of cell debris and proteinaceous supernatant by means of centrifugation at 15 000  $\times$  g for 1.5 h at 4°C and afterwards filtering of supernatant using a 0.22  $\mu\text{m}$  syringe filter was conducted. In the meantime, 1 ml of amylose resin was washed three times with 1 x TE buffer and finally added to the filtered supernatant. Incubation overnight on a tumbler at 4°C conducted binding of MaBP-tagged proteins to the amylose resin beads whilst other untagged proteins did not bind to the resin. The following day, batch elution of MaBP-tagged proteins was carried out by initially spinning down the resin for 5 min at 60  $\times$  g with decreased deceleration. Subsequent washing steps were carried out 3 times using column buffer without supplemented maltose. All supernatants were saved and processed for SDS-PAGE analysis. For elution of proteins, 8 ml of column buffer with maltose was added to the washed beads, incubated for at least 20 min on a rolling mixer at 4°C and centrifuged for 5 min at 60  $\times$  g. This elution step was repeated and samples of elution fractions were processed for determination of concentration via SDS-PAGE. Protein concentrations were estimated by comparison of stained SDS-gels showing a dilution series of BSA proteins of known concentrations. Specimens were stored at -20°C up to further use.

#### Purification of inclusion bodies

In case of limited yield of soluble recombinant proteins which were subjected merely to immunization and subsequent generation of antibodies, the alternative choice of purifying recombinant proteins as inclusion bodies was the method of choice. Therefore, an expression and purification protocol of the company ImmunoGlobe (Himmelstadt) was utilized. Inclusion bodies represent cellular and nuclear protein aggregates which are composed of denatured

proteins formed through excessive overexpression in bacterial cells. Inclusion bodies are not membrane bound and often reversibly misfolded.

Following maxi expression and harvesting of cells, lysis was implemented by resuspending the pellet in 80 ml of lysis buffer and supplementing another 20 ml of lysis buffer with 20 mg of lysozyme. After incubation on ice for 30 min, the sample was sonicated as described above and the lysate was resuspended in 200 ml of Detergent buffer followed by centrifugation at  $5\,000 \times g$  for 10 min. Thereafter the pellet was washed with 200 ml of washing buffer each, until the pellet became solid and less viscous. It was subsequently thoroughly washed once with 70 % ethanol. Finally the pellet was resuspended in 2-5 ml of freshly prepared sterile PBS and sonicated to enable the proteins to pass through a 23 G needle which was used later on for immunization of mice. Protein concentration was estimated by loading the samples onto a SDS-gel and comparison of specimen with the protein ladder to calculate the appropriate amount for immunization. Moreover, the approximate protein concentrations were confirmed by comparing the band intensities with protein bands of known BSA protein concentrations. Inclusion body preparations were stored at  $-20^{\circ}\text{C}$  until further use.

### **2.2.3.3 Immunization of mice and generation of mouse polyclonal antibodies**

Specific immune sera were generated by the immunization of six week-old female NMRI mice. Beforehand, the purified soluble proteins were buffer-exchanged and concentrated using Millipore Amicon centrifugal filters with nominal molecular weight limits suitable for the molecular weight of the protein to be concentrated. Regarding recombinant proteins purified from inclusion bodies, usage of Amicon filters was dispensable. Concentrated protein solution was transferred from the Amicon centrifugal unit and resuspended in sterile 1 x PBS/5 % glycerol, followed by scrutiny of concentration by means of SDS-PAGE. 100  $\mu\text{g}$  of recombinant protein or inclusion bodies for each mouse were dissolved in 200  $\mu\text{l}$  of sterile PBS and emulsified in Freund's incomplete adjuvant which acts as immunopotentiator. After an interval of four weeks, mice were boosted with 100  $\mu\text{g}$  of soluble protein solution or 50  $\mu\text{g}$  of inclusion bodies, respectively, supplemented with Freund's incomplete adjuvant as mentioned above. Ten days later mice were anesthetized by intraperitoneal injection of a mixture of ketamine and xylazine according to the manufacturer's protocol (Sigma-Aldrich), and immune sera were then collected via heart puncture. Sera from non-immunized mice served as control for antibody reagent studies.

### **2.2.3.4 Preparation of parasite lysates and nuclear extract**

Parasite pellets attained by either saponin lysis (section 2.2.1.4) or gametocyte purification (section 2.2.1.5) were lysed subsequently in an appropriate volume of PMSF lysis buffer for 10 min on ice and thereafter sonicated for approximately 30 seconds at 50 % intensity and 50 cycles to degrade DNA. Consecutively the protein solution was separated from the cell debris by centrifugation at  $13\,000 \times g$  for 10 min at  $4^{\circ}\text{C}$ . Resulting supernatant containing parasite proteins was transferred into a sterile pre-chilled 1.5 ml tube and was either stored at  $-20^{\circ}\text{C}$  or preferably used freshly in subsequent SDS-PAGE or kinase activity assays (sections 2.2.3.5 or 2.2.3.8). Total protein concentration was measured by means of Bradford assay (Bio-Rad).

For preparation of nuclear extracts, parasite pellets gained by saponin lysis were initially washed with 1 x PBS and subsequently resuspended in Buffer A supplemented with protease inhibitor cocktail and incubated for 10 min at RT. After centrifugation at 13 000 × g for 10 min at 4°C, the supernatant containing the cytoplasmic fraction was transferred to a new reaction tube and the resultant pellet was resuspended in Buffer B. The resuspended pellet was then shaken vigorously for 2 h at 4°C followed by centrifugation at 13 000 × g for 5 min at 4°C. Nuclear fraction of parasite pellets was represented by the resulting supernatant and purity was confirmed by Hoechst labeling of nuclei (kindly conducted by Dr. Shruti Agarwal). Nuclear extract as well as cytoplasmic fraction was then immediately used for further analyses or kept at -20°C for future purposes.

### 2.2.3.5 SDS polyacrylamide gel electrophoresis

SDS polyacrylamide gel electrophoresis (SDS-PAGE) was utilized for separation of a protein mixture in an electrical field due to their different molecular weights. The strong anionic detergent sodium dodecyl sulfate (SDS) ensures a linearization of proteins and confer a uniform negative charge so that the proteins migrate to the anode and are separated on the basis of their molecular weight. Further denaturation of proteins is ensured by adding β-mercaptoethanol, which reduces disulfide linkages. Varying percentage of resolving gels (in this study 10 % and 12 %) were prepared according to the size of the protein to be identified. A stacking gel of 5 % served as starting zone for the protein separation in the resolving gel, composition given below (Tab. 2.14). TEMED and APS were added lastly to initiate polymerization of the gel.

**Tab. 2.15:** Composition of different SDS gels (stacking and resolving). Volumes refer to one mini-gel.

	Resolving gel		Stacking gel
	10 %	12 %	5 %
<b>H<sub>2</sub>O<sub>bidest</sub></b>	1.9 ml	1.6 ml	1.4 ml
<b>30 % acrylamide</b>	1.7 ml	2.0	0.33 ml
<b>1.5 M Tris pH 8.8</b>	1.3 ml	1.3 ml	-
<b>0.5 M Tris pH 6.8</b>	-	-	0.25 ml
<b>10 % SDS</b>	50.0 µl	50.0 µl	20.0 µl
<b>10 % APS</b>	50.0 µl	50.0 µl	20.0 µl
<b>TEMED</b>	2.0 µl	2.0 µl	2.0 µl

The samples were prepared in 2 x SDS sample buffer supplemented with 25 mM DTT and heated for 10 min at 95°C and afterwards cooled down for 2 min on ice to denature the proteins further. For gel electrophoresis, the Mini-PROTEAN® electrophoresis system was utilized (Bio-Rad, Munich). Specimens were loaded onto the gel and allowed to resolve for approximately 15-20 min at 80 V until they migrated out of the stacking gel. Separation was then run at 120 V until the desired separation was achieved. The gel was subsequently either used in a Western blot analysis (section 2.2.3.6) or washed three times in distilled water for further staining with GelCode®-Blue Stain (Pierce, Thermo Fisher, Rockford, USA) on a Mini rocker shaker according to the manufacturer's protocol. Long-term gel preservation was

conducted by incubating the gel with a solution of 10 % glycerol/20 % ethanol for 30 min and subsequently dried between cellophane sheets in a gel drying frame (Roth, Karlsruhe) for up to two days at RT.

### 2.2.3.6 Western blot analysis

For immunodetection, proteins were separated by SDS-PAGE (section 2.2.3.5) and subsequently transferred to Hybond ECL Nitrocellulose membrane (Amersham Biosciences, Munich). For this purpose, the Mini Trans-Blot® apparatus was employed (Bio-Rad, Munich) and constructed according to the manufacturer's protocol (Fig. 2.11), using transfer buffer. Particular attention was paid that no air bubbles persisted between the gel and the nitrocellulose membrane. The transfer was subsequently transformed for either 2 h at 25 V or overnight at 15 V. The membranes were thereafter washed once for 5 min in 1 x TBS to dispose of the methanol-containing transfer buffer. Subsequently the blocking of non-specific protein binding sites was conducted by incubating the membrane in blocking solution for Western blotting containing BSA and milk powder for at least 1 h at RT. After washing the blocked membrane for three times with 1 x TBS to remove blocking solution, the same was incubated with the respective primary antibodies diluted in TBSM for 2 h at RT or overnight at 4°C under constant agitation.

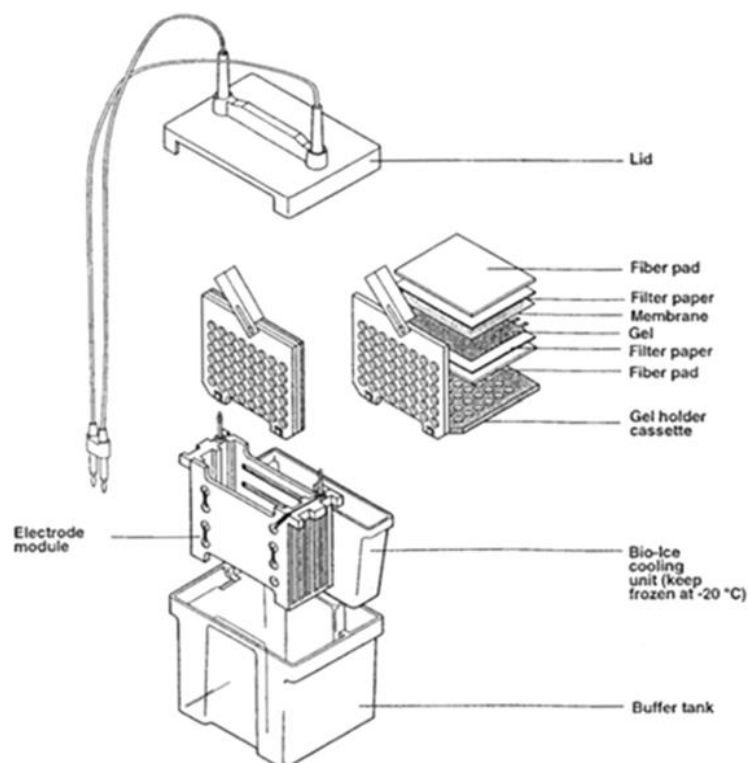


**Fig. 2.11: Assembly of Mini Trans-Blot® Western blotting apparatus from Bio-Rad, Munich.** The cassette holds the gel and the nitrocellulose membrane between buffer-saturated filter papers and fiber pads, followed by vertical insertion of the cassette in the electrode module inside the transfer tank filled with transfer buffer. The cassette is then placed between the anode and the cathode, thus being ready for transferring.

After removing unbound antibodies by washing 10 min each with TBSM, twice with TBSM-T and once again with TBSM, the corresponding secondary antibody conjugated with alkaline

phosphatase was diluted in TBSM and added to the membrane. Binding of the respective secondary antibody was conducted by incubation for 1 h at RT under constant agitation. To remove excessive antibodies, the membrane was subsequently washed once with 1 x TBS, twice with TBS-T and again with 1 x TBS for 10 min each. Thereafter, the membrane was equilibrated for 3 min in equilibration buffer and subsequently the membrane was developed by adding one NBT (nitroblue tetrazoliumchloride)/BCIP (5-bromo-4-chloro-3'-indolylphosphate) tablet (Sigma-Aldrich) which was previously dissolved in 10 ml H<sub>2</sub>O<sub>bidest</sub> for 1 to 15 min, depending on the desired signal intensity and background staining. The detection reaction was then stopped by rinsing the developed membrane in stop buffer.

### **2.2.3.7 Co-immunoprecipitation assay**

Co-immunoprecipitation (Co-IP) is the technique of precipitating a protein antigen out of intact protein complexes using an antibody that specifically binds to the protein of interest, also called bait-antibody. Co-IP is a powerful method for isolation and concentration of this particular protein from a mixed protein sample, together with binding partners of the protein of interest. Initially, parasite lysates attained from wild type NF54 or tagged cultures were processed as described above (section 2.2.1.4) and subsequently pre-cleared by means of successively adding 5 % v/v of pre-immune serum and 20 µl of PBS-washed protein G-beads (Santa Cruz Biotechnology, Heidelberg) and incubation for 30 min each at 4°C. Depending on the origin species of the latter used bait antibody, pre-immune sera was utilized from the same species for pre-purification, in this study pre-immune serum from mouse, rat and rabbit, respectively. Pre-clearing of lysates was then completed by centrifugation of specimens at 3 500 × g for 5 min at 4°C and the supernatant containing the pre-purified parasite protein lysate was transferred in new pre-chilled reaction tubes. Further incubation of the lysates with the appropriate amount of anti-kinase (bait) antibody for at least 1 h at 4°C on a tube agitator was followed by successive incubation with 20 µl of PBS-washed protein G beads each. Incubation of beads was carried out overnight to ensure appropriate binding of the protein-antibody complex to the protein G beads. The following day, the supernatant was removed by centrifugation at 3 500 × g for 5 min at 4°C and the bead-immunocomplexes were washed three to five times with ice-cold 1 x PBS. For succeeding kinase activity assay, the immunocomplexes were washed lastly with 5 x kinase buffer. In case of SDS-PAGE, the specimens were solely resuspended with an equal volume of SDS loading buffer containing DTT (see section 2.2.3.5) and loaded onto an SDS gel for verification or processing via Western blotting.

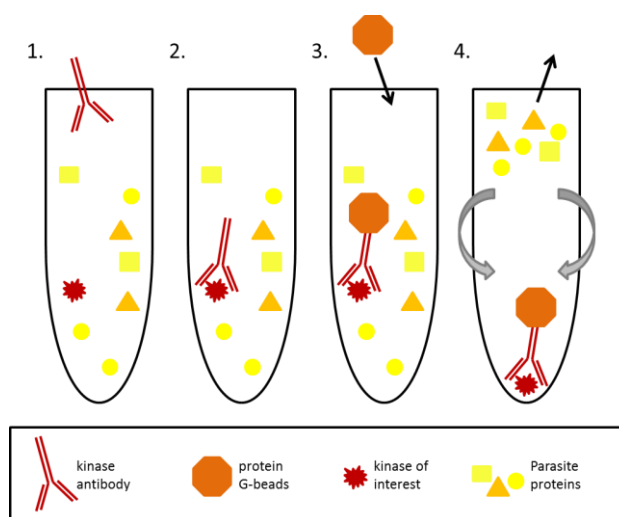


**Fig. 2.12: Schematic depicting the principle of Co-IP.** 1. Specific antibodies are utilized that target the respective kinase in the parasite lysate which 2. then bind the kinase in the solution. 3. Subsequently added protein G coated beads bind the Fc region of the antibodies to form an immunocomplex. 4. Washing and centrifugation of the immunocomplex separates it from the remaining parasite proteins in the solution, which can be thoroughly aspirated.

### 2.2.3.8 Kinase activity assay

For investigating phosphorylation activity of the PfCLK kinases *in vitro*, kinase activity assays were performed with radioactive labeled ATP proceeding co-immunoprecipitation (section 2.2.3.7) of the respective PfCLK from wild type NF54 lysates. The kinase reaction was either supplemented by the exogenous substrates histone H1, myelin basic protein (MBP) and  $\alpha$ - $\beta$ -casein or recombinant plasmodial SR proteins destined to be investigated as putative PfCLK substrates. In case of testing the effect of CLK inhibitors in the kinase activity assays, sorbitol-synchronized ring stages were incubated with the inhibitors at approximate  $IC_{80}$  concentrations for 12 h prior to generation of lysates for immunoprecipitation. In the event of preincubated Npl3p, no further substrates were added as Npl3p was already added to the parasite lysate within the scope of Co-IP. A standard kinase reaction of 30  $\mu$ l was conducted in a standard kinase buffer and prepared as follows:

**Tab. 2.16: Composition of a standard kinase reaction for kinase activity assay.**

Reagent	Volume
5 x kinase buffer	6 $\mu$ l
Exogenous substrates/recombinant protein (10 $\mu$ g)	y $\mu$ l
ATP-mix	5 $\mu$ l
Sterile H <sub>2</sub> O <sub>bidest</sub>	x $\mu$ l
<b>Final volume</b>	<b>30 <math>\mu</math>l</b>

60  $\mu$ M ATP non-radiolabeled was prepared by mixing 75  $\mu$ l dH<sub>2</sub>O<sub>bidest</sub> and 5  $\mu$ l of 1 mM ATP stock. Further, a mixture of 4.75  $\mu$ l 60  $\mu$ M ATP and 0.25  $\mu$ l 0.1 MBq [ $\gamma$ -<sup>32</sup>P] ATP was prepared per reaction. This 5  $\mu$ l mixture of radiolabelled and non-radiolabelled ATP was added to the above 25  $\mu$ l reaction, scaling the final volume of 30  $\mu$ l kinase reaction. Reactions were incubated at 37°C for 1 h under constant agitation and terminated by addition of 8  $\mu$ l of



2 x sample buffer (section 2.1.7) for 5 min at 100°C. Samples were separated on 12 % SDS-PAGE (section 2.1.7 and 2.2.4.4) and the gel was dried followed by exposing it to an X-ray film. The film was incubated at -20°C for 48-90 h and developed to detect the phosphorylation signal. For negative control, purified GST- or MaPB-tag alone was used for substrate in the kinase activity assays. An additional negative control, in which the parasite lysate was replaced by the same volume of 1 x PBS (PBS control), was used to exclude unspecific phosphorylation of reaction components. Recombinantly expressed His<sub>6</sub>-tagged protein kinase 6 (rPK6), purified as previously described (Bracchi-Ricard et al., 2000), was used as a positive control for the kinase activity assay using exogenous substrates. For quantification of inhibition of phosphorylation, the mean grey values (MGV) for the DMSO control were set to 100% to calculate the relative MGV (rMGV).

## 3 Results

### 3.1 Functional characterization of the PfCLKs

The CMGC group of eukaryotic kinases displays the vastest group in the plasmodial kinome. Although members of the CDK, MAPK and GSK3 families have been investigated extensively, scant research has been undertaken up to date regarding the fourth family, the CDK-like kinases (CLK) in *P. falciparum*. The four members belonging to this family, PfCLK-1/LAMMER, PfCLK-2, PfCLK-3 and PfCLK-4, are most probably assigned to be involved in mRNA processing and transport. They represent dual specificity kinases with the ability to autophosphorylate tyrosine residues, but phosphorylate their specific substrate proteins solely on serine/threonine residues (Bullock et al, 2009). Previous studies revealed a primarily nucleus-associated expression of PfCLK-1 as well as PfCLK-2 in asexual parasites, with both kinases revealing essentiality for the replication cycle of asexual parasites (Agarwal, 2010; Agarwal et al., 2011). Furthermore, immunoprecipitated PfCLK-1 and PfCLK-2 exhibited *in vitro* phosphorylation activity on exogenously added substrates (Agarwal, 2010; Agarwal et al., 2011). As scarce research has been conducted regarding the remaining family members PfCLK-3 and PfCLK-4, functional characterization studies were performed by means of immunofluorescence assays and Western blots in the present study in order to scrutinize the stage-specific expression of both kinases. Moreover, the recombinogenicity of the *pfclk-3* and *pfclk-4* loci was determined by reverse genetic approaches in order to permit any reliable forecasts on the essentiality of the plasmodial CLKs. Similarly as it was carried out for PfCLK-1 and PfCLK-2 (Agarwal, 2010), phosphorylation capability of PfCLK-3 and PfCLK-4 was determined by kinase activity assays.

#### 3.1.1 Protein expression analysis of PfCLK-3 and PfCLK-4 in *P. falciparum* stages

The protein expression profile of the two plasmodial CDK-like kinases PfCLK-3 and PfCLK-4 was investigated in this study. For the detection and verification of stage-specific expression of PfCLK-3, attempts to generate a recombinant protein were made using primers from regions covering portions of the catalytic domain. Two different primer pairs were utilized resulting in diverse fragments of the catalytic domain of PfCLK-3 with a size of 41.1 and 30.4 kDa, respectively. The recombinant proteins were fused to an N-terminal GST-tag (26.0 kDa) resulting in a size of 67.1 and 56.4 kDa, respectively and named PfCLK-3 rp1 and PfCLK-3 rp2. Purification of either PfCLK-3 rp1 or rp2 was conducted as soluble proteins as well as inclusion bodies. As the concentration of soluble GST-tagged protein after two independent purification steps was too low for immunization of mice (Fig 3.1) and was diminished furthermore after buffer exchange via Amicon centrifugal units (not shown), merely the inclusion body purified recombinant proteins (Fig. 3.2) were viable and therefore used for immunization of mice.

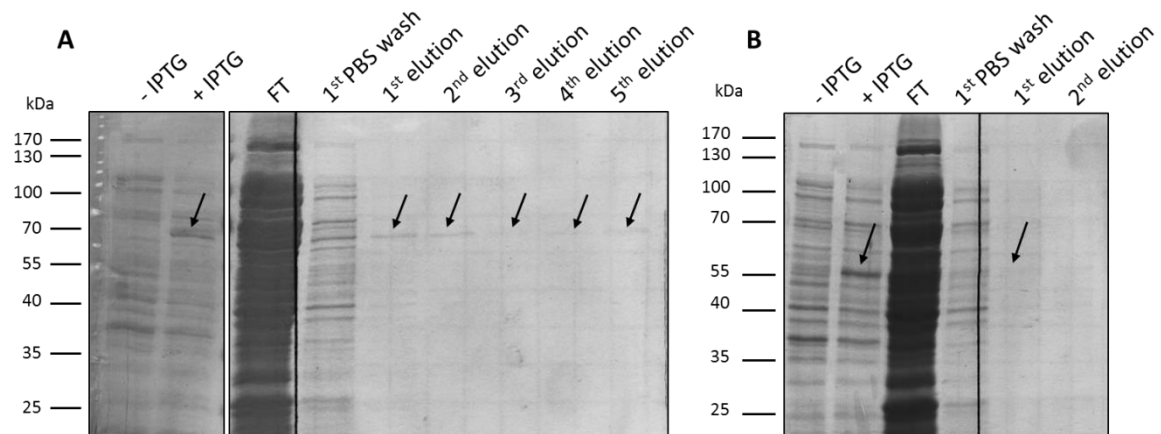


**Fig. 3.1: Generation of GST-tagged recombinant PfCLK-3 fragments as soluble proteins for polyclonal antibody production in mice.** Bacterial overnight cultures of one clone for each plasmid was induced with IPTG (+ IPTG) to induce transcription. Uninduced cultures (- IPTG) were cultivated as negative transcription controls. Large scale purification revealed protein bands migrating at the respective molecular weight of the purified protein by means of SDS-PAGE and subsequent Coomassie blue staining. **A.** A first fragment from the catalytic domain, PfCLK-3 rp1, was recombinantly expressed in *E. coli* at the expected size of 67.1 kDa in all five elution steps, however only in marginal concentrations (indicated by arrows). **B.** A second, 30.4 kDa portion of the catalytic domain of PfCLK-3, rp2, was N-terminally fused with GST and expressed recombinantly with a complete size of 56.4 kDa only in very low concentrations in the first elution step (arrows). FT: flow-through of bacterial protein lysate, PBS wash: flow-through of washed column.

Generated polyclonal mouse antisera based on purified inclusion bodies of PfCLK-3 rp1 were utilized in Western Blot analysis (Fig. 3.3 B) and revealed protein expression in lysates of asexual parasites (ASEX, using the gametocyte-less strain F12) and of gametocytes (GC, using the gametocyte-producing strain NF54). The detected protein bands migrated at the calculated full-length of PfCLK-3 (81.0 kDa).

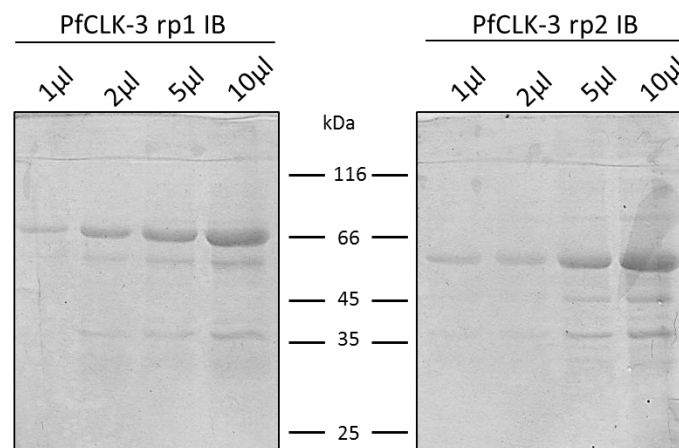


**Fig. 3.2: Synthesis of PfCLK-3 rp1 and rp2 purified from bacterial inclusion bodies.** Inclusion body (IB) specimens were diluted 1:10 in 1x PBS prior to loading onto the SDS gel to avoid overloaded bands due to highly concentrated protein preparations. Preparations were loaded in different volumes for estimation of protein concentration destined to subsequent immunization of mice. Staining of SDS-gels was conducted by means of Coomassie blue staining.

A similar expression pattern was achieved using antibodies against the recombinant fragment PfCLK-3 rp2 (not shown). Full size protein bands were furthermore observed in nuclear pellet fractions of asexual parasites (NP) and cytoplasmic fractions (CF). Preparation of nuclear pellet fractions of asexual parasites, the corresponding cytoplasmic fractions and nuclei verification by means of Hoechst staining were kindly provided and carried out by Dr. Shruti Agarwal (Agarwal, 2010). No protein bands were detected in lysates of uninfected erythrocytes (EC) incubated with the mouse anti-PfCLK-3 antibody or when neutral mouse serum (NMS) was used on asexual parasite lysates (ASEX).

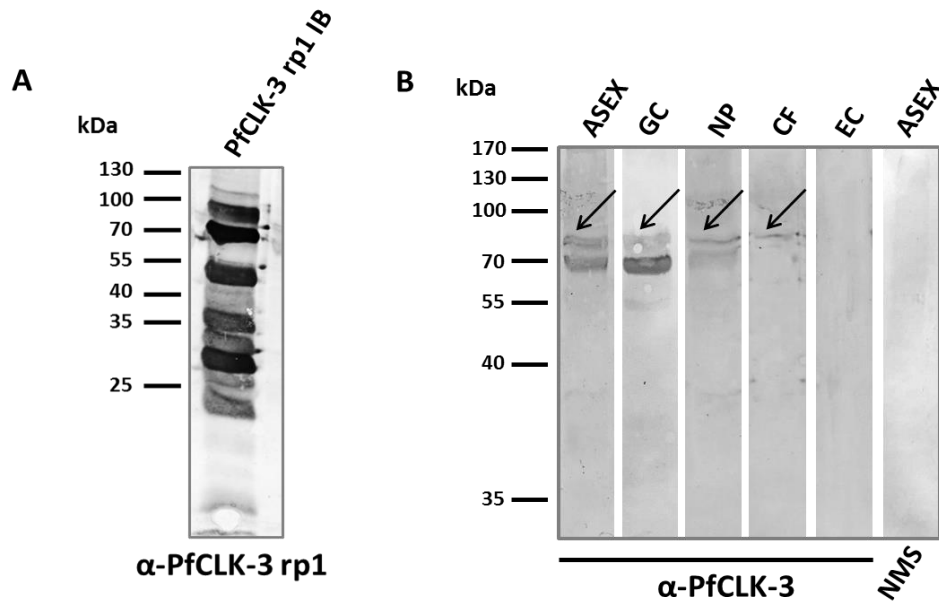


**Fig. 3.3: Verification of PfCLK-3 antisera for expression studies.** **A.** Western Blot on the inclusion body-derived recombinant protein PfCLK-3 rp1 was performed to verify the detection of the 81.0 kDa protein by the antiserum generated against it. Inclusion body preparations were diluted 1:10. **B.** Protein level expression of PfCLK-3 in blood stage parasites by means of Western blot analysis. Protein bands at sizes of 81.0 kDa and approx. 70.0 kDa (indicated by arrows) were detected. For kinase detection in asexual parasites, lysates of the gametocyte-less strain F12 (ASEX) and for detection of gametocytes, lysates of the gametocyte-producing strain NF54 (GC) were utilized. Neither in lysates of uninfected erythrocytes (EC) nor in asexual parasite lysates blotted with neutral mouse serum (NMS), specific bands could be detected.

Antibodies against both fragments raised from inclusion bodies were not capable of detecting the kinase by means of indirect immunofluorescence assays (IFA). For this purpose, antibodies kindly provided by Andrew Tobin (MRC Toxicology Unit, Leicester, UK) were used for expression studies in IFA. Therefore, specific rat antibodies against PfCLK-3 were raised by immunizing rats with peptide YKSKHEENSPDGDSY (AA30-44) and purified by protein G as described previously (Solyakov et al., 2011).

Immunolabeling with rat anti-PfCLK-3 antibody exhibited a labeling of the kinase which is associated with the nucleus of trophozoites. However, in schizonts the kinase seems to be displacing to the parasite cytoplasm (Fig 3.4, upper panel) with a rim-associated expression especially in latter stages. An analogical detection of PfCLK-3 was observed in the cytoplasm of stage IV and stage V gametocytes with a substantial rim-associated labelling pattern (Fig 3.4, lower panel). Asexual parasites were counterstained with antibodies against the

merozoite surface protein MSP-1, and gametocytes were labeled with antibodies against the sexual stage protein *Pfs230*.

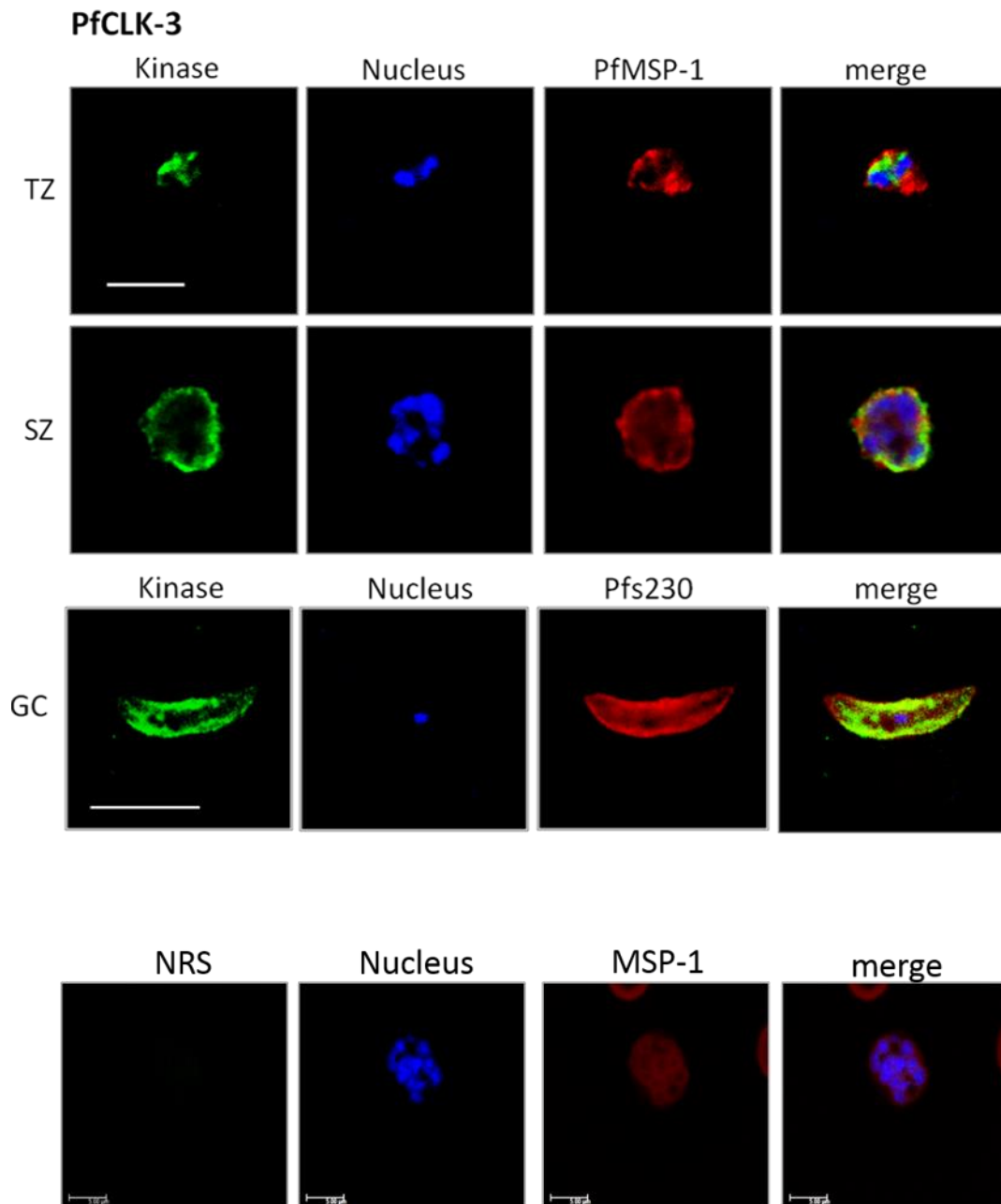


**Fig. 3.4: Expression analysis of PfCLK-3 by the use of rat antisera.** Indirect immunofluorescence assays were performed using rat polyclonal antibodies directed against a portion of the kinase. Whereas the kinase labeling can be detected in association with the parasite nucleus in trophozoites (TZ), the kinase appears to be more distributed into the periphery of the cytoplasm of schizonts (SZ). In gametocytes, a likewise rim-associated labelling of PfCLK-3 is observed. Kinase labeling was visualized with Alexa Fluor488 secondary antibody (green). Neutral rat serum (NRS) was used in IFA and showed no binding (lower panel). Asexual parasites were detected with antibodies against the merozoite surface protein PfMSP-1, whereas gametocytes were labeled with antibodies against the sexual stage protein *Pfs230*. Parasite nuclei were highlighted by means of Hoechst staining.(blue). Bar, 5  $\mu$ m.

For investigation of protein expression of PfCLK-4, a 51.6 kDa fragment of the catalytic domain was selected to be recombinantly expressed in *E. coli*. The recombinant fragment of the catalytic domain sequence was fused to an N-terminal GST-tag with a size of 26.0 kDa, resulting in a 77.6 kDa recombinant fusion protein, PfCLK-4 rp4. Overnight bacterial cultures expressed the fusion protein after transcription induction by means of IPTG (section 2.2.3.1) which was verified by Western blot detection utilizing antisera against the GST-tag (Fig. 3.5 A). Affinity purification (Fig 3.5 B) as well as subsequent buffer exchange and concentration by means of Amicon centrifugal units (Fig. 3.5 C) was carried out and GST-tagged fusion protein PfCLK-4 rp4 was obtained, which was further used for immunization of mice for raising polyclonal antibodies against a region of the catalytic domain of PfCLK-4.

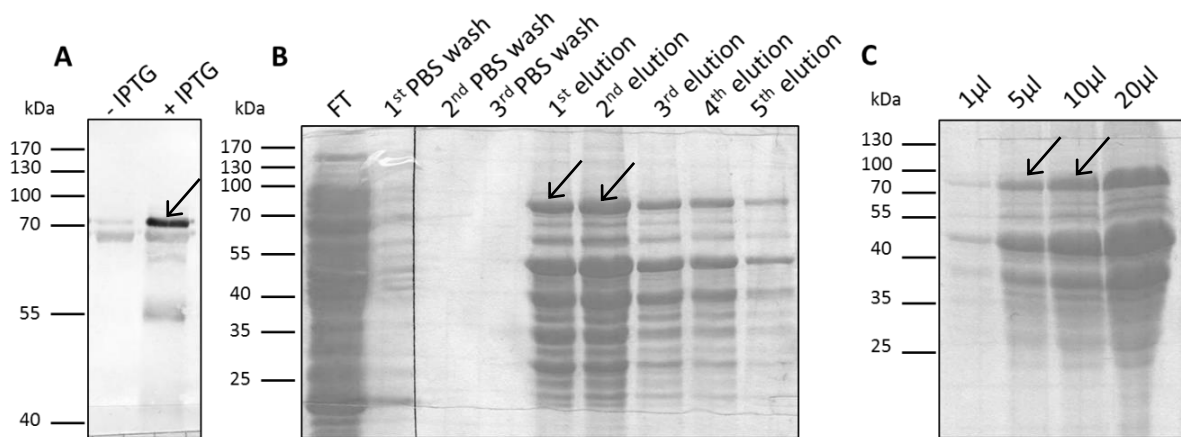


**Fig. 3.5: Generation of GST-tagged recombinant PfCLK-4 rp4.** A fragment from the catalytic domain was fused to GST N-terminally and recombinantly expressed in *E. coli*. **A.** Western Blot of bacterial overnight culture lysates to detect PfCLK-4 rp4-GST by antisera against the GST-tag. Bacterial overnight cultures of one clone for each plasmid was induced with IPTG (+ IPTG) to initiate transcription. Uninduced cultures (- IPTG) were cultivated as negative transcription controls. **B.** SDS-PAGE of large scale purification revealed protein bands migrating at the respective molecular weight of the purified recombinant fusion protein PfCLK-4 rp4 (77.6 kD, arrows). **C.** SDS-PAGE for estimation of protein concentration after buffer exchange and concentration with different dilutions of eluate loaded onto the gel. Staining of SDS-gels was conducted by Coomassie blue staining. FT: flow-through of bacterial protein lysate, PBS wash: flow-through of washed column.

In conformity with transcription data (Agarwal, 2010; Agarwal et al., 2011), immunoblotting revealed protein expression in lysates of asexual blood stages with bands migrating at the calculated full-length molecular weight of PfCLK-4 (157 kDa, Fig. 3.6.B). In addition, bands of lower molecular weight (100 kDa; 70 kDa) were detected in mixed asexual parasite lysates. Similar lower molecular weight bands were obtained in lysates of mature gametocytes (GC) and cytoplasmic fractions (CF) of asexual parasites. To experimentally verify the presence of PfCLK-4 in the parasite nucleus, nuclear pellet fraction from mixed asexual parasite stages was collected and employed in Western blot analysis. A full-length protein of 157 kDa was detected in the nuclear pellet of asexual parasites (NP, Fig. 3.6 B). No protein bands were detected in lysates of uninfected erythrocytes (EC) or in asexual parasites incubated with neutral mouse serum (NMS), both used as negative controls.

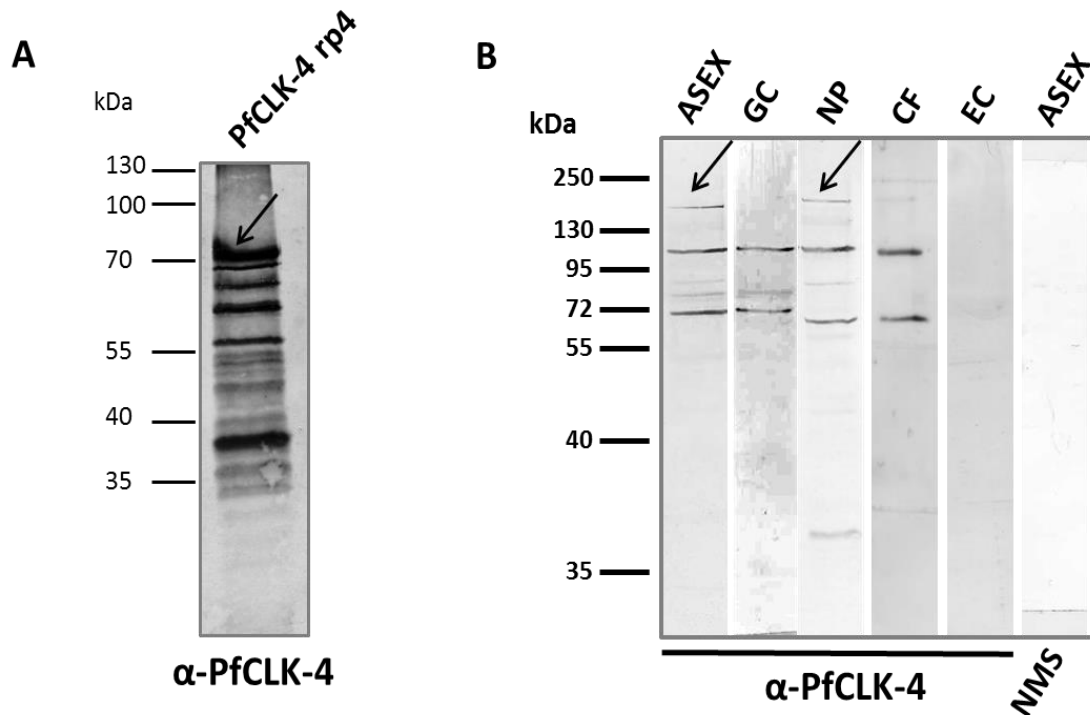


**Fig. 3.6: Determination of antisera directed against PfCLK-4 for expression studies.** **A.** Western blot analysis for evaluation of PfCLK-4 antibodies. Immunoblotting of mouse antiserum directed against GST-tagged fusion protein PfCLK-4 rp4 (diluted 1:20) revealed bands at the expected size of 77.6 kDa. **B.** Western blot analysis for stage-specific expression of PfCLK-4. Mouse-derived polyclonal antibodies against recombinantly expressed fusion protein of PfCLK-4 rp4 revealed protein bands with full-length kinase bands (157 kDa) in asexual parasite lysates (ASEX) as well as nuclear pellet preparations (NP), alongside with processed kinase bands running at 100 and 70 kDa, respectively. Exclusively the truncated kinase fragments could be detected in gametocytes (GC) and cytoplasmic fractions (CF). Neither in lysates of uninfected erythrocytes (EC) nor in asexual parasite lysates incubated with neutral mouse serum (NMS), specific kinase bands could be detected.

Protein expression of PfCLK-4 was scrutinized by immunofluorescence assays on *P. falciparum* wild type strain NF54. Immunolabeling detected the presence of PfCLK-4 in the nucleus and cytoplasm of both asexual stages, trophozoites (TZ) as well as schizonts (SZ). Similarly, in gametocytes the kinase was detected in both cellular compartments with the specific mouse antisera. Kinase labelling was carried out with Alexa Fluor488 secondary antibody and nuclei were highlighted with Hoechst staining. Asexual parasites were counterstained with antibodies against the merozoite surface protein PfMSP-1, and gametocytes were labeled with antibodies against the sexual stage protein *Pfs230*.

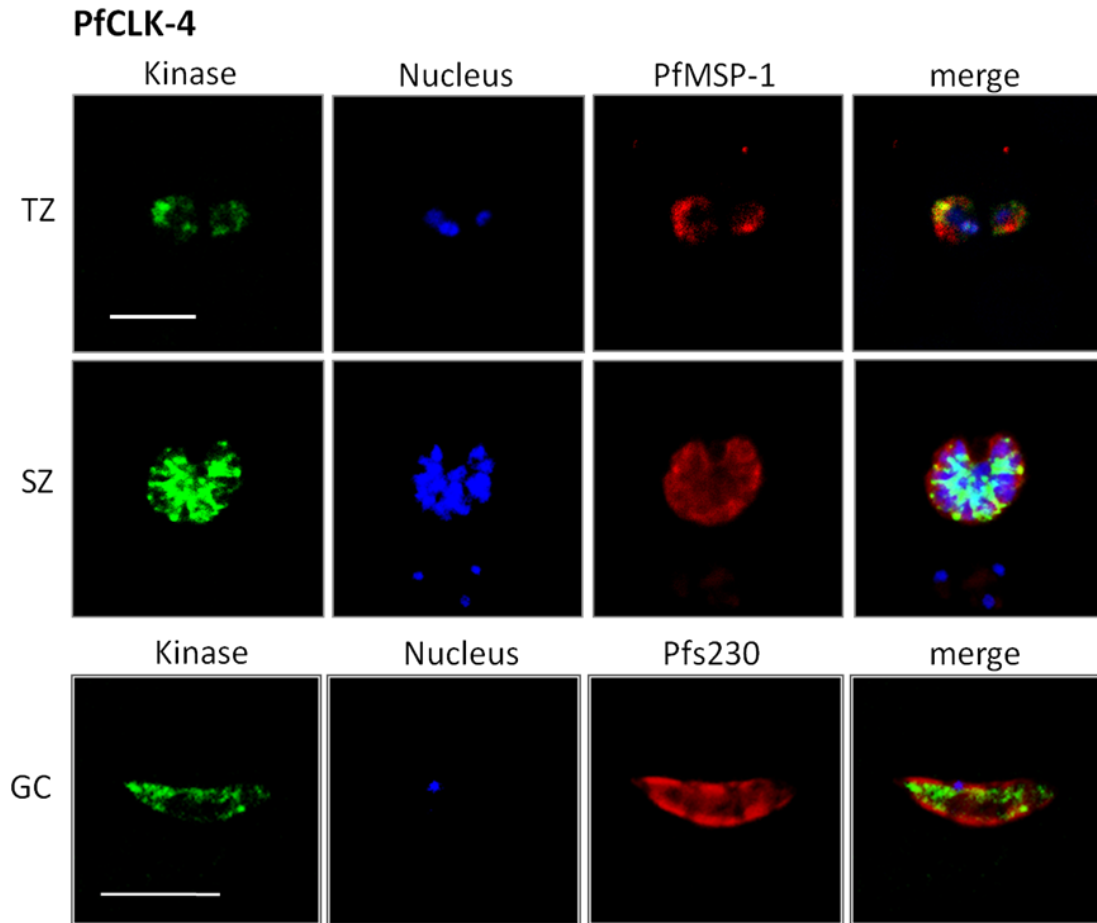


**Fig. 3.7: Protein expression analysis of PfCLK-4.** IFAs were performed using polyclonal antibodies. Whereas the kinase labeling can be detected in association with the parasite nucleus as well as the cytoplasm in both investigated asexual stages, trophozoites (TZ) and schizonts (SZ). In gametocytes (stage IV shown here), a similar distribution can be observed. Kinase labeling was visualized with Alexa Fluor488 secondary antibody (green). Asexual parasites were detected with antibodies against the merozoite surface protein PfMSP-1, whereas gametocytes were labeled with antibodies against the sexual stage protein Pfs230. Parasite nuclei were highlighted by means of Hoechst staining. Bar, 5  $\mu$ m.

### 3.1.2 Reverse genetic studies on PfCLK-3 and PfCLK-4

For investigating the cellular function of the PfCLK kinases, reverse genetic approaches (Dorin-Semblat, 2007) were utilized to confirm whether PfCLK-3 or PfCLK-4 are indispensable for the completion of the asexual replication cycle. This approach aims at the verification whether the kinases play an essential role in the parasite's lifecycle. In an initial attempt, the respective PfCLK knock-out (KO) was aimed to be generated via a single cross-over homologous recombination technique, deploying the pCAM-BSD vector (Sidhu, 2005). This KO-vector encompasses the insert corresponding to a portion of the respective kinase catalytic domain and furthermore a resistance cassette conferring resistance to blasticidine (BSD) to mutant parasites. For a successful homologous recombination, the respective kinase insert of the KO-vector is designed homologous to the endogenous kinase gene, which is attempted to be knocked out. In case of integration of this vector into the genome of *P. falciparum*, a gene-disruptant, pseudo-diploid gene locus arises, in which the ATP-binding



region is disjointed from the proline-glutamate-rich (PE) motif, resulting in a disrupted catalytic domain and thus a non-functional, truncated enzyme. Cloning of KO-pCAM-BSD vector for PfCLK-3 and for PfCLK-4 was kindly carried out by Dr. Shruti Agarwal (Agarwal, 2010).

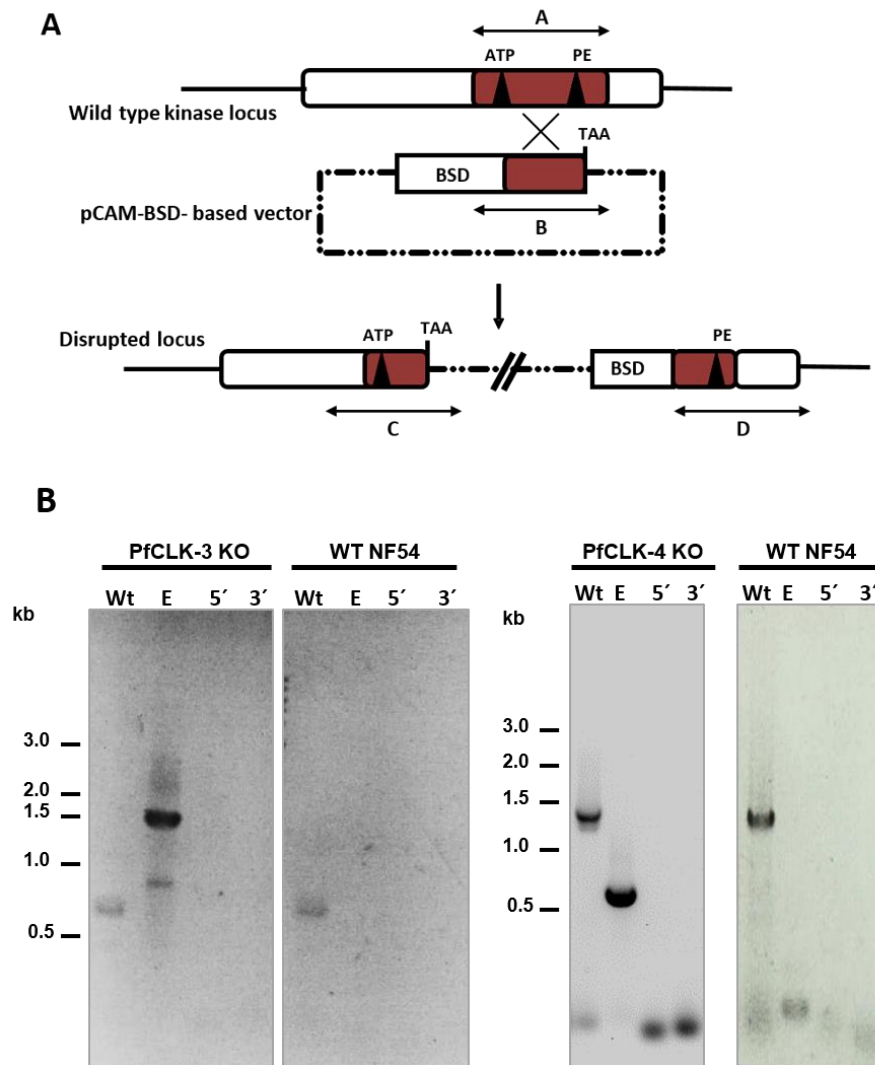


**Fig. 3.8: Generation of gene-disruptant parasites by means of reverse genetics.** **A.** Schematic of knock-out (KO)-strategy by single cross-over homologous recombination utilizing the pCAM-BSD vector. Primer combinations used for discrimination between wild type (A), episomal presence (B), 5'-integration (C) and 3'-integration (D) of the transfection plasmid are indicated by arrows. Modified from Agarwal, 2010; Agarwal et al., 2011. Primer combination A: amplification of wild type (Wt) gene locus; primer B: amplification of episome (E); primers C: diagnostic for 5'-integration of plasmid; primers D: diagnostic for 3'-integration of plasmid. BSD: blasticidine drug resistance cassette. ATP: ATP binding motif. PE: Proline-glutamate motif. **B.** Molecular analysis of PfCLK-3 and PfCLK-4 KO attempts by reverse genetic approaches. Diagnostic PCR from total DNA of pCAM-BSD- PfCLK-3-KO vector transfected parasites showed amplification only for the wild type (Wt, 594 bp) and episomal gene locus (E, 794 bp, observed dimerization of amplicons). No amplification was observed for PfCLK-3-KO attempts at the sizes of the 5'- or 3'-integration concatemers. Similarly as observed for PfCLK-3-KO, no integration of PfCLK-4-KO plasmid was demonstrated. Only the wild type (1.48 kb) and non-integrated episomal band (672 bp) could be detected. Wild type parasites of strain NF54 were used as a control of the wild type locus.

Electroporated parasites were cultivated under the influence of selection medium containing BSD, and after onset of drug pressure for both PfCLK-3 and PfCLK-4, drug-resistant

subpopulations emerged after three weeks, although the number of parasites was initially reduced. For both plasmodial kinases, only parasites containing the non-integrated episomal plasmids were detected by means of diagnostic PCR (section 2.2.2.10), even after prolonged cultivation for more than 20 weeks. In addition, a second attempt of transfection followed by cultivation, gDNA isolation and PCR amplification led to the same result (Fig 3.8 B).

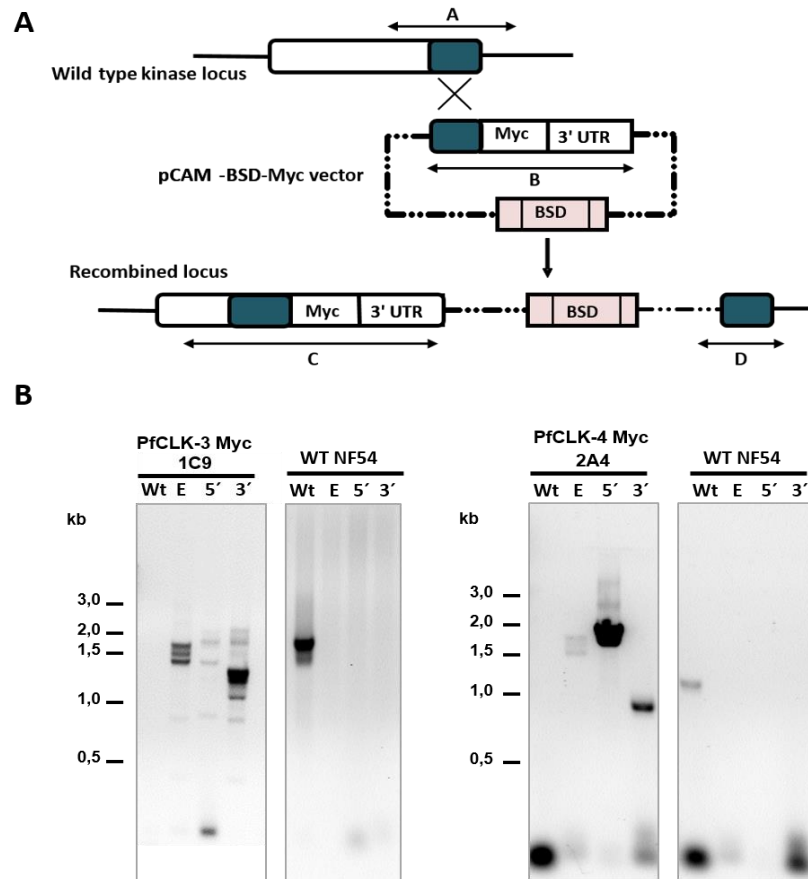


**Fig. 3.9: Gene tagging strategy by reverse genetics.** **A.** Schematic of gene tagging strategy by single cross-over homologous recombination utilizing the pCAM-BSD-tag vector construct. Regions used for discrimination between wild type (A), episomal presence (B), 5'-integration (C) and 3'-integration (D) of the transfection plasmid are indicated by arrows. Modified from Agarwal, 2010; Agarwal et al., 2011. Primer combination A: amplification of wild type (Wt) gene locus; primer combination B: amplification of episome (E); primers C: diagnostic amplification of 5'-integration of plasmid; primers D: diagnostic amplification of 3'-integration of plasmid. BSD: blasticidine drug resistance cassette. Myc: double Myc-tag, exemplary. 3'UTR: 3'-untranslated region from *P. berghei* DHFR-ts gene. **B.** Molecular analysis of successful *in situ* PfCLK-3 and PfCLK-4 tagging attempts by reverse genetic approaches after separation and selection of wild type-devoid clones by limiting dilution. Diagnostic PCR from single clone 1C9 genomic DNA of pCAM-BSD-PfCLK-3-Myc vector transfected parasites showed amplification of episome (E, 1.94 kb) as well as 5'- or 3'-integration-correlating DNA fragments (1.74 kb and 1.39 kb, indicated by arrows), respectively. The single clone population was devoid of wild type indicating band (1.92 bp). Likewise, PfCLK-4-Myc plasmid transfected parasites of the single clone 2A4 showed integration of episome (1.70 kb) as well as bands for 5'- or 3'-integration amplicons (2.0 kb and 900 bp, indicated by arrows), respectively. The clone 2A4 was devoid of wild type sequences (1.40 bp). Wild type parasites of strain NF54 were used as a control of the wild type locus.

To verify the accessibility of the respective gene locus for recombination, a second approach was carried out simultaneously. For this purpose, another pCAM-BSD based vector was generated, containing an insert homologous to the 3'-end of the respective kinase gene. This

insert was fused to the sequence of a c-Myc-epitope followed by the 3'-untranslated region of the *P. berghei dhfr-ts* gene (Fig. 3.9 A). Genomic integration of this vector is resulting in a complete functional kinase that is tagged by a Myc epitope. By means of gene-tagging, recombinogenicity of the respective gene locus can be proven if successful integration of the vector occurs. Cloning and preparation of Myc-tagged pCAM-BSD-vectors was carried out by Dr. Shruti Agarwal (Agarwal, 2010). Electroporation and subsequent treatment of cultures with blasticidine resulted in a subpopulation of drug-resistant parasites after approximately three weeks and diagnostic PCR revealed integration of tagged constructs into the respective gene locus. Both PfCLK-3 and PfCLK-4 could be tagged with a Myc-epitope. To gain parasites devoid of the wild type allele which was still present, single clones were isolated by means of limiting dilution (section 2.2.1.7), which maintained the integrated plasmid even after prolonged cultivation. The clone 1C9 of PfCLK-3-Myc subpopulation was chosen and diagnostic PCR verified the absence of the wild type kinase locus, whereas 5'- and 3'-integration of the tagging vector could be confirmed (Fig 3.9 B). Similarly, the PfCLK-4-Myc clone 2G2 showed complete integration of the respective tagging vector, whilst the parasites were devoid of the wild type allele of the kinase (Fig 3.9.B).

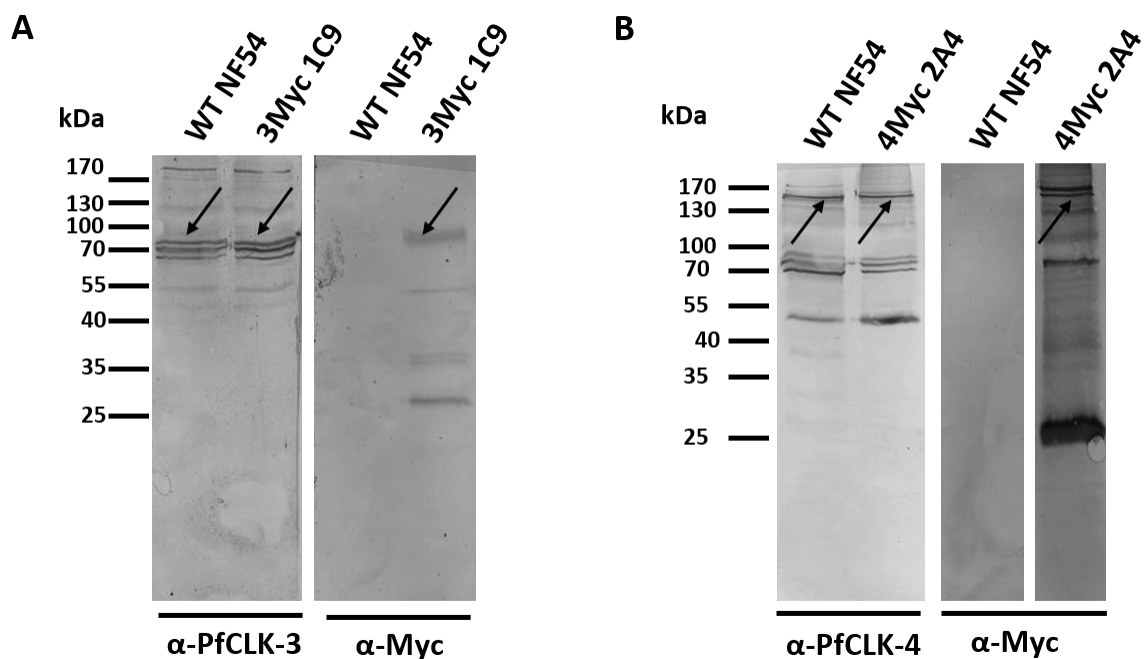


**Fig. 3.10: Phenotype analyses of genetically modified parasites by means of Western Blotting with antisera directed against Myc-tag.** **A.** Lysates of Myc-tagged PfCLK-3 parasites were utilized to detect the integrant parasite population using rabbit anti-Myc antibody via immunoblotting. The protein bands migrated at the expected kinase full size molecular mass of 81 kDa (right lane, indicated by arrows). The same bands occurred when mouse anti-PfCLK-3 antibody was blotted on WT and mutant parasite lysates (left lanes). No protein band was observed in the non-integrated WT lysate used as control (WT NF54). **B.** Western blot utilizing anti-Myc antibody detected the 157 kDa full-length protein band (arrows) as well as an additional processed protein band at 70 kDa in Myc-tagged PfCLK-4 parasite lysates (right lane). No band was observed in the WT control. The same bands with an additional 50 kDa band of processed protein occurred when mouse anti-PfCLK-4 antibody was blotted on WT and mutant parasite lysates (left lanes).

Subsequently, the successful integration of tagged PfCLK-3 and PfCLK-4 was furthermore confirmed by Western blot. Lysates of Myc-tagged PfCLK-3-asexual parasites demonstrated

an immunoreactive band of the full size kinase (81 kDa) when incubated with anti-Myc antisera, whereas in wild type parasites of the strain NF54, no kinase was detected by immunoblotting with anti-Myc antibodies (Fig 3.10 A). Full size bands for PfCLK-3 were observed in both wild type and tagged mutant parasites when incubated with the specific anti-PfCLK-3 antisera. Anti-Myc antibodies were capable of detecting the full size PfCLK-4 (157 kDa) in lysates of integrant parasites of clone line 2A4, similarly to anti-PfCLK-4 mouse antisera in both wild type and mutant parasite lysates (Fig 3.10 B).

Once the mutant parasite lines with the tagged PfCLKs were obtained, they were subsequently deployed for additional characterization by immunofluorescence assays. Therefore, lysates of parasite lines possessing the respective Myc-tagged kinase were immunolabeled with anti-Myc antisera. Both tagged kinases showed expression patterns likewise in WT parasites (Fig 3.11). PfCLK-3 and PfCLK-4 are distributed in the cytoplasm of blood stage schizonts and are not only restricted to the parasite nucleus.

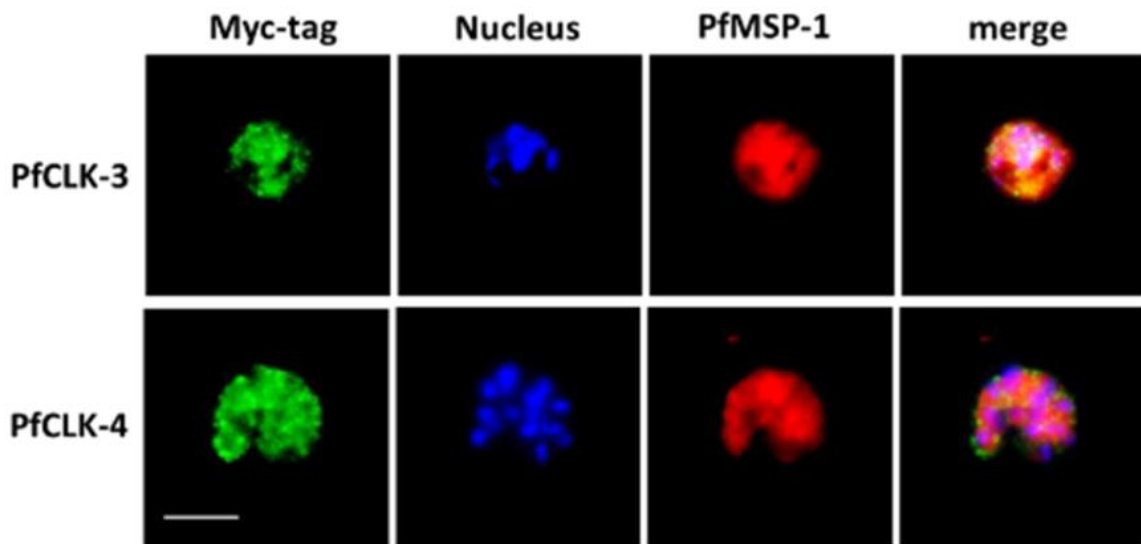


**Fig. 3.11: Subcellular localization of Myc-tagged PfCLK-3 and PfCLK-4 in blood stage schizonts.** Mixed asexual blood stage cultures of the integrant PfCLK-3-Myc and PfCLK-4-Myc lines were methanol-fixed and prepared for IFA (section 2.2.1.2), using rabbit antibodies against the Myc-tag (green). Parasite nuclei were labeled by Hoechst nuclear staining (blue) and schizonts were highlighted with mouse antibodies against PfMSP-1 (red). Bar, 5  $\mu$ m.

### 3.1.3 Kinase activity assays on PfCLK-3 and PfCLK-4-specific precipitate

As previous attempts to use recombinantly expressed PfCLK-1/LAMMER in kinase activity assays were unsuccessful (Agarwal, 2010), solely the kinase activity of endogenous PfCLK-1-4 was investigated in the current study. For the purpose of testing endogenous PfCLKs on their ability to phosphorylate physiological substrates, kinase activity assays were performed as described previously (Reininger et al., 2009, Agarwal et al., 2011). Native kinases were immunoprecipitated using the kinase-specific mouse antisera (section 2.2.3.7) from asexual wild type NF54 parasite lysates (section 2.2.3.4). After washing the immunocomplex, a kinase activity assay was performed adding exogenous substrates histone H1, myelin basic protein (MBP) as well as  $\alpha$ -/ $\beta$ -casein. Subsequently the proteins were destined to separation by SDS gel electrophoresis (section 2.2.3.5), gels were vacuum-dried and phosphorylation signals were finally detected by autoradiography. All four endogenous PfCLK kinases were able to

significantly phosphorylate all three exogenously added substrates (Fig. 3.12, upper panel). As positive control, recombinantly expressed protein kinase 6 (rPK6; Bracchi-Ricard et al., 2000) which predominantly phosphorylates MBP, revealed strong phosphorylation activity of all three exogenously added substrates. The assay was performed without precipitated kinases (PBS control) as negative control and no phosphorylation signal was observed. As loading control, Coomassie blue-stained radiolabelled gels were utilized (Fig. 3.12, lower panel).

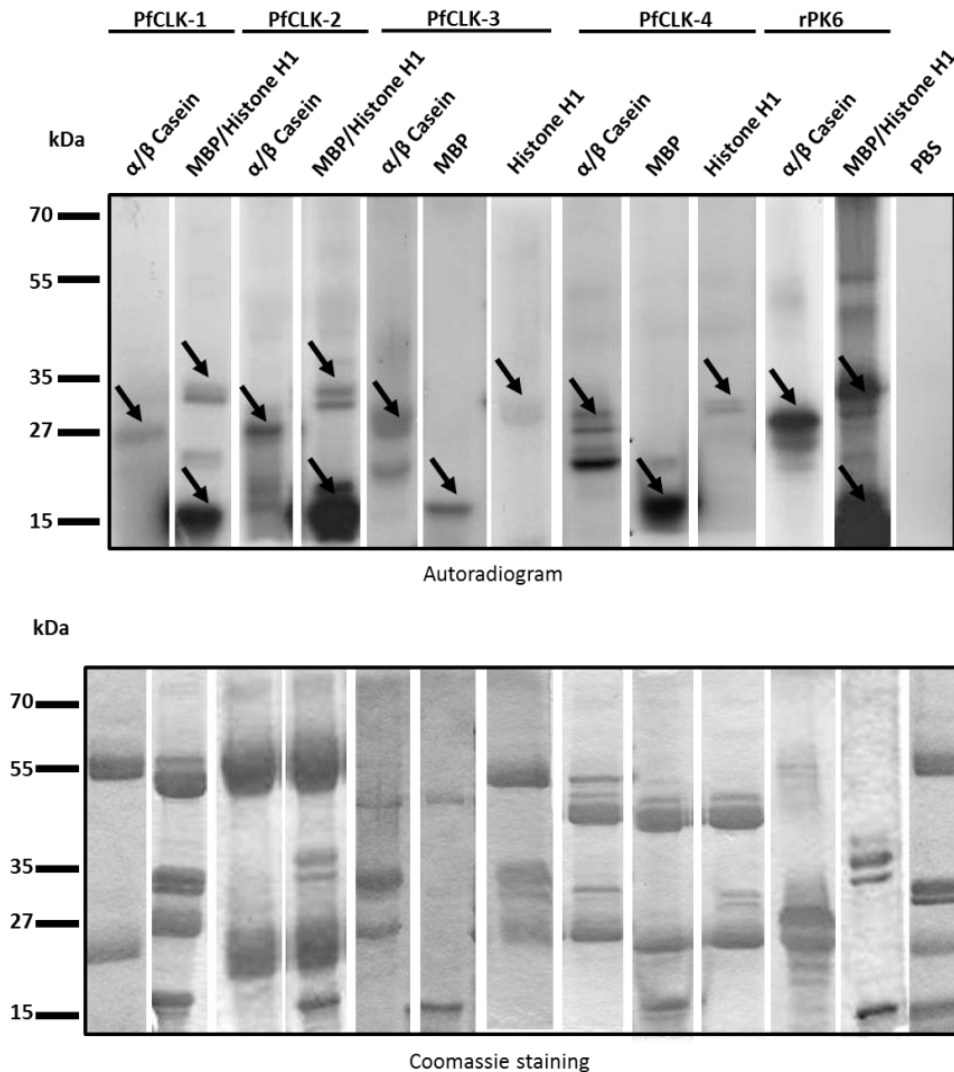


**Fig. 3.12: Kinase activity assays performed on immunoprecipitated PfCLKs.** In order to scrutinize *in vitro* phosphorylation activity, ubiquitous kinase substrates were added to a standard kinase reaction including the precipitated kinases. All four investigated endogenous PfCLKs were capable of phosphorylating  $\alpha$ - $\beta$ -casein, myelin basic protein (MBP) as well as histone H1 *in vitro* (upper panel). Recombinant protein kinase PfPK6 served as phosphorylation control and exhibited similar strong phosphorylation signals. Instead of parasite lysates, immunoprecipitation reactions containing PBS were used as negative control (PBS). Coomassie blue-stained SDS-gels served as loading control (lower panel).

### 3.2 Identification of putative interaction partners of the PfCLKs

In preceding studies, the catalytic domain sequences of all four PfCLKs have been aligned with the homologous yeast kinase Sky1p (Agarwal, 2010; Agarwal et al., 2011), which is a well-

studied kinase of *S. cerevisiae* and involved in mRNA splicing and mRNA transport in this organism (Siebel et al., 1999). Sequence alignment revealed that all conserved kinase domains are present in the PfCLKs (Agarwal, 2010), and further striking matches between substrate binding residues between the kinases of the different organisms were disclosed. In this previous study, this led to having a closer look at the specific substrate protein of Sky1p, which is referred to as Npl3p and displays a shuttle-protein for nucleocytoplasmic transport (Siebel et al., 1999; Lukasiewicz et al., 2007). In the onset of the study of Dr. Agarwal, several plasmodial proteins were found that were homologues to the BLAST searches of the yeast kinase substrate Npl3p as well as mammalian kinase substrate SF2/ASF (Tab. 3.1). Among them were the putative splicing factor PF3D7\_1119800 (PfASF-1), the putative serine/arginine-rich splicing factor PF3D7\_0503300 (PfsRSF12), the putative pre-mRNA splicing factor PF3D7\_1022400 (PfsFRS4) as well as the putative splicing factor PF3D7\_1321700 (PfsF-1).

**Tab. 3.1:** Table displaying homologies between the plasmodial proteins investigated in this study and yeast Npl3p and human SF2/ASF.

Plasmodial protein	Homology with yeast Npl3p	Homology with human SF2/ASF
<b>PfASF-1</b>	32%	44%
<b>PfsFRS4</b>	28%	45%
<b>PfsRSF12</b>	45%	80%
<b>PfsF-1</b>	46%	63%

Noteworthy, all these hits were putative plasmodial splicing factors or at least putatively assigned to RNA binding protein function, possessing one or two RNA recognition motifs (RRM). In order to generate major insights into the individual components of the plasmodial splicing machinery, these four plasmodial factors were investigated in this study. Initially, the plasmodial factors as well as yeast Npl3p were recombinantly expressed in *E. coli*. In a subsequent approach, these recombinant factors were utilized in kinase activity assays for determining whether they display interactions partners for the PfCLKs in vitro. Lastly, localization studies were carried out in order to further characterize the four chosen plasmodial proteins.

### 3.2.1 Expression of recombinant proteins in *E. coli*

To identify putative interactions partners of the PfCLKs, we first recombinantly expressed GST-tagged yeast splicing factor Npl3p in *E. coli* (expression plasmid kindly provided by Dr Gourisankar Gosh, Department of Cellular and Molecular Medicine, University of California, San Diego, California, USA). After several unsuccessful attempts to gain recombinant GST-tagged Npl3p in the elution fraction of the affinity purification, the bacterial flow-through was utilized which was rich of recombinant Npl3p-GST, as verified by SDS-PAGE (Fig. 3.13 A). Further confirmation of the presence of GST-tagged Npl3p was utilized by immunoblotting the bacterial flow-through and detection of protein with anti-GST polyclonal antibodies (Fig. 3.13 B). The recombinant protein possessed an expected molecular mass of 63.4 kDa, resulting in a fusion protein with a molecular mass of 89.4 kDa.

To scrutinize whether plasmodial factors are displaying substrates for the four PfCLKs *in vitro*, four proteins were recombinantly expressed that revealed significant homology to the yeast kinase substrate Npl3p and mammalian SF2/ASF (Tab. 3.1). Towards this aim, either the full size parasite protein (in case of PfASF-1 and PfSRSF12, Fig. 1.7) was bacterially expressed in *E. coli*, or fragments of the respective putative splicing factor (for PfSFRS4 and PfSF-1). Moreover, for PfSF-1 it was feasible to split the recombinant protein into two separate recombinant proteins due to its higher molecular weight compared to the other three chosen proteins. The N-terminal part of the protein which comprises the RS-rich domain was termed PfSR-1 rp1, whereas the C-terminal part consisting of three RNA recognition motifs was expressed separately and referred to as PfSF-1 rp2 (Fig. 1.7).

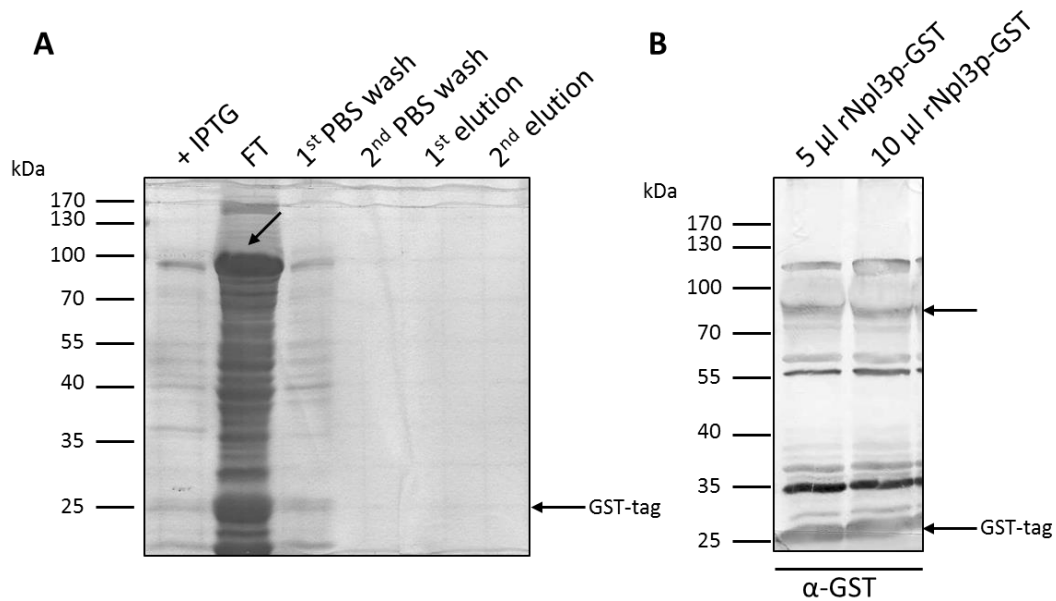


**Fig. 3.13: Recombinant expression of yeast GST-tagged splicing factor Npl3p in *E. coli*.** **A.** Affinity purification of GST-tagged Npl3p did not lead to purified eluted protein with an expected molecular mass of 89.6 kDa, but protein was yielded in the bacterial flow-through of the purification column (FT, arrow). **B.** Western Blot analysis utilizing mouse derived anti-GST antibodies detected the full-length recombinant protein (rNpl3p-GST) running at 89.6 kDa (arrow in the figure) as well as truncated fragments migrating at lower molecular weights. GST-tag alone was also detected by antibodies (arrow). Dilutions of 5 and 10  $\mu$ l of bacterial flow-through were used, respectively.

PfASF-1, which has a predicted molecular weight of 22 kDa, was recombinantly expressed as GST-tagged full size fusion protein. Consecutively, it was purified via affinity chromatography resulting in a 48 kDa recombinant protein (Fig. 3.14 A). Immunoblotting of diluted purified soluble protein with antisera against GST confirmed the presence of GST-tagged PfASF-1 in concentrations that could be utilized in subsequent interaction studies (Fig 3.14 B.).

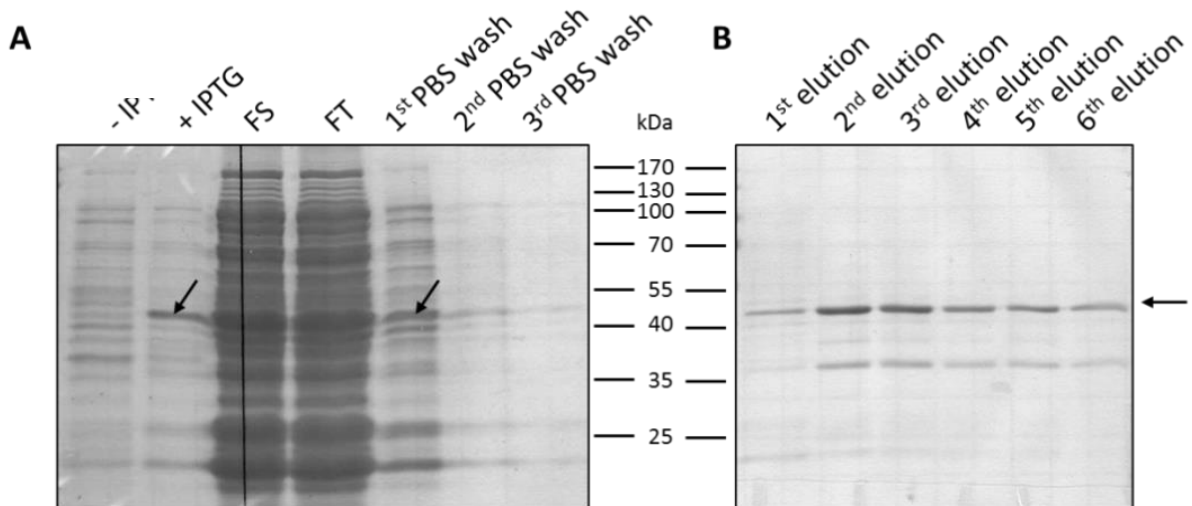


**Fig. 3.14: Generation of GST-tagged recombinant PfASF-1 via affinity purification.** The full-length protein was N-terminally fused to GST, expressed in bacteria and subsequently affinity-purified as soluble protein with a combined molecular weight of 48 kDa (arrows). FS: filtered supernatant, FT: column flow-through.

Portions of the splicing factors PfSRSF12 and PfSFRS4 were likewise bacterially expressed, but these recombinant fragments were tagged with a MaBP-tag with a resulting molecular weight of 73 and 87 kDa, respectively (Fig. 3.15).

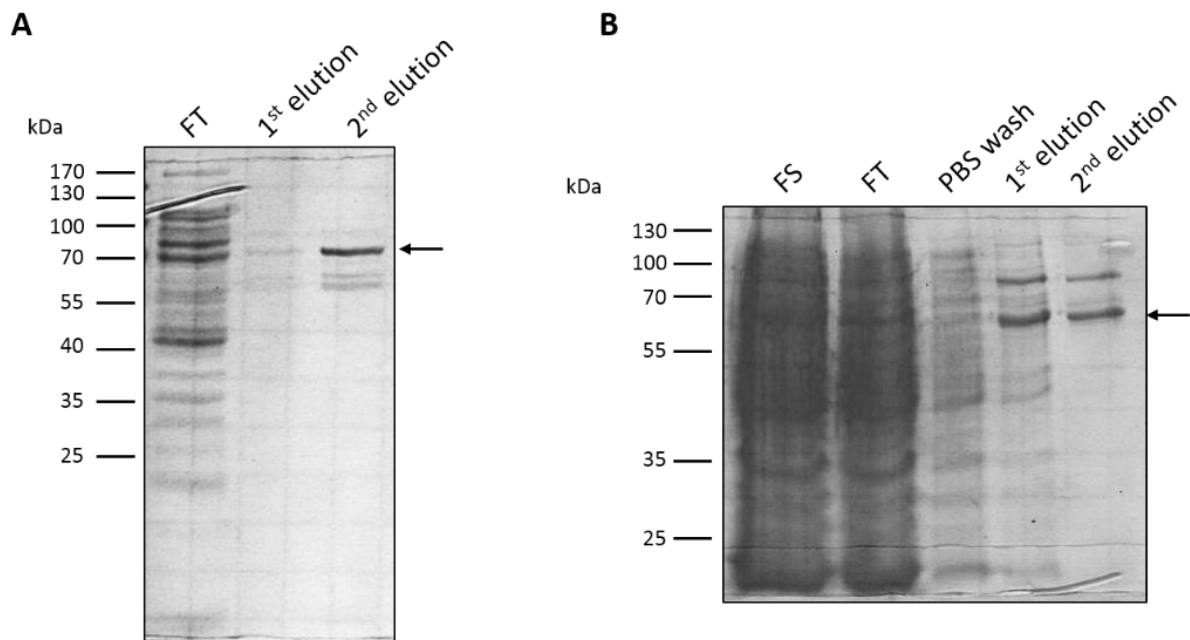


**Fig. 3.15: Generation of recombinant splicing factors PfSRSF12 and PfSFRS4 in *E. coli*.** **A.** Affinity purification of MaBP-tagged recombinant PfSRSF12. The full-length protein was N-terminally fused to MaBP, expressed in bacteria and subsequently affinity-purified as soluble protein with a combined molecular weight of 73.0 kDa (arrows). **B.** Generation of MaBP-tagged recombinant PfSFRS4 via affinity purification. The protein was fused N-terminally with MaBP, expressed in bacteria and subsequently affinity-purified as soluble protein with a combined molecular weight of 65.2 kDa (arrows). FS: filtered supernatant, FT: column flow-through.



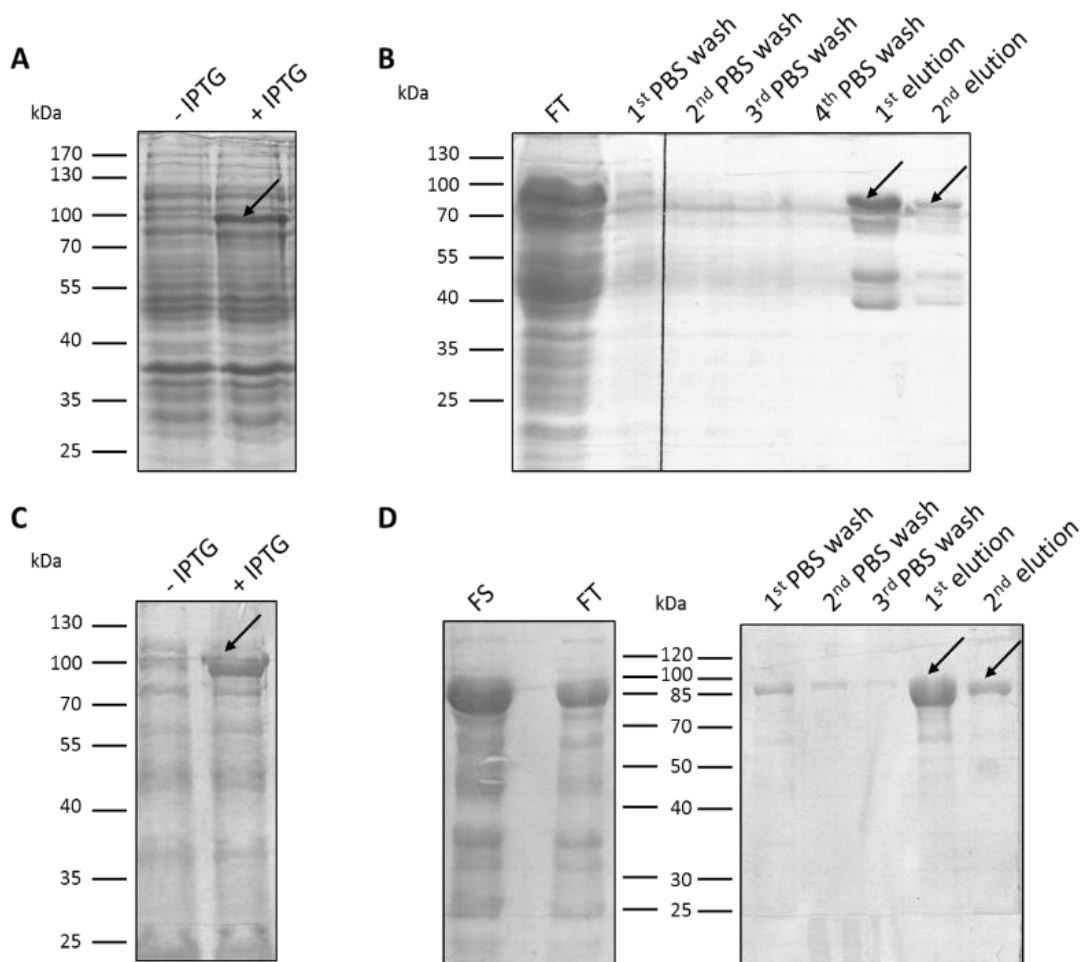


**Fig. 3.16: Generation of MaBP-tagged recombinant PfSF-1 fragments.** They were expressed as soluble proteins for examination of interaction with the PfCLKs. **A.** One clone for the recombinant PfSF-1 rp1 fragment from bacterial overnight cultures was induced with IPTG (+ IPTG) to induce transcription (indicated by arrow). Uninduced cultures (- IPTG) were cultivated as negative transcription controls. **B.** Large scale purification revealed protein bands migrating at the expected molecular weight of the purified protein (94.6 kDa). **C.** One clone for the recombinant PfSF-1 rp2 fragment from bacterial overnight cultures was induced with IPTG (+ IPTG) to induce transcription (indicated by arrow). Uninduced cultures (- IPTG) were cultivated as negative transcription controls. **D.** Large scale purification revealed protein bands migrating at the expected molecular weight of the purified protein (85.7 kDa). FS: filterd supernatant, FT: flow through of bacterial protein lysate, PBS wash: flow through of washed column.

Given the molecular weight of 101 kDa for the fourth chosen plasmodial splicing factor, PfSF-1, two recombinant portions of this protein were expressed recombinantly as MaBP-tagged fusion proteins. PfSF-1rp1 displays the N-terminal part of the physiological protein consisting of the RS-domain which is known to be phosphorylated by kinases (Fig. 1.7). This recombinant protein has a molecular weight of 95 kDa, whereas the C-terminal part consisting of the RRM domains was expressed as 85 kDa fusion protein referred to as PfSR-1 rp2. Both recombinant proteins were affinity purified similarly to the above mentioned proteins and subsequently loaded onto SDS gels to scrutinize the concentration of soluble protein respectively (Fig 3.16).

### 3.2.2 Kinase activity assays with putative SR proteins

For experimental verification whether the yeast splicing factor Npl3p is phosphorylated by the PfCLKs *in vitro*, the recombinant protein yielded in the bacterial flow-through was subsequently utilized in kinase activity assays (section 2.2.3.8). The PfCLKs were therefore immunoprecipitated and recombinant Npl3p was added to each reaction which was supplemented with phosphorus<sup>32</sup>-labeled ATP (Fig. 3.17). Preparations were separated via SDS-PAGE and phosphorylation signals of Npl3p were detected subsequently by autoradiography. Full size bands of the phosphorylated yeast splicing factor were detected when PfCLK-1, PfCLK-2 and PfCLK-4 were precipitated from asexual parasite extracts. In contrast, PfCLK-3 was not capable of interacting *in vitro* with the yeast protein Npl3p. Interestingly, by incubating Npl3p with parasite extract prior to immunoprecipitation with PfCLK-1, Npl3p was phosphorylated as well (Fig. 3.17).

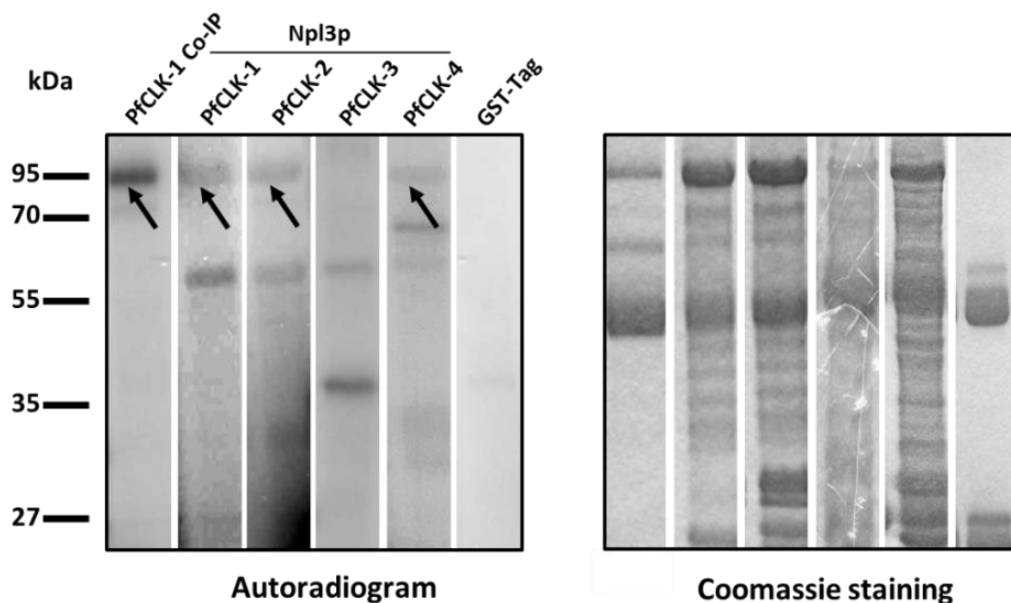


**Fig. 3.17: Phosphorylation of yeast Npl3p by immunoprecipitated PfCLKs.** Phosphorylation signals were observed when recombinant yeast Npl3p-GST was added to the kinase reaction containing immunoprecipitated PfCLK-1, PfCLK-2 and PfCLK-4 (left panel). When Npl3p was added prior to the kinase activity assay, PfCLK-1 was also capable of phosphorylating the yeast factor (PfCLK-1 Co-IP). No interaction of PfCLK-3 was verified *in vitro* with the yeast factor. GST-tag alone as substrate (26 kDa) was used as negative control. Shown here is an assay using PfCLK-1 specific immunoprecipitate, similar results were obtained with immunoprecipitates of other PfCLKs (data not shown). Coomassie blue staining of radiolabeled SDS gels was used as loading control (right panel).

Likewise to Npl3p-GST, recombinant plasmodial SR proteins PfASF-1, PfSRSF12, PfSFRS4 and PfSF-1 were expressed either in fragments or as full size proteins (Fig. 1.7). Affinity-purified recombinant proteins were added to the kinase reactions for each PfCLK kinase and kinase activity assays were carried out as mentioned before (section 2.2.3.8). Bacterially expressed full-length GST-tagged PfASF-1 showed interaction with PfCLK-1 and PfCLK-2, as strong phosphorylation signals were observed (Fig. 3.18). No phosphorylation bands could be detected in kinase reactions containing immunoprecipitated kinases PfCLK-3 and PfCLK-4, when recombinant PfASF-1 was added.

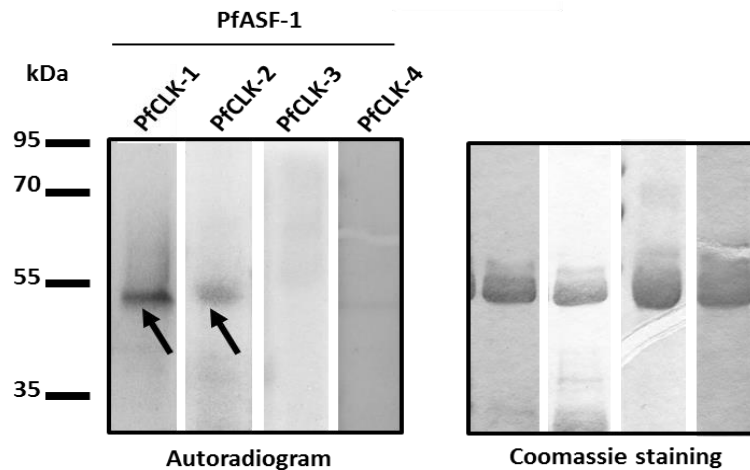


**Fig. 3.18: Phosphorylation of plasmodial SR protein PfASF-1 by immunoprecipitated PfCLKs.** Kinase activity assays were deployed to detect phosphorylation of recombinant PfASF-1 (48 kDa, arrows) by PfCLK-1 and PfCLK-2 (autoradiogram, left panel). For PfCLK-3 and PfCLK-4, no phosphorylation signals could be detected. Coomassie blue staining of radiolabeled SDS gels (right panel) was utilized as loading control.

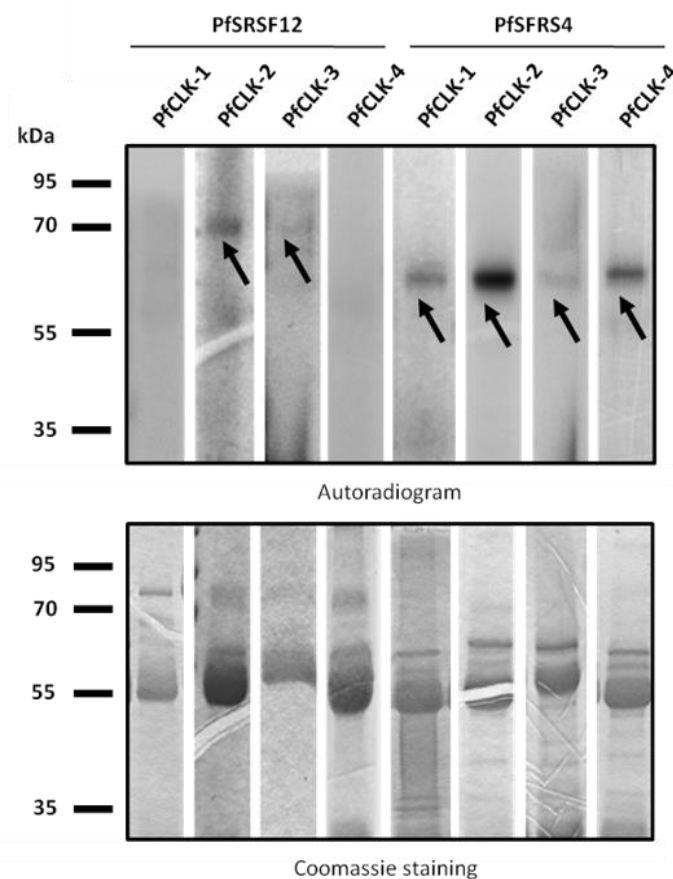


**Fig 3.19: Phosphorylation of plasmodial SR proteins PfSRSF12 and PfSFRS4 by immunoprecipitated PfCLKs.** Kinase activity assays were deployed to detect phosphorylation of recombinant PfSRSF12 and PfSFRS4 (73 kDa, 65.3 kDa, indicated by arrows). PfSRSF12 was solely capable of phosphorylating PfCLK-2 and PfCLK-3 in vitro, whereas phosphorylation of PfSFRS4 by all four PfCLKs was detected in the kinase activity assay.

Deploying recombinant full-length PfSRSF12, this factor was solely phosphorylated by precipitates of PfCLK-2 and PfCLK-3, whereas recombinant PfSFRS4 was phosphorylated by all

four immunoprecipitated plasmodial kinases (Fig. 3.19). Regarding the fourth recombinant parasite splicing factor PfSF-1, this protein was recombinantly expressed as two independent fragments. The N-terminal fragment containing the RS-rich domains and the C-terminal part, which only comprises RNA binding motifs, but no RS-rich repeats (Fig. 1.7). PfSF-1 rp1 displaying the N-terminal RS-rich domain was phosphorylated by the plasmodial CLKs except of PfCLK-3 precipitate (Fig. 3.20 A). On the contrary, no phosphorylation signals were observed in kinase activity assays for the recombinant C-terminal domain PfSF-1 rp2 when incubated with all four precipitated PfCLKs, respectively. Purified GST- and MaBP-tag alone was utilized as substrate instead of the recombinant SR proteins and served as negative control in the described assays (Fig. 3.20 B). No phosphorylation of the two tags was detected in these reactions. Coomassie blue-stained dried gels served as loading control (Fig. 3.20, lower panel).

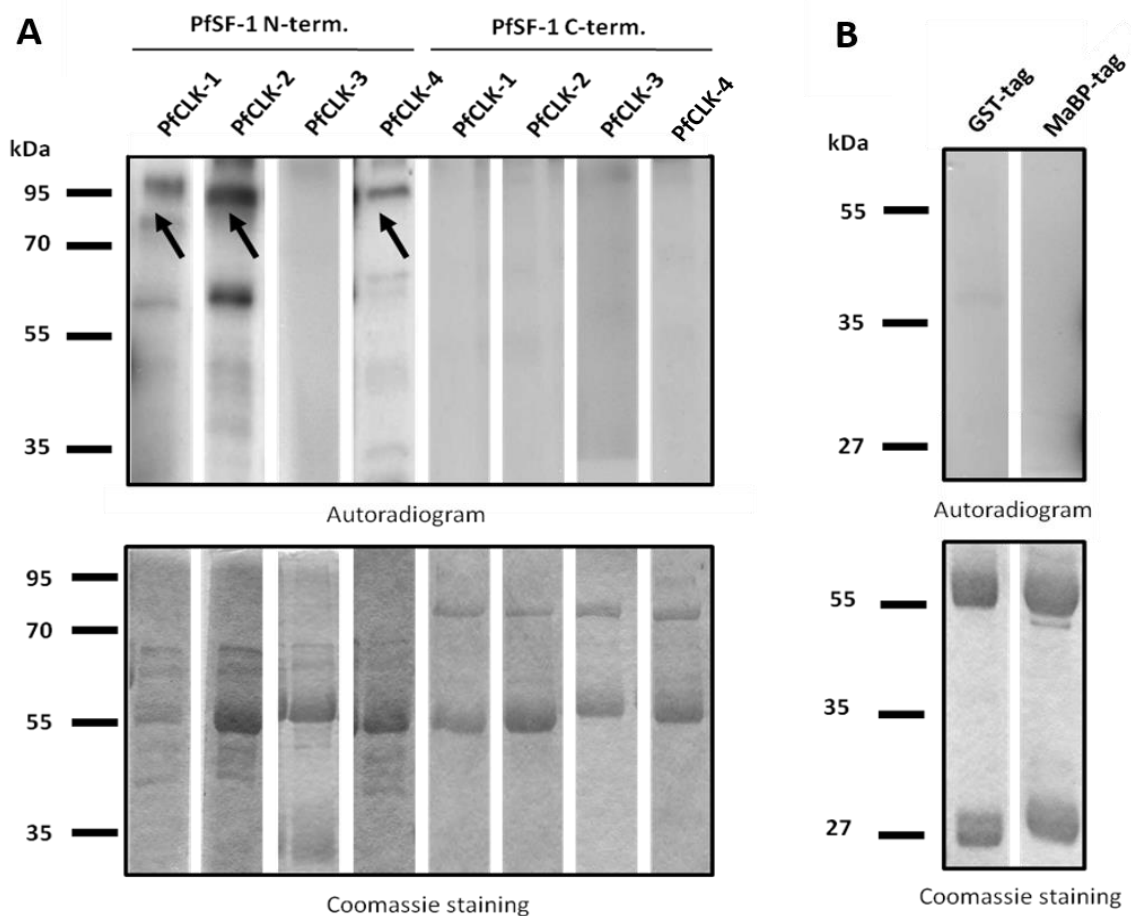


**Fig. 3.20: Phosphorylation of the plasmodial SR protein PfSF-1 by immunoprecipitated PfCLKs.** **A.** The N-terminal fragment (95 kDa, arrows) of recombinant PfSF-1 was phosphorylated by PfCLK-1, PfCLK-2 and PfCLK-4. An additional phosphorylation signal of truncated N-terminal PfSF-1 was visible at approximately 60 kDa. On the contrary, the C-terminal fragment of PfSF-1 showed no phosphorylation by any of the four PfCLKs. **B.** GST-tag (26 kDa) or MaBP-tag (43 kDa) alone was used as substrate control and revealed no phosphorylation when added to immunoprecipitates of PfCLK-1 and PfCLK-4, respectively. Coomassie blue staining of radiolabeled SDS gels (lower panels) was utilized as loading control.

### 3.2.3 Localization studies on putative SR proteins

Available transcriptome data at PlasmoDB point to a predominant transcript expression in the trophozoite stage for all investigated SR proteins (Aurrecochea et al., 2009). For further verification of the subcellular localization of the investigated SR proteins, the soluble recombinant protein fractions (section 3.2.1) were utilized to immunize mice for generation of antisera against the parasite splicing factors. Antisera raised against the full-length plasmodial splicing factor PfASF-1 were utilized in immunofluorescence assays for determining the specific localization. The assays showed faint to no signals in all investigated life cycle stages of *P. falciparum*, whereas the stage-specific labeling was clearly visible (Fig. 3.21). Asexual parasites were counterstained with antibodies against the merozoite surface protein PfMSP-1, and gametocytes were labeled with antibodies against the sexual stage protein Pfs230.

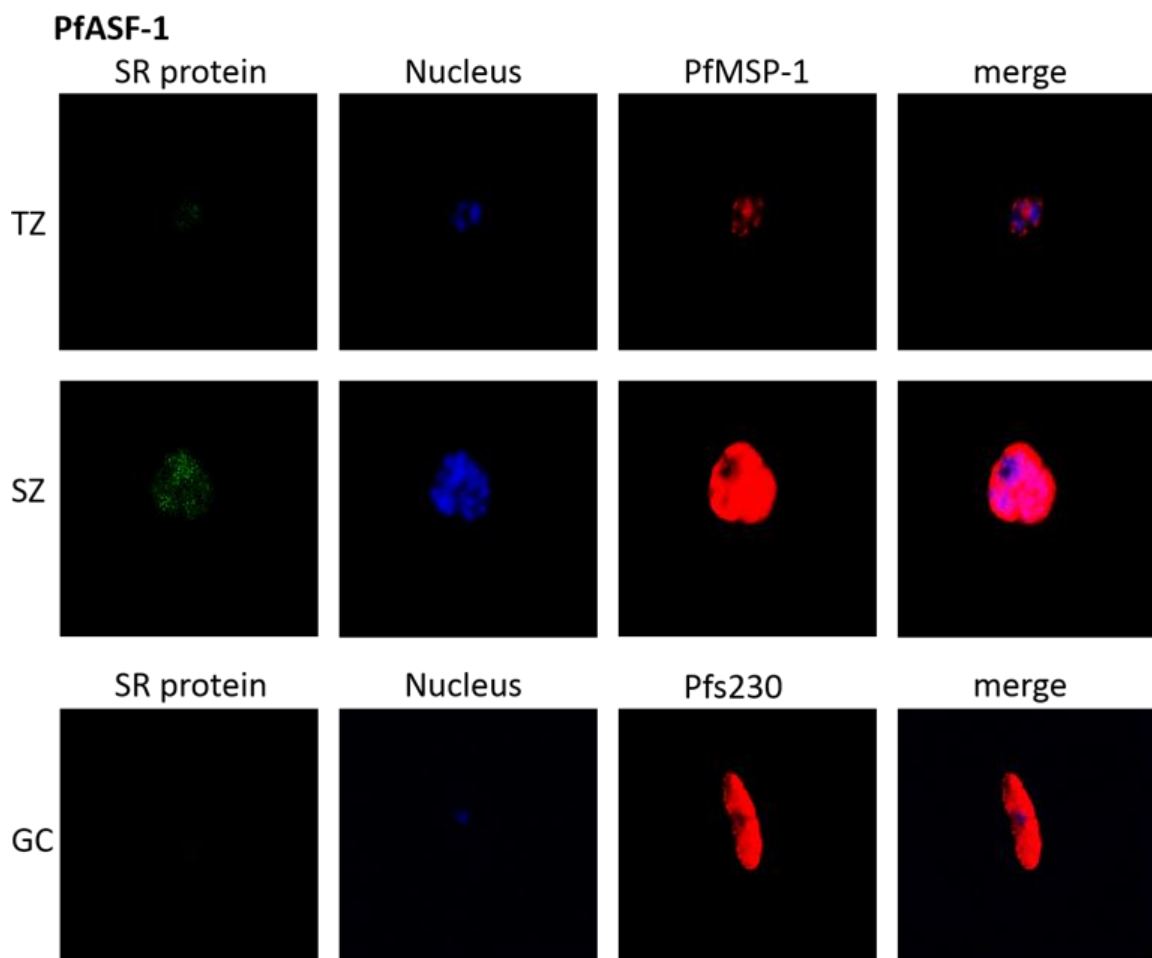


**Fig. 3.21: Subcellular localization of PfASF-1 in blood and gametocyte stages.** Mixed asexual blood stage cultures containing trophozoites (TZ) and schizonts (SZ) as well as mature gametocyte cultures (GC) were fixed with 4 % paraformaldehyde, using mouse-derived antiserum against PfASF-1. Kinase-specific labeling is displayed in green (Alexa Fluor 488), whereas the parasite nuclei are highlighted by Hoechst staining in blue. Asexual blood stage parasites are labeled with rabbit antibodies against PfMSP-1 and gametocytes with rabbit antibodies directed against Pfs230 (red, Alexa Fluor 594). Bar, 5  $\mu$ m.

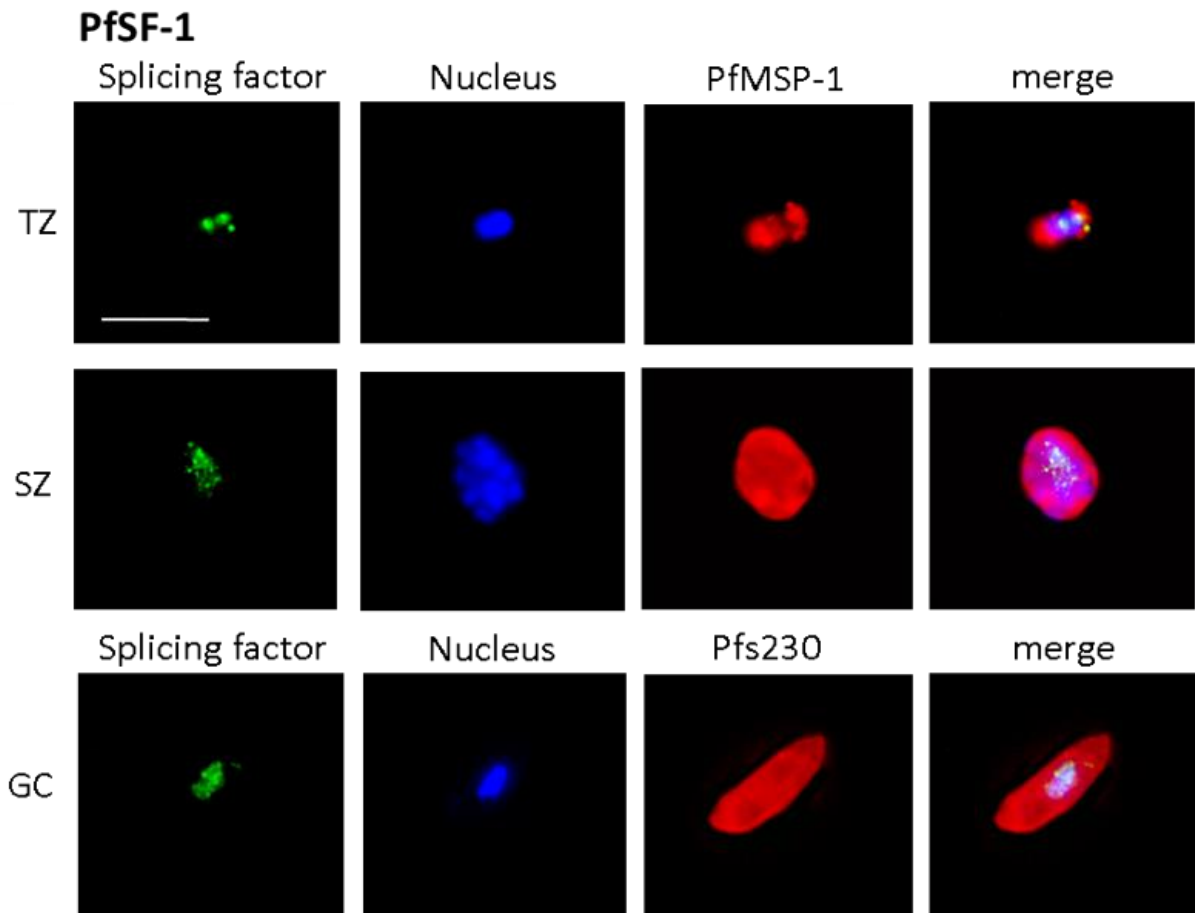


**Fig. 3.22: Subcellular localization of PfSF-1 in blood and gametocyte stages.** Mixed asexual blood stage cultures containing trophozoites (TZ) and schizonts (SZ) as well as mature gametocyte cultures (GC) were fixed with 4 % paraformaldehyde, using mouse-derived antiserum against PfSF-1. Kinase-specific labeling is displayed in green (Alexa Fluor 488), whereas the parasite nuclei are highlighted by Hoechst staining in blue. Asexual blood stage parasites are labeled with rabbit antibodies against PfMSP-1 and gametocytes with rabbit antibodies directed against Pfs230 (red, Alexa Fluor 594). Bar, 5  $\mu$ m.

Investigation of the subcellular localization of PfSF-1, PfsRSF12 and PfsFRS4 by using specific mouse antisera revealed a predominant expression in the nucleus of trophozoites for all three plasmodial factors (Fig. 3.22, 3.23 A, B). By means of these investigations, schizonts exhibited an additional minor labeling for the three SR proteins. In mature gametocytes, presence of PfsRSF12 and PfSF-1 was confirmed via IFA. On the contrary, no PfsFRS4-specific labeling pattern could be observed in these stages (Fig. 3.23 B). Furthermore, more thorough investigations of the localization of the SR proteins PfsRSF12, PfsFRS4 and PfSF-1 in transforming trophozoites (2-nuclei-stage) verified the finding that these splicing factors prevail in distinct areas of the parasite nuclei (Fig. 3.25). In contrast, these factors can not be detected in the cytoplasm of the parasite.

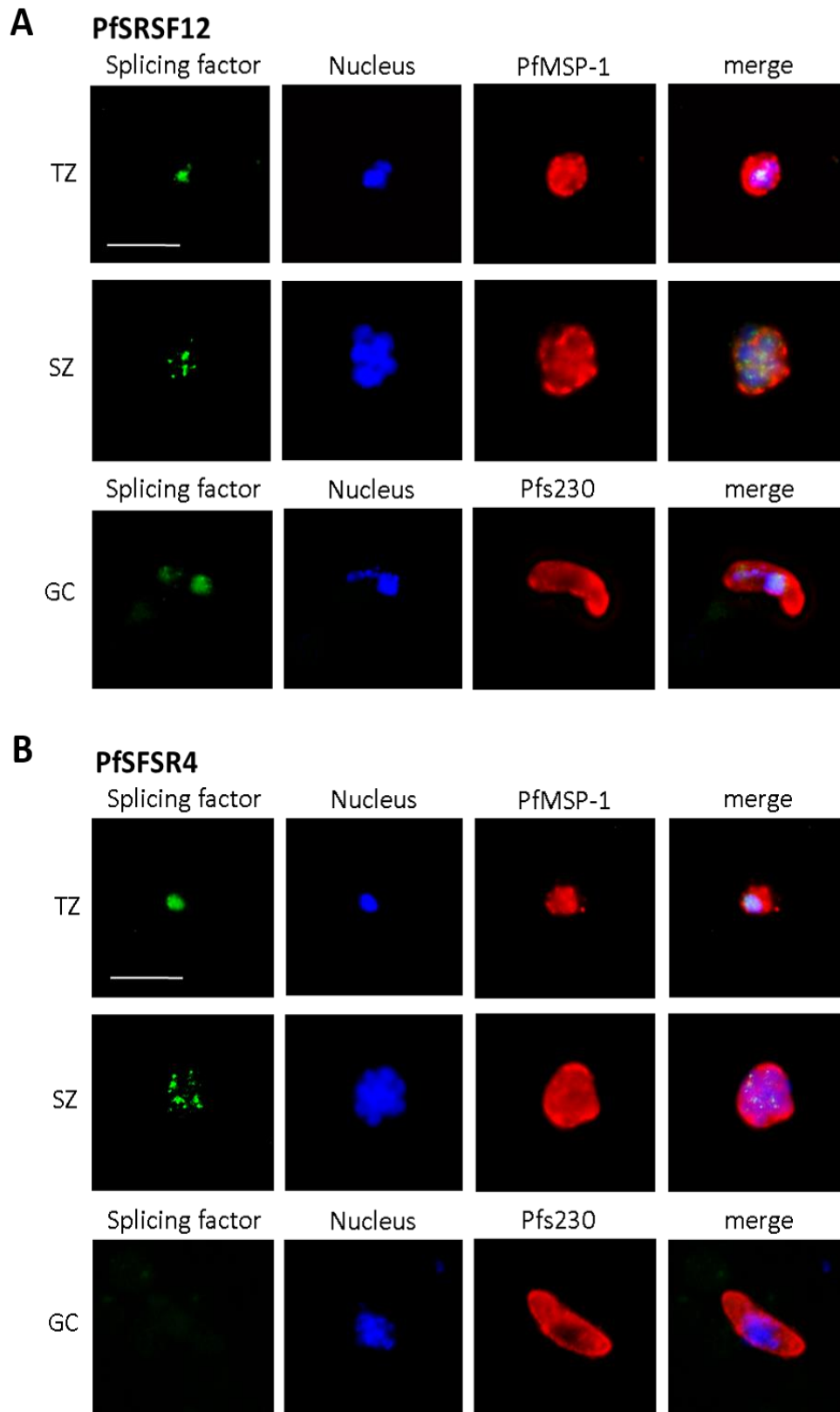


**Fig. 3.23: Subcellular localization of the SR proteins PfSRSF12 and PfSFSR4 in blood and gametocyte stages.** Mixed asexual blood stage cultures containing trophozoites (TZ) and schizonts (SZ) as well as mature gametocyte cultures (GC) were fixed and prepared for IFA, using mouse-derived antiserum against PfSRSF12 (A.) or PfSFSR4 (B.), respectively. Kinase-specific labeling was visualized using Alexa Fluor 488-labeled secondary antibodies (green), whereas the parasite nuclei are highlighted by Hoechst staining in blue. Asexual blood stage parasites were labeled with rabbit antibodies against PfMSP-1 and gametocytes with rabbit antibodies directed against Pfs230 (red, Alexa Fluor 594). Bar, 5  $\mu$ m.

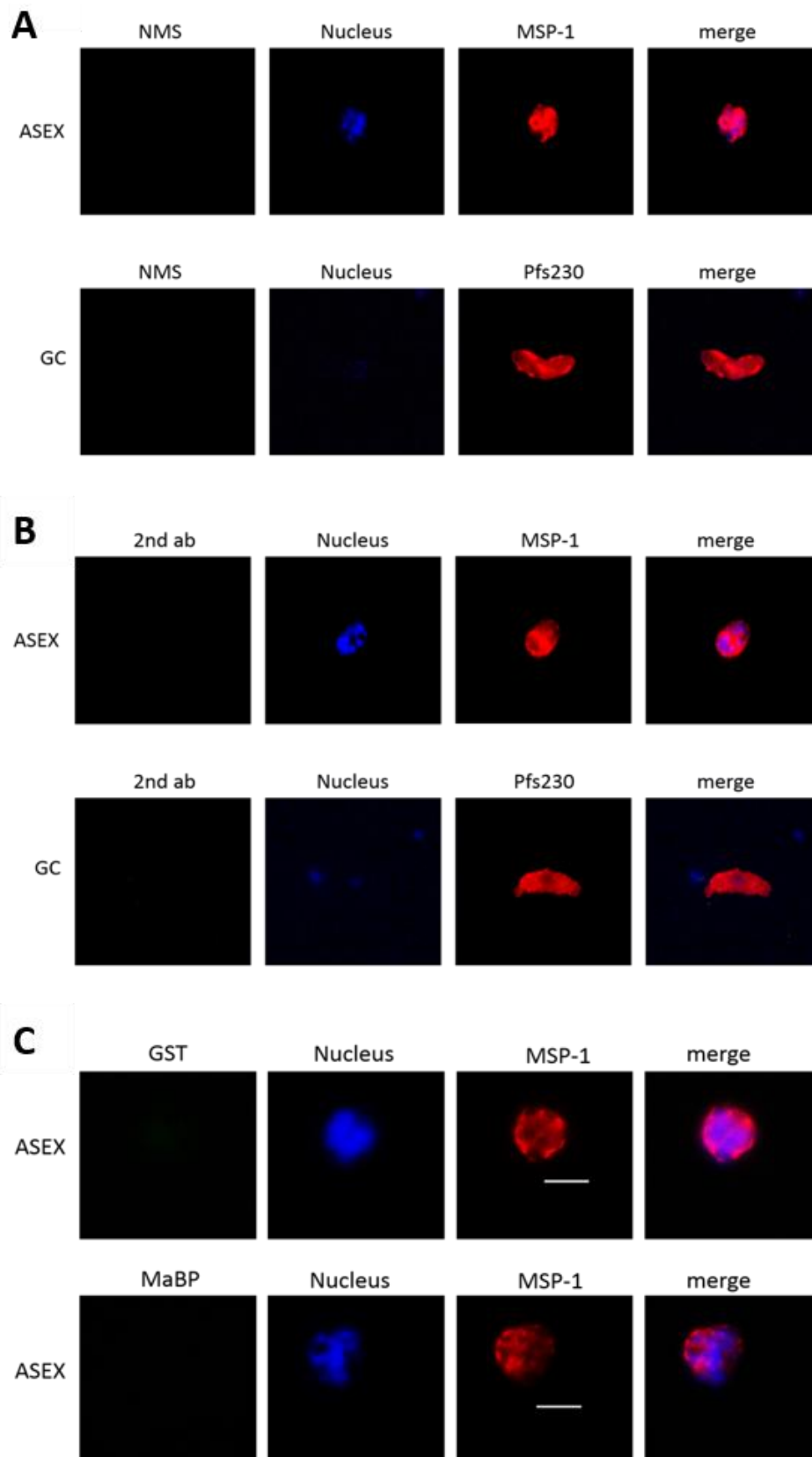


**Fig. 3.24: Control IFAs.** **A.** Neutral mouse serum was used in IFA and showed no binding. Asexual parasites were counterlabeled with antibodies directed against PfMSP-1, whereas sexual stage parasites were counterlabeled with rabbit or mouse anti-Pfs230 serum. **B.** Goat-derived fluorescence-conjugated secondary antibody exhibited no labeling of asexual parasites or gametocytes. **C.** Furthermore antibodies against the GST-tag or the MaBP-tag alone revealed no binding to plasmodium-specific proteins. Bar, 5  $\mu$ m.



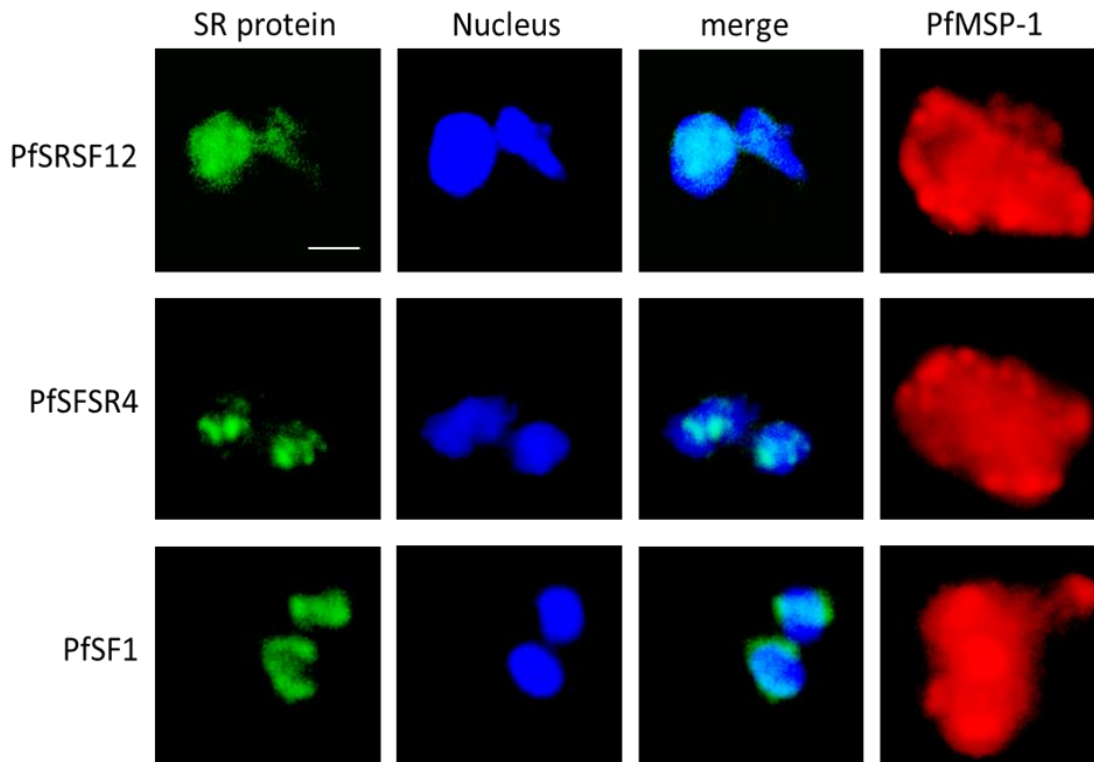


**Fig. 3.25: In depth analysis of the localization of the SR proteins PfSRSF12, PfSFRS4 and PfSF-1 in the parasite nucleus.** Transforming trophozoite stages (2-nuclei-stages) were prepared for IFA as described above and the localization of the SR proteins was verified in the Hoechst-positive nuclei. Counterlabeling was deployed with rabbit antibodies against PfMSP-1 Bar, 5  $\mu$ m.

To confirm co-localization with PfCLK-1, subsequent IFA studies were undertaken which demonstrated an expression of the above mentioned three splicing factors in association with PfCLK-1/LAMMER (Fig 3.26). In a subsequent step, the numbers of parasites positive for the PfCLKs and the three SR proteins PfSRSF12, PfSFRS4 and PfSF-1 were determined. When blood stage schizonts were highlighted by immunolabeling with  $\alpha$ -PfMSP-1 antibody or by Hoechst nuclear staining,  $99 \pm 1\%$  of schizonts labeled for PfCLK-1-3 or PfSF-1,  $96 \pm 2\%$  of schizonts labeled for PfCLK-4,  $92 \pm 2.8\%$  of schizonts labeled for PfSFRS4, and  $94 \pm 0.6\%$  of schizonts labeled for PfSRSF12. Further  $100 \pm 0.9\%$  of Pfs230-positive gametocytes labeled for PfCLK-1,  $98 \pm 1.1\%$  of gametocytes labeled for PfCLK-2,  $84 \pm 2.3\%$  of gametocytes labeled for PfCLK-3,  $94 \pm 1.1\%$  of gametocytes labeled for PfCLK-4,  $96 \pm 1.6\%$  of gametocytes labeled for PfSF-1, and  $96 \pm 0.6$  of gametocytes labeled for PfSRSF12. No labeling was detected when serum of non-immunized mice or secondary antibodies were used in the IFAs (Fig. 3.24 A, B). Further, IFAs using mouse antisera directed against the GST- and MaBP-tag did not result in any labeling of the blood stage parasites (Fig. 3.24 C).

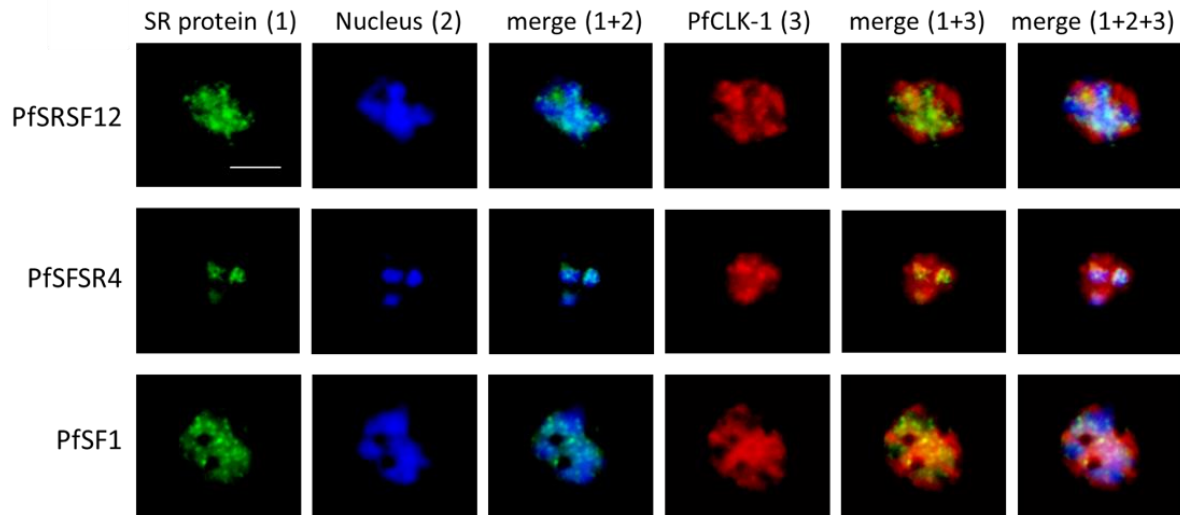


**Fig. 3.26: Co-localization of PfSRSF12, PfSFRS4 and PfSF-1 with PfCLK-1/LAMMER.** Immunolabeling of PfCLK-1 with rabbit antisera (red) detected the kinase in the cytoplasm of schizonts as well as in the nuclei, where it co-localizes with the three SR proteins (green). Schizonts were counterlabelled with rabbit antibodies against PfCLK-1 (red). All nuclei were highlighted by Hoechst staining (blue). Bar, 5  $\mu$ m.

### 3.3 Evaluation of potential PfCLK inhibitors

Knock-out attempts for PfCLK-1, PfCLK-2 (S. Agarwal, 2010; Agarwal et al., 2011; Solyakov et al., 2011) as well as for PfCLK-3 and PfCLK-4 (this study) were unsuccessful; nonetheless locus modification by tagging the respective sequence with an epitope to the 3' end was successfully conducted. As a result of a lack of functional kinase disruptant parasites, we further aimed at chemically knocking out the respective CLK kinase to functionally analyze their roles in plasmodial development and survival. Assuming that the inability to knock out PfCLK-3 and PfCLK-4 displays their essentiality in the asexual replication cycle, the identification of inhibitory compounds can be an initial step to investigate putative plasmodial CLK inhibitors.

On this account, a small compound library of 63 compounds (section 2.1.4; Fedorov et al., 2011; Huber et al., 2012) plus the antiseptic CHX was tested on their antiplasmodial activity in this study. All of these compounds are known to interfere with human or microbial CLKs.

#### 3.3.1 Antiplasmodial activity of CLK inhibitors against asexual blood stages of *P. falciparum*

Initially, the antiplasmodial activity of the compounds was tested on asexual blood stages of the parasite by Malstat viability assay (Makler and Hinrichs, 1993; Makler et al., 1993; Aminake et al., 2011). This *in vitro* screening assay takes advantage of the fact that the plasmodial enzyme lactate dehydrogenase (pLDH) has a high catalytic efficacy to use the synthetic NAD<sup>+</sup> analogue 3-acetylpyridine adenine dinucleotide (APAD) instead of the coenzyme NAD<sup>+</sup> for the oxidation reaction of L-lactate to pyruvate. On the contrary, human LDH is not capable of reducing APAD as NAD<sup>+</sup> analogue with the same enhanced catalytic

efficiency as the parasitic LDH (Gomez et al., 1997). For enzyme-based detection of malaria parasites, this circumstance is taken advantage of in Malstat viability assay (Gomez et al., 1997). The activity of pLDH is measured by a colorimetric reaction, which is verified by measuring the optical density (OD).

A stock solution of 100 mM in 100 % DMSO of each inhibitor was generated, as previous observations showed that the inhibitors were not able to dissolve in AlbuMax II™ medium or H<sub>2</sub>O<sub>bidest</sub> directly. Furthermore, DMSO does not inhibit plasmodial growth in a final concentration of 0.5 % vol. The measurement of the inhibitory effect of the compounds on asexual blood stages of 3D7 strain of *P. falciparum* was conducted by a microdilution assay, where the half-maximal inhibitory concentration (IC<sub>50</sub>) of each of the compounds was determined by measuring the optical density. Therefore, a measurement range between 6.4 nM and 500 μM was chosen.

After determining the antiplasmodial activity of the small library of CLK inhibitors (Tab. 9.1, Appendix), five compounds, C-117, *gea-27*, KH-CARB10, KH-CARB11 and KH-CARB13xHCl were chosen for further examination, as they revealed IC<sub>50</sub> values in the low micromolar range (Tab. 3.2). As a sixth compound, the antibiotic CHX was further examined with an IC<sub>50</sub> value in the nanomolar range (Tab. 3.2).

**Tab. 3.2: Malstat assay results showing IC<sub>50</sub> values of the tested inhibitors.**

Substance name	IC <sub>50</sub> (μm)
C-117	9.3 ± 3.82
<i>gea-27</i>	5.2 ± 0.35
KH-CARB10	7.4 ± 5.75
KH-CARB11	6.1 ± 1.09
KH-CARB13xHCl	7.5 ± 6.13
CHX	0.6 ± 0.40

### 3.3.2 Effect of CLK inhibitors on PfCLK-mediated phosphorylation

In a subsequent attempt, three of the chosen inhibitory compounds (*gea-27*, KH-CARB-13xHCl and CHX) were investigated if the CLK inhibitors specifically affect the phosphorylation activity of the four PfCLKs *in vitro*. For that purpose, synchronized blood stage parasites were incubated for 12 h with the above mentioned compounds at IC<sub>80</sub> concentrations prior to kinase activity assays. The solvent DMSO was used for negative control, and MBP was used as kinase substrate (10 μg per reaction). Kinase activity assays were employed as described in section 2.2.3.8. Likewise described above, the phosphorylation signals of MBP by the respective kinases was perceived by autoradiography of dried SDS gels and the rMGV was measured (section 2.2.3.8). When the parasites were incubated with the inhibitors prior to the immunoprecipitation and the assay, a reduction in the rMGV by 24.1 to 76.4% was observed compared to the DMSO control (Fig. 3.27). No effect on the phosphorylation activity of PfCLK-4 was observed for *gea-27*.

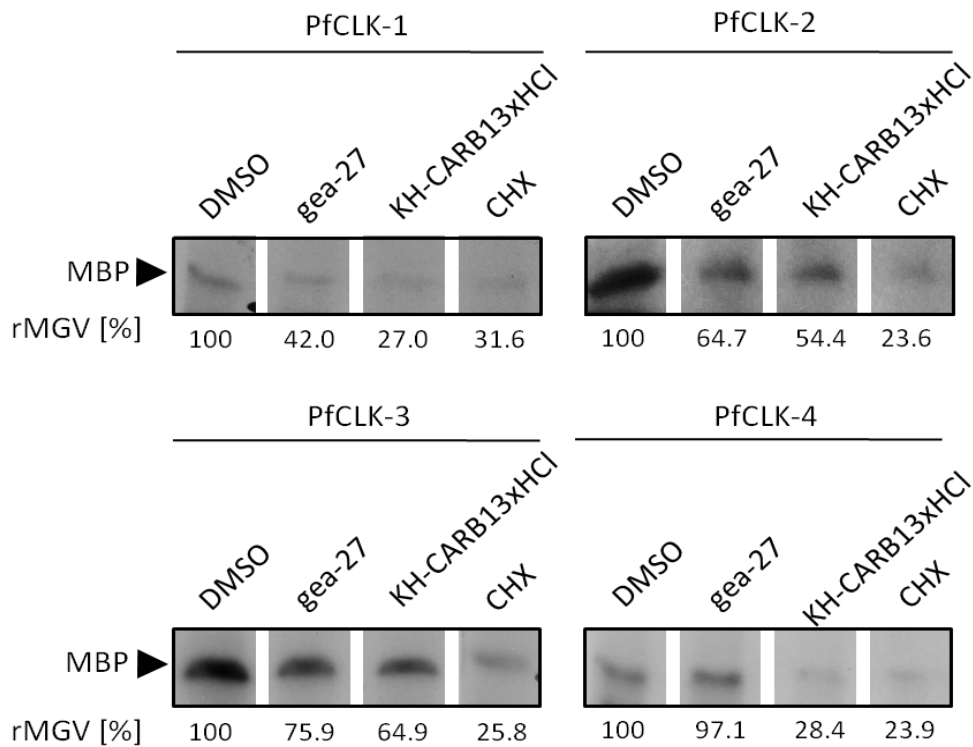


**Fig. 3.27: Effect of CLK inhibitors on CLK-mediated MBP phosphorylation.** Kinase activity assays were performed to determine MBP phosphorylation by immunoprecipitated PfCLKs. The parasites were incubated with the CLK inhibitors at approximate  $IC_{80}$  concentrations or 0.5 % vol. DMSO for 12 h prior to the assays. Specific phosphorylation signals were measured as rMGV (MGV of DMSO-treated parasites set to 100 %).

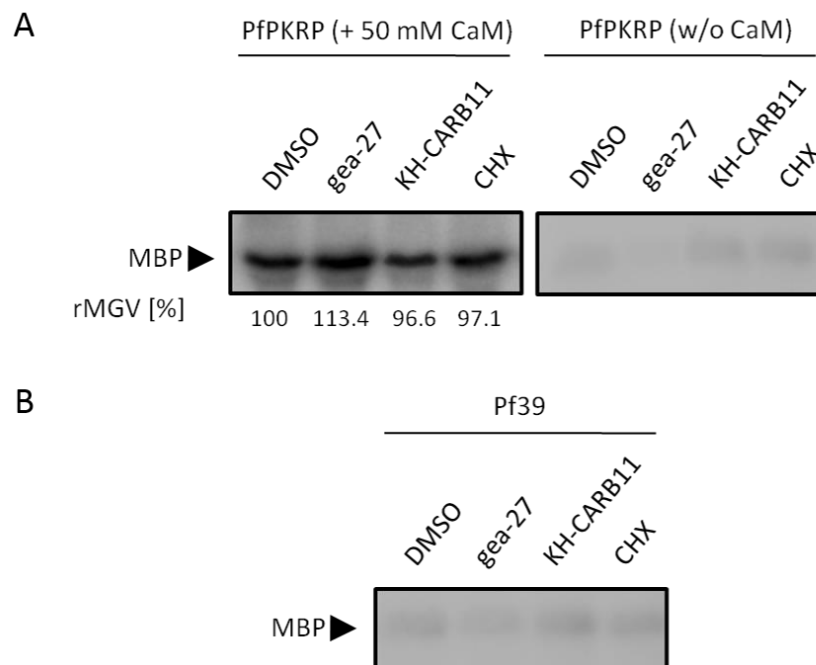


**Fig. 3.28: Controls for kinase activity assays determining the effect of CLK inhibitors on CLK-mediated MBP phosphorylation.** **A.** PfPKRP-specific immunoprecipitate phosphorylates MBP in the presence of 50 mM CaM, independent from prior incubation of the parasites with the CLK inhibitors. When CaM is missing in the kinase assay reaction, no signals of phosphorylation are observed. **B.** Pf39-specific immunoprecipitate was used as a negative control in the assays.

Immunoprecipitates of the non-CLK-kinase PfPKRP was utilized in these assays as control. PfPKRP is a CaM-dependent protein-kinase related protein (reviewed in Ward et al., 2004) and displays a homologue of the *P. berghei* PKRP, which is crucial for parasite transmission to the mosquito (Purcell et al., 2010). It was shown in IFA to be present in asexual blood stages as well as gametocytes (Agarwal, 2010; Brühl, 2011), where it is present throughout sexual stage maturation from stage II to stage V. There, it is localized in the cytoplasm. The control assays were carried out with and without the addition of 50 mM CaM, as PfPKRP is annotated as CaM-dependent kinase of the parasite (reviewed in Ward et al., 2004). In the presence of CaM, the PfPKRP-specific immunoprecipitate was capable of phosphorylating MBP, whereas reactions without CaM did not lead to a detectable MBP phosphorylation signal (Fig. 3.28 A). Noteworthy, the phosphorylation signals (rMGV) were of the same intensity for both inhibitor-treated precipitates and DMSO-treated control parasites.

As a second negative control, the endoplasmic reticulum (ER)-associated plasmodial protein Pf39 (Templeton et al., 1997) was immunoprecipitated by specific antisera for employing in the kinase inhibition assays. Pf39-specific precipitate was not capable of phosphorylating MBP, neither in inhibitor-treated parasite precipitates nor DMSO control precipitates (Fig. 3.28 B).

### 3.3.3 Effect of CLK inhibitors on specific blood stages

Besides proving that the CLK inhibitors specifically impair the activity of the PfCLKs *in vitro*, studies were conducted to scrutinize which particular parasite stage is affected by the inhibitors specifically. Therefore, the stage-of-inhibition assay was carried out as previously described (Barthel et al., 2008; Aminake et al., 2011). The most active inhibitor CHX, as determined by Malstat assay (section 3.3.1; Tab. 3.2), was incubated with synchronized ring stage parasites (T0) at approximate IC<sub>50</sub> and IC<sub>80</sub> concentrations and cultured further as described (section 2.2.1.1). DMSO-treated parasite cultures at a concentration of 0.5% vol. DMSO served as negative controls. Giemsa-stained smears were taken at distinct time points between 12-60 h of incubation and the numbers of different blood stages and dead parasites were counted in a total of 100 infected erythrocytes (Fig. 3.29).

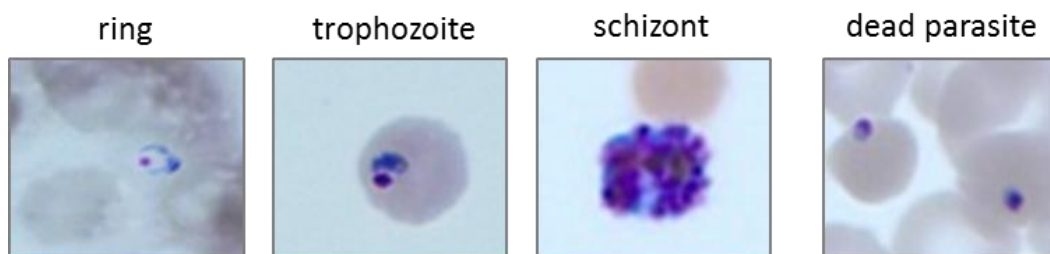
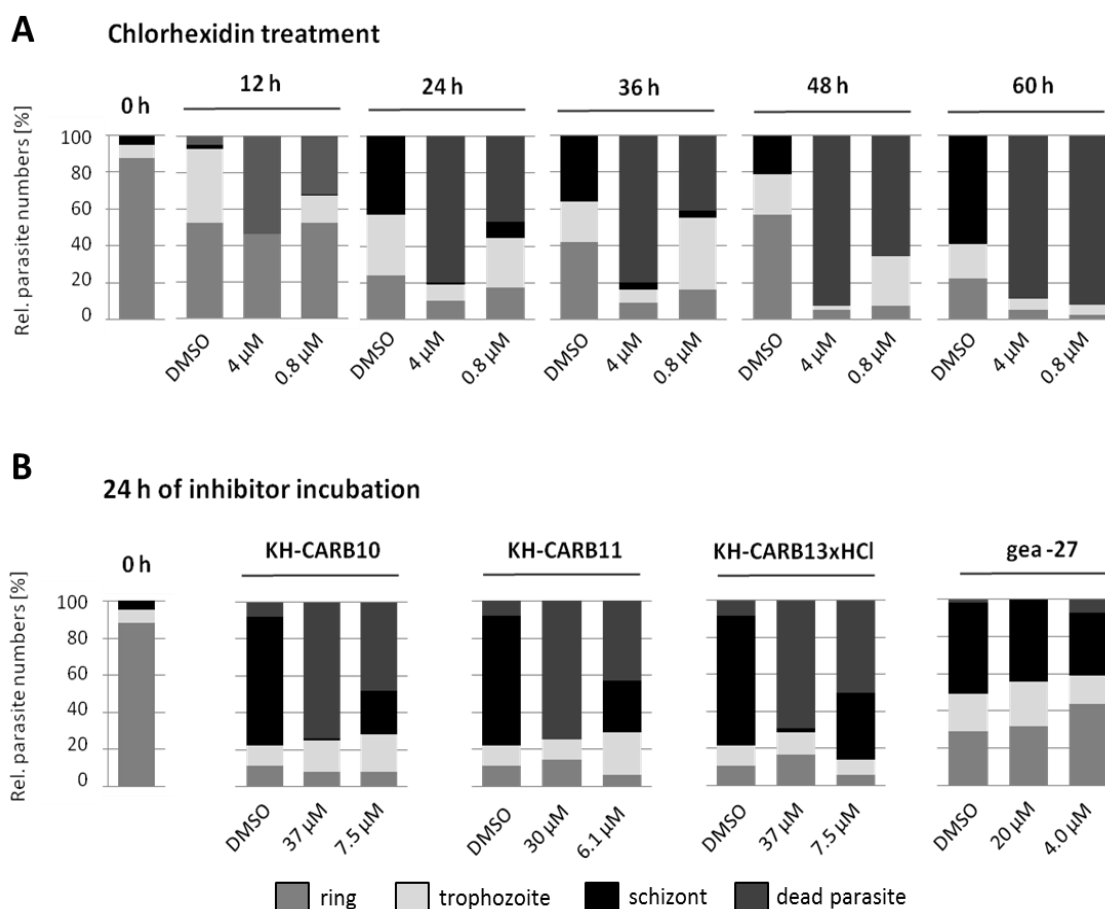


Fig. 3.29: Giemsa-stained asexual parasite stages distinguished in stage-of-inhibition assays.

The Giemsa-stained smears revealed that the CHX-treated asexual parasites developed to trophozoites normally, but the majority of the investigated parasites died before they were able to enter the schizont stage (Fig. 3.30 A). At the given concentrations of CHX, a marginal amount of parasites was able to escape the killing during the first round of replication. These parasites died finally during the second replication cycle where they were not capable of

transforming from trophozoites to schizont stages. DMSO-treated parasites exhibited regular growth and stage-transition during the given cycles of asexual replications, with no or only very few parasites being killed due to prolonged cultivation under the given conditions.



**Fig. 3.30: Effect of CLK inhibitors on blood stage parasites.** **A.** Stage of growth inhibition of asexual blood stage parasites between 12 to 60 h of CHX treatment. The compound at approximate  $IC_{50}$  and  $IC_{80}$  concentrations ( $0.8 \mu\text{M}$  and  $4.0 \mu\text{M}$ , respectively) or 0.5 % vol. of DMSO was added to synchronized ring stage parasites. Giemsa-stained blood smears were prepared at six time points between 0-60 h of incubation with CHX and the numbers of ring stages, trophozoites, schizonts and dead parasites were counted. Histograms display the percentages of developmental stages prevailing in the respective blood smears. **B.** Parasites were treated with CLK inhibitors as described above and the stage of growth inhibition was ascertained at 24 h of compound incubation. A total number of 100 parasites was counted in A and B for each condition.

To determine whether a comparable killing mechanism can be considered for the other investigated CLK inhibitors, stage-of-inhibition-assays were carried out for KH-CARB10, KH-CARB11, KH-CARB13xHCl and gea-27 (Fig. 3.30 B). After incubating the respective inhibitor for 24 h at approximate  $IC_{50}$  and  $IC_{80}$  concentrations and evaluation of Giemsa-stained smears, it was observed that all blood stages died when incubated with each of the four investigated compounds once they entered schizogony. The lowest death rate at 24 h of compound incubation was recorded for gea-27 where schizonts were counted in parasite samples treated with  $IC_{50}$  and  $IC_{80}$  concentrations of this CLK inhibitor. All three investigated oxo- $\beta$ -carboline-derived CLK inhibitors, on the contrary, exhibited the same effective killing effect on parasites treated with both concentrations, respectively.

### 3.3.4 Effect of CLK inhibitors on gametocyte maturation

In order to verify the gametocytocidal effect of a selection of the above mentioned CLK inhibitors, gametocyte toxicity assays were carried out as previously described (Aminake et al., 2011). The observation was made that all CLK inhibitors tested in this assay significantly compromised gametocyte maturation by 40-60% compared to DMSO-treated control parasites (Fig. 3.31). The highest gametocytocidal effect was exhibited by KH-CARB11 with a reduction rate of mature gametocytes by 62.5%. Chloroquine was used as negative control (Buckling et al., 1999) and the proteasome inhibitor epoxomicin was utilized as positive control (Kreidenweiss et al., 2008; Aminake et al., 2011).

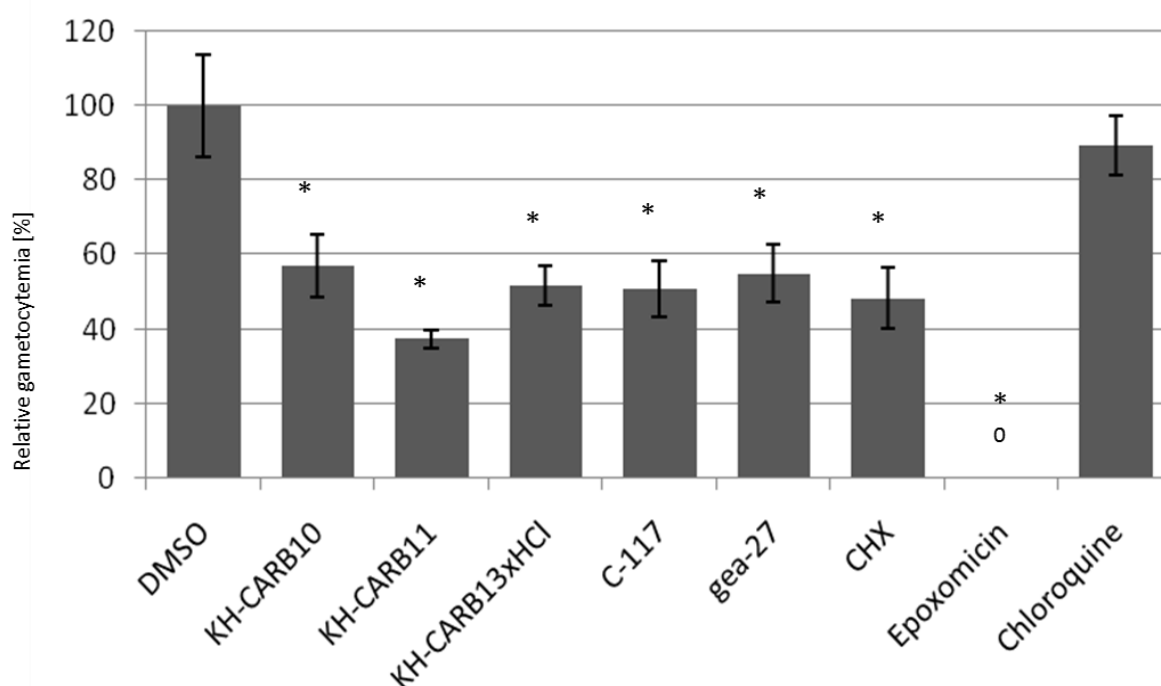


**Fig. 3.31: Gametocyte toxicity assay.** Compounds at  $IC_{50}$  concentrations or 0.5 % vol. DMSO were added to stage II gametocyte cultures for two days. After seven days, the numbers of stage IV and V gametocytes were counted in a total of 1000 RBCs and correlated to the gametocyte numbers of DMSO control, which was set to 100 %. \*, significant reduction of gametocyte numbers ( $p < 0.001$ , student's t-test). Epoxomicin was utilized as positive control, chloroquine was used as negative control.

### 3.3.5 Effect of CLK inhibitors on microgametocyte exflagellation

Exflagellation inhibition assays were conducted subsequently to scrutinize the effect of the CLK inhibitors on microgamete formation. Male gametogenesis was impaired most severely by the oxo- $\beta$ -Carbolines KH-CARB10, KH-CARB11 and KH-CARB13xHCl with  $IC_{50}$  values ranging between 10 and 20  $\mu$ M (Tab. 3.3, Fig 3.32 A). Combined results (mean and SD) of two independent experiments were determined, comprising six counts per sample and concentration in total. Number of exflagellation centers are shown as percentage of DMSO controls (Fig. 3.32 and. 3.33).

**Tab. 3.3:** Summary of observed IC<sub>50</sub> values in exflagellation assays.

Compound	IC <sub>50</sub> (μM)
KH-CARB10	14.0 ± 3.72
KH-CARB11	15.8 ± 0.84
KH-CARB13xHCl	13.8 ± 6.22
C-117	67.5 ± 13.03
gea-27	154.2 ± 56.43
CHX	19.8 ± 0.93

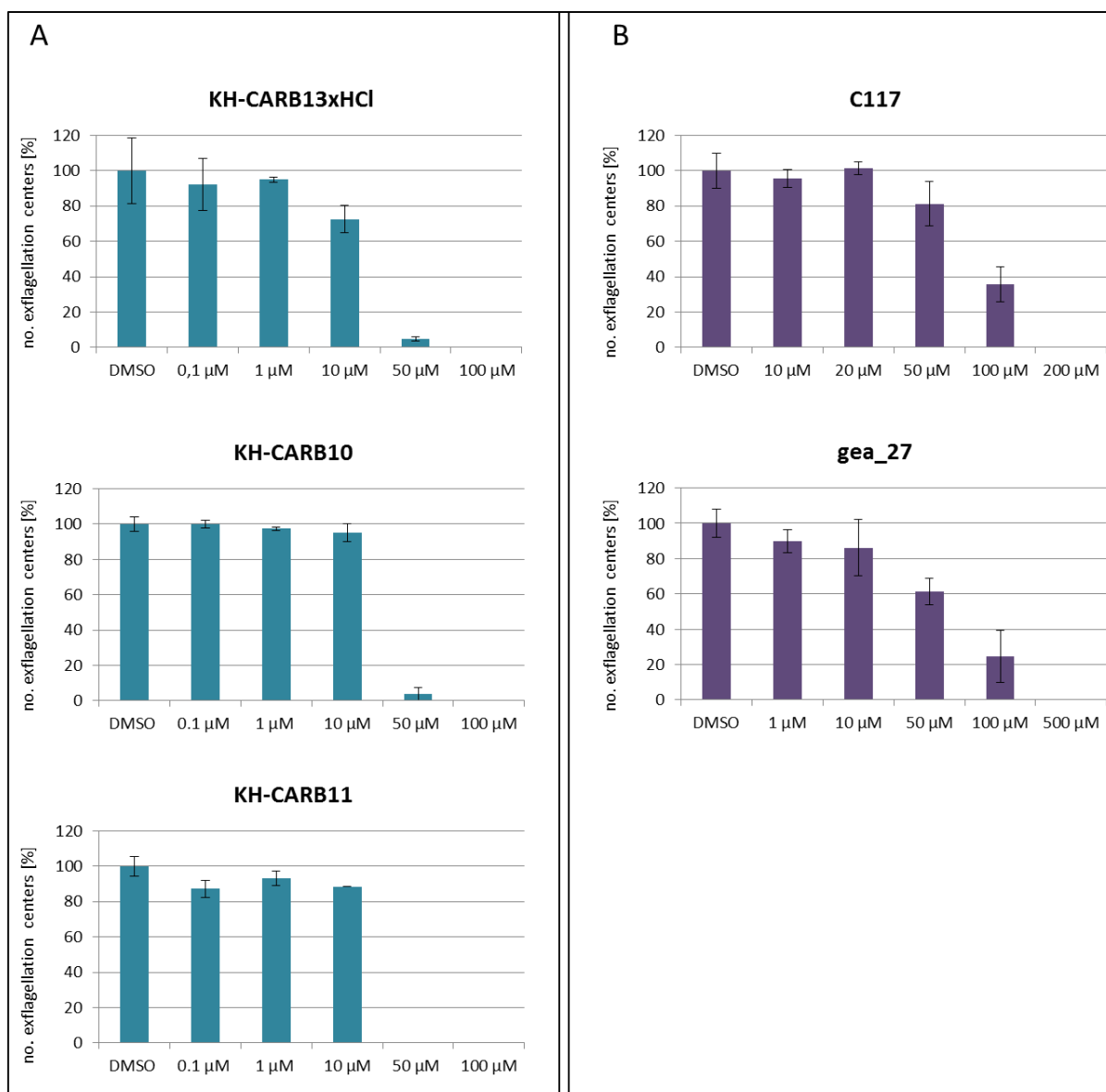


**Fig. 3.32: Transmission blocking potential of selected CLK inhibitors in exflagellation assays.** Compounds at various concentrations (**A.** oxo-β-carbolines and **B.** aminopyrimidines) or 0.5 % volume of DMSO were added to mature gametocyte cultures and activated with XA. The number of exflagellation centers were counted 15 min after activation. Combined results (mean and SD) of two independent experiments, comprising six counts per sample and concentration in total, are shown as percentage of DMSO control.



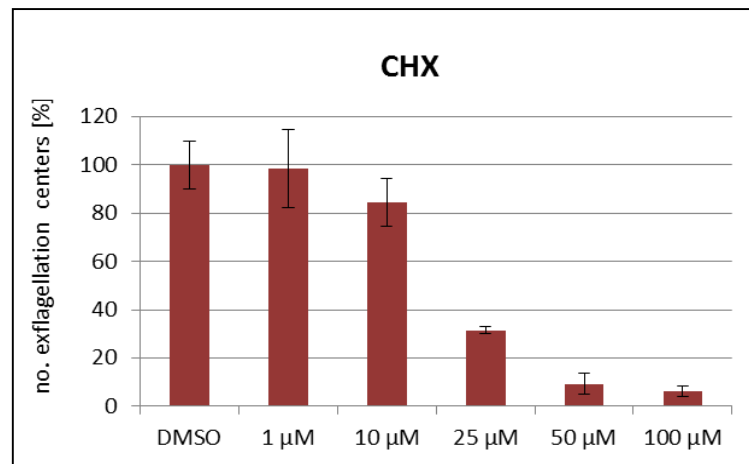


**Fig. 3.33: Impact of CHX on parasite gametogenesis.** CHX at different concentrations or 0.5 % volume of DMSO were added to mature gametocyte cultures and activated with XA. The number of exflagellation centers were counted 15 min after activation; the number of centers was recorded and compared to the number of centers in the untreated DMSO controls. Results of two independent experiments. Mean  $\pm$  SEM.

## 4 Discussion

As one of the world's most devastating diseases, malaria still displays an enormous burden to socio-economic development and public health conditions (reviewed in (Breman et al., 2004; Kokwaro, 2009)). Most severely affected areas are regions in Sub-Saharan Africa, the Amazon region and Southeast Asia (Hyde, 2005), where predominantly malaria tropica is a leading cause of death in children and pregnant women. Numerous factors such as poor health services, poverty, malnutrition and co-infections with tuberculosis or HIV contribute to deteriorate the situation in endemic countries (reviewed in Breman et al., 2004; WHO, 2013). As rising resistances against commonly used medications as well as a lack of an effective vaccine prevail, strategies to counteract malaria have to be enhanced and effective drug targets have to be searched for (reviewed in Greenwood et al., 2008).

Resulting from the sequencing of the genome of *P. falciparum* and succeeding genome annotation, merely one tenth out of 5 300 genes encode for enzymes (Gardner et al., 2002). Two independent genome-wide analyses of *P. falciparum* subsequently led to the identification of 86 or 99 sequences related to kinases, respectively (reviewed in Ward et al., 2004; Anamika et al., 2005), depending on the stringency applied to include borderline sequences (reviewed in Doerig et al., 2008, Solyakov et al., 2011). Representing 1.1-1.6 % of the parasite's coding genes, 65 out of these are evidently related to the eukaryotic protein kinase (ePK) family (Solyakov et al., 2011). Pre-genomic classification distributed ePKs into conventional eukaryotic groups (reviewed in Miranda-Saavedra et al., 2012). Several of the 65 ePKs of *P. falciparum* can be ascribed to the acquainted groups of AGC, CMGC, CK1, CaMK and tyrosine-kinase like groups observed in the human kinome (reviewed in Doerig et al., 2008).

Phylogenetic tree construction led to the classification of plasmodial kinases into seven main groups, with the CMGC group representing the largest of these groups. Amongst cyclin-dependent (CDK), mitogen-activated (MAPK) and glycogen-synthase (GSK) kinases, the CLK kinase family surveyed in this study belongs to this significant group. In other eukaryotes, CLKs play crucial roles regarding mRNA splicing or processing and have been studied extensively, representing corroborated targets for drugs (Talevich et al., 2011). CLKs are conserved throughout eukaryote evolution and possess a unique and conserved LAMMER signature motif, often being referred to as LAMMER kinases (Yun et al., 1994; Bullock et al., 2009). The specific LAMMER signature has been previously suggested to prescribe kinase substrate specificity (Yun et al., 1994). Remarkably, CLKs have been reported to possess dual-specificity properties, being capable of performing autophosphorylation at tyrosine residues as well as phosphorylation of substrates exclusively on serine/threonine residues (Nayler et al., 1997). Tyrosine phosphorylation was actually reported for PfCLK-3 in a global genomic analysis (Solyakov et al., 2011).

Nevertheless, scant research is carried out regarding CLKs as well as mRNA splicing in *P. falciparum* (Dixit et al., 2010; Eshar et al., 2012). Consequently, characterization of malarial CLKs is indispensable as to conceive and disclose the mechanisms of splicing regulation. As alternative splicing displays such an essential cell cycle mechanism in all eukaryotes analyzed

so far (reviewed in Hagiwara, 2005), the exploration of the same in *P. falciparum* will unravel the cascades and components involved in this process and may lead to the identification of additional drug targets. The present study chose the four serine/threonine CLK kinases of *P. falciparum*, namely PfCLK-1/LAMMER (PF3D7\_1445400), PfCLK-2 (PF3D7\_1443000), PfCLK-3 (PF3D7\_1114700) and PfCLK-4 (PF3D7\_0302100) for functional characterization in the parasite life cycle stages. All four plasmodial kinases of the CLK family cluster with the human SRPK1-3 and the human LAMMER kinases CLK1-4, which also phosphorylate SR proteins (reviewed in Ward et al., 2004). Previously described PfCLK-1/LAMMER is related to yeast *kns1* (Li et al., 2001; Prasad et al., 2003), and PfCLK-3 is clearly reported to be an orthologue of human PRP4 (Talevich et al., 2011), which is associated with mRNA splicing and is conserved in most eukaryotic genomes including the *Schizosaccharomyces pombe* genome (Gross et al., 1997; reviewed in Ward et al., 2004). Human SRPK1 was previously reported to phosphorylate SR proteins and homologues are conserved in all eukaryotic genomes (Wang et al., 1999). PfCLK-4 and PfCLK-2 cluster within SRPKs, with both kinases possessing an insertion which is an unmistakable attribute of SRPKs (reviewed in Ward et al., 2004; Dixit et al., 2010; Talevich et al., 2011). Furthermore, preceding studies revealed that the PfCLKs share homologies with the yeast kinase Sky1p (Agarwal, 2010; Agarwal et al., 2011), which is involved in mRNA splicing and transport in *S. cerevisiae* (Siebel et al., 1999; Nolen et al., 2001).

In order to gain deeper insight into the splicing machinery of *P. falciparum*, this study was carried out to identify putative interaction partners of the PfCLKs, which are most likely SR proteins or RNA binding proteins. These proteins function in the RNA processing pathway during splicing events. Additionally, a library of inhibitors of human and microbial CLKs was used to scrutinize the antiplasmodial activity of the used inhibitors. By rendering some of these compounds active against the parasite kinases, they can be used as agents to chemically inhibit the specific PfCLKs and for further identification of the components of the plasmodial splicing machinery.

#### 4.1 Functional characterization of PfCLK-3 and PfCLK-4

Previously, PfCLK-1/LAMMER was described as sexual stage-specific kinase (Li et al., 2001) by measuring the mRNA level of the kinase gene by means of Northern blotting. However, subsequent studies revealed that transcripts of all four plasmodial CLKs are predominantly present in schizonts and gametocytes, conducted by RT-PCR and more sensitive Real Time RT-PCR (Agarwal, 2010; Agarwal et al., 2011). The transcript expression ceases with proceeding parasite development, detecting only low transcript levels for *pfclk-4* in zygotes. None of the other kinase genes studied showed considerable expression in this life cycle stage of *P. falciparum*.

Characterization of protein expression of PfCLK-3 and PfCLK-4 was carried out in this study. To determine the kinase expression on the protein level, mouse antisera raised against the recombinantly expressed catalytic domains of PfCLK-3 and PfCLK-4 were used (Fig. 1.6). Kinase catalytic domains were preferred for antisera production as these protein domains are

fundamental components responsible for kinase activity. Moreover, their presence can be predicted as indispensable for the cellular function of the respective kinase. They are comprised of twelve highly conserved subdomains with distinct functions in ATP binding capability as well as the ensurance of structural stability of the kinase (reviewed in Hanks and Hunter, 1995; Hanks, 2003; reviewed in Ward et al., 2004).

For both PfCLK-3 and PfCLK-4, asexual parasite lysates were obtained from gametocyte-less parasite strain F12, whereas gametocyte lysates were attained by use of wild type strain NF54. Western blot analysis performed on these lysates using mouse antisera against PfCLK-3 detected a full size protein band migrating at 81 kDa. In addition, a processed protein band was revealed at approximately 70 kDa, most likely representing truncated forms of the recombinant protein due to improper translation. The protein expression of both kinases in these life cycle stages is in concordance with previously reported mRNA transcript expression (Agarwal, 2010; Agarwal et al., 2011). The same protein bands were detected in nuclear pellet fractions as well as in cytoplasmic fractions of asexual parasites. Full size PfCLK-4 (157 kDa) was similarly detected in lysates of asexual parasites and nuclear pellet fractions, whereas a processed PfCLK-4 protein only was observed in gametocyte lysates.

The presence of both kinases under study in the parasite nucleus and the cytoplasm is consistent with previous *in silico* analyses which exhibited that PfCLK-3 and PfCLK-4 do not possess nuclear localization signals, unlike PfCLK-1 and PfCLK-2 (Agarwal, 2010; Agarwal et al., 2011). In that study it was observed by *in silico* analysis and immunoelectron microscopy that PfCLK-1 as well as PfCLK-2 possess nuclear localization signals, directing them to subcellular nuclear structures called nuclear speckles. Nuclear speckles are associated with the storage of splicing factors like snRNPs (small nuclear ribonucleoprotein particles) and SR-proteins (reviewed in (Lamond and Spector, 2003; Spector and Lamond, 2011)). Previous studies confirm presence of mammalian Clk/Sty kinases within nuclear speckles. Consequently, these kinases display parts of the splicing machinery in synergy with splicing factors. (reviewed in Lamond and Spector, 2003; Ngo et al., 2005). Given the recent observations in this study, PfCLK-3 and PfCLK-4 are as well located in the parasite nucleus despite the absence of nuclear localization signals (NLS) in these kinases. Several nuclear proteins are reported that lack classic NLS and can still be found inside the nucleus (Eshar et al., 2012). One prominent example is Clk/Sty, which was reported to be localized to the nucleus (Duncan et al., 1997), most probably within nuclear speckles in conjunction with SR proteins (Colwill et al., 1996b). Likely as a consequence of hyperphosphorylation, the proteins remain inside the nuclear speckles through their RS domain (Bullock et al., 2009). Upon phosphorylation, SR splicing factors are released from these sites (Colwill et al., 1996b), presumably “piggy-backing” the associated kinase and thus relocating it to the cytoplasm (Dixit et al., 2010). For PfCLK-4, a similar mechanism has been proposed, since SRPK of mammalian cells is also present in the cytoplasm to phosphorylate the RS domain of SF2/ASF, which leads to its nuclear translocation (Koizumi et al., 1999; Lai et al., 2000; reviewed in Stamm, 2008; Dixit et al., 2010). SF2/ASF is further hyperphosphorylated inside the nucleus by Clk/Sty, resulting in its release from the speckles to the site of mRNA splicing (Dixit et al., 2010). Export to the cytoplasm is subsequently facilitated by dephosphorylation conducted by a protein phosphatase (reviewed in Stamm, 2008). In accordance with previous studies (Dixit et al.,

2010), the findings of this study show that PfCLK-4 (PfSRPK1) is principally located inside the parasite nucleus during early asexual stages and switches to cytoplasmic localization after mid to late trophozoite stages. It was previously observed that PfCLK-4 localization almost permanently coincides with localization of PfSR-1, suggesting an interaction of both proteins in such a way that one partner “piggy-backs” the other in and out of the nucleus (Dixit et al., 2010). Such an interaction of two proteins was reported for non-kinase proteins, as Pfsec13 seems to be specifically associated with another plasmodial protein, which contains a nuclear transport factor (Dahan-Pasternak et al., 2013). Pfsec13 is an integral component of the nuclear pore complex as well as of the vesicle transport system in the parasite cytoplasm and does not possess any NLS.

In addition, the localization of PfCLK-3 and PfCLK-4 was further verified by IFAs on asexual and gametocyte parasite stages. As the mouse antiserum directed against PfCLK-3 was not capable of detecting the endogenous parasite kinase in IFAs, rat antiserum was utilized which was kindly provided by Prof. Dr. Andrew Tobin and was generated as previously described (Solyakov et al., 2011). Both kinases, PfCLK-3 and PfCLK-4, revealed in immunofluorescence assays that they are profusely expressed in asexual blood stages of *P. falciparum*. Similar to previous studies on PfCLK-1 and PfCLK-2, the kinases investigated in this actual study are located to the nucleus of trophozoites. In contrast, both kinases displace to the parasite cytoplasm during schizogony and subsequent gametocytogenesis. In concordance with the recent findings, previous studies reported that PfCLK-4 is predominantly located inside the parasite nucleus in early asexual stages, switching to cytoplasmic distribution from late trophozoites and schizonts (Dixit et al., 2010). Likewise to the current investigations, PfCLK-4 was only detected in the cytoplasm of gametocytes in the preceding study by Dixit et al. In compliance with these findings, it was previously shown that PfCLK-4 is abundantly expressed in gametocytes, but down-regulated once gametogenesis has terminated (Ngwa et al., 2013). This observation is connoting PfCLK-4 to have a particular function during parasite transmission from the human host to the anopheline vector.

Previous attempts to demonstrate any kinase activity of PfCLK-1 by utilizing its recombinant catalytic domain were ineffective (Agarwal, 2010). This failure can most likely be explained due to missing residues in the recombinantly expressed kinase fragment. Therefore for this study, *in vitro* substrate phosphorylation was carried out by precipitating endogenous PfCLKs from parasite lysates with specific antisera against PfCLK-3 and PfCLK-4. Subsequently they were processed in a specific kinase activity reaction by adding  $\gamma$ -<sup>32</sup>P-phosphorus-labeled ATP and common physiological substrates *in vitro*. Likewise to PfCLK-1 and PfCLK-2 (Agarwal, 2010; Agarwal et al., 2011), both kinases under the current study were capable of phosphorylating all offered physiological substrates (section 2.2.3.8) *in vitro*. PfCLK-4 was already reported in previous studies to phosphorylate these substrates *in vitro* as well (Dixit et al., 2010).

## 4.2 PfCLK-3 and PfCLK-4 are essential for the asexual replication cycle

Generation of gene-disruptant parasites was conducted to investigate the correspondent kinase phenotype in asexual parasite cultures. For this purpose, a pervasive strategy was used to disrupt the respective kinase gene by single cross-over homologous recombination (Dorin-Semlat et al., 2007). The disruption was placed into the catalytic domain to separate the ATP binding domain (GXGXXG) from the PE motif which is responsible for the structural stability of the kinase, thus rendering the same non-functional. Up to date, numerous parasite kinases have been reported to be indispensable for the parasite in both *P. berghei* as well as *P. falciparum*. To only mention a few, these are Pbcrk-1, Pfmap-2 or PfCK2 (Rangarajan et al., 2006; Dorin-Semlat et al., 2007; Holland et al., 2009). On the contrary, kinases like Pfmap-1 have been disrupted successfully, while the resulting knock-out parasites revealed a normal phenotype in all parasite stages (Fenell et al., 2009). In summary, 12 plasmodial ePKs were identified in a global kinomic analysis that are definitely dispensable, as demonstrated by viable parasite clones carrying the respective inactivated kinase genes. For further 14 ePKs, they appear to be likely dispensable, as they revealed a strong signal diagnostic for gene disruption in (mixed) transfected populations (Solyakov et al., 2011).

Successfully disrupting genes does not only provide information about the indispensability of the respective kinase regarding replication of asexual parasite stages, but also delivers a powerful tool to determine the application of specific kinase inhibition. Differential inhibition can be applied onto PfCK2 $\alpha$  subunit for example, which can be specifically blocked by ML-7 and Rottlerin (Holland et al., 2009). Whereas these compounds exhibit moderate IC<sub>50</sub> values for inhibiting the plasmodial subunit of CK2 $\alpha$ , the human subunit of this kinase requires an extremely high concentration of these compounds, although CK2 has a high percentage of identity (65 %) between the human and the plasmodial counterparts (Holland et al., 2009).

None of the two investigated *pfclk* loci could be disrupted successfully, which leads to the assumption that either the genomic locus of the kinase is not accessible for homologous recombination, or the kinase is essential for the replication and thus for the survival of asexual stage parasites (Rangarajan et al., 2006). This observation is in concordance with previous studies that showed that the gene loci for PfCLK-1/LAMMER as well as PfCLK-2 can not be disrupted by reverse genetic strategies (Agarwal, 2010; Agarwal et al., 2011; Solyakov et al., 2011). For the purpose of investigating the recombinogenicity of the kinase locus, a Myc-epitope was fused to the 3'-end of the respective kinase gene by means of single cross-over homologous recombination. As a result, gene-tagging was conducted without disrupting the gene and thus no loss-of-function. Integrant populations of kinase-tagged parasites were detected by diagnostic PCR after transfection and single clones were subsequently isolated. Further verification after prolonged culturing was carried out and confirmed the stable integration of the tagging sequence into the genome. As this gene-tagging approach was successful for both PfCLK-3 and PfCLK-4, the recombinogenicity was validated for both gene loci. Earlier studies on the capability of recombining the kinase locus for PfCLK-1 and PfCLK-2 showed that these two kinases can be tagged similarly. These results lead to the assumption that the inability to knock out the respective kinase locus is not caused by locus refractoriness

to recombination, but rather due to the indispensability of both PfCLK-3 and PfCLK-4 for the asexual replication cycle of *P. falciparum*. PfCLK-3 and PfCLK-4 thus display essential components in the parasite asexual life cycle. This finding aligns with the fact that multiple essential kinases are involved in SR protein phosphorylation in diverse cellular compartments in a non-redundant manner. Human ASF is phosphorylated by both SRPK1 and SRPK2 inside the cytosol, thereby triggering its nuclear import and accumulation inside the speckles. A family of CLKs hyperphosphorylates human ASF subsequently and mediates its release from the nuclear speckles again and directing it back to the cytoplasm, after splicing (Misteli et al., 1998; Lai et al., 2000; Aubol et al., 2003). In conclusion, several diverse kinases orchestrate in close collaboration during the event of pre-mRNA processing (Ngo et al., 2005), rendering all individual components indispensable for the entire splicing event. Moreover, none of the involved kinases is capable of compensating another.

Fusing a tag to the 3'-end of kinase sequences by single cross-over homologous recombination leads to a tagged but functional enzyme and does not produce a loss-of-function mutation in contrast to the knock-out strategy. Hence, tagging a specific kinase with a Myc-tag allows on the one hand the investigation of the kinase's role in the parasite life cycle. On the other hand, gene-tagging displays a potent device to further characterize PfCLK-3 and PfCLK-4 by using antibodies directed against one of the tags which was successfully fused to the kinase sequence. By doing so, Western blot assays, IFAs, Pull down or immunoprecipitation assays can be utilized for further scrutinizing the role of the kinases in the parasite's life cycle. Tagged PfCLK-3 and PfCLK-4 were successfully confirmed by means of Western Blot and IFA using the respective antisera against the tag.

Together, given the aforementioned results regarding the study on the essentiality of PfCLK-3 and PfCLK-4, it can be concluded that both kinases play pivotal roles in the parasite asexual development. This conclusion can be drawn as the kinase loci cannot be disrupted but recombined successfully. These findings are in accord with their specific expression profiles throughout the asexual blood stages, both on the mRNA and protein level. Kinome-wide gene knock-out and reverse genetic approaches have been exhibited that out of the 65 identified *P. falciparum* ePKs approximately 50 % are most likely essential for the preservation of parasite viability (Solyakov et al., 2011). Given this lack of redundancy, it is likely to assume that a vast number of protein kinases possess pivotal roles for the parasite erythrocytic asexual cycle. Moreover, there is a hypothetically abundant source of protein kinases as targets for prospective anti-malarial strategies (Solyakov et al., 2011). Amongst all four PfCLKs, there are several protein kinases of *P. falciparum* that have shown to be indispensable by means of reverse genetic studies: for example the MAP kinase Pfmap-2 (Dorin-Semlat et al., 2007), NIMA-related kinase Pfnek-1 (Dorin-Semlat et al., 2011), PfCK2 (Holland et al., 2009) or the cyclin-dependent kinase-related kinase Pfcrk-3 (Halbert et al., 2010).

### 4.3 Identification of putative CLK interaction partners

Furthermore, the aim of this study was to examine putative interaction partners which may act as splicing factors in pre-mRNA processing. CLKs are capable of phosphorylating SR proteins that act as splicing factors in the post transcriptional/pre-mRNA processing pathway (reviewed in Godin and Varani, 2007; Bullock et al., 2009). When being inactive, SR proteins reside inside nuclear speckles, dynamic structures inside the cell nucleus and storage sites for components of the splicing machinery (reviewed in (Lamond and Spector, 2003; Spector and Lamond, 2011)). Nevertheless, SR proteins shuttle between the nucleus and the cytoplasm during a splicing event (Cáceres et al., 1997; Lai et al., 2000). The specific state of activity of SR proteins is controlled by their phosphorylation status (Misteli et al., 1998, reviewed in Graveley, 2000; Dixit et al., 2010). As a consequence of changing their phosphorylation status, SR proteins change their capability to interact with other proteins (reviewed in Fu et al., 1995; Bullock et al., 2009). Post-transcriptional splice site selection of splicing components such as splicing factors is tightly regulated by the concentration and phosphorylation status of SR proteins (reviewed in (Godin and Varani, 2007; Stamm, 2008)). Thus, CLKs play an indirect but nevertheless pivotal role in governing the choice of splice sites, highlighting their significance in alternative splicing events (Velazquez-Dones et al., 2005; reviewed in Stamm, 2008). SR proteins have been investigated extensively in several eukaryotes and have been identified as components in alternative splicing as well as CLK interaction partners and substrates (Colwill et al., 1996 a&b; Duncan et al., 1997; Bullock et al., 2009). Prototypical SR proteins like human SF2/ASF possess two arginine/serine repeat domains consisting of multiple arginine/serine dipeptides (reviewed in (Fu et al., 1995; Graveley, 2000)). Serine residues are subject to phosphorylation by CLKs, thus triggering nuclear import and accumulation in nuclear speckles (Velazquez-Dones et al., 2005, reviewed in Stamm, 2008; Bullock et al., 2009).

In this study, we were able to identify one yeast CLK substrate and four plasmodial SR proteins that revealed interaction with the investigated PfCLKs *in vitro*. Yeast factor Npl3p is reported to be the specific substrate of yeast kinase Sky1p (Siebel et al., 1999; Nolen et al., 2001) and was utilized as alignment template to find the homologous plasmodial factors investigated in this study. All four investigated parasite proteins possess a RNA recognition motif, rendering them as putative splicing factors (reviewed in Graveley, 2000). Except for PfASF-1, these factors also consist of a domain of RS-rich repeats, where presumably phosphorylation by CLKs takes place. Kinase activity assays utilizing the affinity purified recombinant yeast Npl3p revealed that it interacts with PfCLK-1, PfCLK-2 and PfCLK-4 *in vitro*. No phosphorylation signal was observed for PfCLK-3 incubated with recombinant Npl3p. Noteworthy, by incubating Npl3p with parasite extract prior to immunoprecipitation by PfCLK-1 antisera, Npl3p was phosphorylated, indicating that Npl3p is able to form a stable complex with PfCLK-1 *in vitro*, as it was precipitated conjointly with PfCLK-1.

Regarding the four plasmodial factors which function as PfCLK substrates, we additionally recognized diverse phosphorylation preferences for the SR proteins under study. PfASF-1 was phosphorylated *in vitro* by PfCLK-1 and PfCLK-2, whereas recombinant PfSRSF12 showed phosphorylation by anti-PfCLK-2 and anti-PfCLK-3 precipitates. Moreover, PfSFRS4 was



phosphorylated *in vitro* by all PfCLK-specific precipitates. PfCLK-4 was previously described to phosphorylate another AS factor, PfSR-1 (PF3D7\_0517300; Dixit et al., 2010). Whilst the N-terminal RS-domain containing fragment of PfSF-1 was interacting with all PfCLKs except of PfCLK-3, no phosphorylation signals were observed when incubating the kinase immunoprecipitates with the C-terminal part of PfSF-1 lacking the RS domain. This domain was reported previously to be the phosphorylation target of CLKs (Bullock et al., 2009; Velazquez-Dones et al., 2005; reviewed in Stamm, 2008).

Interestingly, PfASF-1 is the only of the four plasmodial splicing factors investigated that does not possess a RS domain but is phosphorylated by the PfCLKs. Presumably PfASF-1 is phosphorylated at location that is unique to the plasmodial ASF-1, since even this plasmodial factor shares homology with the human/mammalian factor, it remains elusive if PfASF-1 definitely is a plasmodial splicing factor.

Different preferences of CLKs and SRPKs for SR protein substrates have already been reported, as SRPK interaction is restricted by a specific docking interaction, whereas CLK activity is less constrained by a determined active-site mediated substrate specificity (Bullock et al., 2009). Domain insertions define the specificity of the conserved LAMMER signature motif in CLKs, displaying distinct binding activities (Velazquez-Dones et al., 2005; Bullock et al., 2009). During splicing events, CLKs and SRPKs often act in close collaboration (Ngo et al., 2005). For all plasmodial proteins investigated in this study except of PfASF-1, phosphorylation sites have been identified (Kern et al., 2014) and the proteins are phosphorylated *in vivo*, as determined in the *P. falciparum* schizont stages (Solyakov et al., 2011; Treeck et al., 2011; Lasonder et al., 2012; Pease et al., 2013).

Once the phosphorylation activity of the four plasmodial factors was confirmed, IFAs were carried out utilizing antisera raised against the SR proteins of interest. Immunolabelling for PfASF-1 could not obtain significant signals, which may be elucidated by either a very low protein expression level in the investigated life cycle stages or, more likely, a non-functional or only poorly performing antibody raised in mice. Due to time restrictions, it was not possible in the course of this study to repeat the generation of functional antibodies. As the recombinant protein of PfASF-1 displayed the full-length protein, it was moreover not feasible to choose a diverse fragment of the plasmodial protein resulting in a more effectively expressed recombinant protein for immunization of mice.

Antibodies raised against the fragments of the remaining three recombinant splicing factors under study, respectively, revealed that PfSRSF12, PfSFRS4 as well as PfSF-1 are located inside the parasite nucleus of trophozoite stages with a fainter labelling in schizonts, but also in co-localization with the parasite nucleus. In gametocytes, nuclear localization of PfSRSF12 and PfSF-1 was detected, whilst PfSFRS4 was not observed in these sexual stages. Transcriptome data point as well to predominant transcript expression for these parasite SR proteins in trophozoites (Aurrecochea et al., 2009). Several other nuclear proteins like PfSR-1 are located to the nucleus despite of the presence of NLS (Cáceres et al., 1997; Eshar et al., 2012). PfSR-1 was reported to be the phosphorylation substrate of PfCLK-4 (Dixit et al., 2010), possessing a RS-domain which is crucial for nuclear localization. Deletion analyses revealed that mutants lacking the RS-domain of PfSR-1 reside in the parasite cytoplasm (Eshar et al., 2012). Therefore, it is indicative for the RS domain to act as NLS similar to the mammalian

SRSF1 (Eshar et al., 2012). Previous studies report that the RS domain is able to function as NLS in SR proteins, affecting the subcellular localization of SR proteins by mediating the interaction with the SR protein nuclear import receptor, transportin-SR (Cáceres et al., 1997; Lai et al., 2000; reviewed in Long and Cáceres, 2009). Furthermore, binding to nuclear export factors of human ASF is increased by dephosphorylation (Huang et al., 2004), therefore pointing to a distinct role of phosphorylation and subsequent dephosphorylation of SR proteins in nucleo-cytoplasmic shuttling of the same. The phosphorylation status of SR proteins also regulates their accumulation inside the cytosol (Lai et al., 2000). Ribonucleoprotein A1 is accumulating in the cytosol succeeding serine phosphorylation of the F-peptide, which represents a motif being central to nuclear import and export (Allemand et al., 2005).

#### **4.4 CLK inhibitors block parasite development and impair PfCLK phosphorylation activity**

There is a serious need of new malaria combat strategies as there arises an increasing spread of resistance against pervasively used antimalarial drugs. Therefore, drugs eliciting novel modes of action and diverse targets have to be explored to combat this devastating tropical infectious disease. Towards this aim, effective novel compounds should not only be capable of killing asexual parasites, but also block the development of sexual stage parasites. Gametocytes are the sole parasite stages that are capable of infecting mosquitoes once they are taken up by the insect vector during a blood meal. Hence, the parasite is able to continue its life cycle inside the vector, resulting in transmitting the parasite to more human hosts when biting them during a subsequent blood meal. Killing of the transmissible sexual stages will lead to a block of the transmission of the parasites from one human host to the other via mosquitoes, hence lowering the infection rate of individuals in close communities. In *P. berghei*, the homologue to PfCLK-4 (SRPK1) was recently reported to be indispensable for the sexual phase, as this kinase is involved in microgamete formation (Tewari et al., 2010). Even though the *pbclk4* (*srpk1*) gene can be knocked out, this phenotype revealed impaired exflagellation ability.

Given the vast divergence between plasmodial kinases and the kinases of their human hosts (reviewed in Doerig and Meijer, 2007), selective inhibition by various compounds is a promising method to combat malaria. A major part of actual kinase inhibitors is presented by chemical compounds that are ATP analogues (reviewed in (Cox et al., 2011; Lamba and Ghosh, 2012)). Out of thousands of drug-like compounds, these ATP-antagonists have been identified as lead compounds, rendering protein kinases as one of the most important druggable targets.

In addition to the aforementioned reasons, this study aimed at finding prospective promising compounds that possess the potential to chemically inhibit the PfCLKs. Previous studies (Solyakov et al. 2011, Agarwal et al., 2011) and this current study revealed that it was not possible to knock out all four PfCLKs, rendering them essential for the asexual replication cycle. To gain access to a powerful tool for chemically knocking out the parasite CLKs despite

the inability to create a genetic knock-out, attempts were made to identify effective PfCLK inhibitors. For this purpose, a small compound library of 63 CLK inhibitors known to inhibit microbial or human CLKs were screened in this study by Malstat assay in a first approach. Measured IC<sub>50</sub> values revealed that a small compartment of the library compounds was capable of inhibiting the PfCLKs in such a manner that these compounds were considered to be utilized in further testing. Interestingly, out of this small compound library it was possible to identify three members of oxo- $\beta$ -carbolines and two members of aminopyrimidines that show antiplasmodial activity with an IC<sub>50</sub> in the micromolar range (Tab. 3.2).

In addition to the chemical compound library, we screened the antiseptic CHX for its anti-CLK activity. In previous studies, CHX exhibited an antiplasmodial activity with IC<sub>50</sub> concentrations of approximately 0.316  $\mu$ M, which was determined by dose-response curves (Geary and Jensen, 1983). In Malstat assays, CHX was capable of inhibiting *P. falciparum* asexual stages with an IC<sub>50</sub> of  $0.6 \pm 0.40$   $\mu$ M. CHX is a potent inhibitor of human CLK kinases. In a cell-based splicing reporter assay which aimed to identify modulators of splicing and splicing-dependent processes, 23 000 compounds have been screened. As one of the modulators, CHX revealed inhibitory effects on alternative splicing events by specifically and selectively inhibiting CLKs and SRPKs (Younis et al., 2010). A different study confirmed the inhibitory effect of CHX on CLKs by blocking CLK-dependent human SR proteins, which are crucial for RNA processing during replication of HIV-1 (Wong et al., 2011). Since CHX reveals high ototoxic effects which can lead to impaired hearing (reviewed in Milestone et al., 2008) and furthermore exhibits hemolytic effects at concentrations of 0.1 mM (Geary and Jensen, 1983), this antibiotic is most likely not applicable as antimalarial compound. Nevertheless, due to its high efficacy in inhibiting PfCLKs specifically, it displays a potent tool for using this compound to generate chemical KOs and therefore dissect the splicing mechanisms in malaria parasites.

Given the fact that the four PfCLKs cannot be knocked out, this study aimed at chemically inhibiting the plasmodial kinases to gain insight into their specific function. Towards this aim, the five identified CLK inhibitors and the antiseptic CHX were screened out of a small compound library to have an effect on asexual stages of *P. falciparum* investigated in this study as well as sexual stage parasites. Given the vast divergence between plasmodial kinases and the kinases of their human hosts (reviewed in Doerig and Meijer, 2007), selective inhibition by various compounds is a promising method to combat malaria. Therefore, kinase activity assays were carried out to determine whether the compounds act specifically on the PfCLKs. The inhibitors revealed an inhibitory effect on the phosphorylation activity on all four PfCLKs, rendering all investigated compounds as specifically acting on the parasite CLKs. The inhibitors act on the *Plasmodium* parasites in the low micromolar range. While it was demonstrated that the CLK inhibitors have no activity against the calmodulin-dependent kinase PfPKRP, other off-target effects of the investigated compounds can currently not be excluded. Morphological analyses on drug-treated parasites showed that the inhibitors arrest the parasites during the trophozoite-to-schizont transition. Moreover, the inhibitors affected gametocyte development and exflagellation, especially the oxo- $\beta$ -carbolines acted on blood stage replication and on exflagellation in similar concentrations. This approach demonstrated that the investigated compounds are qualified for being used to generate chemical KOs of the PfCLKs for further phenotype characterization and identification of mRNA processing

pathways and phosphorylation-dependent signal transduction during splicing events in *P. falciparum*. Noteworthy, 50 % of the identified compounds belong to the class of oxo- $\beta$ -carboline. Members of this substance class have been reported previously to display potent CLK inhibitors with selective properties (Huber et al., 2011). In this study, specific oxo- $\beta$ -carboline selectively inhibit human CLKs in a non-ATP-mimetic manner. Typically, common kinase inhibitors act in such a way that they target the ATP binding cleft of the kinase to be blocked (reviewed in Lamba and Ghosh, 2012). As the ATP binding pocket is highly conserved, the identification and screening of bisubstrate and bivalent kinase inhibitors is of high importance (reviewed in Cox et al., 2011). These new compounds are considered to possess an active site-directed residue which is bound to another ligand that targets a location outside of the ATP-binding cleft. As kinase signalling activity is regulated by regions outside of the ATP-binding cleft, approaches that take advantage of these interactions have the capability to allocate compounds with high target specificity (reviewed in Gower et al., 2014).

To summarize, the combined data gained in this study demonstrated that the four plasmodial members of the CLK family, PfCLK-1-4, have an important role during schizogony and are further crucial during parasite transmission from the human host to the mosquito. All four PfCLKs are phosphorylating plasmodial SR proteins *in vitro*, rendering them as important components of the parasite splicing machinery. The four identified parasite SR proteins are predominantly expressed in the nucleus of trophozoites and reveal co-localization with PfCLK-1. Upon being inhibited by already available CLK inhibitors, phenotypic analyses are feasible by chemical knock-outs. These findings make the PfCLKs potential candidates as targets for antimalarials with transmission blocking properties.

## 5 Conclusions and future perspectives

The present study was conducted to functionally characterize two of four identified members of the ePK family of cyclin-dependent kinase-like kinases (CLK) in the malaria pathogen *P. falciparum*, PfCLK-3 and PfCLK-4 and substrates of all four identified PfCLKs. Reverse genetic approaches revealed that PfCLK-3 as well as PfCLK-4 are indispensable for the completion of the asexual replication cycle. Protein expression studies showed an abundant expression of both kinases in asexual parasites and gametocytes. In particular, the present study exhibited that the two PfCLKs are predominantly present in the parasite nucleus of trophozoites, whereas the localization is more distributed to the cytoplasm in schizonts and gametocytes. In other eukaryotes, CLKs have been manifested to be involved in splicing events by reversibly phosphorylating SR proteins acting as splicing factors. Given the notable homology of all four PfCLKs to yeast SR protein kinase Sky1p, it was feasible to conduct *in vitro* interaction studies to determine putative substrates of the PfCLKs. Sky1p substrate and nuclear shuttle protein Npl3p as well as the plasmodial homologues and SR proteins PfASF-1, PfSRSF12, PfSFRS4 and PfSF-1 were identified as interaction partners of the PfCLKs *in vitro* in this study. These putative parasite splicing factors show an expression profile in association with the nucleus of trophozoites, indicating that they remain in dynamic storage sites for splicing factors inside the nucleus, most likely nuclear speckles. IFAs revealed that PfSRSF12, PfSFRS4 and PfSF-1 also co-localize with PfCLK-1.

To enlarge the scope of the interaction analysis for the four PfCLKs, prospective studies will also encompass the investigation of the co-localization of the identified SR proteins with PfCLK-2, PfCLK-3 and PfCLK-4 by means of IFA studies or additional co-immunoprecipitation assays. Therefore, it should be attempted to generate antibodies against the investigated splicing factors originating from other species than from mice. Future studies will also involve the investigation of additional putative SR proteins of *P. falciparum*. These expanded studies should include the plasmodial SR protein PfSR-1 (PF3D7\_0517300), which has already been characterized and confirmed to display a substrate for PfCLK-4 *in vitro* (Dixit et al., 2010; Eshar et al., 2012). Moreover, the putative RNA-binding protein PF3D7\_1004400 exhibited homology with Npl3p and human SF1/ASF to a notable extent of 45% or 56%, respectively, rendering this plasmodial protein as an additional subject to future interaction studies besides other plasmodial candidates (Eshar et al., 2012). For more in depth analyses, successful attempts to knock-out the parasite SR proteins would gain deeper insight into the hitherto mainly unexplored malarial spliceosomal complex and the mRNA transport machinery. With possibly obtained knock-out parasites, *in vitro* splicing reactions and *in vitro* RNA binding assays could be conducted to unravel the functions of the plasmodial SR proteins. In addition, Yeast 2-Hybrid assays could confirm the findings that were achieved regarding the *in vitro* phosphorylation interaction in the present study by kinase activity assays utilizing recombinant parasite proteins.

Out of a small library, five compounds have been identified that showed inhibitory effects on malaria parasites. In addition, the antiseptic CHX exhibited a considerable inhibitory effect on

asexual parasites as well as gametocytes. The specific inhibition of PfCLKs by these compounds was confirmed in this study in an initial attempt, as it was demonstrated that the identified PfCLK inhibitors do not have any activity against the calmodulin-dependent kinase PfPKRP. Nevertheless, other eligible off-target effects of the inhibitors can not be ruled out at present. As the PfCLKs cannot be knocked out, the identified compounds investigated in this doctoral thesis display a useful tool for generation of chemical kinase knock-outs for subsequent more in depth phenotypic analyses on asexual stages as well as sexual stage parasites.

## 6 Summary

Besides HIV and tuberculosis, malaria still is one of the most devastating infectious diseases especially in developing countries, with *Plasmodium falciparum* being responsible for the frequently lethal form of malaria tropica. It is a major cause of mortality as well as morbidity, whereby pregnant women and children under the age of five years are most severely affected. Rapidly emerging drug resistances and the lack of an effective and safe vaccine hamper the combat against malaria by chemical and pharmacological regimens, and moreover the poor socio-economic and healthcare conditions in malaria-endemic countries are compromising the extermination of this deadly tropical disease to a large extent. Malaria research is still questing for druggable targets in the parasitic protozoan which pledge to be refractory against evolving resistance-mediating mutations and yet constitute affordable and compliant antimalarial chemotherapeutics.

The parasite kinome consists of members that represent most eukaryotic protein kinase groups, but also contains several groups that can not be assigned to conservative ePK groups. Moreover, given the remarkable divergence of plasmodial kinases in respect to the human host kinome and the fact that several plasmodial kinases have been identified that are essential for the intraerythrocytic developmental cycle, these parasite enzymes represent auspicious targets for antimalarial regimens. Despite elaborate investigations on several other ePK groups, merely scant research has been conducted regarding the four identified members of the cyclin-dependent kinase-like kinase (CLK) family, PfCLK-1-4. In other eukaryotes, CLKs are involved in mRNA processing and splicing by means of phosphorylation of serine/arginine-rich (SR) proteins, which are crucial components of the splicing machinery in the alternative splicing pathway. All four PfCLKs are abundantly expressed in asexual parasites and gametocytes, and stage-specific expression profiles of PfCLK-1 and PfCLK-2 exhibited nucleus-associated localization and an association with phosphorylation activity. In the course of this study, PfCLK-3 and PfCLK-4 were functionally characterized by indirect immunofluorescence, Western blot analysis and kinase activity assays. These data confirm that the two kinases are primarily expressed in the nucleus of trophozoites and both kinases possess *in vitro* phosphorylation activity on physiological substrates. Likewise PfCLK-1 and PfCLK-2, reverse genetic studies exhibited the indispensability of both PfCLKs on the asexual life cycle of *P. falciparum*, rendering them as potential candidates for antiplasmodial strategies. Moreover, this study was conducted to identify putative SR proteins as substrates of all four PfCLKs. Previous alignments revealed a significant homology of the parasite CLKs to yeast SR protein kinase Sky1p. Kinase activity assays showed *in vitro* phosphorylation of the yeast Sky1p substrate and SR protein Npl3p by precipitated PfCLKs. In addition, four homologous plasmodial SR proteins were identified that are phosphorylated by PfCLKs *in vitro*: PfASF-1, PFSRSF12, PFSFRS4 and PFSR-1. All four parasite SR splicing factors are predominantly expressed in the nuclei of trophozoites. For PfCLK-1, a co-localization with the SR proteins was verified.

Finally, a library of human and microbial CLK inhibitors and the antiseptic chlorhexidine (CHX) was screened to determine their inhibitory effect on different parasite life cycle stages and on the PfCLKs specifically. Five inhibitors out of 63 compounds from the investigated library were selected that show a moderate inhibition on asexual life cycle stages with  $IC_{50}$  values ranging between approximately 4 and 8  $\mu$ M. Noteworthy, these inhibitors belong to the substance classes of aminopyrimidines or oxo- $\beta$ -carbolines. Actually, the antibiotic compound CHX demonstrated an  $IC_{50}$  in the low nanomolar range. Stage-of-inhibition assays revealed that CHX severely affects the formation of schizonts. All of the selected CLKs inhibitors also affect gametocytogenesis as well as gametogenesis, as scrutinized in gametocyte toxicity assays and exflagellation assays, respectively. Kinase activity assays confirm a specific inhibition of CLK-mediated phosphorylation of all four kinases, when the CLK inhibitors are applied on immunoprecipitated PfCLKs. These findings on PfCLK-inhibiting compounds are initial attempts to determine putative antimalarial compounds targeting the PfCLKs. Moreover, these results provide an effective means to generate chemical kinase KOs in order to phenotypically study the role of the PfCLKs especially in splicing events and mRNA metabolism. This approach of functionally characterizing the CLKs in *P. falciparum* is of particular interest since the malarial spliceosome is still poorly understood and will gain further insight into the parasite splicing machinery.



## 7 Zusammenfassung

Neben HIV und Tuberkulose stellt Malaria vor allem in Entwicklungsländern immer noch eine der verheerendsten Infektionskrankheiten dar, wobei *Plasmodium falciparum* für die oft tödlich verlaufende Form der Malaria tropica verantwortlich ist. Sie ist eine der Hauptgründe für Mortalität und Morbidität, von der vor allem schwangere Frauen und Kinder unter fünf Jahren am schlimmsten betroffen sind. Das Fehlen eines effektiven und ungefährlichen Impfstoffes und sich schnell ausbreitende Medikamentenresistenzen erschweren die Bekämpfung von Malaria mit Arzneimitteln. Darüber hinaus beeinträchtigen die schlechten sozioökonomischen Bedingungen und der mangelhafte Zustand des Gesundheitssystems in Malaria-endemischen Ländern die Elimination dieser tödlichen Tropenkrankheit in hohem Maße. Die Malariaforschung ist immer noch auf der Suche nach vielversprechenden Angriffspunkten im Parasiten, die widerstandsfähig gegenüber sich entwickelnden resistenzvermittelnden Mutationen sind und dennoch erschwingliche und verträgliche Chemotherapeutika gegen Malaria darstellen.

Das Kinom des Parasiten besteht aus Vertretern der meisten eukaryotischen Proteinkinase-Gruppen und enthält zudem einige Gruppen, die keiner der konventionellen Gruppen zuordenbar sind. Darüber hinaus stellen Kinasen vielversprechende Angriffspunkte für Malariamedikamente dar, da das Parasitenkinom bemerkenswerte Divergenzen gegenüber dem Wirtskinom aufweist und zudem einige Parasitenkinasen identifiziert wurden, die unerlässlich für den Replikationszyklus von asexuellen Parasiten sind. Trotz umfangreicher Untersuchungen anderer Kinasegruppen des Parasiten wurden die vier identifizierten Vertreter der Zyclin-abhängige-Kinase-ähnlichen Kinasen (cyclin-dependent kinase-like kinases, CLKs) bisher kaum untersucht. In anderen Eukaryoten sind CLKs an der mRNA-Prozessierung und am Spleißen durch die Phosphorylierung von Serin/Arginin-reichen (SR-) Proteinen beteiligt, welche wiederum Komponenten der Spleißmaschinerie sind. Alle vier PfCLKs sind abundant exprimiert in asexuellen Parasiten sowie Gametozyten, und stadienspezifische Expressionsprofile von PfCLK-1 und PfCLK-2 zeigten eine Kern-assoziierte Expression sowie Phosphorylierungsaktivität in *in vitro*-Aktivitätsstudien. Im Verlauf dieser Studie wurden PfCLK-3 und PfCLK-4 mittels indirekter Immunfluoreszenzstudien, Western Blot-Analysen und Kinaseaktivitätsassays funktionell charakterisiert. Die Ergebnisse bestätigen, dass beide Kinasen vorrangig im Nukleus von *P. falciparum*-Trophozoiten lokalisiert sind und Phosphorylierungsaktivität gegenüber physiologischen Substraten *in vitro* aufweisen. Ähnlich wie für PfCLK-1 und PfCLK-2 konnte in Reverse-Genetik-Studien gezeigt werden, dass sowohl PfCLK-3 als auch PfCLK-4 essentiell für den asexuellen Replikationszyklus von *P. falciparum* sind. Dieser Umstand macht beide Kinasen zu potenziellen Angriffspunkten für antiplasmodiale Bekämpfungsstrategien. Des Weiteren wurde diese Studie ausgeführt, um mögliche Interaktionspartner aller vier PfCLKs zu identifizieren. Vorangegangene Sequenzabgleiche brachten eine bemerkenswerte Homologie der Parasiten-CLKs zur SR-Proteinkinase Sky1p der Bäckerhefe zu Tage. Kinaseaktivitätsassays zeigten Phosphorylierung des Sky1p-Substrates und SR-Proteins Npl3p durch präzipitierte PfCLKs *in vitro*. Außerdem

wurden vier homologe plasmodiale SR-Proteine bzw. mutmaßliche Spleißfaktoren identifiziert, die ebenso von den PfCLKs *in vitro* phosphoryliert werden: PfASF-1, PFSRSF12, PFSFRS4 und PfSR-1. Alle vier Parasiten-Spleißfaktoren sind vorwiegend in Kernen von Trophozoiten exprimiert. Für PfCLK-1 konnte eine Ko-Lokalisation mit den SR-Proteinen nachgewiesen werden.

Abschließend wurden eine Sammlung humaner und mikrobieller CLK-Inhibitoren sowie das Antiseptikum Chlorhexidin (CHX) auf ihren hemmenden Effekt auf verschiedene Lebenszyklusstadien von *P. falciparum* und gezielt auf die PfCLKs überprüft. Es wurden fünf Inhibitoren aus einer Sammlung von 63 Substanzen auserwählt, die eine moderate Hemmung auf asexuelle Lebenszyklusstadien aufwiesen, mit IC<sub>50</sub>-Werten zwischen ungefähr 4 und 8 µM. Das Antibiotikum CHX zeigte sogar einen IC<sub>50</sub>-Wert im niedrigen nanomolaren Bereich. Nachfolgende Stage-of-Inhibition-Assays deckten auf, dass CHX die Entwicklung von Schizonten enorm beeinträchtigt. Wie in Gametozyten-Toxizitätsassays und Exflagellationsassays ermittelt wurde, hemmen alle ausgewählten CLK-Inhibitoren ferner sowohl die Gametozytogenese als auch die Gametogenese. Kinaseaktivitätsassays bestätigen eine spezifische Hemmung der CLK-vermittelten Phosphorylierung aller vier Kinasen, wenn die CLK-Inhibitoren auf immunopräzipitierte PfCLKs angewendet wurden. Diese Erkenntnisse über PfCLK-hemmende Substanzen sind erste Ansätze, um mögliche Wirkstoffe gegen Malaria zu finden, die die PfCLKs als Angriffspunkte haben. Zudem stellen diese Resultate ein wirksames Mittel zur Verfügung, um chemische Kinase-Knockout-Parasiten zu generieren. Diese können dann verwendet werden, um die Rolle der PfCLKs vor allen in Bezug auf Spleißvorgänge und mRNA-Metabolismus phänotypisch zu untersuchen. Der Ansatz, die CLKs des Parasiten funktionell zu charakterisieren, ist von besonderem Interesse, da das Spleißosom des Malariaparasiten immer noch nicht ausreichend erforscht ist. Dadurch können weitere Erkenntnisse über die Spleißmaschinerie des Parasiten gewonnen werden.

## 8 References

- Abdi A., Eschenlauer S., Reininger L., Doerig C. (2010).** SAM domain-dependent activity of PfTKL3, an essential tyrosine kinase-like kinase of the human malaria parasite *Plasmodium falciparum*. *Cell Mol Life Sci.* 67(19):3355-3369.
- Abdi A., Carvalho T.G., Wilkes J.M., Doerig C. (2013).** A secreted *Plasmodium falciparum* kinase reveals a signature motif for classification of tyrosine kinase-like kinases. *Microbiology.* 159(Pt 12):2533-2547.
- Agarwal S. (2010).** Functional characterization of four CDK-like kinases and one Calmodulin-dependent kinase of the human malaria parasite *Plasmodium falciparum*. PhD thesis, University of Wuerzburg, Wuerzburg.
- Agarwal S., Kern S., Halbert J., Przyborski J.M., Baumeister S., Dandekar T., Doerig C., Pradel G. (2011).** Two nucleus-localized CDK-like kinases with crucial roles for malaria parasite erythrocytic replication are involved in phosphorylation of splicing factor. *J Cell Biochem.* 112(5):1295-1310.
- Aird W.C., Mosnier L.O., Fairhurst R.M. (2014).** *Plasmodium falciparum* picks (on) EPCR. *Blood.* 123(2):163-167. Review.
- Allemand E., Guil S., Myers M., Moscat J., Cáceres J.F., Krainer A.R. (2005).** Regulation of heterogenous nuclear ribonucleoprotein A1 transport by phosphorylation in cells stressed by osmotic shock. *Proc Natl Acad Sci U S A.* 102(10):3605-3610.
- Alving A.S., Carson P.E., Flanagan C.L., Ickes C.E. (1956).** Enzymatic deficiency in primaquine-sensitive erythrocytes. *Science* 124:484-485.
- Aminake M.N., Schoof S., Sologub L., Leubner M., Kirschner M., Arndt H.D., Pradel G. (2011).** ThioStrepton and derivatives exhibit antimalarial and gametocytocidal activity by dually targeting parasite proteasome and apicoplast. *Antimicrob Agents Chemother.* (4):1338-1348.
- Anamika, Srinivasan, N., Krupa, A. (2005).** A genomic perspective of protein kinases in *Plasmodium falciparum*. *Proteins.* 58(1):180-189.
- Arai M., Billker O., Morris H.R., Panico M., Delcroix M., Dixon D., Ley S.V., Sinden R.E. (2001).** Both mosquito-derived xanthurenic acid and a host blood-derived factor regulate gametogenesis of *Plasmodium* in the midgut of the mosquito. *Mol Biochem Parasitol.* 116(1):17-24.
- Ashley E.A., Dhorda M., Fairhurst R.M., Amaratunga C., Lim P., Suon S., Sreng S., Anderson J.M., Mao S., Sam B., Sopha C., Chuor C.M., Nguon C., Sovannaroeth S., Pukrittayakamee S., Jittamala P., Chotivanich K., Chutasmit K., Suchatsoonthorn C., Runcharoen R., Hien T.T., Thuy-Nhien N.T., Thanh N.V., Phu N.H., Htut Y., Han K.T., Aye K.H., Mokuolu O.A., Olaosebikan R.R., Folaranmi O.O., Mayxay M., Khanthavong M., Hongvanthong B., Newton P.N., Onyamboko M.A., Fanello C.I., Tshefu A.K., Mishra N., Valecha N., Phyo A.P., Nosten F., Yi P., Tripura R., Borrmann S., Bashraheil M., Peshu J., Faiz M.A., Ghose A., Hossain M.A., Samad R., Rahman M.R., Hasan M.M., Islam A., Miotto O., Amato R., MacInnis B., Stalker J., Kwiatkowski D.P., Bozdech Z., Jeeyapant A., Cheah P.Y., Sakulthaew T., Chalk J., Intharabut B., Silamut K., Lee S.J., Vihokhern B., Kunasol C., Imwong M., Tarning J., Taylor W.J., Yeung S., Woodrow C.J.,**

- Flegg J.A., Das D., Smith J., Venkatesan M., Plowe C.V., Stepniewska K., Guerin P.J., Dondorp A.M., Day N.P., White N.J.; Tracking Resistance to Artemisinin Collaboration (TRAC). (2014). Spread of artemisinin resistance in *Plasmodium falciparum* malaria. *N Engl J Med.* 371(5):411-423.
- Aubol B.E., Chakrabarti S., Ngo J., Shaffer J., Nolen B., Fu X.D., Ghosh G., Adams J.A. (2003). Processive phosphorylation of alternative splicing factor/splicing factor 2. *Proc Natl Acad Sci U S A.* 100(22):12601-12606.
- Aubol B.E., Plocinik R.M., Hagopian J.C., Ma C.T., McGlone M.L., Bandyopadhyay R., Fu X.D., Adams J.A. (2013). Partitioning RS domain phosphorylation in an SR protein through the CLK and SRPK protein kinases. *J Mol Biol.* 425(16): 2894-2909.
- Aurrecochea C., Brestelli J., Brunk B.P., Dommer J., Fischer S., Gajria B., Gao X., Gingle A., Grant G., Harb O.S., Heiges M., Innamorato F., Iodice J., Kissinger J.C., Kraemer E., Li W., Miller J.A., Nayak V., Pennington C., Pinney D.F., Roos D.S., Ross C., Stoeckert C.J. Jr, Treatman C., Wang H. (2009). PlasmoDB: a functional genomic database for malaria parasites. *Nucleic Acids Res.* 37:D539-D543.
- Barik S., Taylor R.E., Chakrabarti D. (1997). Identification, cloning, and mutational analysis of the casein kinase 1 cDNA of the malaria parasite, *Plasmodium falciparum*. Stage-specific expression of the gene. *J Biol Chem.* 272(42):26132-26138.
- Baldauf S.L. (2003). The deep roots of eukaryotes. *Science.* 300(5626):1703-1706.
- Barnes K.I., Little F., Smith P.J., Evans A., Watkins W.M., White N.J. (2006). Sulfadoxine-pyrimethamine pharmacokinetics in malaria: pediatric dosing implications. *Clin Pharmacol Ther.* 80(6):582-596.
- Barthel D., Schlitzer M., Pradel G. (2008). Telithromycin and quinupristin-dalfopristin induce delayed death in *Plasmodium falciparum*. *Antimicrob Agents Chemother.* 52(2):774-777.
- Berendt A.R., Simmons D.L., Tansey J., Newbold C.I., Marsh K. (1989). Intercellular adhesion molecule-1 is an endothelial cell adhesion receptor for *Plasmodium falciparum*. *Nature* 341: 57-59.
- Beutler E. (1959). The hemolytic effect of primaquine and related compounds: a review. *Blood.* 14:103-139. Review.
- Billker O., Lindo V., Panico M., Etienne A.E., Paxton T., Dell A., Rogers M., Sinden R.E., Morris H.R. (1998). Identification of xanthurenic acid as the putative inducer of malaria development in the mosquito. *Nature.* 392(6673):289-292.
- Black D.L. (2003). Mechanisms of alternative pre-messenger RNA splicing. *Annu Rev Biochem.* 72:291-336. Review.
- Bousema T. and Drakeley C. (2011). Epidemiology and infectivity of *Plasmodium falciparum* and *Plasmodium vivax* gametocytes in relation to malaria control and elimination. *Clin Microbiol Rev.* 24(2):377-410. Review.
- Bozdech Z., Llinás M., Pulliam B.L., Wong E.D., Zhu J., DeRisi J.L. (2003). The transcriptome of the intraerythrocytic developmental cycle of *Plasmodium falciparum*. *PLoS Biol.* 1(1):E5.
- Bracchi-Ricard V., Barik S., Delvecchio C., Doerig C., Chakrabarti R., Chakrabarti D. (2000). PfPK6, a novel cyclin-dependent kinase/mitogen-activated protein kinase-related protein kinase from *Plasmodium falciparum*. *Biochem J.* 347(1):255-263.

- Breman J.G., Alilio M.S., Mills A. (2004).** Conquering the intolerable burden of malaria: what's new, what's needed: a summary. *Am J Trop Med Hyg.* 71(2 Suppl):1-15. Review.
- Briolant S., Wurtz N., Zettor A., Rogier C., Pradines B. (2010).** Susceptibility of *Plasmodium falciparum* isolates to doxycycline is associated with pftetQ sequence polymorphisms and pftetQ and pfmdt copy numbers. *J Infect Dis.* 201(1):153-159.
- Bruce M.C., Alano P., Duthie S., Carter R. (1990).** Commitment of the malaria parasite *Plasmodium falciparum* to sexual and asexual development. *Parasitology.* 100(2):191-200.
- Brügl T. (2011).** Functional characterization of two members of the calmodulin-dependent protein kinase family, PfPK2 and PfPKRP, in *Plasmodium falciparum*. Diploma thesis, University of Wuerzburg, Wuerzburg.
- Buckling A., Ranford-Cartwright L.C., Miles A., Read A.F. (1999).** Chloroquine increases *Plasmodium falciparum* gametocytogenesis *in vitro*. *Parasitology.* 118(4):339-346.
- Bull P.C., Lowe B.S., Kortok M., Molyneux C.S., Newbold C.I., Marsh K. (1998).** Parasite antigens on the infected red cell surface are targets for naturally acquired immunity to malaria. *Nat Med.* 4(3):358-360.
- Bullock A.N., Das S., Debreczeni J.E., Rellos P., Fedorov O., Niesen F.H., Guo K., Papagrigoriou E., Amos A.L., Cho S., Turk B.E., Ghosh G., Knapp S. (2009).** Kinase domain insertions define distinct roles of CLK kinases in SR protein phosphorylation. *Structure.* 17(3):352-362.
- Cáceres J.F., Misteli T., Sreaton G.R., Spector D.L., Krainer A.R. (1997).** Role of the modular domains of SR proteins in subnuclear localization and alternative splicing specificity. *J Cell Biol.* 138(2):225-238.
- Carvalho P.A., Diez-Silva M., Chen H., Dao M., Suresh S. (2013).** Cytoadherence of erythrocytes invaded by *Plasmodium falciparum*: Quantitative contact-probing of a human malaria receptor. *Acta Biomater.* 9(5): 6349-6359.
- Cohen, P. (2001).** The role of protein phosphorylation in human health and disease. The Sir Hans Krebs Medal Lecture. *Eur J Biochem.* 268(19):5001-5010.
- Cohen P. (2002).** Protein kinases--the major drug targets of the twenty-first century? *Nat Rev Drug Discov.* 1(4):309-315.
- Colwill K., Feng L.L., Yeakley J.M., Gish G.D., Cáceres J.F., Pawson T., Fu X.D. (1996a).** SRPK1 and Clk/Sty protein kinases show distinct substrate specificities for serine/arginine-rich splicing factors. *J Biol Chem.* 271(40):24569-24575.
- Colwill K., Pawson T., Andrews B., Prasad J., Manley J.L., Bell J.C., Duncan P.I. (1996b).** The Clk/Sty protein kinase phosphorylates SR splicing factors. *EMBO J.* 15(2):265-275.
- Courtin D., Oesterholt M., Huismans H., Kusi K., Milet J., Baadaut C., Gaye O., Roeffen W., Remarque E.J., Sauerwein R., Garcia A., Luty A.J. (2009).** The quantity and quality of African children's IgG responses to merozoite surface antigens reflect protection against *Plasmodium falciparum* malaria. *PLoS One.* 4(10):E7590.
- Cox K.J., Shomin C.D., Ghosh I. (2011).** Tinkering outside the kinase ATP box: allosteric (type IV) and bivalent (type V) inhibitors of protein kinases. *Future Med Chem.* 3(1):29-43. Review.

- Cox-Singh J., Davis T.M., Lee K.S., Shamsul S.S., Matusop A., Ratnam S., Rahman H.A., Conway D.J., Singh B. (2008). *Plasmodium knowlesi* malaria in humans is widely distributed and potentially life threatening. *Clin Infect Dis.* 46(2):165-171.
- Curd F.H., Rose F.L., et al. (1946). Synthetic antimalarials. *J Chem Soc.* 343-84.
- Dahan-Pasternak N., Nasereddin A., Kolevzon N., Pe'er M., Wong W., Shinder V., Turnbull L., Whitchurch C.B., Elbaum M., Gilberger T.W., Yavin E., Baum J., Dzikowski R. (2013). PfSec13 is an unusual chromatin-associated nucleoporin of *Plasmodium falciparum* that is essential for parasite proliferation in human erythrocytes. *J Cell Sci.* 126(14):3055-3069.
- Dastidar E.G., Dayer G., Holland Z.M., Dorin-Semblat D., Claes A., Chêne A., Sharma A., Hamelin R., Moniatte M., Lopez-Rubio J.J., Scherf A., Doerig C. (2012). Involvement of *Plasmodium falciparum* protein kinase CK2 in the chromatin assembly pathway. *BMC Biol.* 10(5).
- Davies A. (1975). The mode of action of chlorhexidine. *J Periodontal Res.* 8(Suppl 12):68-75.
- Deutsch K., Duraisingh M., Dzikowski R., Gunasekera A., Khan S., LeRoch K., Llinas M., Mair G., McGovern V., Roos D., Shock J., Sims J., Wiegand R., Winzeler E. (2007). Mechanisms of gene regulation in *Plasmodium*. *Am J Trop Med Hyg.* 77(2):201-208. Review.
- Deng W., Baker D.A. (2002). A novel cyclic GMP-dependent protein kinase is expressed in the ring stage of the *Plasmodium falciparum* life cycle. *Mol Microbiol.* 44(5):1141-51.
- Diaz C.A., Allocco J., Powles M.A., Yeung L., Donald R.G., Anderson J.W., Liberator P.A. (2006). Characterization of *Plasmodium falciparum* cGMP-dependent protein kinase (PfPKG): antiparasitic activity of a PKG inhibitor. *Mol Biochem Parasitol.* 146(1):78-88.
- Dixit A., Singh P.K., Sharma G.P., Malhotra P., Sharma P. (2010). PfSRPK1, a novel splicing-related kinase from *Plasmodium falciparum*. *J Biol Chem.* 285(49):38315-38323.
- Doerig C.M., Parzy D., Langsley G., Horrocks P., Carter R., Doerig C.D. (1996). A MAP kinase homologue from the human malaria parasite, *Plasmodium falciparum*. *Gene.* 177(1-2):1-6.
- Doerig C., Endicott J., Chakrabarti D. (2002). Cyclin-dependent kinase homologues of *Plasmodium falciparum*. *Int J Parasitol.* 32(13):1575-1585. Review.
- Doerig, C. (2004). Protein kinases as targets for anti-parasitic chemotherapy. *Biochim Biophys Acta.* 1697(1-2):155-168. Review.
- Doerig C., Billker O., Pratt D., Endicott J. (2005). Protein kinases as targets for antimalarial intervention: Kinomics, structure-based design, transmission-blockade, and targeting host cell enzymes. *Biochim Biophys Acta.* 1754(1-2):132-150. Review.
- Doerig C. and Meijer L. (2007). Antimalarial drug discovery: targeting protein kinases. *Expert Opin Ther Targets.* 11(3):279-290. Review.
- Doerig C., Billker O., Haystead T., Sharma P., Tobin A.B., Waters N.C. (2008). Protein kinases of malaria parasites: an update. *Trends Parasitol.* 24(12):570-577. Review.
- Doerig C., Abdi A., Bland N., Eschenlauer S., Dorin-Semblat D., Fennell C., Halbert J., Holland Z., Nivez M.P., Semblat J.P., Sicard A., Reininger L. (2010). Malaria: targeting parasite and host cell kinomes. *Biochim Biophys Acta.* 1804(3):604-612. Review.
- Dondorp A.M., Nosten F., Yi P., Das D., Phyo A.P., Tarning J., Lwin K.M., Arie F., Hanpithakpong W., Lee S.J., Ringwald P., Silamut K., Imwong M., Chotivanich K., Lim

- P., Herdman T., An S.S., Yeung S., Singhasivanon P., Day N.P., Lindegardh N., Socheat D., White N.J. (2009). Artemisinin resistance in *Plasmodium falciparum* malaria. *N Engl J Med.* 361(5):455-467.
- Dondorp A.M., Ringwald P. (2013). Artemisinin resistance is a clear and present danger. *Trends Parasitol.* 29(8):359-360.
- Dorin D., Alano P., Boccaccio I., Ciceron L., Doerig C.M., Sulpice R., Parzy D., Doerig C. (1999). An atypical mitogen-activated protein kinase (MAPK) homologue expressed in gametocytes of the human malaria parasite *Plasmodium falciparum*. Identification of a MAPK signature. *J Biol Chem.* 274(42):29912-29920.
- Dorin D., Le Roch K., Sallicandro P., Alano P., Parzy D., Poulet P., Meijer L., Doerig C. (2001). Pfnek-1, a NIMA-related kinase from the human malaria parasite *Plasmodium falciparum* Biochemical properties and possible involvement in MAPK regulation. *Eur J Biochem.* 268(9):2600-2608.
- Dorin D., Semblat J.P., Poulet P., Alano P., Goldring J.P., Whittle C., Patterson S., Chakrabarti D., Doerig C. (2005). PfPK7, an atypical MEK-related protein kinase, reflects the absence of classical three-component MAPK pathways in the human malaria parasite *Plasmodium falciparum*. *Mol Microbiol.* 55(1):184-96.
- Dorin-Semblat D., Quashie N., Halbert J., Sicard A., Doerig C., Peat E., Ranford-Cartwright L. (2007). Functional characterization of both MAP kinases of the human malaria parasite *Plasmodium falciparum* by reverse genetics. *Mol Microbiol.* 65(5):1170-1180.
- Dorin-Semblat D., Schmitt S., Semblat J.P., Sicard A., Reininger L., Goldring D., Patterson S., Quashie N., Chakrabarti D., Meijer L., Doerig C. (2011). *Plasmodium falciparum* NIMA-related kinase Pfnek-1: sex specificity and assessment of essentiality for the erythrocytic asexual cycle. *Microbiology.* 157(Pt 10):2785-94.
- Dormoi J., Savini H., Amalvict R., Baret E., Pradines B. (2014). *In vitro* interaction of lumefantrine and piperazine by atorvastatin against *Plasmodium falciparum*. *Malar J.* 13:189.
- Duffy P.E., Mutabingwa T.K. (2006). Artemisinin combination therapies. *Lancet.* 367(9528):2037-2039.
- Duncan P.I., Stojdl D.F., Marius R.M., Bell J.C. (1997). *In vivo* regulation of alternative pre-mRNA splicing by the Clk1 protein kinase. *Mol Cell Biol.* 17(10):5996-6001.
- Eziefula A.C., Staedke S.G., Yeung S., Webb E., Kamya M., White N.J., Bousema T., Drakeley C. (2013). Study protocol for a randomised controlled double-blinded trial of the dose-dependent efficacy and safety of primaquine for clearance of gametocytes in children with uncomplicated *falciparum* malaria in Uganda. *BMJ Open.* 3(3).
- Eziefula A.C., Pett H., Grignard L., Opus S., Kiggundu M., Kamya M.R., Yeung S., Staedke S.G., Bousema T., Drakeley C. (2014). Glucose-6-Phosphate Dehydrogenase status and risk of hemolysis in *Plasmodium falciparum*-infected African children receiving single-dose primaquine. *Antimicrob Agents Chemother.* 58(8):4971-4973.
- Eriksen J., Mwankusye S., Mduma S., Veiga M.I., Kitua A., Tomson G., Petzold M.G., Swedberg G., Gustafsson L.L., Warsame M. (2008). Antimalarial resistance and DHFR/DHPS genotypes of *Plasmodium falciparum* three years after introduction of sulfadoxine-pyrimethamine and amodiaquine in rural Tanzania. *Trans R Soc Trop Med Hyg.* 102(2):137-142.

- Eshar S., Allemand E., Sebag A., Glaser F., Muchardt C., Mandel-Gutfreund Y., Karni R., Dzikowski R. (2012). A novel *Plasmodium falciparum* SR protein is an alternative splicing factor required for the parasites' proliferation in human erythrocytes. *Nucleic Acids Res.* 40(19):9903-9916.
- Farooq U. and Mahajan R.C. (2004). Drug resistance in malaria. *J Vector Borne Dis.* 41(3-4):45-53. *Review.*
- Feachem R. and Sabot O. (2008). A new global malaria eradication strategy. *Lancet.* 371(9624):1633-1635.
- Feachem R.G., Phillips A.A., Hwang J., Cotter C., Wielgosz B., Greenwood B.M., Sabot O., Rodriguez M.H., Abeyasinghe R.R., Ghebreyesus T.A., Snow R.W. (2010). Shrinking the malaria map: progress and prospects. *Lancet.* 376(9752):1566-1578. *Review.*
- Fedorov O., Huber K., Eisenreich A., Filippakopoulos P., King O., Bullock A.N., Szklarczyk D., Jensen L.J., Fabbro D., Trappe J., Rauch U., Bracher F., Knapp S. (2011). Specific CLK inhibitors from a novel chemotype for regulation of alternative splicing. *Chem Biol.* 18(1):67-76.
- Fernandez-Reyes D., Craig A.G., Kyes S.A., Peshu N., Snow R.W., Berendt A.R., Marsh K., Newbold C.I. (1997). A high frequency African coding polymorphism in the N-terminal domain of ICAM-1 predisposing to cerebral malaria in Kenya. *Hum Mol Genet.* 6: 1357-1360.
- Ferreira P.E., Culleton R., Gil J.P., Meshnick S.R. (2013). Artemisinin resistance in *Plasmodium falciparum*: what is it really? *Trends Parasitol.* 29(7):318-320.
- Fowkes F.J., Richards J.S., Simpson J.A., Beeson J.G. (2010). The relationship between anti-merozoite antibodies and incidence of *Plasmodium falciparum* malaria: A systematic review and meta-analysis. *PLoS Med.* 7(1):e1000218. *Review.*
- Fu X.D. (1995). The superfamily of arginine/serine-rich splicing factors. *RNA.* 1(7):663-680. *Review.*
- Garcia C.R. (1999). Calcium homeostasis and signaling in the blood-stage malaria parasite. *Parasitol Today.* 15(12):488-91. *Review.*
- Gardner M.J., Hall N., Fung E., White O., Berriman M., Hyman R.W., Carlton J.M., Pain A., Nelson K.E., Bowman S., Paulsen I.T., James K., Eisen J.A., Rutherford K., Salzberg S.L., Craig A., Kyes S., Chan M.S., Nene V., Shallom S.J., Suh B., Peterson J., Angiuoli S., Pertea M., Allen J., Selengut J., Haft D., Mather M.W., Vaidya A.B., Martin D.M., Fairlamb A.H., Fraunholz M.J., Roos D.S., Ralph S.A., McFadden G.I., Cummings L.M., Subramanian G.M., Mungall C., Venter J.C., Carucci D.J., Hoffman S.L., Newbold C., Davis R.W., Fraser C.M., Barrell B. (2002). Genome sequence of the human malaria parasite *Plasmodium falciparum*. *Nature.* 419(6906):498-511.
- Geary T.G., Jensen J.B. (1983). Effects of antibiotics on *Plasmodium falciparum* in vitro. *Am J Trop Med Hyg.* 32(2):221-5.
- Gilbert W., Siebel, C. W., Guthrie, C. (2001). Phosphorylation by Sky1p promotes Npl3p shuttling and mRNA dissociation. *RNA.* 7(2):302-313.
- Godin, K.S. and Varani, G. (2007). How arginine-rich domains coordinate mRNA maturation events. *RNA Biol.* 4(2):69-75. *Review.*
- Gomez M.S., Piper R.C., Hunsaker L.A., Royer R.E., Deck L.M., Makler M.T., Vander Jagt D.L. (1997). Substrate and cofactor specificity and selective inhibition of lactate



- dehydrogenase from the malarial parasite *P. falciparum*. *Mol Biochem Parasitol.* 90(1):235-246.
- Good M.F. (2001).** Towards a blood-stage vaccine for malaria: are we following the leads? *Nat Rev Immunol.* 1(2):117-125. *Review.*
- Gower C.M., Chang M.E., Maly D.J. (2014).** Bivalent inhibitors of protein kinases. *Crit Rev Biochem Mol Biol.* 49(2):102-115. *Review.*
- Graveley B.R. (2000).** Sorting out the complexity of SR protein functions. *RNA.* 2000, 6(9):1197-1211. *Review.*
- Graves P.M., Gelband H., Garner P. (2014).** Primaquine or other 8-aminoquinoline for reducing *P. falciparum* transmission. *Cochrane Database Syst Rev.* 6.
- Greenwood B.M., Fidock D.A., Kyle D.E., Kappe S.H., Alonso P.L., Collins F.H., Duffy P.E. (2008).** Malaria: progress, perils, and prospects for eradication. *J Clin Invest.* 118(4):1266-1276. *Review.*
- Gross T., Lutzberger M., Weigmann H., Klingenhoff A., Shenoy S., Kaufer N.F. (1997).** Functional analysis of the fission yeast Prp4 protein kinase involved in pre-mRNA splicing and isolation of a putative mammalian homologue. *Nucleic Acid Res.* 25(5):1028-1035.
- Gui J.F., Lane W.S., Fu X.D. (1994).** A serine kinase regulates intracellular localization of splicing factors in the cell cycle. *Nature.* 369(6482):678-682.
- Hagiwara M. (2005).** Alternative splicing: A new drug target of the post-genome era. *Biochim Biophys Acta.* 1754(1-2):324-331. *Review.*
- Halbert J., Ayong L., Equinet L., Le Roch K., Hardy M., Goldring D., Reininger L., Waters N., Chakrabarti D., Doerig C. (2010).** A *Plasmodium falciparum* transcriptional cyclin-dependent kinase-related kinase with a crucial role in parasite proliferation associates with histone deacetylase activity. *Eukaryot Cell.* 9(6):952-959.
- Hanks S.K., Quinn A.M. (1991).** Protein kinase catalytic domain sequence database: identification of conserved features of primary structure and classification of family members. *Methods Enzymol.* 200:38-62.
- Hanks S.K. and Hunter T. (1995).** Protein kinases 6. The eukaryotic protein kinase superfamily: kinase (catalytic) domain structure and classification. *FASEB J.* 9(8):576-596. *Review.*
- Hanks S.K. (2003).** Genomic analysis of the eukaryotic protein kinase superfamily: a perspective. *Genome Biol.* 4(5):111.
- Hegeman A.D., Rodriguez M., Han B.W., Uno Y., Phillips G.N.Jr, Hrabak E.M., Cushman J.C., Harper J.F., Harmon A.C., Sussman M.R. (2006).** A phyloproteomic characterization of *in vitro* autophosphorylation in calcium-dependent protein kinases. *Proteomics.* 6(12):3649-64.
- Hill A.V. (2006).** Pre-erythrocytic malaria vaccines: towards greater efficacy. *Nat Rev Immunol.* 6(1):21-32. *Review.*
- Ho M. (2014).** EPCR: holy grail of malaria cytoadhesion? *Blood.* 123(2):157-159.
- Holland Z., Prudent R., Reiser J.B., Cochet C., Doerig, C. (2009).** Functional analysis of protein kinase CK2 of the human malaria parasite *Plasmodium falciparum*. *Eukaryot Cell.* 8(3):388-397.

- Huang Y. and Steitz J.A. (2005). SRprises along a messenger's journey. *Mol Cell*. j17(5):613-615. Review.
- Hull R. and Dlamini Z. (2014). The role played by alternative splicing in antigenic variability in human endo-parasites. *Parasit Vectors*. 7:53. Review.
- Hyde J.E. (2005). Drug-resistant malaria. *Trends Parasitol*. 21(11):494-498. Review.
- Hyde J.E. (2007). Drug-resistant malaria - an insight. *FEBS J*. 274(1):4688-4698. Review.
- Inoue J., Lopes D., do Rosário V., Machado M., Hristov A.D., Lima G.F., Costa-Nascimento M.J., Segurado A.C., Di Santi S.M. (2014). Analysis of polymorphisms in *Plasmodium falciparum* genes related to drug resistance: a survey over four decades under different treatment policies in Brazil. *Malar J*. 13:372.
- Iriko H., Jin L, Kaneko O., Takeo S., Han E.T., Tachibana M., Otsuki H., Torii M., Tsuboi T. (2009). A small-scale systematic analysis of alternative splicing in *Plasmodium falciparum*. *Parasitol Int*. 58(2):196-9.
- Jelinek T., Schelbert P., Löscher T., Eichenlaub D. (1995). Quinine resistant *falciparum* malaria acquired in East Africa. *Trop Med Parasitol*. 46(1):38-40.
- Jongwutiwes S., Buppan P., Kosuvin R., Seethamchai S., Pattanawong U., Sirichaisinthop J., Putaporntip C. (2011). *Plasmodium knowlesi* malaria in humans and macaques, Thailand. *Emerg Infect Dis*. 17(10):1799-1806.
- Kamali M., Sharakhova M.V., Baricheva E., Karaqodin D., Tu Z., Sharakhov I.V. (2011). An integrated chromosome map of microsatellite markers and inversion breakpoints for an Asian malaria mosquito, *Anopheles stephensi*. *J Hered*. 102(6):719-726.
- Kappes B., Doerig C.D., Graeser R. (1999). An overview of *Plasmodium* protein kinases. *Parasitol Today*. 15(11):449-454. Review.
- Kariuki M.M., Kiaira J.K., Mulaa F.K., Mwangi J.K., Wasunna M.K., Martin S.K. (1998). *Plasmodium falciparum*: purification of the various gametocyte developmental stages from *in-vitro* cultivated parasites. *Am J Trop Med Hyg*. 59(4):505-508.
- Keren H. and Lev-Maor G., Ast G. (2010). Alternative splicing and evolution: diversification, exon definition and function. *Nat Rev Genet*. 11(5):345-355. Review.
- Kern S., Agarwal S., Huber K., Gehring A.P., Strödke B., Wirth C.C., Brügl T., Abodo L.O., Dandekar T., Doerig C., Fischer R., Tobin A.B., Alam M.M., Bracher F., Pradel G. (2014). Inhibition of the SR protein-phosphorylating CLK kinases of *Plasmodium falciparum* impairs blood stage replication and malaria transmission. *PLoS One*. 9(9):e105732.
- Kirchgatter K. and Del Portillo H.A. (2005). Clinical and molecular aspects of severe malaria. *An Acad Bras Cienc*. 77(3):455-75. Review.
- Knapp B., Nau U., Hundt E., Küpper H.A. (1991). Demonstration of alternative splicing of a pre-mRNA expressed in the blood stage form of *Plasmodium falciparum*. *J Biol Chem*. 266(11):7148-7154.
- Koizumi J., Okamoto Y., Onogi H., Mayeda A., Krainer A.R., Hagiwara M. (1999). The subcellular localization of SF2/ASF is regulated by direct interaction with SR protein kinases (SRPKs). *J Biol Chem*. 274(16):11125-11131.
- Kokwaro G. (2009). Ongoing challenges in the management of malaria. *Malar J*. 8(Suppl 1):S2. Review.

- Kreidenweiss A., Kreamsner P.G., Mordmüller B. (2008).** Comprehensive study of proteasome inhibitors against *Plasmodium falciparum* laboratory strains and field isolates from Gabon. *Malar J.* 7:187.
- Krishna S. and Kreamsner P.G. (2013).** Antidogmatic approaches to artemisinin resistance: reappraisal as treatment failure with artemisinin combination therapy. *Trends Parasitol.* 29(7):313-317. Review.
- Krudsood S., Patel S.N., Tangpukdee N., Thanachartwet W., Leowattana W., Pornpininworakij K., Boggild A.K., Looareesuwan S., Kain K.C. (2007).** Efficacy of atovaquone-proguanil for treatment of acute multidrug-resistant *Plasmodium falciparum* malaria in Thailand. *Am J Trop Med Hyg.* 76(4):655-658.
- Kuehn A, Pradel G. (2010).** The coming-out of malaria gametocytes. *J Biomed Biotechnol.* 2010:976827. Review.
- Kuhn S., Gill M.J., Kain K.C. (2005).** Emergence of atovaquone-proguanil resistance during treatment of *Plasmodium falciparum* malaria acquired by a non-immune north American traveller to west Africa. *Am J Trop Med Hyg.* 72(4):407-409.
- Kumar N. and Zheng H. (1990).** Stage-specific gametocytocidal effect in vitro of the antimalaria drug qinghaosu on *Plasmodium falciparum*. *Parasitol Res.* 76(3):214-218.
- Kumar P., Tripathi A., Ranjan R., Halbert J., Gilberger T., Doerig C., Sharma P. (2014).** Regulation of *Plasmodium falciparum* development by calcium-dependent protein kinase 7 (PfCDPK7). *J Biol Chem.* 289(29):20386-20395.
- LaCount D.J., Vignali M., Chettier R., Phansalkar A., Bell R., Hesselberth J.R., Schoenfeld L.W., Ota I., Sahasrabudhe S., Kurschner C., Fields S., Hughes R.E. (2005).** A protein interaction network of the malaria parasite *Plasmodium falciparum*. *Nature.* 438(7064):103-107.
- Lamba V. and Ghosh I. (2012).** New directions in targeting protein kinases: focusing upon true allosteric and bivalent inhibitors. *Curr Pharm Des.* 18(20):2936-2945. Review.
- Lamond A.I. and Spector D.L. (2003).** Nuclear speckles: a model for nuclear organelles. *Nat Rev Mol Cell Biol.* 4(8):605-612. Review.
- Lai M.C., Lin R.I., Huang S.Y., Tsai C.W., Tarn W.Y. (2000).** A human importin-beta family protein, transportin-SR2, interacts with the phosphorylated RS domain of SR proteins. *J Biol Chem.* 275(11):7950-7957.
- Lasonder E., Green J.L., Camarda G., Talabani H., Holder A.A., Langsley G., Alano P. (2012).** The *Plasmodium falciparum* schizont phosphoproteome reveals extensive phosphatidylinositol and cAMP-protein kinase A signaling. *J Proteome Res.* 11(11):5323-5337.
- Le Roch K.G., Johnson J.R., Florens L., Zhou Y., Santrosyan A., Grainger M., Yan S.F., Williamson K.C., Holder A.A., Carucci D.J., Yates, J.R. 3rd, Winzeler E.A. (2004).** Global analysis of transcript and protein levels across the *Plasmodium falciparum* life cycle. *Genome Res.* 14(11):2308-2318.
- Leroux-Roels G., Leroux-Roels I., Clement F., Ofori-Anyinam O., Lievens M., Jongert E., Moris P., Ballou W.R., Cohen J. (2014).** Evaluation of the immune response to RTS,S/AS01 and RTS,S/AS02 adjuvanted vaccines: Randomized, double-blind study in malaria-naïve adults. *Hum Vaccin Immunother.* 10(8).

- Li J., Cox L.S. (2000). Isolation and characterisation of a cAMP-dependent protein kinase catalytic subunit gene from *Plasmodium falciparum*. *Mol Biochem Parasitol*. 109(2):157-63.
- Li J.L., Targett G.A., Baker D.A. (2001). Primary structure and sexual stage-specific expression of a LAMMER protein kinase of *Plasmodium falciparum*. *Int J Parasitol*. 31(4):387-392.
- Lim C., Hansen E., DeSimone T.M., Moreno Y., Junker K., Bei A., Brugnara C., Buckee C.O., Duraisingh M.T. (2013). Expansion of host cellular niche can drive adaptation of a zoonotic malaria parasite to humans. *Nat Commun*. 4:1638.
- Lim D.C., Cooke B.M., Doerig C., Saeij JP. (2012). *Toxoplasma* and *Plasmodium* protein kinases: roles in invasion and host cell remodelling. *Int J Parasitol*. 42(1):21-32. Review.
- Lobo C.A. and Kumar N. (1999). Differential transcription of histone genes in asexual and sexual stages of *Plasmodium falciparum*. *Int J Parasitol*. 29(9):1447-1449.
- Long J.C. and Cáceres J.F. (2009). The SR protein family of splicing factors: master regulators of gene expression. *Biochem J*. 417(1):15-27. Review.
- Lucet I.S., Tobin A., Drewry D., Wilks A.F., Doerig C. (2012). *Plasmodium* kinases as targets for new-generation antimalarials. *Future Med Chem*. 4(18):2295-2310. Review.
- Lun Z.R., Ferreira P.E., Fu L.C. (2014). Artemisinin resistance in *Plasmodium falciparum*. *Lancet Infect Dis*. 14(6):450-451.
- Maina C.V., Riggs P.D., Grande A.G. 3rd, Slatk, B.E., Moran L.S., Tagliamonte J.A., McReynolds L.A., Guan C.D. (1988). An *Escherichia coli* vector to express and purify foreign proteins by fusion to and separation from maltose-binding protein. *Gene*. 74(2):365-373.
- Makler M.T., Ries J.M., Williams J.A., Bancroft J.E., Piper R.C., Gibbins B.L., Hinrichs D.L. (1993). Parasite lactate dehydrogenase as an assay for *Plasmodium falciparum* drug sensitivity. *Am J Trop Med Hyg*. 48(6):739-741.
- Makler M.T., Hinrichs D.J. (1993). Measurement of the lactate dehydrogenase activity of *Plasmodium falciparum* as an assessment of parasitemia. *Am J Trop Med Hyg*. 48(2):205-10.
- Manning G., Whyte D.B., Martinez R., Hunter T., Sudarsanam S. (2002). The protein kinase complement of the human genome. *Science*. 298(5600):1912-1934. Review.
- Milestone A.M., Passaretti C.L., Perl T.M. (2008). Chlorhexidine: expanding the armamentarium for infection control and prevention. *Clin Infect Dis*. 46(2):274-81. Review.
- Miller L.H., Baruch D.I., Marsh K., Doumbo O.K. (2002). The pathogenic basis of malaria. *Nature* 415:673–679. Review.
- Miller L.H., Ackerman H.C., Su X.Z., Wellems T.E. (2013). Malaria biology and disease pathogenesis: insights for new treatments. *Nat Med*. 19: 156-167. Review.
- Miranda-Saavedra D., Gabaldón T., Barton G.J., Langsley G., Doerig C. (2012). The kinomes of apicomplexan parasites. *Microbes Infect*. 14(10): 796-810. Review.
- Misteli T., Cáceres J.F., Clement J.Q., Krainer A.R., Wilkinson M.F., Spector D.L. (1998). Serine phosphorylation of SR proteins is required for their recruitment to sites of transcription *in vivo*. *J Cell Biol*. 143(2):297-307.
- Muhia D.K., Swales C.A., Eckstein-Ludwig U., Saran .S, Polley S.D., Kelly J.M., Schaap P., Krishna S., Baker D.A. (2003). Multiple splice variants encode a novel adenylyl cyclase

- of possible plastid origin expressed in the sexual stage of the malaria parasite *Plasmodium falciparum*. *J Biol Chem*. 278(24):22014-22022.
- Naro C. and Sette C. (2013)**. Phosphorylation-mediated regulation of alternative splicing in cancer. *Int J Cell Biol*. 2013:151839. Review.
- Nayler O., Stamm S., Ullrich A. (1997)**. Characterization and comparison of four serine- and arginine-rich (SR) protein kinases. *Biochem J*. 326(Pt3):693-700.
- Ndiath M.O., Mazonot C., Sokhna C., Trape J.F. (2014)**. How the malaria vector *Anopheles gambiae* adapts to the use of insecticide-treated nets by African populations. *PLoS One*. 9(6):e97700.
- Ngo J.C., Chakrabarti S., Ding J.H., Velazquez-Dones A., Nolen B., Aubol B.E., Adams J.A., Fu X.D., Ghosh G. (2005)**. Interplay between SRPK and Clk/Sty kinases in phosphorylation of the splicing factor ASF/SF2 is regulated by a docking motif in ASF/SF2. *Mol Cell*. 20(1):77-89.
- Ngwa C.J., Scheuermayer M., Mair G.R., Kern S., Brügl T., Wirth C.C., Aminake M.N., Wiesner J., Fischer R., Vilcinskas A., Pradel G. (2013)**. Changes in the transcriptome of the malaria parasite *Plasmodium falciparum* during the initial phase of transmission from the human to the mosquito. *BMC Genomics*. 14:256.
- Nunes M.C., Goldring J.P., Doerig C., Scherf A. (2007)**. A novel protein kinase family in *Plasmodium falciparum* is differentially transcribed and secreted to various cellular compartments of the host cell. *Mol Microbiol*. 63(2):391-403.
- Nunes M.C., Okada M., Scheidig-Benatar C., Cooke B.M., Scherf A. (2010)**. *Plasmodium falciparum* FIKK kinase members target distinct components of the erythrocyte membrane. *PLoS One*. 5(7):e11747.
- O'Meara W.P., Mangeni J.N., Steketee R., Greenwood B. (2010)**. Changes in the burden of malaria in Sub-Saharan Africa. *Lancet Infect Dis*. 10(8):545-555. Review.
- Otto T.D., Wilinski D., Assefa S., Keane T.M., Sarry L.R., Böhme U., Lemieux J., Barrell B., Pain A., Berriman M., Newbold C., Llinás M. (2010)**. New insights into the blood-stage transcriptome of *Plasmodium falciparum* using RNA-Seq. *Mol Microbiol*. 76(1):12-24.
- Pajares M.J., Ezponda T., Catena R., Calvo A., Pio R., Montuenga L.M. (2007)**. Alternative splicing: an emerging topic in molecular and clinical oncology. *Lancet Oncol*. 8(4):349-357. Review.
- Pease B.N., Huttlin E.L., Jedrychowsky M.P., Talevich E., Harmon J., Dillman T., Kannan N., Doerig C., Chakrabarti R., Gygi S.P., Chakrabarti D. (2013)**. Global analysis of protein expression and phosphorylation of three stages of *Plasmodium falciparum* intraerythrocytic development. *J Proteome Res*. 12(9):4028-4045.
- Ponnudurai T., Leeuwenberg A.D., Meuwissen J.H. (1981)**. Chloroquine sensitivity of isolates of *Plasmodium falciparum* adapted to *in vitro* culture. *Trop Geogr Med*. 33(1):50-54.
- Pradel G. (2007)**. Proteins of the malaria parasite sexual stages: expression, function and potential for transmission blocking strategies. *Parasitology*. 134(Pt.14):1911-1929. Review.
- Pradel G. and Schlitzer M. (2010)**. Antibiotics in malaria therapy and their effect on the parasite apicoplast. *Curr Mol Med*. 10(3):335-349. Review.
- Prasad J., Manley J.L. (2003)**. Regulation and substrate specificity of the SR protein kinase Clk/Sty. *Mol Cell Biol*. 23(12):4139-4149.

- Praygod G., de Frey A., Eisenhut M. (2008).** Artemisinin derivatives versus quinine in treating severe malaria in children: a systematic review. *Malar J.* 7(210). Review.
- Pukrittayakamee S., Supanaranond W., Looareesuwan S., Vanijanonta S., White N.J. (1994).** Quinine in severe *falciparum* malaria: evidence of declining efficacy in Thailand. *Trans R Soc Trop Med Hyg.* 88(3):324-327.
- Qian F., Wu Y., Muratova O., Zhou H., Dobrescu G., Duggan P., Lynn L., Song G., Zhang Y., Reiter K., MacDonald N., Narum D.L., Long C.A., Miller L.H., Saul A., Mullen G.E. (2007).** Conjugating recombinant proteins to *Pseudomonas aeruginosa* ExoProtein A: a strategy for enhancing immunogenicity of malaria vaccine candidates. *Vaccine.* 25(20):3923-3933.
- Qian F., Rausch K.M., Muratova O., Zhou H., Song G., Diouf A., Lambert L., Narum D.L., Wu Y., Saul A., Miller L.H., Long C.A., Mullen G.E. (2008).** Addition of CpG ODN to recombinant *Pseudomonas aeruginosa* ExoProtein A conjugates of AMA1 and Pfs25 greatly increases the number of responders. *Vaccine.* 26(20):2521-2527.
- Rached F.B., Ndjembo-Ezougou C., Chandran S., Talabani H., Yera H., Dandavate V., Bourdoncle P., Meissner M., Tatu U., Langsley G. (2012).** Construction of a *Plasmodium falciparum* Rab-interactome identifies CK1 and PKA as Rab-effector kinases in malaria parasites. *Biol Cell.* 104(1):34-47.
- Ranson H., N'guessan R., Lines J., Moiroux N., Nkuni Z., Corbel V. (2011).** Pyrethroid resistance in African anopheline mosquitoes: what are the implications for malaria control? *Trends Parasitol.* 27(2):91-98. Review.
- Reininger L., Tewari R., Fennell .C., Holland Z., Goldring D., Ranford-Cartwright L., Billker O., Doerig C. (2009).** An essential role for the *Plasmodium* Nek-2 Nima-related protein kinase in the sexual development of malaria parasites. *J Biol Chem.* 284(31):20858-20868.
- Rogerson S.J., Hviid L., Duffy P.E., Leke R.F.G., Taylor D.W. (2007).** Malaria in pregnancy: pathogenesis and immunity. *Lancet Infect Dis.* 7(2):105-117. Review.
- Roll Back Malaria Partnership. (2008).** The global malaria action plan. World Health Organization. <http://www.rbm.who.int/gmap/gmap.pdf>.
- Rosario, V. (1981).** Cloning of naturally occurring mixed infections of malaria parasites. *Science.* 212(4498):1037-1038.
- Sachs J. and Malaney P. (2002).** The economic and social burden of malaria. *Nature.* 415(6872):680-685. Review.
- Santos G., Torres N.V. (2013).** New targets for drug discovery against malaria. *PLoS One.* 8(3).
- Schlitzer M. (2007).** Malaria chemotherapeutics part I: History of antimalarial drug development, currently used therapeutics, and drugs in clinical development. *Chem Med Chem.* 2(7):944-986. Review.
- Schneider A.G. and Mercereau-Puijalon O. (2005).** A new Apicomplexa-specific protein kinase family: multiple members in *Plasmodium falciparum*, all with an export signature. *BMC Genomics.* 6(30).
- Schumacher R.F. and Spinelli E. (2012).** Malaria in children. *Mediterr J Hematol Infect Dis.* 4(1): e2012073. Review.
- Schwartz L., Brown G.V., Genton B., Moorthy V.S. (2012).** A review of malaria vaccine clinical projects based on the WHO rainbow table. *Malar J.* 11(11):1-22. Review.

- Sherman I.W., Eda S., Winograd E. (2003). Cytoadherence and sequestration in *Plasmodium falciparum*: defining the ties that bind. *Microbes Infect.* 5(10):897-909. Review.
- Shiu S.H. and Li W.H. (2004). Origins, lineage-specific expansions, and multiple losses of tyrosine kinases in eukaryotes. *Mol Biol Evol.* 21(5):828-840.
- Sibley C.H., Brophy V.H., Cheesman S., Hamilton K.L., Hankins E.G., Wooden J.M., Kilbey B. (1997). Yeast as a model system to study drugs effective against apicomplexan proteins. *Methods.* 13(2):190-207.
- Sidhu A.B., Valderramos S.G., Fidock, D.A. (2005). *Pfmdr1* mutations contribute to quinine resistance and enhance mefloquine and artemisinin sensitivity in *Plasmodium falciparum*. *Mol Microbiol.* 57(4):913-926.
- Silvestrini F., Alano P., Williams J.L. 2000. Commitment to the production of male and female gametocytes in the human malaria parasite *Plasmodium falciparum*. *Parasitology.* 121(5):465-471.
- Sims P.F. and Hyde J.E. (2006). Proteomics of the human malaria parasite *Plasmodium falciparum*. *Expert Rev Proteomics.* 3(1):87-95. Review.
- Singh N., Preiser P., Rénia L., Balu B., Barnwell J., Blair P., Jarra W., Voza T., Landau I., Adams J. H. (2004). Conservation and developmental control of alternative splicing in *maebl* among malaria parasites. *J Mol Biol.* 343(3):589-599.
- Sologub L., Kuehn A., Kern S., Przyborski J., Schillig R., Pradel G. (2011). Malaria proteases mediate inside-out egress of gametocytes from red blood cells following parasite transmission to the mosquito. *Cell Microbiol.* 13: 897-912.
- Solyakov L., Halbert J., Alam M.M., Semblat J.P., Dorin-Semblat D., Reininger L., Bottrill A.R., Mistry S., Abdi A., Fennell C., Holland Z., Demarta C., Bouza Y., Sicard A., Nivez M.P., Eschenlauer S., Lama T., Thomas D.C., Sharma P., Agarwal S., Kern S., Pradel G., Graciotti M., Tobin, A.B., Doerig, C. (2011). Global kinomic and phospho-proteomic analyses of the human malaria parasite *Plasmodium falciparum*. *Nat Commun.* 2(565).
- Sorber K., Dimon M.T., DeRisi J.L. (2011). RNA-Seq analysis of splicing in *Plasmodium falciparum* uncovers new splice junctions, alternative splicing and splicing of antisense transcripts. *Nucleic Acids Res.* 39(9):3820-3835.
- Spector D.L. and Lamond A.I. (2011). Nuclear speckles. *Cold Spring Harb Perspect Biol.* 3(2). Review.
- Stamm S. (2008). Regulation of alternative splicing by reversible protein phosphorylation. *J Biol Chem.* 283(3):1223-1227. Review.
- Stojdl D.F. and Bell J.C. (1999). SR protein kinases: the splice of life. *Biochem Cell Biol.* 77(4):293-298. Review.
- Sutanto I., Suprijanto S., Kosasih A., Dahlan M.S., Syafruddin D., Kusriastuti R., Hawley W.A., Lobo N.F., Ter Kuile F.O. (2013). The effect of primaquine on gametocyte development and clearance in the treatment of uncomplicated *falciparum* malaria with dihydroartemisinin-piperaquine in South Sumatra, Western Indonesia: an open-label, randomized, controlled trial. *Clin Infect Dis.* 56(5):685-693.
- Talevich E., Mirza A., Natarajan K. (2011). Structural and evolutionary divergence of eukaryotic protein kinases in Apicomplexa. *BMC Evol Biol.* 11:321.
- Trager W. and Jensen J.B. (1976). Human malaria parasites in continuous culture. *Science.* 193(4254):673-675.

- Trecek M., Sanders J.L., Elias J.E., Boothroyd J.C. (2011).** The phosphoproteomes of *Plasmodium falciparum* and *Toxoplasma gondii* reveal unusual adaptations within and beyond the parasites' boundaries. *Cell Host Microbe*. 10(4):410-419.
- Talman A.M., Domarle O., McKenzie F.E., Ariey F., Robert V. (2004).** Gametocytogenesis: the puberty of *Plasmodium falciparum*. *Malar J*. 3(24). Review.
- Udhayakumar V., Kariuki S., Kolczack M., Girma M., Roberts J.M., Oloo A.J., Nahlen B.L., Lal A.A. (2001).** Longitudinal study of natural immune responses to the *Plasmodium falciparum* apical membrane antigen (AMA-1) in a holoendemic region of malaria in western Kenya: Asembo Bay Cohort Project VIII. *Am J Trop Med Hyg*. 65(2):100-107.
- Vaid A., Sharma P. (2006).** PfPKB, a protein kinase B-like enzyme from *Plasmodium falciparum*: II. Identification of calcium/calmodulin as its upstream activator and dissection of a novel signaling pathway. *J Biol Chem*. 281(37):27126-33.
- Velazquez-Dones A., Hagopian J.C., Ma C.T., Zhong X.Y., Zhou H., Ghosh G., Fu X.D., Adams J.A. (2005).** Mass spectrometric and kinetic analysis of ASF/SF2 phosphorylation by SRPK1 and Clk/Sty. *J Biol Chem*. 280(50):41761-41768.
- Vogel G. (2010).** The 'Do unto others' malaria vaccine. *Science*. 328(5980):847-848.
- Walliker D, Quakyi I.A., Wellems T.E., McCutchan T.F., Szarfman A., London W.T., Corcoran L.M., Burkot T.R., Carter R. (1987).** Genetic analysis of the human malaria parasite *Plasmodium falciparum*. *Science*. 236(4809):1661-1666.
- Wang H.Y., Arden K.C., Bermingham J.R.Jr., Viars C.S., Lin W., Boyer A.D., Fu X.D. (1999).** Localization of serine kinases, SRPK1 (SFRSK I) and SRPK2 (SFRSK2), specific for the SR family of splicing factors in mouse and human chromosomes. *Genomics*. 57(2):310-315.
- Ward P., Equinet L., Packer J., Doerig C. (2004).** Protein kinases of the human malaria parasite *Plasmodium falciparum*: the kinome of a divergent eukaryote. *BMC Genomics*. 5(79). Review.
- Warsame M., Abdillahi A., Duale O.N., Ismail A.N., Hassan A.M., Mohamed A., Warsame A. (2002).** Therapeutic efficacy of chloroquine and sulfadoxine/pyrimethamine against *Plasmodium falciparum* infection in Somalia. *Bull World Health Organ*. 80(9):704-708.
- White N.J. (1998).** Preventing antimalarial drug resistance through combinations. *Drug Resist Updat*. 1(1):3-9.
- White N.J. (2004).** Antimalarial drug resistance. *J Clin Invest*. 113(8):1084-1092. Review.
- White N.J. (2013).** Primaquine to prevent transmission of *falciparum* malaria. *Lancet Infect Dis*. 13:175-181.
- World Health Organization. (2013).** World malaria report 2013.  
[http://www.who.int/malaria/publications/world\\_malaria\\_report\\_2013/report/en/](http://www.who.int/malaria/publications/world_malaria_report_2013/report/en/)
- Wiesner J., Ortmann R., Jomaa H., Schlitzer M. (2003).** New antimalarial drugs. *Angew Chem Int Ed Engl*. 42(43):5274-5293. Review.
- Witkowski B., Amaratunga C., Khim N., Sreng S., Chim P., Kim S., Lim P., Mao S., Sopha C., Sam B., Anderson J.M., Duong S., Chuor C.M., Taylor W.R., Suon S., Mercereau-Puijalon O., Fairhurst R.M., Menard D. (2013).** Novel phenotypic assays for the detection of artemisinin-resistant *Plasmodium falciparum* malaria in Cambodia: *in-vitro* and *ex-vivo* drug-response studies. *Lancet Infect Dis*. 13:1043-49.



- Wong R., Balachandran A., Mao A.Y.Q., Dobson W., Gray-Owen S., Cochrane A. (2011).** Differential effect of CLK SR kinases on HIV-1 gene expression: potential novel targets for therapy. *Retrovirology*. 8:47.
- Wongsrichanalai C., Pickard A.L., Wernsdorfer W.H., Meshnick S.R. (2002).** Epidemiology of drug-resistant malaria. *Lancet Infect Dis*. 2(4):209-218. *Review*.
- Wu Y., Ellis R.D., Shaffer D., Fontes E., Malkin E.M., Mahanty S., Fay M.P., Narum D., Rausch K., Miles A.P., Aebig J., Orcutt A., Muratova O., Song G., Lambert, L., Zhu D., Miura K., Long C., Saul A., Miller L.H., Durbin A.P. (2008).** Phase 1 trial of malaria transmission blocking vaccine candidates Pfs25 and Pvs25 formulated with montanide ISA 51. *PLoS One*. 3(7):e2636.
- Younis I., Berg M., Kaida D., Dittmar K., Wang C., Dreyfuss G. (2010).** Rapid-response splicing reporter screens identify differential regulator of constitutive and alternative splicing. *Mol Cell Biol*. 30(7):1718-1728.
- Yun B., Farkas R., Lee K., Rabinow L. (1994).** The Doa locus encodes a member of a new protein kinase family and is essential for eye and embryonic development in *Drosophila melanogaster*. *Genes Dev*. 1994, 8(10):1160-1173.
- Zalis M.G., Pang L., Silveira M.S., Milhous W.K., Wirth D.F. (1998).** Characterization of *Plasmodium falciparum* isolated from the Amazon region of Brazil: evidence for quinine resistance. *Am J Trop Med Hyg*. 58(5):630-637.
- Zhang X., Tolzmann C.A., Melcher M., Haas B.J., Gardner M.J., Smith J.D., Feagin J.E. (2011).** Branch point identification and sequence requirements for intron splicing in *Plasmodium falciparum*. *Eukaryot Cell*. 10(11):1422-1428.

## 9 Appendix

### 9.1 Antiplasmodial activity of the CLK inhibitor library

**Tab. 9.1:** Measured IC<sub>50</sub> values for the inhibitor library by Malstat assays. Compounds marked with an asterisk were further investigated in subsequent studies.

Substance name	Single Malstat assays (µm)				Mean IC <sub>50</sub> (µm) ± SD
<b>C-117*</b>	5.5	9.4	13.0	-	<b>9.3 ± 3.82</b>
<b>C81</b>	36.1	77.8	40.2	-	<b>51.4 ± 22.98</b>
<b>C-129</b>	>100	>100	-	-	<b>&gt;100</b>
<b>C-666-42-72</b>	>100	-	-	-	<b>&gt;100</b>
<b>C-667</b>	>100	>100	-	-	<b>&gt;100</b>
<b>EK-28</b>	>100	-	-	-	<b>&gt;100</b>
<b>Kast-24</b>	30.7	58.9	42.7	-	<b>44.1 ± 14.15</b>
<b>Kast-25</b>	99.7	75.8	-	-	<b>87.8 ± 16.90</b>
<b>Kast-27</b>	>100	>100	-	-	<b>&gt;100</b>
<b>Kast-50</b>	11.0	9.9	19.3	6.7	<b>11.7 ± 4.65</b>
<b>Kast-73</b>	>100	>100	-	-	<b>&gt;100</b>
<b>Kast180-HCl</b>	>100	>100	-	-	<b>&gt;100</b>
<b>Puzik-V8</b>	>100	>100	-	-	<b>&gt;100</b>
<b>Puzik-V12</b>	16.4	28.6	37.7	-	<b>27.6 ± 10.69</b>
<b>Puzik-V16</b>	55.7	25.3	-	-	<b>40.5 ± 21.50</b>
<b>Puzik-V23.1</b>	39.1	32.9	34.9	-	<b>35.6 ± 3.16</b>
<b>gea-27*</b>	5.4	4.9	-	-	<b>5.2 ± 0.35</b>
<b>gea-50</b>	>100	-	-	-	<b>&gt;100</b>
<b>gea-70</b>	>100	>100	-	-	<b>&gt;100</b>
<b>gea-75</b>	3.6	33.8	-	-	<b>18.7 ± 21.35</b>
<b>KH-CARB13xHCl*</b>	6.4	2.0	14.1	-	<b>7.5 ± 6.13</b>
<b>Pohl-2</b>	121.1	61.8	72.8	-	<b>85.2 ± 31.54</b>
<b>Pohl-17</b>	>100	>100	-	-	<b>&gt;100</b>
<b>KH-CARB1</b>	72.2	119.1	-	-	<b>95.7 ± 33.16</b>
<b>KH-CARB8</b>	59.5	49.5	-	-	<b>54.5 ± 7.07</b>
<b>KH-CARB3A</b>	>100	>100	-	-	<b>&gt;100</b>
<b>KH-CARB3B</b>	>100	>100	-	-	<b>&gt;100</b>
<b>KH-CARB7</b>	>100	>100	-	-	<b>&gt;100</b>
<b>KH-CARB9</b>	>100	>100	-	-	<b>&gt;100</b>
<b>KH-CARB10*</b>	9.2	9.1	4.8	6.6	<b>7.4 ± 5.75</b>
<b>KH-CARB11*</b>	7.1	6.4	5.0	-	<b>6.1 ± 1.09</b>
<b>KH-CARB2</b>	142.4	63.2	-	-	<b>102.8 ± 56.00</b>

<b>KH-DTCMA</b>	8.1	23.5	-	-	<b>15.8 ± 10.92</b>
<b>KH-CARB6</b>	76.3	60.3	-	-	<b>68.3 ± 11.31</b>
<b>KH-AMTC</b>	6.0	11.9	-	-	<b>9.0 ± 4.17</b>
<b>KH-CB5</b>	>100	-	-	-	<b>&gt;100</b>
<b>KH-CB19T</b>	>100	-	-	-	<b>&gt;100</b>
<b>NIH85</b>	>100	>100	-	-	<b>&gt;100</b>
<b>AR7</b>	>100	>100	-	-	<b>&gt;100</b>
<b>KH-HP05</b>	36.0	46.8	41.2	-	<b>41.3 ± 5.40</b>
<b>KH-HP11</b>	29.3	43.8	43.7	-	<b>38.9 ± 8.34</b>
<b>KH-HP01</b>	>100	>100	-	-	<b>&gt;100</b>
<b>KH-HP02</b>	32.6	47.4	-	-	<b>40.0 ± 10.47</b>
<b>KH-HP03</b>	90.4	52.4	-	-	<b>71.4 ± 26.87</b>
<b>KH-HP04</b>	>100	-	-	-	<b>&gt;100</b>
<b>KH-HP06</b>	>100	>100	-	-	<b>&gt;100</b>
<b>KH-HP07</b>	>100	-	-	-	<b>&gt;100</b>
<b>KH-HP08</b>	56.8	57.3	-	-	<b>57.1 ± 0.35</b>
<b>KH-HP09</b>	37.4	66.1	-	-	<b>51.8 ± 20.29</b>
<b>CS-14</b>	59.6	29.9	97.2	79.0	<b>66.4 ± 24.93</b>
<b>CS02</b>	>100	>100	-	-	<b>&gt;100</b>
<b>CS04</b>	>100	-	-	-	<b>&gt;100</b>
<b>CS06</b>	>100	>100	-	-	<b>&gt;100</b>
<b>CS07</b>	>100	>100	-	-	<b>&gt;100</b>
<b>gea-11</b>	>100	-	-	-	<b>&gt;100</b>
<b>gea-49</b>	25.8	64.0	-	-	<b>44.9 ± 27.01</b>
<b>gea-55</b>	67.2	64.3	-	-	<b>65.6 ± 2.05</b>
<b>NIH11</b>	23.0	55.0	17.7	-	<b>32.0 ± 4.77</b>
<b>NIH16</b>	50.5	91.3	34.4	-	<b>58.7 ± 29.33</b>
<b>KH-CM16</b>	78.2	130.8	-	-	<b>104.5 ± 37.19</b>
<b>NIH08</b>	>100	>100	-	-	<b>&gt;100</b>
<b>NIH39</b>	>100	-	-	-	<b>&gt;100</b>
<b>NIH54</b>	>100	>100	-	-	<b>&gt;100</b>
<b>CHX*</b>	0.4	0.8	0.7	-	<b>0.6 ± 0.40</b>

## 9.2 Sequences of genes investigated in this study

### A Kinase sequences (5'→3')

PfCLK-3 (PF3D7\_1114700)

Coding sequence: 2100 bp

Recombinant protein primers: **rp1**; **rp2**

**pCAM-BSD-KO primers**

**pCAM-BSD tagging primers**

*CATALYTIC DOMAIN*

ATGTCCAAAGATAAGAGAACTCGTTTGCATCCAATTCTTTTGATTCTAGCAACGACGAA  
 AAAAAATCTAAGAATGGAAATAAAATTTATAAATCAAACATGAAGAGAATAGTCCTGAT  
 GGTGATTCATATAAAATAAATAACGAAAAAGAGAAAAGTAAAGAAAAATTAACAAAA  
 GATCAAAAGAAAAATCTAAAGAAATTTATAATTCATTTAATTCTCCTAATTCTACTAGT  
 AGCGATTCGGATGGAAATGGATTACATCTAAATTTTTCCAACGCATCAAGTTCGAGTAGT  
 GAAAACGGATTTAAGATACTACGAACACAAGAAAATGAGGATAAACTTCTAGAAGAAAGA  
 AGAAGAAAAAGAGAAGCATTAAAGAAAAATTAACAAACATGGTTAAGGAAAATGAACAA  
 AATAATGATGCGAATGAAATACTACAGAATGATCAGATAAATAAAGATTATAACAATGAA  
 ACTTTTTTGTAAAGTAAAATAAAATGATAATGATATAATAACAAATGAAATACCATCT  
 AATCCATCATATATCGACCAAATGATGCGGCCTGCATTTTCGCACCCAACAATGATGTT  
 ATTGAAGATACGTGCTCATCACTCTCATCAGATCATGAAATTATAGAAGAAAAACAAAT  
 AAAGAAAACCAGAAGCAGTAAAGAGTGTAGTGATTTGTATAATGATTTAAAAA  
 ATTGATGAAGAAAAGGCCAAAATTAGGTCATTTATAATCAAACAGAAAGAATTACATGAA  
 AGATTAATAATGAATGTGGATGATAGTTTATATGTGAATAAAAGT**AAGGGAAATGCAGAT**  
**ACA**CATAATAATTTAACTAATAAGAAGAGTCCTCTTGAAAATGAAGAAGATGAAATGCAA  
 GAAGAATACGATGAGGATAAT**GATGATTTTGATATGTTTTCTGT**GTACAAGCAAATAAA  
 AAAAGAAAAGTTGAAAAGTACATATACTGATTATTACACAACAGGAAATAATGCAAAT  
 TTGTCAGATAATTGGAATGACTCAGAGGATATTACAAGGCTATGGTTGGCGAGGTTATT  
 GATAAAAGATAC**AGTGTGTGTGGAAGTGGTGGGAAAGGTGTTTTTCAAATGTATTA**  
**AAGTGTTATGATATGGTAAATAAAAT****CCTGTAGCTGTAAAAGTT****ATTAGAGATAATGAT**  
**ATGATGAAAAGGCTGCAGAAAAAGAAATATCTATTTGAAGAAGTTAAATCAATATGAT**  
**AAGACAATAAAAGGCACATCATTGTTTATTAAGTAGTATAAAATATAAAATCATTTA**  
**TGTTTAGTATTTGAGTGGATGTGGGTAAGTAAAGTAAAGTAAATCAATATGAT**  
**GGACATGGACTAAACGCAACAGCCGTTATTGTTACACAAAACAATTATTTATAGCCCTA**

AGACATATGAGAAAATGTCGAATAATGCATGCTGATCTAAAACCGGATAATATTCTTATT  
 AATGAAAAATTTAACGCCTTAAAAGTTTGGCATTGGAAGTGCAAGTGATATATCA GAA  
 AATGAAATTACGTCATATTTAGTTAGTAGATTTTATAGAGCA CCTGAAATTATTTGGGT  
 TTTGATACGACGCTCAGATTGATGTATGGTCAGCTGCTGCAACTGTTTTGAATTAGCA  
 ACGGGTAAAATCTTGTTCGGGTAAATCAAATAATCATATGATAAAACTGATGATGGAA  
 TATAAGGGCAAATTTTACATAAAATGATAAAAGGTGGGCAATTTTATTCTCAACATTTT  
 AATGAAAATTTAGATTTTCTTTATGTGGATAGAGATCATTATTCCAAAAAGAAGTTGTT  
 AGAGTTATATCTGATTTGAGACCTACGAAAAATATAACATGTGATTTATTGGAGCATCAA  
 TATGGTTGAAGGGAAATAGCCCTAAAATGCAATTTTGAAAAAAAAAAATAAAACAATA  
 GGAGATTTATTAGAGAAATGTTAATTCTAGATCCATCTAAACGATATACTCCAGATCAA  
 GCTTTACAACATCCTTATTTAAGAGAATCTATTCATTTTCAAAAATCTCAAAATGAA TAA

PfCLK-4 (PF3D7\_0302100)

Coding sequence: 4017 bp

Recombinant protein primers

pCAM-BSD-KO primers

pCAM-BSD tagging primers

*CATALYTIC DOMAIN*

ATGAGTTTTAGTAATACATGCTCACTATCCAATAACAGCAACAGTTCTAGTAGTAGTGAA  
 GATGCTACTTCTGGTAAATTACAATACACCGAAAGTGATGATGAAGGAAGTGATGAATAC  
 TGCGAAGGAGGGTATCACCCAGTCAAATTAATGAAATATATAATGATAGA TATAGAATT  
 GAAGGAAAATTAGGTTGGGACATTTTCAACCGTTTGGGTTGCTACTGATTTAAAAGT  
 AAACCCTTAAAATTTGTTGCTATAAAAATTCAAAAAGGATCAGAACTTATACTGAATCA  
 GCCAAATGTGAAATTAATTATTTAAATACAGTCAAAGTAAATTCTTTTGATTCTTCATGG  
 GTTGAATTAAGAACAACAAGAGAAAGATTATTCATTATAATATGACTAAAGGAGTT  
 GTCTCTTTTATTGATAGTTTGAACATAAAGGTCCAATGGTACTCATATTTGTATGGTC  
 TTTGAATTTATGGTCCTAATTTATTATCCCTAATAAAACATTATGATTATAAAGGAATT  
 CCATTAAATTTGGTCAGAAAAATTGCTACACATGTGTTAATAGGAATGCAATATTTACAT  
 GATGTCTGTAAAATTATACATAGTGATATCAAACCAGAAAATGTTTTGGTCTCACCATTG  
 ACTACTATTCCAAAACCAAAGGATTATACCAAAGATAAATTAGAATCAAATAAATCTAAC  
 CAAGTTGAAAAAAAAAGAAAATGACCAAATGTAGATAAGAAATTAATTACTACAATGAAT

AATAACATAAATACAAATCTAAGTGAAAAAAAAAAGTTATTAATGATACACAAAAAAT  
GATAAAAAATATAGAATATGATCAAAAA**TGTACGAGCAGTAAAGAA**AATATTGAAGATAAT  
GTATCCTTTGTAAATGATCCAAGTGATCCTAATCAAAGAATAATCTAAATAATAATATA  
ACGGATAATAATATCATACCCAGTAATGTACAAATAGAAAAACAATCTACATTAAGTAAA  
AATAAAAAAATGAAAAAGATTCATATATAAATATAAACAATTCTCTTACAAATGATGAT  
CAAATTTAAAAAGAGAAGATATCAAATTTAATGAT**AAAGCGGAAGGGATTACCAA**TAT  
GATATGTTAAATATTAATAATAATATATCTATTAAAGAAAAATAAATGATTGTCATTCA  
CCCAATGAAAATAAAAAATAAGATAATCATAATCAATGTGAAGACAATTCGATCAACATA  
TGTAATAACAAAAATAATAATATTCAAACAAATAATATTAATGATAACACTGTTAACGAA  
AAAATTAATAATACATCAAAGAAGGATATGTTAAATAATACACAAAATAATAAT**GATTCC**  
**GAAAAGAACGAC**GTTGTTATTGAACAACAATTGGTAAATGAAGATATTTTAAAAAAAAA  
AACAAACAAACAAAAAAAAAAAAAAAAAATAAATGAACCTCCATATGTTAAACATAAACTA  
AGACCATCAAATTCGGATCCTTCTTTGCTCACATCTTATTCTAATATACATGCACTTCAA  
GAAACCTTGACAAGGAAACCATATCATTATAATACCTATTTTTTAAACAACCCCGAAAAA  
TATAGAGATAATAAATGAATCCATACTTACACAGATTGCCAAATGATTGCTTGAAAAA  
ATCGATCAAGATGATAGTGATGAAACGGAAGAGGAGGATGATCTTTCAGATGTAGACCAA  
AATAAGGAACAAAATAAGAACCAATTAGAGGTCAACTTGCCAAATAATAAATATCCAAAT  
TCCAATGATGTGTATAAATTTTTTGAAAAGATATTAATAAATTTCCCATATACTGCGAC  
ATGTTTAAATCATCTTATACATCCAGAAGCCTTACGATTACATGAATTATATATGAAAAAT  
AAAAAAAACATCGATTCTAACAATACAATGAATGATTTAGGTAATAATCAAATAGTCAT  
AAAGTAGTATATATAAATACTGAAGATGGAGAATATTGTATTAGGCCATACGATCCGTCT  
GTTTATTATCATGAAAAATCATGTTATAAAATATGTGACCTAGGAAATAGTTTGTGGATA  
GATGAATCAAGATATGCCGAAATTCAAACCTAGACAATATCGAGCCCCTGAAGTTATTTTA  
AAAAGTGGGTTCAATGAAACAGCAGATATATGGTCCTTTGCATGCATGGTATTCGAATTA  
GTAACAGGAGACTTTTTATTTAATCCACAAAAGGTGATAGATATGATAAAAATGAAGAA  
CATTTAAGTTTTATAATTGAAGTGTTAGGAAATATACCAAAGCATATGATTGATGCAGGG  
TATAATTCCATAAATATTTTAAACAAAATAATTATCGACTTAAAAATATAAGAAATATT  
AAAAAATATGGTTTATATAAAATATTAATAATAAATATAATCTTCCTGAAAAGGAAATT  
AGCCCCTTATGTAGTTTCTTATTACCCATGTTATCTGTGGATCCACAAACGCGCCCCTCA  
GCATATACCATGCTTCAACACCCATGGCTTAATATGGTATCATTAGAAGAAGGGGATGAC

ATGTATATTAATGATGAATCATATTCTATTAATAATGATAGAAACATGAAAAATAATAGT  
AATAGTAATAATTTTCATCTACGACGGTCATAATAGTAGTAAAAATAAAAAATCTTCAAA  
AAAAAAAAAATTGATGTAAACTACAAAATTGGTAATAATGGAAATAATGCTTATAACGAT  
AACTATTATAATAAAAAATTATAAAAAATAAAAAATAAAAAATTTTAATGATGATGTT  
GTAGAACCATCACCAGATCAATATATGCATGCAAATTATAATAATGATATTGTGCATGCA  
GTTTTGTATGAAAAGCCATATAATTCAAATAATGTCATTTTCATACACTAATAACAAAGGA  
CATAAAAAATAATTTTGATATTAATTATTTACAACATAGGAATGATAATAATTCGAACAAA  
CAAAATATTTTCATTAECTACAAACGATTATACATTTAATTCGGATTATATTGCTAATATG  
ATGGATCATGACACATATAGAAAACAAATAATAAAAAATATTCCTGCACATCAAATTTCA  
AACTAAAAGATGGTAAAAATTTTAAGGCATATAATGAATCTATTCAATATGAAATGCAT  
GATTTTCAACAATACAATGAACATGATTTTGAATACAAATTTAATAAAAGATTTGAACAT  
GCACATCATATAAAAGAAATGAAACATAACGATGATGATTACGAGGAGGAAGATGAAGAT  
GAAGATGACGATGATGAAGATTATGAAAGTGATGTTGATTATGATGATGATGATGAATAT  
GATGAAGGACAAGAACATGATGCTGATCAAGATGAAAAAACAACGATAACGAAAAACAA  
CAAGAACAACAAAATTACGGTGAAAAATATAATTATGAACATTATGAAAATAATATGGGT  
TATAATAAAAACATTCAACAATTGTCATATACAAATAATAATGATGATGAAAATAATTTT  
TGTGAGACACAAAATATATATATATTACAAAACAAAAGAGATATAAATTTTAAAGAATGT  
ACACCACGAAATAATATCAACAAAGAAATAAAAAGTGATAAATATCAATCCAGTAAAGTT  
ATAAATCAAAAAGATAATTATTGGAATTACAAAATCAAAGAAAACACAAAATTAAGAGAA  
CATGCAAAAAACAACATTATAGCAACAACAATAATATCAATAAAAAATGATAACTAAT  
ATAATGAACCAAATAGATACCAAAGATCAAATATCCAAAAATTTACATGATTTATCAACA  
AATAACAATATGGACCAAAAACACGGTGCATTACAAAAATGCATATGAACGAAAAACA  
AACCAAGACAAACCATTAAATGACGAAGAAATTTAATCGAAAATAGAGATGACCAGAAT  
GTTAATAAAATCAATTGCAAAGTTATTAACAAAAAAAACTCTTGTGCATATACTTAA

**B SR protein sequences (5'→3')**

PfASF-1 (PF3D7\_1119800)

Coding sequence: 603 bp

**Recombinant protein primers**

**ATGAAAAGTTAATTAATTGTGGC**AATAGATTATATGTTGGTAATATTCCAGGCTCAGCA  
ACAAGACAAGAATTAATAAAAATATTTGAAGAATATGGAAAGATATCAGATATCGATATA  
AAATATAATCGTAATAGTAATGGAACGAATTATGCATTTATCGAATATGAGAACCCTAAG  
AGTGCTGAGAAAAC TATACAAAAAGGAATGGAAAAAATTTAAAGTTATATGTTAAAA  
GTAGAATATAGTATAGAAAAAATAAGAGATTTGAATGATATATATAGATCTGAATAC  
AGAGTTGTTGTAAAACATTTCCCGAGATTTTTTAAAAATATAAAGAATTTTTATCAAGA  
GCAGGAAAAGTACTTTATATTCATAAAGATAATGGTCTTATTATTGCTGAATATGAAGAT  
AAAGAAAGTATGATTAAAGCTATTAGTACATTAGATAGAACCATCTATAATTCAAAAAGA  
AAAGTTTATGTTTCGAGTATTTAAAGACATACCTTATGATTATTCGGATGTAAATCTTATT  
GATTATAATATGGTCTTCTCATCTACAAAAATGAAAATATA**TCTCCAAGGAACTAAAT**  
TAA

PfSRSF12 (PF3D7\_0503300)

Coding sequence: 927 bp

**Recombinant protein primers**

**ATGGGGCCATATATAAATCAG**AAGAATCAACCCATGTCGTTATTGATAAGAAAATTAAG  
TTTGATACATCCCATCAATTGTAAGAGAAAAGTTTAAAAGATTTGGAGCGATTAAAGAT  
GTATATTTACCAATAGATTATTATACGAAAGAACCTCGAGGGTTTGGTTTCGTAGAATTT  
TATGATGCAAAGATGCTGAACAAGCATTAAAGAAATGAATGGTTCAGAAATTGATGGA  
AGTAGAATAGAAGTTTTTGTAGCACAGAAAGGAAGATCAGATCCAAGACATATGAGATAT  
AAAGAAAAGGAGGTTATGCATATAGAAAAATCCAGATAATAAATAAGAAGAAGATAT  
ATATCGAAATCAAATCAAGATATGGTTCATATCAAGAGATAAATAAGAAGACGCGAA  
AGATCAAAGAAAGATTTAGATATAGAAGTAGTTATGATAGAAAAATGAGTAGTTACCGA



GATCGAAAAAATTATCATATGAAAAGTTATGACAAATATCGTGATAGAAATCATGACCGA  
AGTTTAAAGTAGAAGATCAAGAGAATATCGTAATAATACATCAAGATATAGAGATAAAAGA  
AGATATGATAAATATTATAGAAGTACTAGTCGAAGAGCTAGTAGACATGAAAAAAGAAAT  
GAAAATTATAAATCTAAATATAATCATAGTAACGATGACTATAGTGATGAAACCAGAAAC  
TCAAGTAAGCATTCAAGAAAAGAACATGTGTCCAGATCTATTTCTTTTAATTCGGAAAAA  
GATGATGCCAAAAAGAAAAACGATAATACAAGTGAGAGAGATAAATTCAAATGATTGGAAA  
GGAAGTGAACAAAGAAAAGAGGAAGAAGATGAGGAAGTAGAA**AAGGAGAAGGAAAATGAA**  
GAAGAGGAAGAAGCAATTTATGATTAA

PfSFRS4 (PF3D7\_1022400)

Coding sequence: 1617 bp

#### Recombinant protein primers

ATGAGTTTTAAACCAAGATTCAGTAAATCATCTTCATGCATATATGTAGGAAATTTACCA  
GGCAATGTCATTGAAGAAGAAGTTTACGATTTATTTGGAAAGTATGGGCGTATAAAGTAC  
ATAGATATAAAGCCATCAAGATCTTCCTCTAGTTCCTTATGCTTTTGTTCATTATTATGAT  
TTGAAAGATGCAGATTATGCAATAGAAAGAAGAGATGGATATAAATTTGATGGATTTTCGT  
TTACGTGTTGAACATTCAGGAGAAAACAGAAGTTTTGGAAAATATAGAAAAAA**GATGAT**  
**GGTGTGGTCCA**CTATAAGA ACTGAAAATAGAGTAATTGTTACTAATTTACCAGATAAT  
TGCAGGTGGCAACATTTAAAAGATATTATGAGACAATGTGGTGATGTGGGATATGCTAAT  
ATTGAACGAGGAAAAGGTATAGTAGAATTTGTAAGTTATGATGATATGTTATATGCAATT  
GAAAAATTTGATGGTGCAGAATTTAAAGTGTATGACGATGTTACAAATATTTAAAGTTAGA  
AGAGATAAAAGAGGTTCTTCTTATATGAAAAGATATAGAAATGATTATAGTCCTAAATAT  
AAAAAAGACGTAGATATAGTAATGAATCGGGATTATCAGATAGAGATCGATCAAGATCT  
AGAAGATACAGTAAATCTAGTAATTCATCAAACAAAAGAAATAATAAATATGAATCTCAT  
AGTCAAAGTTTAAAGCGATAATAGAAATAGTTACAGAAATAGAAGTAAGGGTAAAAAAGA  
AGTGGATATAAAGGGAAAAGAAGTTATAGTTCTTATGAAAACCAAACGATGATGTTAGT  
AGGAGTAGATCTGATCATGGATCAAGAAGTGGTGATAGAAGTTATAGAAAGAAAAAAT  
AAAAATGAAAGCTCTAGTGATGTATTAAGTAAACATTCTAGTGCATACCGAGATAGCGAT  
AGTGAAAAAATAAAAGCTATAGAAAACGTTTATCAAGTGATAACAGAAGTCATAGCAGA

CGAAGAACTGTAAGTGAAGATAGAAGTGAAAGAAGGAGAAGTTTAAGTGAAGATAGAAGT  
AATAGTAGAAAAAGGAACGCAAGCAGCGACTTCAAAGAGAACTAAATTCAGATGATGAT  
AAAAAAGTAAAAAAAAAAGAAGCTATAGCGCTTCACCGGGATCGGCATATAAGAGCAGT  
TCACGTGAGTTAAAAAGTCAAGATAAAAGCAATGATAGATTAAGTGAATCAAAAAAGAGT  
TATAAATCTCAAAGTGCTTCTGTTAGATACAATAGCACAGAAGAGAAAAAAGCGATGAT  
GAACTGTAAACCTAAGAGAGGTGGTAGGGGAAATGCAAAGAATACAGGGAAGAATAAG  
AATACTAAAGGAAGTAAAAAGGTGCTAAACAGAAGAAAATCATGATTCTAAAAGTGTT  
TCCAATGATAGAAAATAAAGTGATAAATCCGAAGAAAAAGAAAAACCTGAAGTTGTAAGT  
AAAGATGAAGAAGATAAGAAAACAGGAGGTGCAGAAGTAAACCTAAGAGAGGAAGAAGA  
GGAAGAAAAAAGCTAATGCAGCAGATGAAAATGCAAATGGTAATGTTAGCAACTAA

PfSF-1 (PF3D7\_1321700)

Coding sequence: 2595 bp

Recombinant protein primers: **rp1**; **rp2**

ATGGAAGAGAACTCATATTTTGAGGCA GTAGAAAACTTTTTGAAATTAAAAATTCAAA  
GAAGATAAAATAAATGGAAGTAGTAGTAATAAGGATGAATTAATTGAAAATAAAGAATTA  
AAAAATGATAACTTGAATAATAACTTGTGATAGTGATAAAAAGAAAACAAACAAAAGA  
GAAGTCAAAGAAAAAGTAAAGTTATCAATGATAATAAAATAGATAATGAAAACAAAAT  
ACAAAAGGAAAAAAAAAAACAAATGGTGTGTCGATATAAATATAGATGAAAATTTTGAT  
GAAGATAATGATGAAAATGTTGATAAAAATGTTGATAAAAATGTTGATAAAAATGTTGAT  
AAAAATGATGATGAAGATGATGGTGAAGATGATGGTGAAGATGATGGTGAAGATGATGGT  
GAACACGATGGTGAAGATGACGGTGAAGATGATAGTGATGAAGATAAACATGAAAATATT  
CCTAAAAATAAAGCAGATACTTTGAAAGAAGAGTCTGATGTATCAGATAACCATCATAAC  
AACAGAAAATCTAAAAATATAAAAAATCTATAAGGAGTAAGAGTAGTAATAGTAAAACA  
AAAAAGAAGATGATGATAATAATATTCATTGTAATAATAGTTTCGCAGGAAAATGAACAA  
AAGCGTAAGGAACAGCTTTTGAAAAATAAAGACAATAAGAAGGAGGGGAAAAATACAAAT  
TCCTCTAAAGTTAAAAAAGATATCATACTAGTAGTGATGAAAATGATAGGAATAATGAT  
AATACATCATCAGAGGAAGAAAGGACAAAAGTCGAAAAAGAAACATAAAAAATGATAAC  
AGTGATAAAAAAATGAAAATAGAGTAGTAGACTATTCGTCGTCGTCTTCTCCTCCTCT

GATGCTTCAAATGAATATAGCTCAAGTGATGAAGAAAGAGATCATAAAAAAGAAAAATA  
AGAAAAACAAACCGATCTAGGAGAATTTCCAGATCATCTAGTGAAAGTAATTCAGTACA  
GACAATGATAAACGTGGTACATCAAGAAGCAGTGAAGAAAAAGTGTACTCCAAATATGAT  
AAGATGAAAAGAAGAGATAGAGAAAGAGAAAGAGATAGGGATAGAGACAGAGATAGGGAT  
AGAGACAGAGACAGGGATAGAGACAGAGATAGGGATAGAGACAGAGATAGGGATAGAGAA  
AGAGAAAAGGATAAGGATCGAGATAGAGACCATGACCGATATAGAGATAGAGAACGTGAT  
CGATATAGAGATAGAGAAAGAGAGCGAAGAAAAGATAGAGAAAGGGAAAGAGAAAGGGAA  
AGGGAAAAAGAAAGAATAAGAAGAGAAAATGAAAGAGAAAGATTAAGGAAAGAAAGAGAA  
CTGGAAAGAGAAAGAAGAGAAAAAATAAGA **GAAGAAAGAAGATTAAAAGAAGAAATGGAA**  
**GAAGCAAAAAGGGAT**GATTTAACAGTACTTGTATTAAATTTGGATTTAAAAGCAGATGAA  
AGAGATATATATGAATTTTTTTTCAGAAGTAGCTGGAAAGGTTAGGGATATACAATGTATA  
AAAGATCAAAGGTCAGGAAAATCAAAGGAGTAGCATATGTAGAATTTTACACTCAAGAA  
GCAGTAATAAAAGCATTAGCAGCAAATGGCATGATGTTAAAAAATCGACCAATAAAAAATA  
CAATCATCTCAGGCAGAAAAAATAGAGCAGCAAAGCAGCAAACATCAACCTATAGAT  
CCAAACGATATTCCATTAAAATTATATATCGGTGGATTATTAGGTCCATTAAGTAATATA  
ACAGAACAAGAATTAAAACAATTATTTAATCCTTTTGGTGATATATTAGATGTAGAAATA  
CATAGAGATCCTTATACAGGGAAATCTAAAGGATTTGGTTTTATTCAATTTTCATAAAGCC  
TCTGAAGCCATTGAAGCATTAACTGTTATGAATGGAATGGAGGTAGCGGGTAGAGAAATT  
AAAGTAGGATATGCACAAGATTCTAAATATCTCTTAGCATGTGATAATACTCAAGAAAAT  
ATATTAAGCAACAGCAAATGGCAAAAAATATAAACACTGAAGAGGAAGAACAAGATAAT  
GAGAAAATTGATAACGATGATGGAGACGGCGGTGGGCTCATAGCTGGCACTGGTAGCAAA  
ATAGCATTAATGCAGAAGCTTCAGAGGGATAGTATCATAGATCCTAATATAACCCAGTAGG  
TATGCCACTGGAGCCAATGCTATTATGGCAAGGAATTCCTTCGTTCCCTCAACCAATAAT  
ATAAATAATAATGTGACAACATAATTTAGTATTAAGCAATATGTTTTTCATCAAATGATGAA  
AATATAGGAAGCGACCCCGATTTCTTTAATGACATACTTGAAGATGTTAAAGAAGAAATGT  
AGCAAATATGGAAAGGTTGTAACATTTGGCTAGATACCAAGAACATTGATGGTAAGATT  
TACATAAAATATTCTAATAATGATGAATCATTAAAATCATTTCAATTTTTAAATGGAAGG  
TATTTTGGAGGCTCACTAATAAACGCGTATTTTATTTCAAAC **GATGTATGGGATATGACT**  
**TGTCTTCCAAG**TAG

### 9.3 List of abbreviations

aa	Amino acid
AB	Antibody
ACT	Artemisinin combination therapy
Amp	Ampicillin
AP	Alkaline phosphatase
APAD	3-Acetylpyridine adenine dinucleotide
approx.	Approximately
APS	Ammonium peroxide sulphate
AS	Alternative splicing
ATP	Adenosine tri-phosphate
bp	Base pairs
BSA	Bovine serum albumin
BSD	Blasticidin
CaM	Calmodulin
CF	Cytoplasmatic fraction
CHX	Chlorhexidine
CIP	Calf intestinal phosphatase
Co-IP	Co-immunoprecipitation
CQ	Chloroquine
DMSO	Dimethylsulfoxide
DNA	Deoxyribonucleic acid
dNTP	Deoxynucleotide
DTT	1,4-Dithiothreitol
EC	Erythrocyte control
EDTA	Ethylenediaminetetraacetic acid
EGTA	Ethylene glycol tetraacetic acid
ePK	Eukaryotic protein kinase
ER	Endoplasmatic reticulum
EtBr	Ethidium bromide
Fig.	Figure
FS	Filtered supernatant
FT	Column flow-through
GC	Gametocytes
GST	Glutathione-S-transferase
H <sub>2</sub> O <sub>bidest</sub>	Double-distilled water
HEPES	4-(2-Hydroxyethyl)piperazine-1-ethanesulfonic acid, N-(2-Hydroxyethyl)piperazine-N'-(2-ethanesulfonic acid)
HIV	Human immunodeficiency virus
hLDH	Human lactate dehydrogenase
IB	Inclusion bodies
ICM	Incomplete medium
IFA	Immunofluorescence assay
IgG	Immunoglobulin G
IPTG	Isopropyl-β-D-thiogalactopyranoside
kb	Kilobase
kDa	Kilodalton
KO	Knock-out
LB	Lysogeny broth

MaBP	Maltose binding protein
MBP	Myeline basic protein
mRNA	Messenger RNA
NBT	Nitroblue tetrazolium
NGS	Neutral goat serum
NLS	Nuclear localization signal
NMS	Neutral mouse serum
NP	Nuclear pellet
NRS	Neutral rabbit serum
NTF	Nuclear transport factor
OD	Optical density
PAGE	Polyacrylamide gel electrophoresis
PBS	Phosphate buffered saline
PCR	Polymerase chain reaction
PIC	Protease inhibitor cocktail
PK	Protein kinase
pLDH	Parasite lactate dehydrogenase
PML	Promyelotic bodies
PMSF	Phenylmethanesulfonyl fluoride
PYR	Pyrimethamine
RBC	Red blood cell
rMGV	Relative mean grey value
RNA	Ribonucleic acid
rp	Recombinant protein
rpm	Revolutions per minute
RRM	RNA recognition motif
RS	Arginine-serine
RT	Room temperature
SD	Standard deviation
SDS	Sodium dodecyl sulphate
SDX	Sulfadoxine
SOC	Super optimal broth with catabolite repression
SR	Serine-arginine
SZ	Schizonts
Tab.	Table
TAE (buffer)	Tris-acetate-EDTA (buffer)
TBD	Transmission blocking drugs
TBS	Tris buffered saline
TBSM	Milk powder in TBS
TBSM-T	TBSM-Tween
TBS-T	TBS-Tween
TBV	Transmission blocking vaccines
TEMED	N,N,N',N'-Tetramethylethylenediamine
term.	Terminal
TLR	Toll-like receptor
TZ	Trophozoites
UV	Ultraviolet
WHO	World Health Organization
XA	Xanthurenic acid
$\alpha$	Anti

## 9.4 List of tables

Tab. 2.1:	List of CLK-inhibitors used in the present study. ....	26
Tab. 2.2:	List of commercial kits and enzymes used in this study and their suppliers.....	32
Tab. 2.3:	List of solutions, reagents and buffers used and their compositions.....	32
Tab. 2.4:	List of media and solutions for <i>P. falciparum</i> cultivation. ....	35
Tab. 2.5:	List of media and agar used in this study for bacterial cultivation.....	36
Tab. 2.6:	List of antibodies used in this study, their properties and suppliers.....	39
Tab. 2.7:	List of primers used in this study for recombinant protein expression and gene modification.....	41
Tab. 2.8.:	List of primers used in this study for genotype characterization. ....	42
Tab. 2.9:	Gene IDs of investigated genes proteins. ....	43
Table 2.10:	Pipetting scheme for PCR reactions using GoTaq® or Phusion® Polymerase, respectively. ....	53
Table 2.11:	Thermocycler programs for GoTaq® and Phusion® polymerase.....	53
Tab. 2.12:	Pipetting scheme for digestion reactions.....	55
Tab. 2.13:	Pipetting scheme for ligation reactions.....	55
Tab. 2.14:	Pipetting scheme for control digestion of purified plasmid DNA from transformant bacterial colonies. ....	56
Tab. 2.15:	Composition of different SDS gels (stacking and resolving). ....	61
Tab. 2.16:	Composition of a standard kinase reaction for kinase activity assay.....	64
Tab. 3.1:	Table displaying homologies between the plasmodial proteins investigated in this study and yeast Npl3p and human SF2/ASF.....	78
Tab. 3.2:	Malstat assay results showing IC <sub>50</sub> values of the tested inhibitors. ....	91
Tab. 9.1:	Measured IC <sub>50</sub> values for the inhibitor library by Malstat assays.....	130

## 9.5 List of figures

Fig. 1.1:	Worldwide distribution of vivax and falciparum malaria.....	1
Fig. 1.2:	Representative asexual blood stage parasites in Giemsa-stained blood smears....	4
Fig. 1.3:	Schematic of the life cycle of <i>P. falciparum</i> (modified from Bousema and Drakeley, 2011).....	4
Fig. 1.4:	Gametocytes of <i>P. falciparum</i> in Giemsa-stained blood smears.....	5
Fig. 1.5:	Schematic of the typical ePK catalytic subdomain structure. ....	12
Fig. 1.6:	Domain structures of the PfCLKs. ....	17
Fig. 1.7:	Domain structures of yeast splicing factor Npl3p and the four homologous plasmodial factors.....	19
Fig. 2.1:	Vector map of the expression vector pGEX-4T-1 .....	37
Fig. 2.2:	Vector map of the expression vector pIH902 .....	38
Fig. 2.3:	Vector map of pCAM-BSD for disrupting a specific gene locus.....	38
Fig. 2.4:	Vector map of pCAM-BSD-Myc for gene-tagging. ....	38
Fig. 2.5:	The DNA molecular weight standards for agarose gel electrophoresis..	43
Fig. 2.6:	The protein molecular weight standards used for SDS-PAGE. ....	44
Fig. 2.7:	Preparation of a thin blood smear for determination of parasitemia..	46
Fig. 2.8:	Neubauer hemocytometer and schematic representation of counting grid..	47
Fig. 2.10:	Malstat plate depicting a typical Malstat assay. ....	49
Fig. 2.11:	Assembly of Mini Trans-Blot® Western blotting apparatus from Bio-Rad, Munich..	62
Fig. 2.12:	Schematic depicting the principle of Co-IP. 1.....	64
Fig. 3.1:	Generation of GST-tagged recombinant PfCLK-3 fragments as soluble proteins for polyclonal antibody production in mice. ....	67
Fig. 3.2:	Synthesis of PfCLK-3 rp1 and rp2 purified from bacterial inclusion bodies .....	67
Fig. 3.3:	Verification of PfCLK-3 antisera for expression studies.....	68
Fig. 3.4:	Expression analysis of PfCLK-3 by the use of rat antisera .....	69
Fig. 3.5:	Generation of GST-tagged recombinant PfCLK-4 rp4.....	70
Fig. 3.6:	Determination of antisera directed against PfCLK-4 for expression studies.....	71
Fig. 3.7:	Protein expression analysis of PfCLK-4 .....	72
Fig. 3.8:	Generation of gene-disruptant parasites by means of reverse genetics .....	73
Fig. 3.9:	Gene tagging strategy by reverse genetics.....	74
Fig. 3.10:	Phenotype analyses of genetically modified parasites by means of Western Blotting with antisera directed against Myc-tag .....	75
Fig. 3.11:	Subcellular localization of Myc-tagged PfCLK-3 and PfCLK-4 in blood stage schizonts. ....	76
Fig. 3.12:	Kinase activity assays performed on immunoprecipitated PfCLKs.....	77
Fig. 3.13:	Recombinant expression of yeast GST-tagged splicing factor Npl3p in <i>E. coli</i> .....	79
Fig. 3.14:	Generation of GST-tagged recombinant PfASF-1 via affinity purification.....	80
Fig. 3.15:	Generation of recombinant splicing factors PfSRSF12 and PfSFRS4 in <i>E. coli</i> .....	80
Fig. 3.16:	Generation of MaBP-tagged recombinant PfSF-1 fragments.....	81
Fig. 3.17:	Phosphorylation of yeast Npl3p by immunoprecipitated PfCLKs.....	82
Fig. 3.18:	Phosphorylation of plasmodial SR protein PfASF-1 by immunoprecipitated PfCLKs. ....	83
Fig 3.19:	Phosphorylation of plasmodial SR proteins PfSRSF12 and PfSFRS4 by immunoprecipitated PfCLKs. ....	83

---

Fig. 3.20:	Phosphorylation of the plasmodial SR protein PfSF-1 by immunoprecipitated PfCLKs.....	84
Fig. 3.21:	Subcellular localization of PfASF-1 in blood and gametocyte stages.....	85
Fig. 3.22:	Subcellular localization of PfSF-1 in blood and gametocyte stages.....	86
Fig. 3.23:	Subcellular localization of the SR proteins PfSRSF12 and PfSFRS4 in blood and gametocyte stages.....	87
Fig. 3.24:	Control IFAs.....	88
Fig. 3.25:	In depth analysis of the localization of the SR proteins PfSRSF12, PfSFRS4 and PfSF-1 in the parasite nucleus.....	89
Fig. 3.26:	Co-localization of PfSRSF12, PfSFRS4 and PfSF-1 with PfCLK-1/LAMMER.....	90
Fig. 3.27:	Effect of CLK inhibitors on CLK-mediated MBP phosphorylation.....	92
Fig. 3.28:	Controls for kinase activity assays determining the effect of CLK inhibitors on CLK-mediated MBP phosphorylation.....	92
Fig. 3.29:	Giemsa-stained asexual parasite stages distinguished in stage-of-inhibition assays.....	93
Fig. 3.30:	Effect of CLK inhibitors on blood stage parasites.....	94
Fig. 3.31:	Gametocyte toxicity assay.....	95
Fig. 3.32:	Transmission blocking potential of selected CLK inhibitors in exflagellation assays.....	96
Fig. 3.33:	Impact of CHX on parasite gametogenesis.....	97



